Optimal power system operation and planning of investments in new lines, energy storage and continuous serial compensation of power lines

Luburić, Zora

Doctoral thesis / Disertacija

2021

Degree Grantor / Ustanova koja je dodijelila akademski / stručni stupanj: **University of Zagreb, Faculty of Electrical Engineering and Computing / Sveučilište u Zagrebu, Fakultet elektrotehnike i računarstva**

Permanent link / Trajna poveznica: https://urn.nsk.hr/urn:nbn:hr:168:797084

Rights / Prava: In copyright / Zaštićeno autorskim pravom.

Download date / Datum preuzimanja: **2025-03-03**

Repository / Repozitorij:

FER Repository - University of Zagreb Faculty of Electrical Engineering and Computing repozitory

DIGITALNI AKADEMSKI ARHIVI I REPOZITORIJI

University of Zagreb

FACULTY OF ELECTRICAL ENGINEERING AND COMPUTING

Zora Luburić

OPTIMAL POWER SYSTEM OPERATION AND PLANNING OF INVESTMENTS IN NEW LINES, ENERGY STORAGE AND CONTINUOUS SERIAL COMPENSATION OF POWER LINES

DOCTORAL THESIS

Zagreb, 2021

University of Zagreb

FACULTY OF ELECTRICAL ENGINEERING AND COMPUTING

Zora Luburić

OPTIMAL POWER SYSTEM OPERATION AND PLANNING OF INVESTMENTS IN NEW LINES, ENERGY STORAGE AND CONTINUOUS SERIAL COMPENSATION OF POWER LINES

DOCTORAL THESIS

Supervisor: Associate Professor Hrvoje Pandžić, PhD

Zagreb, 2021

Sveučilište u Zagrebu
FAKULTET ELEKTROTEHNIKE I RAČUNARSTVA

Zora Luburić

OPTIMALNI POGON ELEKTROENERGETSKOGA SUSTAVA I PLANIRANJE INVESTICIJA U VODOVE, SPREMNIKE ENERGIJE I KONTINUIRANU SERIJSKU KOMPENZACIJU PRIJENOSNIH VODOVA

DOKTORSKI RAD

Mentor: izv. prof. dr. sc. Hrvoje Pandžić

Zagreb, 2021.

The doctoral thesis was completed at the University of Zagreb Faculty of Electrical Engineering and Computing, Department of Energy and Power Systems, Zagreb, Croatia.

Supervisor: Associate Professor Hrvoje Pandžić, PhD

The doctoral thesis has: 123 pages

The doctoral thesis number: ___________

About the Supervisor

Hrvoje Pandžić was born in 1984 in Zagreb, Croatia. He received his Masters and PhD degrees from the University of Zagreb Faculty of Electrical Engineering and Computing (UNIZG-FER) in 2007 and 2011, respectively. After being a postdoctoral researcher at the University of Washington, Seattle, 2012-2014, he became an Assistant Professor at UNIZG-FER in 2014. Currently, he is an Associate Professor at UNIZG-FER and the Head of the Department of Energy and Power Systems.

He has been coordinating many European and national projects focused on electricity markets, energy storage, batteries, electric vehicles, microgrids and power system flexibility. He published over 40 papers in journals categorized as Q1/Q2 according to JCR.

He received numerous awards, including the Award Science by the Government of the Republic of Croatia, 2018; Award for the highest scientific and artistic achievements in Croatia by the Croatian Academy of Science and Arts for 2018; Award Vera Johanides by the Croatian Academy of Engineering, 2015. He has been an Associate Member of the Croatian Academy of Science and Arts since 2020.

He is an Editor of IEEE Transactions on Power Systems and Energies journals.

He is an IEEE Senior Member, as well as a member of INFORMS and CIGRE.

Besides research achievements, he has led 10 technical studies for commercial partners.

O mentoru

Hrvoje Pandžić rođen je 1984. godine u Zagrebu. Završio je diplomski studij 2007. i doktorski studije 2011. godine na Sveučilištu u Zagrebu Fakultetu elektrotehnike i računarstva (UNIZG-FER). Nakon pozicije poslijedoktoranda na Sveučilištu Washington u Seattleu 2012-2014., postaje docent na UNIZG-FER 2014. godine. Trenutno je izvanredni profesor i predstojnik Zavoda za visoki napon i energetiku.

Vodio je mnoge europske i nacionalne projekte usmjerene na energetska tržišta, spremnike energije, baterije, električna vozila, mikromreže i fleksibilnost elektroenergetskog sustava. Objavio je preko 40 znanstvenih radova u znanstvenim časopisima kvalificiranima kao Q1 ili Q2 prema JCR.

Dobitnik je mnogih nagrada, uključujući nagradu Znanost Republike Hrvatske za 2018. godinu, nagradu za najviše znanstvene i umjetničke uspjehe Hrvatske akademije znanosti i umjetnosti za 2018. godinu te nagrade Vera Johanides Hrvatske akademije tehničkih znanosti za 2015. godinu. Član-suradnik je Hrvatske akademije znanosti i umjetnosti od 2020. godine.

Urednik je časopisa IEEE Transactions on Power Systems i Energies.

Član je profesionalnih udruženja IEEE (Senior Member), INFORMS i CIGRE.

Osim znanstvenih uspjeha, vodio je 10 tehničkih projekata za komercijalne naručitelje.

Acknowledgements

This thesis is based on the research conducted in the period 2016 to 2020 as a part of the project ”SIREN - Smart Integration of RENewables” funded by the Croatian Transmission System Operator (HOPS) and the Croatian Science Foundation under grant number I-2583-2015 and supervised by professor Hrvoje Pandžić, PhD.

I wish to express my sincere appreciation to my supervisor, professor Hrvoje Pandžić, who has the spirit of a true leader. He convincingly guided and encouraged me to be professional and do the right thing even when the road became tough. I am very grateful for his invaluable contribution and constructive suggestions during the planning and execution of this research work. Without his persistent help, the goal of this research would not have been realized.

I also wish to show my gratitude to professor Miguel Carrión, who gave me valuable advices and suggestions during my PhD exchange program at the University of Castilla-La Mancha, School of Industrial Technical Engineering in Toledo, Spain.

I would also like to express my deepest gratitude to my friends and colleagues from the Department of Energy and Power Systems, especially to Štefica Vlahović and Mirna Gržanić. Words cannot describe the gratitude and appreciation for your friendship.

I wish to acknowledge the support and great love of my family, my parents, Ivan and Draženka; my sisters, Ivana and Magdalena; and my brothers, Josip, Matej and Karlo. They kept me going on and this work would not have been possible without their support.

Finally, I thank my God, my good Father, for leading me through all the difficulties. I have experienced Your guidance day by day. I will keep on trusting You day by day. Thank you, Lord!

Abstract

Modern power systems tend to increase the capacity of integrated Renewable Energy Sources (RES). While the RES contribute to power system decarbonisation, on the other hand their variable generation is often characterized as poorly predictable and controllable, often away from the load centers. Transmission of electricity in periods of high production might cause line congestion. However, there are devices that can improve efficiency of electricity transmission and provide flexibility to the grid, such as Energy Storage (ES) and Flexible Alternating Current Transmission Systems (FACTS) devices. This thesis deals with ES performing energy arbitrage and deferring transmission investment, while FACTS devices also defer investment by changing the line impedance thus reducing the line congestion. The first part of the thesis is based on operational models in transmission power systems with increased share of non-controllable renewable generation using direct- (DC) and alternating-current (AC) network models. Impact of the two technologies, i.e. ES and FACTS, on power system flexibility and security is exhaustively researched. The second part of the thesis presents Transmission Expansion Planning (TEP) which is developed considering new lines, ES and series compensation of power lines using AC network model of power flows. The TEP problem is solved using Benders decomposition.

The most relevant conclusions of the thesis are: ES is more efficient in reducing system operating costs than FACTS devices, while the wind curtailment is effectively reduced by both technologies. However, the effectiveness of energy storage of reducing system operating costs and wind curtailment significantly depends on the wind profile. The current prices of ES and FACTS are still quite high, making the investment in new lines still the most attractive option. However, for lower ES costs, ES is installed at multiple buses, reducing the wind curtailment, but also taking part in voltage control. Investment in FACTS is less attractive and yields lower returns than the investment in new lines. However, it also complements the ES and can come handy at locations where installation of new lines is not possible.

Keywords: Energy storage, FACTS devices, Transmission power system, Unit commitment, Mixed-integer optimization, Power system planning, Benders decomposition

Prošireni sažetak

Optimalni pogon elektroenergetskog sustava i planiranje investicija u vodove, spremnike energije i kontinuiranu serijsku kompenzaciju prijenosnih vodova

Sve značajnijom integracijom obnovljivih izvora u moderni elektroenergetski sustav (EES) javljaju se dodatni izazovi u planiranju i pogonu samog sustava. Zbog koncentriranih lokacija pogodnih za gradnju vjetroelektrana, a koje su često udaljene od velikih centara potrošnje električne energije, javlja se problem zagušenja prijenosnih vodova. Tako uslijed male učestalosti zagušenja tijekom povećane proizvodnje vjetroelektrana i sezonskih tokova snaga, povećanje kapaciteta i/ili gradnja novih postojećih prijenosnih vodova često nije najekonomičnije rješenje. Povrh toga, gradnja dugačkih trasa vodova često otvara mnoga pravna pitanja i tendenciju dugotrajnijeg procesa izgradnje. U zadnje vrijeme nameću se nova rješenja koja mogu poboljšati učinkovitost prijenosa električne energije i pružiti značajnu količinu fleksibilnosti u sustavu, a neka od njih su spremnici energije i FACTS uređaji.

Općenito, glavne značajke koje doprinose povećavaju popularnosti ugradnje spremnika energije su sposobnost skladištenja energije iz obnovljivih izvora, brza vremena punjenja/pražnjenja te kratko vrijeme instalacije, dajući time prednost u odnosu na konvencionalne tehnologije. Međutim, manje atraktivne komponente spremnika energije su visoki troškovi ugradnje, samopražnjenje te različite gustoće energije samih spremnika energije. Postoji nekoliko tipova spremnika energije. Dok su neki od njih komercijalno dostupni, drugi su još uvijek u fazi razvoja. Moguća energija i snaga po jedinici težine, nazvana specifična energija i specifična snaga, od velike su važnosti za primjene. Prema tome, najčešća klasifikacija prema omjeru energije i snage spremnika energije je na -tip energija i -tip snaga. Spremnik energije -tip energija ima visoku energetsku gustoću i kraći životni vijek. Primjer su kemijski spremnici energije, skladišta komprimiranog zraka itd. Spremnik energije -tip snaga ima veliku gustoću energije, duži životni vijek, mogućnost bržeg punjenja/pražnjenja. Primjer su elektromagnetski spremnici energije i zamašnjaci. Na temelju navedenih značajki, spremnici energije mogu doprinijeti povećanju sigurnosti pogona elektroenergetskog sustava te razvoju tržišta električne energije.

Iako veliki izvor financijske dobiti dolazi od energetske arbitraže i skladištenja električne energije iz volatilnih obnovljivih izvora energije (preuzimanje viška proizvodnje električne energije iz vjetroelektrana te predaja pohranjene energije u trenucima niskog opterećenja vodova, odnosno niske proizvodnje vjetroelektrana), spremnici energije također mogu uprihoditi značajan dio i od pružanja usluga regulacije napona i frekvencije.

FACTS uređaji su druga skupina uređaja koja je bila predmet ovog istraživanja. Glavne prednosti FACTS uređaja su: povećanje sigurnosti i dostupnosti prijenosne mreže te upravljanje zagušenjima u mreži. FACTS tehnologija zasnovana je na energetskoj elektronici, odnosno na elektroničkim ventilima i tiristorima (GTO i IGBT). Vrijeme upravljanja je unutar nekoliko milisekundi, što znači da su u stanju kontinuirano upravljati karakterističnim varijablama sustava. Njihova ugradnja u već postojeća postrojenja iziskuje mnogo manje prostora u usporedbi s izgradnjom novog prijenosnog voda. Područje njihovog djelovanja je lokalnog karaktera. FACTS uređaji dijele se na tri skupine: i) poprečni: SVC (engl. Static Var Compensator) i STATCOM (engl. Static Compensator), ii) serijski: SSSC (engl. Static Synchronous Series Compensator) i TCSC (engl. Thyristor Controlled Series Capacitors), iii) kombinirani: UPFC(engl. Unified Power Flow Controller). Poprečni FACTS uređaji reguliraju iznos napona putem kontroliranog injektiranja jalove snage, dok serijski FACTS uređaji reguliraju tokove snaga pomoću injektiranog izvora napona u serijskom spoju s vodom. Kombinirani FACTS uređaji istodobno reguliraju iznos napona i tokove djelatne i jalove snage na vodu na kojem su priključeni. Predmetom doktorske disertacije u kategoriji serijskih FACTS uređaja je TCSC uređaj. Princip njegova rada bazira se na povećanju razlike napona susjednih čvorišta pomoću kontinuirane promjene reaktancije uz korištenje tiristorskog kuta upravljanja (engl. firing angle). TCSC uređaji utječu na tokove snaga te se njihovim korištenjem mogu opteretiti slabije opterećeni vodovi te rasteretiti zagušeni vodovi promjenom impedancije voda. Povećavanjem impedancije na zagušenim vodovima, TCSC-om se može utjecati na tok snage na nedovoljno iskorištene vodove u blizini. Obrnuto, smanjenje impedancije voda može povećati tok snage koji se prenosi na tom vodu pod pretpostavkom da nisu ugrožena toplinska ograničenja voda. TCSC uređaji najčešće su instalirani na dužinom prijenosnim vodovima.

Kroz doktorsku disertaciju *Optimalni pogon elektroenergetskog sustava i planiranje investicija u vodove, spremnike energije i kontinuiranu serijsku kompenzaciju prijenosnih vodova* ostvareni su sljedeći izvorni znanstveni doprinosi:

- **Optimizacijski model pogona elektroenergetskog sustava koji uključuje spremnike energije i kontinuiranu serijsku kompenzaciju prijenosnih vodova**
  Općenito, glavni ciljevi pogona elektroenergetskog sustava su sigurnost, pouzdanost i učinkovitost. Iako primarna zadaća sustava uključuje sigurnost i pouzdanost, također

važan aspekt EES-a je i učinkovitost njegova pogona. Sukladno tome, prvi doprinos odnosi se na usporedbu načina rada spremnika energije u dereguliranom tržišnom okruženju te zajednički pogon spremnika energije i FACTS uređaja u okomito integriranom modelu za različite razine integracije vjetroelektrana. Operator prijenosnog sustava u dereguliranom tržištu ima manju mogućnost upravljanja nad resursima sustava, a dispečiranje proizvodnih jedinica izravno je povezano s čišćenjem tržišta po nediskriminirajućim uvjetima. Prema tome, vlasnik spremnika energije želi maksimizirati svoju dobit, što nije nužno u skladu s minimiziranjem ukupnih pogonskih troškova sustava ili maksimiziranjem društvenog blagostanja. S druge strane, glavna značajka okomito integriranog modela je centralizirani pogon sustava koji utječe na dispečiranje proizvodnih jedinica. Sve investicijske i pogonske odluke donose se s jedinim ciljem, a to je minimiziranje ukupnih pogonskih troškova sustava. Osim modela, nova značajka doprinosa uključuje koordinirani pogon spremnika energije i TCSC uređaja na način koji je optimalan i ekonomičan za sustav.

Prema istraživanju, u okomito integriranom sustavu, spremnici energije postižu uštede do 1,3% na predloženoj studiji slučajeva. Uštede su veće za dane u kojima je bila veća proizvodnja iz vjetroelektrana. Ovim rezultatom se pokazuje da elektroenergetski sustavi s velikom proizvodnjom iz obnovljivih izvora energije imaju veće prednosti ukoliko imaju instalirane spremnike energije. Nadalje, spremnici energije smanjuju odbačenu energiju iz vjetra, što ujedno smanjuje proizvodnju iz konvencionalnih izvora energije. Smanjena je i vršna proizvodnja iz konvencionalnih elektrana. S druge strane, u elektroenergetskom sustavu utemeljenom na tržišnom modelu spremnika energije, dobit se iz spremnika energije dobiva na temelju razlike u čvorišnim cijenama (LMP metoda) tijekom dana i/ili tjedna. Čak i relativno niska dobit iz spremnika energije rezultira znatno većim (do 10 puta) povećanjem društvenog blagostanja. Jedan od razloga za to su tržišta ponuda/potražnja iz spremnika energije, dok je drugi razlog značajno smanjenje odbačene energije iz vjetra. Također je istraženo da spremnik energije na tržištu električne energije nudi električnu energiju na način koji je što neutralniji za čvorišne cijene. Ukoliko spremnik energije utječe na tržište, ono ujedno ometa i njegove mogućnosti zarade. Stoga se ne mogu očekivati značajna odstupanja cijena kao posljedica njegovog rada na tržištu električne energije. Iako spremnik energije može ostvariti dobit na tržištu električne energije, ta dobit nije dovoljna da opravda takvo ulaganje. Stoga je potrebno složiti više izvora prihoda kako bi se opravdalo samo ulaganje u spremnike energije.

- **Algoritam planiranja prijenosne mreže koji uključuje investicijske opcije u nove vodove, spremnike energije i serijsku kompenzaciju temeljen na optimizacijskom modelu s izmjeničnim tokovima snaga i Bendersovoj dekompoziciji**

  S progresivnom integracijom obnovljivih izvora energije glavni naglasak stavlja se na

povećanje njegove fleksibilnosti, odnosno mogućnosti brzog odgovora na pojavu nesigurnosti u elektroenergetskom sustavu. U disertaciji se predlaže model ulaganja koji pronalazi optimalnu kombinaciju neproizvodnih fleksibilnih jedinica na razini prijenosnog sustava: spremnika energije i uređaja za kontinuiranu serijsku kompenzaciju prijenosnih vodova (TCSC uređaj) te prijenosnih vodova kao tradicionalne opcije. Za razliku od FACTS uređaja koji su usmjereni samo na jalovu komponentu snage, spremnik energije ima mogućnost upravljanja i radnom i jalovom komponentom snage.
Predloženi model planiranja koristi linearizirani model tokova snaga AC OPF te zbog efikasnijeg izračuna koristi iterativni postupak Bendersove dekompozicije za dobivanje optimalnog rješenja. U istraživanju je simuliran model pomoću pet reprezentativnih dana kojima je pomno obuhvaćena cijela godinu. Svaki reprezentativni dan predstavlja pogonske podprobleme, dok se za glavni problem ulaganja koristi mješoviti linearni program (MILP).
Osim samog modela, predložene su i dvije nove stavke. Prvo, modeliran je dinamički pogon TCSC-a za linearno mješovito-cjelobrojni model (MILP). Dinamički pogon TCSC-a znači da se vrijednost kompenzacije aktivno podešava u svakoj jedinici vremena između nule i instaliranog kompenzacijskog kapaciteta. Drugo, spremnik energije je modeliran ne samo sa svrhom injektiranja ili preuzimanja radne snage pražnjenjem ili punjenjem baterije, što je uobičajeno u literaturi, već se njegov izmjenično-istosmjerni pretvarač koristi i za injektiranje ili preuzimanje jalove snage, čime se regulira napon mreže. Navedeno daje dodatnu vrijednost upotrebi spremnika energije, što je dosad u literaturi bilo ignorirano. Predstavljena studija slučaja ilustrira korisnost modela za različite investicijske troškove spremnika energije i politike ulaganja.

Najvažniji zaključci disertacije su sljedeći:

- Spremnici energije učinkovitije smanjuju pogonske troškove EES-a od FACTS uređaja, dok obje tehnologije smanjuju odbacivanje proizvodnje iz vjetroelektrana. Međutim, učinkovitost pohrane energije u smislu smanjenja pogonskih troškova sustava i smanjenja odbačene proizvodnje iz vjetroelektrana značajno ovisi o profilu proizvodnje vjetroelektrana.
- Za sadašnje cijene spremnika energije i TCSC-a ulaganje u nove prijenosne vode i dalje je najekonomičnija opcija na analiziranim studijama slučajeva. Međutim, za niže investicijske troškove spremnika energije model rezultira ulaganjima na nekoliko lokacija, smanjujući pritom odbacivanje proizvodnje iz vjetroelektrana, ali sudjelujući i u regulaciji napona. Ulaganje u TCSC manje je atraktivno i donosi manje dobiti u odnosu na ulaganje u nove prijenosne vodove. Međutim, važno je napomenuti da obje fleksibilne opcije mogu biti pogodne za investiciju ukoliko instalacija novih vodova u nekim dijelovima

mreže nije prihvatljiva opcija zbog imovinsko-pravnih odnosa ili strukture terena.

Ključne riječi: Spremnik energije, FACTS uređaj, Prijenosni sustav, Optimalni pogon sustava, Mješovito-cjelobrojna optimizacija, Planiranje prijenosne mreže, Bendersova dekompozicija

Contents

Chapter 1

Introduction

This chapter presents the background and motivation for this thesis, followed by the problem definition, solution methodology and the main research contributions.

1.1 Background and Motivation

The power system transition all around the world is already well beyond the starting phase as policy makers have intensified their strategy and goals. The share of renewable energy in Europe Union (EU) has almost doubled between 2004 and 2020 [1]. Since renewable energy is at the core of the Energy Union's priorities, the revised Directive (EU) 2018/2001 set a future-proof framework towards meeting the binding Union's target of at least 38%-40% renewable energy in the gross final consumption by 2030 [2]. The whole vision is complemented by the Clean Energy for All Europeans, called the fourth Clean Energy Package (CEP) [3].

Although the penetration of renewable energy sources is gaining momentum in the global energy mixture due to investment cost reductions [4], the integration of large quantities of intermittent renewable energy resources into the grid, comes with economic and technical challenges. In general, to transform an energy system towards the one dominated by renewable energy, flexibility has to be harnessed in all parts of the power system. A lack of system flexibility can reduce the ability to respond quickly to a disturbance in power systems, or lead to a loss of substantial amounts of clean electricity through their curtailment. Power system flexibility unifies various services (long-term to real-time), resource capabilities (from more flexible generation to stronger transmission and distribution systems, storage and flexible demand [5]), and time frameworks (planning horizon to millisecond horizon), accompanied by the improvement in digitalization [6]. Future energy systems will be marked by a stronger integration of all participants from the Transmission System Operator (TSO) to the Distribution System Operator (DSO), which will increase the overall flexibility of the system. While these factors are leading to a structural shift in the performance of power systems, they need to be better planned and operated. The reason behind is the nature of renewable generators, which can provide intermittent and uncertain energy flows in the grid. Moreover, the geographic location of bulk renewable farms contributes to worse impact to the circumstances as they are usually distant from load centers. As result of high unpredictability of renewable production, network congestion may occur. Technically this means that power flows in the transmission line are higher than the flow allowed by operating reliability limits [7]. The list of solutions are many consisting of geographic distribution of renewable generators, restructuring markets to remunerate flexibility, enhancing grid structure, developing advance battery technologies, developing demand-side management programs. Although a significant effort is needed in the isolated islands, this need is also well recognized in the large interconnected systems, and in making stronger connection to the distribution systems.

1.2 Problem Statement

As it is described above, the successful deployment of set of technological solutions which enable increasing a higher penetration of clean energies includes fostering transmission networks, developing demand side management, incorporating more flexible generators and storage units. Due to the fact that giving the place to the clean energy could significantly stop all environment issues, the power system is affected with a lot of challenges. In order to respond to all challenges among which the most important ones are: i) maintain frequency and reduce the cost on the balancing markets, ii) improve the opportunities in the network with reducing network congestion, iii) find the way for less renewable energy curtailment, iv) improve cross-border regional collaboration in assuring system security. In general, all the mentioned issues are connected with strengthening the whole power system flexibility capacity through various specter of options. There are plenty of them already developed and summarized as technical and non-technical methods [8]. The scope of interest of our research are technical methods such as improving system loadability using FACTS devices, and integration of new power transmission lines, and on the other side incorporating ES units for a reduction of renewable curtailment. The thesis covers two main fields in which it deals with increasing the flexibility of the power system network: i) operation and ii) planning algorithms. In the first part the algorithms express operation models of battery ES and FACTS devices in Unit Commitment (UC) and compare the performance of ES in a deregulated market environment for different scenarios of wind power production. The second part of the thesis deals with the transmission planning model of new power lines - somehow traditional components of the network, and ES units and Thyristor-Controlled Series Capacitor (TCSC) - new innovative solutions under linearized form of AC Optimal Power Flow (OPF).

1.3 Contributions

The thesis contributes to the modeling of two of the most important decision-making problems of power systems, the transmission system operation and transmission system planning. The network models present transmission power system under heavily connected renewable energy resources, such as wind power plants. First part of thesis describes models that capture the operational pattern of energy storage in a vertically-integrated utility and in a deregulated market environment. The modeling of continuous serial compensation of power lines at utility scale relaying on power system economics are also performed. This means that the operation of power system is done with the goal to minimize operation costs while reducing curtailment of cheap renewable energy. The second part of the thesis continues with the description of an algorithm of transmission system expansion including new power lines, energy storage and series compensation of power lines using AC model of power flows. Since the modeling of the AC model is non-linear and non-convex, but also, even when relaxed it can be computationally demanding in terms of time and memory. Hence, a decomposition method is used in order to contribute to a better execution of model. Moreover, a part of novelty of the research presents dynamic operation of TCSC which means that its compensation value is actively adjusted at each operating time period between zero and the installed compensation capacity. Second, as mentioned above, we use ES not only to inject or withdraw active power by discharging or charging the battery, which is customarily in the literature, but its AC/DC converter is also used to inject or withdraw reactive power, thus affecting network voltages. This adds another stream of value to the ES installation that has so far been ignored in the literature.

Development and implementation of models are done using CPLEX - The General Algebraic Modeling System (GAMS) solver. The models use network, load and wind production data from IEEE test systems. Data manipulation is done using Matlab.

The scientific contributions of the conducted research are:

- Optimization model of power system operation including energy storage and continuous serial compensation of power lines
- Algorithm of transmission expansion including investment options in new lines, energy

storage and serial compensation based on optimization model with AC OPF and Benders decomposition.

1.4 Thesis Structure

The thesis is structured as follows: Chapter 2 gives a comprehensive scientific overview of the existing solutions and algorithms related to system operation and planning of energy storage and FACTS device, and new power lines. Through the classification of the relevant literature, the position of the research is more briefly described. The analyzes and comparisons are made in order to systematically show the related work as follows: i) the general characteristic and type of energy storage, and FACTS devices - TCSC; ii) the overview of main operation models under division on traditional vertically models (UC) considering both energy storage and TCSC devices, and self-scheduling market models considering only energy storage, here representing classification of these models according to market delivery time (Day-ahead, Intraday, and Balancing markets); iii) the overview of planning models with accent to the transmission expansion models under DC and AC models, here a detailed description and purpose of Benders' decomposition is described. After exhausted overview of relevant literature, Chapter 3 shows in detail the main scientific contributions of the thesis. The contributions are substantiated under Chapter 4 where each articles gives different segments of the research contributions, and as well as authors' contribution in all presented articles. At the end, all conclusion are summarized and future directions are presented in Chapter 5.

Chapter 2

Research Position

This chapter provides a comprehensive scientific overview of the general characteristics and classifications of energy storage and FACTS devices, existing solutions and algorithms related to system operation and planning of these devices, and new power lines. Through the classification of the relevant literature, the position of the research is more briefly described.

2.1 Energy Storage

Although the storing of energy has already been well-known for many decades, it gained further popularity in last few years due to massive integration of renewables in power systems. The quality of voltage and frequency, influence of renewables on system reliability and adequacy, as well as power system security are all challenges that have arisen recently. While power systems can operate effectively without ES, cost-effective ways of storing electrical energy can help to make the network more efficient and reliable, resulting in reduced transmission losses [9]. Consequentially, it changes the paradigm of electricity from a just-in-time to a time-adjustable commodity. Moreover, some storage technologies could be implemented much faster than conventional grid upgrades. With the current trend of electricity production being decentralized and fluctuating, storage can be used to improve generation, transportation and distribution layers.

2.1.1 Energy storage applications

In general, the main performances that increase the popularity for installation of energy storage are fast charge-discharge times, ability to provide energy in time, and short time of installation, which give it an advantage versus conventional technologies. However, the less attractive components of energy storage are high cost, self-discharge, various energy densities. Different types of ES are being developed. While some of them are available commercially, others are still in the development stage. The energy and power available per unit weight, called the specific energy and specific power, are of great importance in some applications. Thus, according to the energy/power ratio, the most common classification is on energy-type energy storage and power-type energy storage. Energy-type energy storage has high energy density, and short life cycle, such as most chemical energy storage, compressed air energy storage, etc. Power-type energy storage has high power density, long life cycle, high-rate charge and discharge capacity, such as most electromagnetic energy storage, flywheel energy storage. Consequently, through ES provides many benefits to the power system network. If these types are connected with their ability for provide some of applications, they can be summarized as in Table 2.1. While the main contribution to the ES profits comes from the energy arbitrage and renewable energy time shift, ES can also generate significant profits from voltage regulation and frequency regulation services [10].

Table 2.1: Energy storage applications (table from [11])

Energy applications	**Power applications**
Energy arbitrage	Frequency regulation
Renewable energy time shift	Voltage support
Demand charge reduction	Small signal stability
Time-of-use charge reduction	Frequency droop
T&D upgrade deferral	Synthetic inertia
Grid resiliency	Renewable capacity firming

2.1.2 Energy storage classification

Due to the fact that direct storing of electricity is almost impossible, electric energy can be stored in form of potential, chemical, magnetic or kinetic energy. However, the classification based on the technology form of stored energy is as follows: i) mechanical storage, ii) chemical storage, iii) electromagnetic storage, iv) thermal storage, v) electrochemical storage [12]. Comparison of ES and their characteristics including their advantages and disadvantages are provided in Table 2.2.

2.1.2.1 Mechanical storage

The most well-known type of energy storage is mechanical storage based on Pumped Hydro Storage (PHS). At the end of the first half of 2020, 167.790 GW of pumped-hydro power plant capacity was operational according to [13]. The most common purpose of PHS is in reducing the long-term variations, e.g. load-shifting. Therefore, its contribution to the system flexibility is counted on a large scale [14]. Despite the fact that this technology can store significant amounts of energy for a long period, PHS are constrained by specific locations with the required geographical features. Other two types of energy storage from this group, however, less utilized, are flywheels [15] and Compressed Air Energy Storage (CAES) [16]. Due to their rapid response, they are usually called power type energy storage technologies.

2.1.2.2 Chemical storage

Hydrogen, ammonia, and methane are some of the most common chemical energy storage materials [17]. According to its specifications, hydrogen fuel cell is a representative of chemical storage. Although hydrogen is the most abundant element on Earth, it rarely exists alone, and therefore is produced by extracting it from its compound. Moreover, it has the potential to be a clean, reliable and affordable energy source, and some forecasts are that it will play a major role in the future. Energy efficiency of fuel cells can be as high as 25-35% [18], and if it is used in hydrogen-oxygen fuel cell, the electricity is directly produced [12].

2.1.2.3 Electromagnetic storage

An interesting new type of energy storage is electromagnetic storage which can be divided into two main mechanisms [19]. In the first one, the electrostatic energy is stored in the electric field, while in the second one the relationship between electrical and magnetic phenomena is used. It will be seen that both of these mechanisms are most applicable to situations in which there is a requirement for storing modest amounts of energy under abrupt transient conditions [20], for relatively short times and occasionally at high rates [21]. The best representative of the first mechanism is the ultracapacitor. It involves storing charge in the electrical double-layer at or near the electrolyte-electronic material interface. Its main characteristics are low specific energy, high specific power, short charge times, very high number of cycles, high self-discharge, and high cost per watt-hour [20]. The second mechanism shows the capability of electromagnets that can be much greater than the one of capacitors. The well-conducted research was done in the application of superconducting magnetic energy storage due to their high-efficiency [22].

2.1.2.4 Thermal storage

Although the current number of thermal energy storage system applications is much lower, their popularization is growing. Thermal energy storage works by heating the storage medium during the charging period and then releasing the heat when the energy is needed [23]. They can be classified into two main groups: i) Latent Heat Storage (LHS) and ii) Sensible Heat Storage (SHS) [24]. While SHS stores thermal energy by raising the temperature of a solid or liquid without the occurrence of a phase change, LHS makes use of the heat absorbed or released by the storage material when it experiences a phase change between solid and liquid or liquid and gas. Current applications include thermal building processes [25], solar applications such as air heating systems [26], greenhouses and concentrated solar power plants [27] and solar tower power plants [28].

2.1.2.5 Electrochemical storage

Due to their specific characteristics that favour all the challenges of RES integration, electrochemical energy storage has become the most investigated ES technology type. The electrochemical storage consists of an elementary cell that comprises two electrodes immersed in an electrolyte. Usually, the electrodes are in the solid state while the electrolyte is in the liquid one [29]. The two electrodes are respectively qualified as positive and negative, and the terms such as anode and cathode should be avoided. The reason behind is that each electrode changes its role depending on whether it is in the process of charging or discharging process. The detail characteristics are further described in the following sections.

2.1.3 Battery energy storage

In general, the most widely used name for electrochemical energy storage is battery. Batteries can be primary or non-rechargeable and secondary or rechargeable. Primary batteries cannot be recharged after the first discharge cycle, while the secondary battery can perform multiple discharge and charge cycles. The main process taking place in secondary batteries is

Table 2.2: Energy storage main characteristic per storing technology type (table adapted from [30])

ES storing type	Technology	Response time	Number of cycles	Advantages & Disadvantages
Mechanical	PHS	Min	Unrestricted	Large capacity, fast output, charge rate, low operating cost and environmental constraints
Mechanical	CEAS	Min	Unrestricted	Large ES capacity, dependable of geological conditions
Chemical	Hydrogen	> Min	40,000	High energy density, clean technology, high efficient, short service life, high cost
Electromagnetic	Ultracapacitor	< Sec	> 1,000,000	Fast charging and discharging, low energy density, short discharging time
Electromagnetic	Flywheel	< Sec	> 100,000	High efficiency, fast response, long life, high cost, technology to be improved
Electromagnetic	Superconducting magnet	Millisec	> 100,000	High power, low energy density, high cost, maintenance needed
Thermal	Latent	< Min	Unknown	Low range of thermal conductivity
Electrochemical	Li-ion battery	< Sec	10,000	High energy density, good discharge possibilities, long life, no special need for maintenance, low internal resistance, short charging time and low self-discharge rate

conversion of electrical energy to chemical potential energy and storing it until the time this energy is needed, when the chemical potential energy is converted back to electricity. This process is derived within an electrochemical cell where an anode and a cathode are immersed into an electrolyte. During the charging process, the electrolyte is ionized, while in the opposite direction (discharging) the reactions take place to recover the chemical potential energy stored in the ions. By definition, an anode is the electrode at which the oxidation occurs (electrons release), and a cathode is the electrode at which the reduction occurs (electrons reception). The most utilized battery energy storages (BES) are i) lead-acid batteries, ii) nickel-based batteries, and iii) Lithium-ion (Li-ion) batteries [17]. The principal requirements for ES include energy density, power density, charging speed, life expectancy, cost, weight, and size. As distributed RES are appearing in the network, the need for incorporation smaller size batteries to solve local voltage or current congestion issues is growing. Since ES enables spatio-temporal arbitrage, the problem with intermittent production can be mitigated. The main idea here is the positioning of ES at strategic locations in the network for consumption at a later time or further transmission when the network is less congested. In addition, distributed energy storage can be used for real-time system balancing, and post-contingency corrective actions. Three distinctive battery technologies, i.e. lead-acid battery, nickel-based, and li-ion, are presented below.

Table 2.3: Performance comparison of different battery ES (table adapted from [21])

Battery ES type	Specific energy (Wh/kg)	Energy density (Wh/L)	Specific power (W/kg)	Life cycle (-)	Energy efficiency (%)
Lead-acid	35	100	180	1,000	80
Nickel-based	50-60	60	100-150	2,000	75
NaS	150-240	-	150-230	4,500	80
Li-ion	118-225	200-400	200-430	10,000	97

2.1.3.1 Lead-acid batteries

Among all types of electrochemical energy storage, lead-acid batteries have the highest technical maturity, lowest cost and the wide-spread application. They are mostly preferred when high discharge power is required. The overall cycle efficiency is relatively high, around 70% to 90% [12]. The lifetime of lead-acid batteries depends on various factors, such as selected component materials, and in general amounts to 3 to 10 years, depending on the utilization regime. Moreover, lead–acid batteries have fast response times, low daily self-discharge rates (<0.3%), and low capital costs (50–600 $/kWh) [31]. It is a popular storage choice for power quality, Uninterruptible Power Supply (UPS) and some spinning reserve applications. Its application for energy management, however, has been very limited due to its limited life cycle (500–1,000 cycles) and low energy density (30–50 Wh/kg) due to the inherent high density of lead [32]. Currently, the research and development of lead–acid batteries focuses on: i) innovating materials for performance improvement, such as extending cycling times and enhancing the deep discharge capability, ii) implementing the battery technology for applications in the wind, photovoltaic power integration and automotive sectors [33].

2.1.3.2 Nickel-based batteries

Before the actual commercial start of NiMH batteries in 1995, NiCd batteries had been in commercial use since 1915. NiCd batteries constitute of a nickel hydroxide positive electrode plate, a cadmium hydroxide negative electrode plate, a separator, and an alkaline electrolyte [32]. However, because of the toxicity of cadmium, these batteries are presently used only for some stationary applications. Today, NiMH batteries are replacing NiCd in many applications where a high specific energy is imperative. In NiMH batteries, a hydrogen-absorbing alloy instead of cadmium is used as the electrode. At low rates of discharge NiMH batteries can reach specific energies up to 80 Wh/kg and in special designs can deliver specific power up to 1 kW/kg [33]. Specific capabilities of these batteries are overcharging and over-discharging. In addition, moderate number of cycles (above 1,000 cycles), higher power capability, and dense electrode structure are advantageous for this battery technology [34]. Compared to lead-acid batteries, nickel-based batteries have higher power density, slightly better energy density and achieve higher number of cycles. They have a wide range of applications, from portable products to Electric Vehicle (EV) and potential industrial standby applications, such as UPS devices [35].

2.1.3.3 NaS battery

A sodium-sulphur battery consists of molten liquid sulphur at the positive electrode and molten liquid sodium at the negative electrode. The active materials are separated by a solid beta alumina ceramic electrolyte. This electrolyte allows only the positive sodium ions (Na+) to go through it and combine with sulphur to form sodium polysulphides. In general, positive Na+ ions during the discharge process flow through the electrolyte while the electrons flow in the external circuit of the battery producing 2.0 V [32]. In the reversible process (charging), sodium polysulphides release the positive sodium ions back through the electrolyte to recombine as elemental sodium. High conductivity is obtained by heating the battery to a temperature of 270–360 Celsius [36]. Some typical characteristics of NaS batteries are high life cycle of 4,500 cycles, energy density in the range of 150–240 Wh/kg, while power density in the range of 150–230 W/kg, and have a discharge time of 6.0 hours to 7.2 hours [37]. The main advantages of these batteries are efficient cycles, around 75-90%, pulse power capability over six times their continuous rating, which makes NaS batteries as economical and widely used in combined power quality and peak shaving applications.

2.1.3.4 Li-ion battery

A Li-ion battery consists of a cathode made of lithium metal oxide, and an anode that is a graphitic carbon cell. Electrolyte can be a non-aqueous solution made of an organic solvent and a dissolved lithium salt or a solid polymer. During discharge, the ions flow from the anode to the cathode through the electrolyte and separator, and in opposite direction (charge) the ions flow from the cathode to the anode [36]. The lifetime cycle of a Li-ion battery is a function of its average operating temperature, which depends on the outside temperature and the heat generated by the application itself, on the Depth-of-Discharge (DoD) attained and the charge conditions applied. High temperatures, deep discharges and poorly-managed charge profiles reduce the lifetime of a battery in terms of the number of cycles [29]. There are six most common types of Li-ion batteries, as summarized in Table 2.4. Batteries have high energy density, good discharge possibilities, long life, no special need for maintenance, low internal resistance, good Coulomb efficiency, simple charging algorithm, short charging time and low self-discharge rate. However, disadvantageous are a need for a well-performing battery management system (BMS), degradation at high temperatures and voltages, and difficult or impossible charging at low temperatures. The current research focuses for the Li-ion battery include: i) increasing battery power capability, ii) enhancing battery specific energy by developing advanced electrode materials and electrolyte solutions. According to that, the improved material developments have led to improvements in terms of the energy density which is increased from 75 to 200 Wh/kg, and increased life cycle to as high as 10,000 cycles. Moreover, the efficiency of Li-ion batteries can reach up 97% [31]. Despite very good characteristics, the main hurdle is their high cost, however these costs are constantly reducing.

2.1.4 Energy storage challenges

In general, there are few widely presented challenges connected with battery energy storage. The result of this conclusion comes from the assessment of storage deployment which is generally described by the speed with which battery storage technologies and their applications are evolving, and to the multiplicity and flexibility of battery storage [38]. The main challenges are : i) Initial investment costs, ii) Lack of standardization, iii) Outdated regulatory policy and market design.

In general, all projections show a decline in capital costs, with cost reductions by 2025 of 6-48% , 26-63% capital cost reductions by 2030 and 44-78% cost reductions by [39]. The storage cost captures a total system cost, where the system cost (in $/kWh) is the power component divided by the duration plus the energy component. According to the following cost

Table 2.4: Comparison of different Li-ion batteries (table adapted from [36])

	Li-Co	**Li-Mn**	**NMC**	**Li-phosphate**	**Li-Al**	**Li-Ti**
Voltage (V)	3.60	3.70	3.60	3.20	3.60	2.40
Specific energy (Wh/kg)	150-200	100-150	150-220	90-120	200-260	50-80
Charge (C-rate)	0.7-1	0.7-1	0.7-1	1	0.7	1
Discharge (C-rate)	1	1	1	1	1	10
Life cycle	500-1,000	300-700	1,000-2,000	> 2,000	500	3,000-7,000
Applications	Mobile phones	Power tools	E-bikes	High load currents	Medical devices	UPS

projections, presented as "low" to a "mid" to a "high", if the initial cost in 2019 was \$380/kWh [40], the storage costs is assumed to be \$124/kWh, \$207/kWh, and \$338/kWh in 2030 and \$76/kWh, \$156/kWh, and \$258/kWh in 2050, respectively [39].

Although the costs have been decreasing very quickly, some decision-makers around the world still do not make decisions in correlation with that statement. The transition of incorporating ES into the power system is demanding time and effort. The standardization should capture common energy storage terms (wording), energy storage metrics — efficiency, capacity, power ratings, system inefficiencies and testing methods. Standard testing methods must be outlined not only for proving component functionality but for system functionality at the point of connection to the grid [41]. Also, the technical requirements for services, such as the frequency regulation services and updated grid codes [42], should be elaborated in detailed in order to enable ES to simply compete among other technologies in markets.

According to the third point, regulatory policy needs to reach mature instruments for existing energy storage technologies. This relates to the additional incentives for pilot projects which will increase awareness for investing in such technologies. Therefore, the European Commission has identified battery energy storage as a strategic value chain where the EU must step up towards investment and innovation to strengthen the industrial policy strategy [43].

2.1.5 Mathematical modelling

The most important aspect of energy storage mathematical modelling is to provide as accurate as possible energy storage model. The main idea here is to use material characteristics and physical parameters in the battery cell design in order to predict voltage and charge capacity [44]. Battery models can be classified by the physical domain and consider State of Charge (SoC), temperature, and degradation [45]. The further classification of SoC models can be organized as a function of the units they use to define capacity: i) electrical energy, ii) electrical charge, and iii) chemical concentration. Electrical energy SoC models are mostly linear and consider energy efficiency and power charge/discharge limits. The electrical charge SoC model works by predicting the battery string voltage, while chemical SoC models are based on chemical concentrations. Temperature function considers both the heat generation and its transfer. While entropy, overpotential losses, and resistive heating are processes responsible for heat generation, they are transferred through conduction, radiation, and convection. Therefore, the variations of the temperature models are based on the level of representation of these two phenomena. Battery degradation can be assumed by the underlying physical mechanisms or empirically. Empirical stress factor models isolate the impacts of time, current, SoC, temperature, and DoD or battery State of Health (SoH). Through a few simplifying assumptions, these stress factors can be represented using regularization norms. Physical degradation models are usually classified into models of side-reactions and those of material fatigue.

For an appropriate sizing of the storage device, both the discharge efficiency and the maximum allowed DoD in discharging models should be considered [46]. A high load current lowers the battery voltage and the end-of-discharge voltage threshold is often set lower to prevent premature cutoff. The cutoff voltage should also be lowered when discharging at very low temperatures [36, 47], as the battery voltage drops and the internal battery resistance rises [48].

Battery charging process is more complex to model than the discharging process [49, 50]. The most commonly used method for charging batteries is the so-called Constant Current (CC)-Constant Voltage (CV) [51]. CC-CV charging is achieved through several phases, as shown in Figure 2.1. The blue line presents current, while red dash line shows the voltage. In the first phase (constant-current phase), when the battery voltage is low, the battery is charged with a constant current and the voltage rises all the way to its nominal value. The SoC of the battery after the first phase is around 65-80%, depending on the charging current. In the second phase, a constant voltage is maintained and the battery is charged with lower and lower current until the current drops to around 3-5% of the nominal value, when the charging process is terminated. Additionally, a third and fourth phases can be added. The third phase shows the standby state

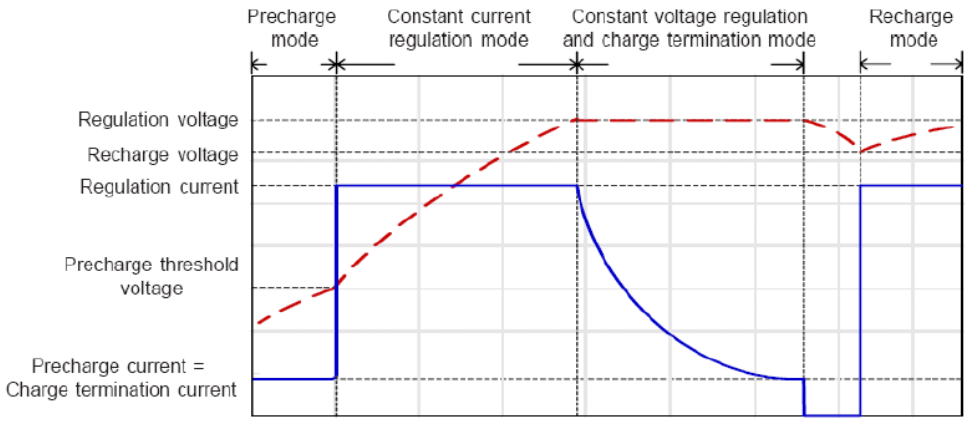

Figure 2.1: Li-ion battery charge stages (figure from [51])

of the battery, and there is no electricity, but the voltage drops slightly. The voltage rises to the level of 3.7-3.9 V. Finally, the fourth phase presents an additional charging/saturation current that returns the voltage to the nominal value. The optimal temperature during solid electrolyte inter-phase plays a big role and presents a strong function of charge rate and energy density [52]. However, for any high-level optimization problem, the battery models need to reach sufficient accurness [53, 54]. An accurate charging model of battery energy storage introduced by a laboratory procedure to obtain the dependence of the battery charging capacity on its state of energy is highly required before any application [55]. The most representative models are: i) the constant charging power limit - Base model [56], ii) charging power limit with linear reduction at the constant voltage part of the charging curve - Linear reduction model [57], iii) piecewise linear approximation of the available charging energy - Piecewise linear approximation model [55].

2.1.5.1 Base model

The base model formulation is used in the thesis algorithms, and it presents the most common used formulation in the literature. The state of charge (soc) is an indication of the amount of electricity still available in the battery in relation to its capacity in given conditions [29]. Equation (2.1) calculates battery energy storage state of charge ($soc_b(t)$) of battery unit b at time period t, established by the state of charge in the previous time period $(t-1)$ and (dis)charged energy in time period t considering battery energy efficiencies ($\eta_b^{\mathrm{ch}}, \eta_b^{\mathrm{dis}}$). SoC is constrained by minimum/maximum possible battery state of charge ($soc_b^{\max}$), as presented in (2.2). Constraints (2.3) and (2.4) represent battery charging and discharging constraints, where

$ch_b^{\max}$ and $dis_b^{\max}$ represent parameters for maximum battery charging and discharging power.

$$soc_b(t) = soc_b(t-1) + p_b^{\text{ch}}(t) \cdot \eta_b^{\text{ch}} - \frac{p_b^{\text{dis}}(t)}{\eta_b^{\text{dis}}} \quad \forall b \in B, t \in T \tag{2.1}$$

$$soc_b^{\min} \leq soc_b(t) \leq soc_b^{\max} \quad \forall b \in B, t \in T \tag{2.2}$$

$$p_b^{\text{ch}}(t) \leq ch_b^{\max} \qquad \forall b \in B, t \in T \tag{2.3}$$

$$p_b^{\text{dis}}(t) \leq dis_b^{\max} \qquad \forall b \in B, t \in T \tag{2.4}$$

2.1.5.2 Linear reduction model

Charging power limit with linear reduction at the constant voltage part of the charging curve is state which occurs in the third phase in Figure 2.1. Since that current starts decreasing in this stage, the charging power reduces significantly as the energy stored is at its maximum value. The formulation of Base model is slightly changed by introducing the mentioned issue [57], only occur when switching constraint (2.3) by two constraints (2.5)-(2.6).

$$p_b^{\text{ch}}(t) \leq ch_b^{\max} \qquad \forall b \in B, t \in T \tag{2.5}$$

$$p_b^{\text{ch}}(t) \leq ch_b^{\max} \cdot \frac{soc_b^{\max} - soc_b(t)}{soc_b^{\max} - soc_b^{\text{CC,CV}}} \qquad \forall b \in B, t \in T \tag{2.6}$$

Parameter $soc_b^{\text{CC,CV}}$ presents the state of charge when the constant-current changes to the constant-voltage mode. While constraint (2.5) limits maximum charging rate for all states of energy, the stricter charging limit for state of energy above $soc_b^{\text{CC,CV}}$ are set by constraint (2.6). It means that for $soc_b(t) = soc_b^{\text{CC,CV}}$, parameter $ch_b^{\max}$ linearly decrease to zero at $soc_b(t) = soc_b^{\max}$.

2.1.5.3 Piecewise linear approximation model

New approach for battery charging model considers battery's ability to absorb energy as a function of the current state of energy [55]. The state of energy (soe) is the ratio of the amount of energy still available to the total amount of energy stored. In other words, this means that $\Delta soe_b(t)$ indicates how much energy can be charged in the battery b in the following time period t. It is shown that for lower charging currents (C-rates less than 0.5), during the CC phase, the ability of the battery to absorb energy reduces. On the other side, for the higher charging current (C-rates close to 1), the rising part is not being appeared since CC phase is shorter than one hour (if one hour is set as standard time step). However, due to nonlinearities introduced by component $soe_b(t) - \Delta soe_b(t)$, the function if piecewise linearized as in Figure 2.2 [55]. The Based model is supplemented with the following constraints where the constraint on battery charging (2.3) is replaced by set of constraints (2.7)-(2.10).

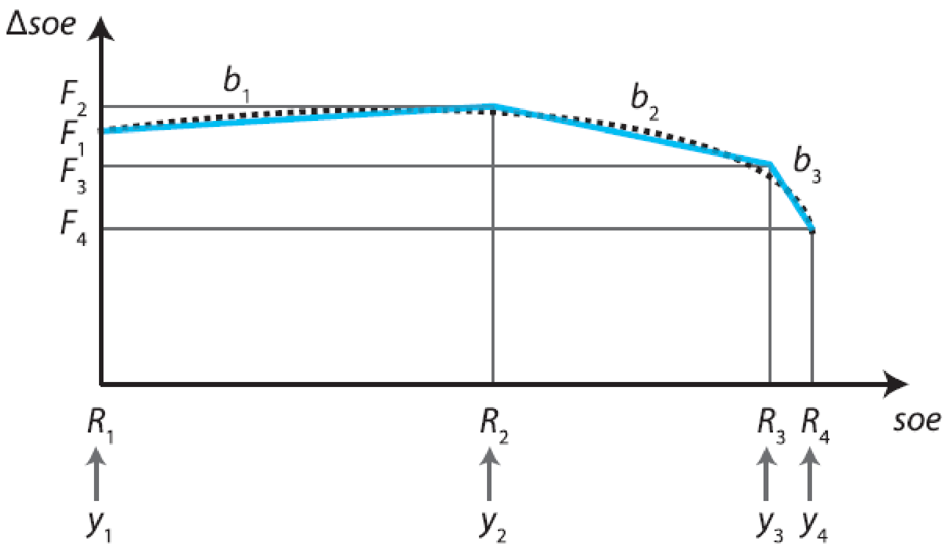

Figure 2.2: Piecewise linear approximation of $soe_b(t) - \Delta soe_b(t)$ (figure from [55])

$$soe_b(t) = \sum_{i=1}^{I-1} soe_{b,i}(t) \qquad \forall b \in B, t \in T \tag{2.7}$$

$$soe_{b,i}(t) \leq R_{i+1} - R_i \qquad \forall i \in I, b \in B, t \in T \tag{2.8}$$

$$\Delta soe_b(t) = F_1 + \sum_{i=1}^{I-1} \frac{F_{i+1} - F_i}{R_{i+1} - R_i} \cdot soe_{b,i}(t-1) \qquad \forall b \in B, t \in T \tag{2.9}$$

$$p_b^{\mathrm{ch}}(t) \leq \frac{\Delta soe_b(t)}{\Delta t \cdot \eta_b^{\mathrm{ch}}} \qquad \forall b \in B, t \in T \tag{2.10}$$

2.2 Flexible AC Transmission Systems

2.2.1 Classification and overview

FACTS are considered to be a key technology for better utilization of transmission network capacity based on power-electronic controllers [58]. Evolution of the FACTS started by the development of new solid-state electrical switching devices. Progressively, the use of the FACTS has given rise to new controllable systems that bring more flexibility to the power system. By providing the increased flexibility, FACTS controllers can enable a line to carry power closer to its thermal rating. These opportunities arise from the ability of FACTS devices to control the interrelated parameters that govern the operation of transmission systems including series impedance, shunt impedance, current, voltage, phase angle, and the damping of oscillations at various frequencies below the rated frequency [59]. The full potential of AC/DC converter technology was better realized once mercury-arc valves were replaced by the solid-state switching devices called thyristors. Thyristors offer controlled turn-on of currents but not their interruption [60].

Generally, FACTS devices can be categorized into three types: i) shunt devices, such as Static Var Compensator (SVC), ii) variable-impedance series devices, such as TCSC, and iii) doubled devices, such as Unified Power Flow Controller (UPFC) [61]. An SVC nominally consists of a fixed shunt capacitor in parallel with a reactor controlled by two thyristors connected to form a bidirectional switch. Consequently, shunt devices are usually used for bus voltage magnitude control and reactive power compensation, thus not suitable for real power flow control [60]. They provide rapidly controllable reactive shunt compensation for dynamic voltage control through utilisation of high-speed thyristor switching/controlled reactive devices [62]. On the other hand, both variable-impedance series devices and phase shifters can be used in real power flow control. A TCSC device comprises of a thyristor-controlled variable capacitor protected by a metal-oxide varistor (MOV) and an airgap. It offers several benefits, such as fast and continuous control of the series compensation level, dynamic control of power flow, reduction of system losses, mitigation of sub-synchronous resonance and improved transient stability [63]. Due to its distinct ability to control the active and reactive power flows in the transmission line, UPFC contributes to a stable operation of the transmission system [64]. The UPFC consists of both the Static Synchronous Compensator (STATCOM) and the Static Synchronous Series

Compensator (SSSC). It can control the magnitude and phase angle of transmission voltage and impedance of the line simultaneously. Since the thesis models TCSC in power system planning and operation models, a detailed description of its characteristics and applications is presented below.

2.2.2 Thyristor-Controlled Series Capacitor

2.2.2.1 Main Characteristic

The basic conceptual TCSC module comprises a series capacitor C, in parallel with a thyristor-controlled reactor, L_S, as shown in Figure 2.3. In the common TCSC configuration, a thyristor-controlled variable capacitor is protected by a metal-oxide varistor (MOV) and an air-gap. This helps preventing the occurrence of high-capacitor over-voltages. Besides this feature, it also allows the capacitor to remain in circuit even during fault conditions and helps improve the transient stability [58]. With the rapid developments in the power electronics technology, TCSC offers several benefits, such as fast and continuous control of the series compensation level, dynamic control of power flow by increasing power transfer, reduction of system losses, and mitigation of sub-synchronous resonance [63]. Furthermore, it also increases responsiveness of power flow in the series-compensated line from the outage of other lines in the system.

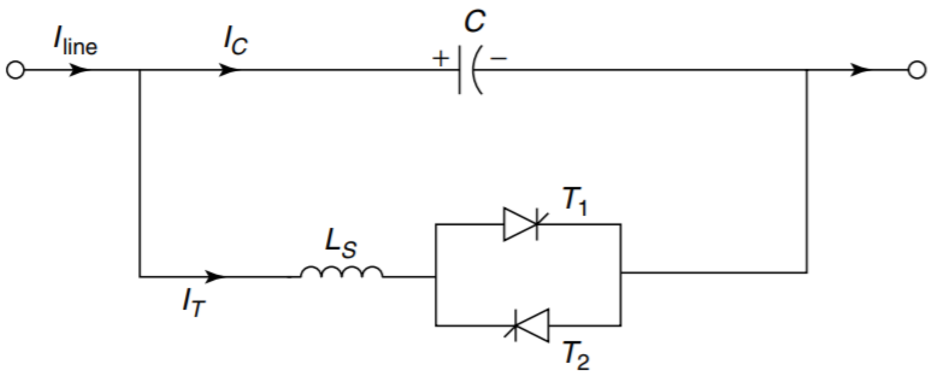

Figure 2.3: TCSC (figure from [58])

As already mentioned, TCSC consists of series capacitor shunted by Thyristor-Controlled Reactor (TCR). The combination of TCR and capacitor enables a smooth control of the capacitive reactance over a wide range as well as switching upon command to a condition where the bidirectional thyristor pairs conduct continuously and insert an appropriate reactance into the line. The series controller may be a variable capacitor, inductor or a variable frequency source.

With the help of series capacitors, it increases the reactive power as the square of line current. This means that TCSC reduces the transmission losses, increases the available capacity transform and improves the voltage profile [65]. By increasing the impedance on congested lines, TCSC can shift power to underutilised transmission lines nearby. Vice versa, decreasing the impedance of a transmission line can increase the power transferred on that line assuming thermal limits have not been reached [66]. Although incorporation of FACTS devices, especially TCSC and UPFC, in power system has contributed to many technical and economic benefits, they introduced some negative effects as well. Operation of such FACTS devices introduces harmonics and non-linearity in power system and causes fast changes in line impedance [63]. In order to tackle this, the impact of these controllers on the performance of distance protection scheme should be studied. This includes fault detection, fault zone identification, fault classification and fault location estimation [67]. Hence, to solve these issues, different algorithms based on soft-computing approaches are heavily investigated. Incorporating a transmission switching with FACTS devices and their coordination can help improve power system network state. As the system operators begin to utilize these tools, it is essential to understand the interdependence between them at various stages, such as planning and operation [68].

2.3 Operational Models in Transmission System Network

In general, the main objectives of power system operation are safety, reliability and efficiency. While the safety and reliability are considers primary, the efficiency of the power system operation is also important. In other words, the power system is optimized in and economically effective manner while complying with reliability and safety requirements [69]. There are plenty classifications of operational models, however, this thesis presents the ones that include energy storage and/or TCSC devices at the transmission system level. Operational models are usually formulated as Linear Program (LP) or Mix Integer Linear Program (MILP) optimization problems, due to good computational performance of such algorithms. They usually have short-term time framework which indicates the importance of obtaining results quickly and implementing the decisions.

According to the level of uncertainty in modelling techniques [70], the operation models are mostly categorized and represented as: i) Deterministic [71], ii) Stochastic [72], iii) Robust [73], iv) Interval [74], v) Chance-constrained [75].

In general, the difference between the deterministic approach and the remaining models listed above is that all uncertain parameters, e.g. demand or renewable generation, are replaced by their expected values. This means that they always produce anticipated results from a given starting condition or initial state, without any allowance of the forecast error [76]. However, this formulation could also ensure some level of flexibility in power system, such as modelling of reserves using approximate methods, such as the NREL's 5+3% rule [77]. With an increasing integration of RES, it is desirable to put more effort in investigation of the other, more rigorous reserve scheduling methods.

Stochastic models assume that probability distributions of uncertain parameters are known. Therefore, these distributions can be afterwards represented using a set of plausible realizations of the uncertain parameters or scenarios. These parameters can be related to generation, especially non-controllable RES, or to demand [78]. Previously, a strong accent was placed on forecasting the demand [79]. Traditional methods such as time series [80], regression [81], econometric [82], An Autoregressive Integrated Moving Average (ARIMA) [83] as well as soft computing techniques such as fuzzy logic [84], genetic algorithm [85], and neural networks [86] are being extensively used for demand side predictions. On the other side, since non-controllable RES introduced an additional factor of uncertainly, their predicted production models started to draw attention of the research community. As the highest rate of clean energy is introduced by wind power with total wind energy globally installed of 651 GW [87] at the end of 2019, the prediction tools for the wind production are carefully investigated [88]. Apart from wind production, photovoltaic power production [89] is the most important RES technology with 584.84 GW of installed capacity [1]. Evaluating these forecasts is very important, especially because the forecast errors can be related to costs and, ideally, an ex-post evaluation should provide information on these expected costs.

The aim of the robust formulation is to minimize the objective function while maintaining feasibility under all possible realizations of uncertain parameters within some specified uncertainty set [90]. It is based on the worst-case outcomes and is criticized as being too conservative for some applications. However, the level of conservatism can be controlled by adjusting the uncertainty budget [91].

Interval formulation can be viewed as an alternative to the stochastic and robust formulations [74]. The reason for that is reduced set of scenarios to three distinct ones: the central forecast, the upper limit, and the lower limit scenario [92]. According to that, the interval formulation is less computationally demanding than the stochastic formulation [93].

Probabilistic optimization or chance-constrained optimization is formulation that deals with random processes where one or several constraints or the objective function must be satisfied with high probability [94]. Consequently, it usually tries to solve the problem of wind power [95] and or demand uncertainties [96].

2.3.1 Unit commitment models

Traditionally, utilities were vertically-integrated and generation, transmission and distribution were optimized under one entity. A typical model of vertically-integrated approach is the UC problem [97]. However, the UC problem remains one of the most investigated problems in the field of power system economics as the US-style markets, i.e. markets operated by an Independent System Operator, are centralized and operate under the UC framework.

UC is an optimization problem that determines the operational schedule of generating units during a given planning horizon, usually one day, with varying loads and generations under different generational, environmental and technical constraints with the aim of minimizing the operating costs [98]. It includes technical aspects and constraints of generation units such as generators' ramp constraints, minimum and maximum output limits, minimum run and off times, as well as economic aspects such as start-up and fuel costs as well as generation efficiencies. This problem is mathematically more complex than a LP as it includes a mix of integer (binary) and continuous variables, and it is usually referred to as MILP. With higher integration of RES in power system, new technologies are being investigated and adopted. In this sense, the usage of ES and TCSC devices is the focal point of this thesis. Energy storage can be considered as an asset optimized in a cost-effective manner and cannot affect the energy price. Under this assumption, an ES is called price-taker [99]. However, in case of large ES, it can affect electricity prices, acting as a price-maker. While energy storage can provide wide spectre of applications to the power system [100, 11], TCSC device enhances base-power flow and loadability of the series-compensated line. Also it reduces the short-circuit current due to ability of switching from the controllable-capacitance the controllable-inductance mode, thereby restricting the short-circuit current [58]. In this thesis the point of interest are models at the transmission system. Hence, a summary of operation models looking into different ES and FACTS operational aspects are presented in Table 2.5 and explained in the following subsections.

2.3.1.1 Deterministic unit commitment (DUC)

DUC models solve the problem of committing and dispatching production units to meet the expected load incorporating the forecasted production of RES. In order to increase flexibility of such power system affected by uncertainty, many formulations deal with introduction of energy storage models. Since the uncertainty is of main importance to deal with, *Zhou et al.* [102] propose multistage methods for solving the scheduling problem of thermal

Table 2.5: Unit commitment models classified according to application of ES and FACTS devices

Application	DUC	SUC	RUC	IUC	CC-UC
Energy arbitrage	[101, 102, 103]	[104, 105]	[106, 107]		[108, 109]
Balancing services	[110, 111, 112]	[111, 113, 114]		[110]	[108, 115, 116]
Virtual Inertia					[117]
Congestion/Imbalance	[101, 112, 103, 118]	[119]			
Criteria N-1	[120]	[105]			
Minimising Losses	[121]				

units and ES while ensuring solution robustness and nonanticipativity: explicit and implicit decision methods. Utilization of energy storage is also investigated in various environments, such as post-contingency corrective actions. *Almassalkhi et al.* [103] propose and demonstrate a three-level framework for coordinating day-ahead, near real-time and minute-by-minute control actions of conventional generating units and distributed energy storage. This approach shows the effectiveness both in terms of UC economics and operational reliability. Similarly, the utility energy storage in [101] reduces the overall operating costs by performing arbitrage and corrective actions, thus reducing the spinning reserve needed to deal with contingencies. An interesting analysis is made by incorporating different policy aspects into the problems with conventional power generation units, such as emission and pricing the environmental impact. *Xia et al.* [121] incorporate this type of policy into the Economic Dispatch (ED) problem by using an emission function for each generator based on its power output, and a fixed cap on the total emissions of the steam units across all time periods. They also consider transmission losses and network flow constraints. As the integration of RES does not affect only transmission system but the distribution system as well, *Elliott et al.* [118] address the problem of sharing the energy storage capacity among transmission and distribution entities. It describes and demonstrates a method for coordinating the transmission-level congestion relief with local, distribution-level services in systems that lack centralized markets. Regarding the security of power system, energy storage is rarely investigated. *Guerrero-Mestre et al.* [120] presents a multiperiod probabilistic security-constrained UC that includes the probabilities of generation and transmission contingencies for optimal reserve sizing, sourcing, allocation, and activation. This formulation incorporates the ability of energy storage to provide the contingency reserve. In order to increase the utilization of each asset in the power system network, deterministic UC usually combines the day-ahead and the intraday operations [110, 111], additionally performing Transmission Switching (TS) in [112]. Transmission switching in combination with variable-impedance series FACTS devices can provide efficiency gains through controlling the power flows. As the system operators begin to utilize these tools, it is essential to understand the interdependence between them at various stages, i.e. planning and operation. Moreover, the results presented in [69] indicate that the cost savings achieved via combination of FACTS and TS can be substantially higher compared to an exclusive employment of either of the two technologies. The loadability of the power systems is utilised to quantify the impacts of FACTS devices to improving the security of system [122]. With approximation of the full AC network constraints and modelling accurately the non-linear nature of SVC and TCSC devices, more realistic operation solutions can be provided.

2.3.1.2 Stochastic unit commitment (SUC)

As the penetration of non-dispatchable resources increases, the total reserve cost in the power system increases. The formulation that deals with various levels of uncertainty is stochastic formulation, highly represented in literature. *Pozo et al.* [111] show that in systems with penetration of RES the total operational cost decreases by including storage units performing energy arbitrage. *Hreinsson et al.* [113] introduce a continuous time stochastic multistage reserve unit commitment. Compared to the conventional unit commitment formulation, the authors propose energy storage devices with limited energy capacity which address load uncertainty through a multi-variate scenario tree and models and through a piece-wise polynomial approximation as well as continuous-time changes in load and generation. The benefits of energy storage include smoothing of the load pattern by lowering on-peak and increasing the off-peak generation loads. Combination of energy arbitrage and N$-$1 contingency analysis is performed by a stochastic model [105] where the short-term profitability of energy storage is proved under different levels of renewable penetrations. Operational models of ES performing balancing services in stochastic environment are not sufficiently analyzed due to complexity issues. *Tang et al.* [114] evaluate the reserve provision ability of ES in six operation modes and show that by fully considering all these modes, the ESS indeed can provide up to 30-50% more reserves than the simplified models. Consequently, the fully utilization of ESS's flexibility in providing reserves and mitigating uncertainties are enabled.

2.3.1.3 Robust unit commitment (RUC)

RUC typically requires solving a bi-level optimization problem, where the outer level is a MIP, and the inner level is usually a bi-linear program. *Jurković et al.* [106] show that energy arbitrage of ES in such models provides lower operation costs than the cases that do not consider ES. The other application, such as load shifting, also contributes to a reduced operation cost [107]. With changing the values of the cost deviation factor, the system operators can adjust the degree of conservatism of the operation strategy against the load demand uncertainty [104].

The authors showed that the advancement of lithium-ion battery technology and reduced manufacturing cost decreases the battery degradation cost, and further increases the attractiveness of utilization of batteries in power system.

2.3.1.4 Interval unit commitment (IUC)

As mentioned before, the best utilization of energy storage in power system is in coordination with other assets. *Bruninx et al.* [110] propose coordination of ES and controllable generation in interval UC. The cost-effective regulating capabilities offered by the ES yield significant operational cost reductions in both models, while the increase in calculation times is limited.

2.3.1.5 Chance-constrained unit commitment (CC-UC)

CC-UC is another type of stochastic optimization problem that can deal with the random distributions of uncertain parameters [123]. While for other types of optimization methods some constraints cannot always be satisfied, for CC-UC the probabilities of meeting all or part of the inequality constraints are relaxed to preset levels lower than 1.0 [124]. Chance constraints have different confidence levels to limit the deviation of the actual power output. Due to its computation complexity it is a less attractive formulation. However, ES models have been investigated in this environment under few applications. The effect of the daily cycling on the battery degradation is proposed in [109]. *Chen et al.* [108] deal with both arbitrage and balancing services in order to achieve a reasonable trade-off between robustness and costs. A very similar problem is investigated in [115, 116], where the line flow limits are introduced as chance constraints in which power system reliability requirements are to be satisfied with a presumed level of high probability. Finally, under the chance-constrained formulation battery energy storage is investigated to provide inertia and primary reserve in [117].

2.3.2 Self-scheduling models

Energy storage progressively contributes to a competitive and secure electricity supply. Since it provides an economically interesting alternative to grid expansion and load shedding, it becomes very important in new market designs. Market mechanisms for flexibility and security of supply and specific storage regulation aim at establishing a competitive energy-storage-suitable market. Based on market time scale, the following classification applies i) long term contracts (up to years scale), ii) forward and future markets (up to weeks and months scale), iii) day-ahead market (the following day scale), iv) intraday markets (up to an hour scale), and to v) balancing markets (real-time scale).

There are differences in electricity market design across the world. For example, the US-style markets use Local Marginal Pricing (LMP) within each balancing authority area. LMPs reflect the price of electricity and cost of congestion and losses at different points across the network. These prices serve as instantaneous signals used by buyers and sellers in wholesale markets. They also give information to guide decisions on infrastructure investments, promote grid reliability and provide competitive markets from the most economic and reliable sources of power considering the network constraints [125].

European electricity markets have zonal market design, known as Market Coupling (MC) [126]. Market coupling uses uniform pricing within each bidding zone (represents national markets) and clears market-to-market interchanges within the Europe-wide day-ahead, and intraday energy markets, implicitly allocating transmission capacity between zones [127]. Recently, balancing markets are being coordinated in Europe by developing a framework for cross-zonal platform for activation of reserves [128]. The European balancing platforms also employ zonal network models [129].

In transition to a clean power system, both the US and European markets strongly work on incorporating the clean energy solutions. Their main tendency is to increase power system flexibility, which is one of the main characteristics of energy storage. ES in general can participate in many markets, especially batteries, which are due to their technological characteristics best-suited for markets close to real-time. This thesis brings up the overview of the day-ahead, intraday and balancing operational models. In the manner of ES role and behaviour in the market, ES can act as a price taker or a price maker. While acting as a price-taker, ES is considered as an asset being self-scheduled in a cost- effective manner and inable (due to its size) to affect market prices [99]. On the other side, if the capacity of an ES is not negligible as compared to the system size, the energy storage strategically competes and can affect the market prices. Such assumption defines a price-maker ES [130].

2.3.2.1 Market-based models classification − ES

Markets other than the balancing markets are cleared well in advance of energy delivery and thus the production and consumption levels scheduled in these markets can differ from the actual production and consumption. Many formulations try to respond to the needs of the power system and in the same time maximize ES revenues. Some of them are presented in Table 2.6. The most common approach in mathematical programming for strategic ES is to employ duality theory or Karush-Kuhn-Tucker optimality conditions to reformulate the initial bi-level problem into a single-level problem [138]. Bi-level models are usually very complex. In the upper level the ES usually seeks for profit maximization, while the lower level simulates market clearing [56]. The basic approach uses deterministic values of all parameters. However, stochastic formulation in the bidding approach creates a more realistic position for ES, as it evaluates multiple scenarios. *Krishnamurthy et al.* [135] propose a stochastic formulation of a storage owner's arbitrage profit maximization problem under uncertainty in both the DA and the ID markets. As already mentioned, such approach helps storage owners assess the the economic viability of their asset. Furthermore, intraday trading of ES can also provide significant revenues. This refers mainly on developing the trading strategies in the continuous intraday market to exploit renewable sources with uncertain real-time production [136]. Very similar approach is the selection of the optimal sequence of orders that maximizes its revenues over the entire trading horizon. It shows the ability of the agent to learn an optimal policy that results in higher revenues [137].

A significant point affecting the economic viability of a battery storage is its level of degradation. This feature is present both when performing energy arbitrage and ancillary services. *Padmanabhan et al.* [131] presents battery storage operational cost function model considering degradation cost, based on depth-of-discharge rate. The model seeks to maximize the battery's economic cost in both the day-ahead and the balancing markets, as well as to ensure technical benefits for the transmission system operator.

Pandžić et al. [132] propose ES to be as part of a virtual power plant in day-ahead market as price taker, while in the balancing market it serves as an asset helping with a correction of the whole energy deviations with respect to its day-ahead schedule.

From the strategic point of view, there are few stohastic bi-level optimization models that aim to determine the pool strategy of a price-maker storage system in both the day-ahead and the balancing markets, while considering net load uncertainty [134]. *Nasrolahpour et al.* [133] propose an ES strategic model in all markets and explain how strategic decisions in multiple markets are dependent on each other.

Table 2.6: Market-based models classified according to application of ES and FACTS devices

	Deterministic	**Stochastic**
Day-ahead	[14, 56, 55, 131]	[132, 133, 134, 135]
Intra-day	[136, 137]	[135]
Balancing	[14, 133, 131]	[132, 133]

2.4 Planning Models in Transmission System Network

2.4.1 Classification of models

Expansion planning models usually solve problems on how the power system, generation and transmission evolve over a long time horizon. It is usually based on optimization techniques that minimize the net present value of operating and investing in new capacity units, or maximizing specific entity's profits to meet the load [139]. The thesis incorporates TEP models which resolve the optimal expansion or reinforcement of an existing electricity transmission network. Hence, the overview represents TEP models that considers ES [140] and TCSC devices.

2.4.1.1 ES investment models

Since the TEP models are highly complex, they usually incorporate a decomposition technique. *Xu et al.* [141] implement a primal decomposition and a subgradient-based cutting-plane method in order to present a bi-level formulation that optimizes the location and size of energy storage systems which perform energy arbitrage and provide regulation services. They show that the profitability of investments in energy storage by enforcing a rate-of-return constraint is possible in such models. The sensitivity of these siting decisions has been studied with respect to different ES technologies, the rate-of-return on ES investments, and regulation market policies. The results indicate that increasing the rate-of-return requirement greatly reduces the deployment of ES. Similar, but with an addition of sensitivity analyses on the price of carbon emissions, *Olsen and Kirschen* [142] show that a carbon price affects the ES investment decisions to high extent. With higher integration of RES, the uncertainty level in power systems becomes more serious. In order to deal with such level of uncertainly, *Nikoobakht et al.* [143] propose an interval-based robust optimization model to investigate the best location for ES in the transmission network while providing fast ramping capability to mitigate wind power uncertainty. In such models, due to still high investment costs of ES, it is of great importance to know both the power and energy ratings of the storage units distributed across a transmission network [144]. Thus, the TEP models that include ES deal with spatio-temporal energy arbitrage, and determining both the optimal sites and energy-to-power ratios [145]. Among other applications, battery ES can also improve power system oscillation damping [146]. *Nasrolahpour et al.* [147] propose a bi-level model for strategic sizing of a storage facility considering market uncertainties. The upper-level problem models the planning and operation decisions of the storage facility. Bids/offers in terms of both the price and the quantity, are strategically made in the upper-level problem.

Finally, the most complex formulation of TEP models are multilevel models, such as trilevel models. Multilevel optimization problems are mathematical models which have a subset of their variables constrained to be an optimal solution of other models parameterized by their remaining variables. As pure mathematical programs deal with bi-level programing, tri-level programing results when the lower-level problems are bi-level models themselves [148]. In this manner, *Pandžić et al.* [149] propose a tri-level model where the upper-level problem optimizes the system operator's transmission line and energy storage investments, the middle-level problem determines the merchant energy storage investment decisions, while the lower-level problem simulates the market clearing process for representative days. Similarly, *Dvorkin et al.* [150] present co-optimize merchant the electrochemical storage siting and sizing problem with centralized transmission expansion planning problem. The upper level takes the merchant storage owner's perspective and aims to maximize the lifetime profits of the storage, while ensuring a given rate-of-return on investments. The middle level optimizes the centralized decisions on transmission expansion, while the lower level simulates market clearing. The proposed model is recast as a bi-level equivalent, which is solved using the column-and-constraint generation technique. From a system perspective, co-planning of storage and transmission expansion achieves greater operating cost savings than solely the deployment of storage. Finally, the rated power, capacity, charging-discharging regime, and initial energy for all storage levels were set in a three-level stochastic planning by *Hemmati et al.* [151]. The proposed model shows the benefit of minimization of the total energy cost in the network after investment in ES.

2.4.1.2 TCSC investment models

Determination of optimal locations and compensation levels of FACTS devices has been extensively researched. The mathematical formulations of such devices are originally nonlinear and non-convex, and according to that various methods have been proposed to solve the FACTS allocation problem. Since this thesis includes series-variant impedance FACTS devices, the overview of the planning models including TCSC are presented below. These models are based on AC OPF models linearized in order to preserve computation feasibility.

Ugranli and Karatepe [152] propose a TEP model for optimal reactive power planning as well as for the allocation of TCSC devices coordinated to minimize the investment in transmission lines, reactive power sources, and TCSC devices along with the sum of the generation costs and load curtailment penalties. The model is formulated using a linearized AC power flow equations. Due to a possibility of TCSC to alter power flows, all the lines equipped with it should be monitored for thermal flow violation to ensure TCSC injections remain within the device's reactance control range [153]. Additionally, the coordination of few FACTS devices results in a better utilization of power flows in the grid. In that manner, *Alhasawi and Milanovic* [154] propose a TEP model that coordinates both the TCSC and the SVC devices in a transmission network to facilitate wind power integration. The objective function takes into account the cost of generated active and reactive power, the cost of wind power integration and the cost of allocated FACTS devices for a range of operating conditions for several load growth profiles and over the lifetime of the FACTS devices. The model successfully identifies the congested areas and provides financial gains.

Besides the deterministic formulation, stochastic formulations in TEP TCSC models have also been studied. *Zhang et al.* [66] present a bi-level optimization model that seek to optimally allocate Variable Series Reactor (VSR) and Phase Shifting Transformer (PST) under a high level of renewable production using a decomposition technique. The objective function in the upper level minimizes the investment of series FACTS, the cost of wind power curtailment and possible load shedding. The disadvantage of this model is that ignores power losses and reactive power in the network. For more detailed voltage and angular stability limits analysis, the obtained FACTS locations need to be deeply evaluated by using a full AC power flow model. In that manner, *Ziaee and Choobineh* [155] formulate a mixed-integer nonlinear model and propose a novel decomposition procedure for determining the optimal location of TCSCs and their size. In order to obtain an effective solution, Benders' decomposition is used. One of the interesting insights of the presented research is that the computation time and the number of allowed TCSCs in the system are not in a direct relationship.

2.4.2 Benders decomposition

As shown in the overview of the TEP models, the resulting complex models are non-linear and non-convex and thus need to be decomposed to reduce the computational time. One of the most well-known decomposition techniques is the Benders' decomposition [156]. It is an iterative approach that is generally used in formulations with complicating variables. Since this thesis incorporates formulation of the Benders decomposition in the developed investment model, this section presents the initial problem structure and presents overview of such models.

2.4.2.1 Problem structure

The initial problem structure is as following [156]:

$$\text{Minimize} \quad \sum_{i=1}^{n} c_i \cdot x_i + \sum_{j=1}^{m} d_j \cdot y_j \tag{2.11}$$

subject to:

$$\sum_{i=1}^{n} a_{li} \cdot x_i + \sum_{j=1}^{m} e_{lj} \cdot y_j \leq b^{(l)} \quad l = 1,...,q \tag{2.12}$$

$$0 \leq x_i \leq x_i^{\text{up}} \quad i = 1,...,n \tag{2.13}$$

$$0 \leq y_j \leq y_j^{\text{up}} \quad j = 1,...,m \tag{2.14}$$

where $x_i (i = 1,...,n)$ are complicating variables.

Since complicating variables commonly make the problem statement (2.11)–(2.14) highly intractable, by fixing them the problem becomes possible to solve in an effective manner. The alternative solution is decomposed into the following structure:

$$\text{Minimize} \quad \sum_{i=1}^{n} c_i \cdot x_i + \alpha(x_1,...,x_n) \tag{2.15}$$

subject to:

$$0 \leq x_i \leq x_i^{\text{up}} \quad i = 1,...,n \tag{2.16}$$

where

$$\alpha(x_1,...,x_n) = \text{Minimize} \sum_{j=1}^{m} d_j \cdot y_j \tag{2.17}$$

subject to:

$$\sum_{j=1}^{m} e_{lj} \cdot y_j \leq b^{(l)} - \sum_{i=1}^{n} a_{li} \cdot x_i \quad l = 1,...,q \tag{2.18}$$

$$0 \leq y_j \leq y_j^{\text{up}} \quad j = 1,...,m \tag{2.19}$$

where $\alpha(x_1,...,x_n)$ is the function that provides the optimal objective function value of the problem (2.18)–(2.19) for given values of the complicating variables $x_1,...,x_n$. The execution of such structure is possible due to convex construction of function $\alpha(x_1,...,x_n)$.

The application to the expansion models is to decompose the initial non-linear and intractable problem into a master problem, which contains complicating variables (investment decision variables), and subpoblems, where these complicating variables are fixed in order to execute the operational model. The master problem in these formulations usually presents the planning stage, where investment variables are obtained in order to minimize the investment costs. After the optimization of the master problem, the decision investment variables are fixed for the operation stage where the optimization problem minimizes the operation costs in order to set the most economically effective operation points for generators in the given power system (includes the new assets from the master problem). The connection between these two stages is achieved through Benders cuts, which consider the subproblems' sensitivities and add new constraints to the master problem in each iteration.

Benders' decomposition is extensively used in the security-constrained UC problems [101, 157, 120, 119] as well as chance-constrained UC [108]. The incorporation of Benders' decomposition is also widely used in strategic siting and sizing of energy storage. *Nasrolahpour et al.* [147] propose a stochastic bi-level optimization problem which is converted into a computationally tractable formulation using an iterative approach of the Benders' decomposition. Similar behaviour introduces a need for decomposition in TCSC optimization problems [155, 66], but these types of problems are not much studied in the literature.

Chapter 3

Main Scientific Contribution of the Thesis

The focus of the thesis is to develop operational and planning optimization models using flexible assets while aiming to increase the flexibility of the power system. The first part of the thesis represents unit commitment and self-scheduling operational models by assessing the benefits energy storage and continuous serial compensation of power lines (TCSC devices). The second part of the thesis develops an expansion planning algorithm for optimal allocation and sizing of flexible and traditional options i.e. transmission power lines. Finally, with regards to the the achieved scientific contribution of the research, the following section briefly describes them both:

1. **Optimization model of power system operation including energy storage and continuous serial compensation of power lines**
   In general, the main objectives of power system operation are safety, reliability and efficiency. While the safety and reliability are considered to be primary, the efficiency of the power system operation is becoming increasingly important. In that manner, I develop a comparison of the operational pattern of an energy storage in a deregulated market environment within a vertically integrated utility (equivalent to the US-style markets) for different levels of wind integration. The system operator in a deregulated market has less power over the system resources and commitment as the dispatch decisions are a result of the market clearing procedure. In this setting, the ES owner aims at maximizing its profit, which might not be in line with minimizing overall system operating costs or maximizing social welfare. On the other side, the main feature of a vertically integrated utility (or US-style markets) is centralized decision-making process (usually modeled through the unit commitment formulation). All the investment and operating decisions are made with a single goal of minimizing the overall system operating costs. The novelty of this contribution is the integration of both the energy storage and TCSC devices in which they

are operated in a way that optimizes the cost-efficient operation of the power system.

2. **Algorithm of transmission expansion including investment options in new lines, energy storage and serial compensation based on optimization model with AC OPF and Benders decomposition**

   With progression integration of renewable energy sources, the main stress is placed on increasing the power system flexibility – the possibility of efficiently accommodating the uncertainties in the power system. The thesis proposes an investment model that finds an optimal mix of transmission-level non-generation flexible assets: battery energy storage (BES), thyristor-controlled series compensators (TCSC), and the traditional option – transmission lines. Role of BES is to offset renewable generation in time, but its power converter is additionally utilized to provide voltage regulation by injecting/withdrawing reactive power. TCSC is used to alter power flows and increase the existing lines' capacity, while new power lines are used to increase bulk power transfer. The proposed planning model uses linearized AC OPF and employs Benders' decomposition to develop an iterative procedure for obtaining the optimal solution. Besides the model itself, two novelties are introduced. First, dynamic operation of TCSC is modeled in a mixed-integer linear fashion (the models in the existing literature are nonlinear). Dynamic TCSC operation means that the compensation value of TCSC is actively adjusted at each operating time period between zero and the installed compensation capacity. Second, the BES is not only used to inject or withdraw active power by discharging or charging the battery, which is customarily in the literature, but its AC/DC converter is also used to inject or withdraw reactive power, thus affecting the network voltage levels. This adds another stream of value to the BES installation that has so far been ignored in the literature.

Chapter 4

Overview of Scientific Work of Thesis

4.1 List of Scientific Qualification Articles

The main scientific publications, both journal and conference ones, related to the thesis are listed below.

4.1.1 Journal publications

[Article 1] Luburić, Zora; Pandžić, Hrvoje; Plavšić Tomislav, "Assessment of energy storage operation in vertically integrated utility and electricity market" Energies 10, no. 5 (2017): 683. DOI: https://doi.org/10.3390/en10050683

[Article 2] Luburić, Zora; Pandžić, Hrvoje, "FACTS devices and energy storage in unit commitment" International Journal of Electrical Power Energy Systems 104 (2019): 311-325. DOI: https://doi.org/10.1016/j.ijepes.2018.07.013

[Article 3] Luburić, Zora; Pandžić, Hrvoje; Carrión, Miguel, "Transmission Expansion Planning Model Considering Battery Energy Storage, TCSC and Lines Using AC OPF" IEEE Access, vol. 8, pp. 203429-203439, 2020, DOI: 10.1109/ACCESS.2020.3036381.

4.1.2 Conference publications

[Conference 1] Luburić, Zora; Pandžić, Hrvoje; Carrión, Miguel; Plavšić Tomislav, "Valuation of Energy Storage Operation in an AC Power Flow Model" // In 2018 IEEE International Conference on Environment and Electrical Engineering and

2018 IEEE Industrial and Commercial Power Systems Europe (EEEIC/ICPS Europe), pp. 1-6. IEEE, 2018. DOI: 10.1109/EEEIC.2018.8493859

[Conference 2] Miletić, Marija; Luburić, Zora; Pavić, Ivan; Capuder, Tomislav; Pandžić, Hrvoje; Andročec, Ivan; Marušić, Anton, "A Review of Energy Storage Systems Applications" // 11th Mediterranean Conference on Power Generation, Transmission, Distribution and Energy Conversion (MEDPOWER 2018), Dubrovnik, Croatia, 2018. 94-6. DOI: 10.1049/cp.2018.1926

4.2 Author's Contributions to the Publications

The results presented in this thesis are based on the research carried out during the period from year 2016 to 2020 at the University of Zagreb Faculty of Electrical Engineering and Computing, Department of Energy and Power Systems (Unska 3, 10000 Zagreb, Croatia) under the guidance of supervisor Assoc. Prof. Hrvoje Pandžić, PhD. The work was mostly carried out within the research project "SIREN - Smart Integration of RENewables" funded by the Croatian Transmission System Operator (HOPS) and the Croatian Science Foundation under grant number I-2583-2015.

Additionally, significant work was performed during a research exchange visit at the University of Castilla-La Mancha, School of Industrial Technical Engineering in Toledo, Spain during the winter semester of the academic year 2017/2018 in collaboration with Prof. Miguel Carrión.

The thesis includes five publications written in collaboration with coauthors of the published papers.

[Article 1] In journal paper "Assessment of energy storage operation in vertically integrated utility and electricity market" [158], the author performed experiments and prepared the literature review. Mathematical formulation was designed by the supervisor Prof. H. Pandžić, while the author modeled the optimization models in GAMS. Furthermore, the author participated in defining scenarios, as well as discussions on the results and model implications. All graphic design of results are performed in MATLAB.

[Article 2] In journal paper "FACTS devices and energy storage in unit commitment" [159], the author and the supervisor conceived, designed and performed the optimization framework for unit commitment. The author modeled the optimization models in GAMS. The author processed the results and discussed them with the coauthors. All graphic design of results are performed in MATLAB.

[Article 3] In journal paper ”Transmission Expansion Planning Model Considering Battery Energy Storage, TCSC and Lines Using AC OPF” [160], the author developed the optimisation methodology for incorporating ES, series compensation (TCSC) and traditional reinforcement into transmission planning practice under the iterative approach of the Benders' decomposition. The author and the supervisor conceived and designed the experiments. The author also prepared the literature overview and modeled the optimization models in GAMS. Processing of results and paper writing was also mostly performed by the author. All graphic design of results are performed in MATLAB.

[Conference 1] In conference paper ”Valuation of Energy Storage Operation in an AC Power Flow Model”, the author developed the optimization problem and made literature review. Together with other authors, the author contributed with designing the case study. The author wrote the paper and discussed and altered the simulation in accordance to the co-authors' inputs.

[Conference 2] In conference paper ”A Review of Energy Storage Systems Applications”, the author, along with other authors, contributed with preparing and discussing the extensive literature review.

Finally, all proposed papers are presented in Chapter 6 as their final published versions.

Chapter 5

Conclusion and Future Directions

The first part of the presented doctoral research was to develop a framework that finds the most economical solution to the energy storage operation problem considering thyristor-controlled series compensators while minimizing the power system costs at the transmission level. This resulted in an evolution of such model published in journal papers ”Assessment of energy storage operation in vertically integrated utility and electricity market” and ”FACTS devices and energy storage in unit commitment”. Consequently, the following contribution was achieved: Optimization model of power system operation including energy storage and continuous serial compensation of power lines.

The second goal of the research was to develop a transmission expansion planning algorithm for optimal siting and sizing of energy storage, TCSC devices, and new power lines using linearized AC OPF and Benders' decomposition. This resulted in obtaining two novelties, i.e. a dynamic operation of TCSC device and reactive power control provided by ES. TCSC compensation value is actively adjusted at each operating time period between zero and the installed compensation capacity. The algorithm was published in journal paper ”Transmission expansion planning model considering battery energy storage, TCSC and lines using AC OPF”, resulting in the following contribution: Algorithm of transmission expansion including investment options in new lines, energy storage and serial compensation based on optimization model with AC OPF and Benders decomposition.

Both parts of the contribution render very important results in the field of operation and planning of energy storage, TCSC devices, and transmission lines. The comparison analysis of two different operational model structures shows that energy storage can obtain benefits in both formulations while performing arbitrage. System-level savings due to ES are in close correlation to the level of variable electricity generation from renewable sources. The higher level of uncertainty generally provides increased benefits both to the system and to the energy storage owner. One of the indicators of a positive effect on the overall system are reduced wind curtailment and, consequently, better utilization of low carbon technologies. On the other side, introduction of TCSC devices into unit commitment impacts the capability and the capacity of the transmission network and optimizes its utilization with respect to the production from RES. While separately both devices are efficient at reducing the number of committed generating units, the highest reduction in the number of committed generating units is achieved in the case of their coordinated operation. Finally, arbitrage-only profits of ES are insufficient to justify its investment. Therefore, multiple streams of revenue need to be stacked to justify investment in ES, at least considering its current investment costs. With this in mind, future research can be directed toward the modeling and utilization of stacked services of energy storage and exploring the benefits both from the power system and the ES owner's perspective. Since the developed operational models only consider deterministic approach, the future intention should focus on considering uncertainty and providing sensitivity analysis.

Regarding the second part of the contribution, an exhaustive analyses was conducted and important conclusions were derived from the proposed investment algorithm that chooses between flexible options such as ES and TCSC devices, and transmission power lines as the traditional option. This research also provides insights on both the ES and TCSC impact on relevant network parameters, such as voltage, reactive power and network losses. The voltage magnitudes are slightly decreased at buses after installation of TCSC, but increased in periods of low consumption and increased reactive power flows during the night. Additionally, ES provides reactive power support instead of only active power control. Reactive power is controlled by the ES converter to reduce the overall reactive power flows and losses in the surrounding network while preserving voltage deviations within a given range. The results of the case study indicate that for the current prices of ES and TCSC, the investment in new lines is still the most attractive option. However, for lower ES costs assumed in the future, the model results in ES installations at multiple buses, reducing the wind curtailment, but also taking part in voltage control. Investment in TCSC is less attractive and yields lower returns than the investment in new lines. However, it also complements the ES and can come in handy at locations where installation of new lines is not possible.

Besides the energy arbitrage and voltage support, energy storage can provide many other applications. Thus, the focus of future research should be on investigating the role and benefits of ES providing balancing services from both the owner's and the power system operator's perspective. New frameworks are required for developing models that consider the uncertainty and awareness of reserve activation to ensure both a more economic operation of ES and preserve reliability of the power system.

Chapter 6

Publications

Article 1 - Assessment of Energy Storage Operation in Vertically Integrated Utility and Electricity Market

Luburić, Zora; Pandžić, Hrvoje; Plavšić Tomislav, "Assessment of energy storage operation in vertically integrated utility and electricity market" Energies 10, no. 5 (2017): 683.
DOI: https://doi.org/10.3390/en10050683

– 16 pages

energies

MDPI

Article

Assessment of Energy Storage Operation in Vertically Integrated Utility and Electricity Market †

Zora Luburić [1,*], Hrvoje Pandžić [1] and Tomislav Plavšić [2]

1 Faculty of Electrical Engineering and Computing, University of Zagreb, Unska 3, Zagreb 10000, Croatia; hrvoje.pandzic@fer.hr

2 Croatian Transmission System Operator Ltd., Kupska 4, Zagreb 10000, Croatia; tomislav.plavsic@hops.hr

* Correspondence: zora.luburic@fer.hr; Tel.: +385-01-6129-986

† This paper is an extended version of our paper published in Luburić, Z.; Pandžić, H.; Plavšić, T. Comparison of Energy Storage Operation in Vertically Integrated and Market-Based Power System. In Proceedings of the IEEE International Conference on Environment and Electrical Engineering 2016, Florence, Italy, 7–10 June 2016.

Academic Editor: Rodolfo Araneo

Received: 15 February 2017 ; Accepted: 10 May 2017; Published: 12 May 2017

Abstract: The aim of this paper is to compare the operational pattern of an energy storage system (ESS) in a vertically-integrated utility and in a deregulated market environment for different levels of wind integration. As the main feature of a vertically-integrated utility is a centralized decision-making process, all of the investment and operating decisions are made with a single goal of minimizing the overall system operating costs. As a result, an ESS in such an environment is operated in a way that is optimal for the overall system economics. On the other hand, the system operator in a deregulated market has less power over the system resources, and commitment and dispatch decisions are a result of the market clearing procedure. In this setting, the ESS owner aims at maximizing its profit, which might not be in line with minimizing overall system operating costs or maximizing social welfare. To compare the ESS operation in these two environments, we analyze the storage operation in two different settings. The first one is a standard unit commitment model with the addition of centrally-controlled storage. The second one is a bilevel model, where the upper level is a coordinated ESS profit maximization problem, while the lower level a simulated market clearing. The case study is performed on a standardized IEEE RTS-96 system. The results show a reduction in the generation dispatch cost, online generation capacity and wind curtailment for both models. Moreover, ESS significantly increases social welfare in the market-based environment.

Keywords: energy storage; unit commitment; mixed-integer linear programming; day-ahead electricity market

1. Introduction

Electric power systems worldwide are experiencing a decarbonization process, which results in high installed capacity of renewable energy sources (RES). The majority of the RES capacity is installed in China (145 GW), the USA (74.5 GW) [1] and the EU, where Germany (45 GW) and Spain (23 GW) [2] are the major investors. This huge RES capacity may cause difficulties for transmission system operators (TSOs) in running the system in a secure and cost-effective manner. Some of the issues RES can cause include questionable predictability of the RES output, its volatility, i.e., sudden and severe changes in output, and decreased capacity of controllable units in operation. Fabbri et al. [3] used a general probabilistic methodology to calculate the cost of wind power prediction error. The results indicate that the cost of the prediction error reduced wind power plant income by 10%. However, it was also concluded that the time horizon for prediction should be decreased and energy should be sold closer to the real-time operation. In a similar context, Ortega-Vazquez et al. [4] presented the impact of an increasing level of wind power on the whole power system costs, such as dispatch cost, start-up cost, emission cost and cost of losing load. Results showed how small changes in the forecasts had a negative effect on the stability of the power system since they were compared to the ideal case of the forecasts. In that case, the actual wind power generation could not be penetrated, and wind needs to be spilled.

The large installed wind power capacity enables wind power producers to impact the market prices. Baringo et al. [5] proposed a stochastic mathematical program in which a wind power producer acts as a price-maker in the day-ahead market and as a deviator in the balancing market. Considering the balancing market at the day-ahead stage may increase the overall profit of a wind power producer. On the other hand, Zugno et al. [6] proposed a model in which the wind power producer participates as a price-taker in the day-ahead market and as a price-maker in the balancing market. Uncertainty of wind production is also modeled through scenarios. They showed that the improvement is between 1% and 3% as opposed to the non-strategic behavior. Furthermore, Delikaraoglou et al. [7] presented the strategic behavior of a wind power producer in both the day-ahead and the balancing market. Results presented a better position at the market as the day-ahead quantity offers were adjusted. However, the amount of the flexible capacity in the power system was increased.

Considering the imbalances in the real-time production, the authors of [8] investigate the effect of wind production on the power system in Northern Europe. They had simulated a model through five scenarios and concluded that the need for reserve capacity and its activation would have been greater if the installed capacity of wind increased over time. Moreover, the integration of the connecting areas is proposed since system balancing costs are lower in the case of fully-integrated markets.

Intermittent production of wind power plants made a case for energy storage investments. The most widespread energy storage technology is pumped-hydro power plants with over 150 GW of installed capacity, which accounts for 99% of the total energy storage capacity in the world [9]. However, other types of energy storage, e.g., solid state batteries, flow batteries, flywheels, compressed air energy storage and thermal storage, are being developed and implemented at various demonstration sites. Large-scale energy storage affords many benefits to the power system. It improves the reliability and stability of the transmission system, reduces congestion and curtailment of RES output, resulting in overall cost reductions. In this paper, we compare the operation of a power system with high penetration of RES combined with bulk energy storage system (ESS) in two different environments: the operation of ESS is under the control of a vertically-integrated power utility in a regulated environment and when ESS is an independent asset in a deregulated market environment [10].

Pozo et al. in [11] propose a stochastic real-time unit commitment introducing ideal and generic battery systems in order to assess their abilities to deal with the intermittency of renewable resources. Furthermore, the authors have compared this model with a deterministic unit commitment and showed a three-fold contribution of energy storage devices, (i) reducing the total power system operational costs; (ii) smoothing of the power generation profile and (iii) using energy storage in an auxiliary service acting as a reserve device.

Yan et al. in [12] model a large-scale energy storage system considering its power, capacity, maintenance time and ramp rate and implemented it in a modern power system consisting of a large quantity of wind farms. The economic dispatch is solved, and the results showed that the energy storage system can cause coupled power flow distribution on a daily basis, as well as that the load distribution of the wind turbine reduces the cost of power generation. A two-stage stochastic unit commitment model with storage is formulated by Li et al. in [13]. Its solution is used in the second stage to extract the flexible schedule for energy storage in economic dispatch with a limited time horizon. The results of using energy storage in the first stage show a reduction in wind curtailment, as well as load and reserve deficits. Furthermore, the non-flexibility of a fixed-schedule approach is established in the second stage, and the authors suggest to use the approach of the flexible operating range in the real-time dispatch for energy storage units due to higher cost savings.

Kyriakopoulos et al. in [14] explore issues, such as: the availability of renewable technologies now and in the following decades by type and policy and, also, possible problems in their implementations. The authors have discussed specific political initiatives, such as the Sustainable Development Goals and the Millennium Development Goals, and their inclusion into the development of electricity generation. Furthermore, different types of energy storage technologies have been investigated, as well as their applicability, operation and the economic side of implementation. Kyriakopoulos et al. in [15] propose an extensive four-fold overview based on worldwide utilization of renewable sources, global utilization of biomass for electricity production and general technology overview. The authors show the limitations and the challenges in a large-scale application of biofuel production. However, the main deficiencies can be problems with the transportation grid and machines with low utilization efficiency, causing great environmental pollution. The authors also highlight the importance of an economical approach in the determination of which type of renewable technology could have the main role in the modernized power system markets.

Sioshansi et al. [16] analyze a model that estimates the capacity value of energy storage in a power system with no transmission constraints. The results show that the capacity values of ESS are susceptible to energy prices and loss of load probabilities. Correspondingly, capacity values increase up to 40% due to the volatility of energy prices at peak hours and are significantly lower if the transmission constraints are included in the model. The authors also show that optimizing the siting of energy storage has a significant impact on the installed capacity. Wogrin et al. [17] present a DC model for optimizing technical aspects of storage and its operation in the transmission system. The results show that the distribution of storage units is affected by the needs of the network. Meneses de Quevedo et al. [18] propose a model to obtain the best location of ES devices under the intermittent production of wind power plants in a distribution network. Distribution of storage installations is considered by Pandžić et al. [19], as well, where the authors propose a three-stage planning procedure for bulk energy storage siting and sizing: optimal storage locations are determined in the first stage, storage capacities at the second stage, while the final stage verifies the quality of the obtained solution. The results show that the location and capacity of storage are correlated with the production of the wind power plants in the system. The profit of ESS depends on the variability of the local marginal prices (LMPs) in the grid. Dvorkin et al. [20] propose an expanded model for siting and sizing energy storage. This model analyzes the profitability for the owners of ESS and proposes a model that ensures the profitability of storage investment.

Hu et al. [21] investigate the operation of ESS for both peak-load shaving and reserve providing purposes. The authors conclude that both start-up and operation costs reduce as the capacity of ESS increases. However, ESS investment cost is not included in the objective function.

ESS integration is a great challenge in restructured electricity markets. This is because their investment costs need to be compared to the revenue they are able to collect. However, this revenue comes from multiple sources (day-ahead market, balancing market, reserves, capacity market, etc.), and every storage operation needs to be attributed to a specific purpose. Sioshansi et al. [22] analyze issues regarding the ESS ownership, identify barriers and propose policies for their removal. Some of the major energy storage applications are arbitrage, generation capacity investment deferral, ancillary services, contingency reserves, ramping, transmission and distribution deferral and renewable curtailment. Pandžić and Kuzle [23] propose a bi-level ESS profit maximization model, where ESS exercises arbitrage in the day-ahead market. The market prices are obtained from the market clearing simulation in the lower-level problem, while the ESS bidding decisions are made in the upper-level problem. The results show low profits from the arbitrage-only application, thus indicating that an ESS should act in other markets and provide other services as well in order to be profitable. On the other hand, Miranda et al. [24] analyzed the role of ESS in European market designs. They show that ESS is negatively correlated with the interconnections, because interconnection capacity reduces the market value of ESS. Furthermore, the integration of ESS is restricted because of their limited participation in the ancillary services.

With respect to the literature review above, the main contribution of this paper is a comparison between the ESS operation in a vertically- and market-oriented power system. We assess storage operation and profits, while analyzing the impacts on the operational aspects of the power system and market participants, i.e., generating units. This issue is very important, as there are still no clear property and operation rules for energy storage units.

2. Model Description

This section formulates two models that include ESS: (1) vertically integrated and (2) market–based power system. We presume a linear DC optimal power flow with no line losses.

2.1. Vertically-Integrated Power System

In a vertically-integrated power system, the objective is to minimize the overall operating costs of a power system. Thus, the objective function (1) minimizes overall generating costs, which are in (2) defined as the sum of the fixed, the variable and the start-up costs of all generators. Binary variable $x_i(t)$ indicates if generator i is online during time period t, while binary variable $y_i(t)$ indicates if generator i is started up during time period t. Expression (3) sets generator outputs to the sums of their cost curve segments. Generator minimum outputs are enforced in (4), while maximum output on each cost curve segment is limited in (5). Constraints (6) and (7) define generator binary variables' logic, which sets appropriate values to on/off, start up and shut down binary variables. The minimum up and down time of generators are enforced in (8)–(10).

$$\text{Minimize} \sum_{t=1}^{T} \sum_{i=1}^{I} C_i(t) \tag{1}$$

subject to:

$$C_i(t) = f_i \cdot x_i(t) + \sum_{c=1}^{C} o_{i,c} \cdot g_{i,c}(t) + start_i \cdot y_i(t) \quad \forall c \in C, i \in I, t \in T \tag{2}$$

$$g_i(t) = \sum_{c=1}^{C} g_{i,c}(t) \quad \forall c \in C, i \in I, t \in T \tag{3}$$

$$g_i(t) \geq g_i^{\text{min}} \cdot x_i(t) \quad \forall i \in I, t \in T \tag{4}$$

$$g_{i,c}(t) \leq g_{i,c}^{\text{max}} \quad : \gamma_{i,c}(t) \quad \forall c \in C, i \in I, t \in T \tag{5}$$

$$y_i(t) - z_i(t) = x_i(t) - x_i(t-1) \quad \forall i \in I, t \in T \tag{6}$$

$$y_i(t) + z_i(t) \leq 1 \quad \forall i \in I, t \in T \tag{7}$$

$$\sum_{t=1}^{V_i^{\text{up,min}}} (1 - x_i(t)) = 0 \quad \forall i \in I \tag{8}$$

$$\sum_{tt=t}^{t+g_i^{\text{up}}-1} x_i(tt) \geq g_i^{\text{up}} \cdot y_i(t) \quad \forall V_i^{\text{up,min}} + 1 \leq t \leq T - g_i^{\text{up}} + 1, i \in I \tag{9}$$

$$\sum_{tt=t}^{T} (x_i(tt) - y_i(t)) \geq 0 \quad \forall T - g_i^{\text{up}} + 2 \leq t \leq T, i \in I \tag{10}$$

Constraints (11)–(14) model the ESS operation. Equation (11) calculates the ESS state of charge, which is restricted in (12). Constraints (13) and (14) limit storage charging and discharging power. Simultaneous charging and discharging is disabled by binary variable $x_b^{\text{ch}}(t)$.

$$soc_b(t) = soc_b(t-1) + p_b^{\text{ch}}(t) \cdot \eta_b^{\text{ch}} - \frac{p_b^{\text{dis}}(t)}{\eta_b^{\text{dis}}} \quad \forall b \in B, t \in T \tag{11}$$

$$soc_b^{\min} \leq soc_b(t) \leq soc_b^{\max} \quad \forall b \in B, t \in T \tag{12}$$

$$p_b^{\mathrm{ch}}(t) \leq ch_b^{\max} \cdot x_b^{\mathrm{ch}}(t) \quad : \phi_b^{\mathrm{ch}}(t) \quad \forall b \in B, t \in T \tag{13}$$

$$p_b^{\mathrm{dis}}(t) \leq dis_b^{\max} \cdot (1 - x_b^{\mathrm{ch}}(t)) \quad : \phi_b^{\mathrm{dis}}(t) \quad \forall b \in B, t \in T \tag{14}$$

Constraint (15) is the power balance equation for each node. Equation (16) calculates power flows through all lines. Line limits are imposed by Constraints (17) and (18).

$$\sum_{w=1}^{W} k_w(t) + \sum_{b=1}^{B} p_b^{\mathrm{dis}}(t) + \sum_{i=1}^{I}\sum_{c=1}^{C} g_{i,c}(t) - \sum_{l=1|\{n,m\}\in l}^{L} pf_{n,m}^{-}(t) + \sum_{l=1|\{n,m\}\in l}^{L} pf_{n,m}^{+}(t) = d_n(t) + \sum_{b=1}^{B} p_b^{\mathrm{ch}}(t) \quad \forall n \in N, t \in T \tag{15}$$

$$pf_{n,m}(t) = sus_{n,m} \cdot (a_n(t) - a_m(t)) \quad : \beta_l(t) \quad \forall \{n,m\} \in L, t \in T \tag{16}$$

$$pf_{n,m}(t) \leq pf_{n,m}^{\max} \quad : \kappa_l^{\max}(t) \quad \forall \{n,m\} \in L, t \in T \tag{17}$$

$$pf_{n,m}(t) \geq -pf_{n,m}^{\max} \quad : \kappa_l^{\min}(t) \quad \forall \{n,m\} \in L, t \in T \tag{18}$$

2.2. Market-Based Power System

The market-based power system is characterized by multiple players with often opposing goals. In order to explore the profitability of ESS in the market environment, we formulate a bilevel program where the ESS owner seeks to maximize its profit pertaining to the objective function (19). The ESS makes a profit from the difference in the dual variable $\alpha_n(t)$, representing locational market prices (LMP) at nodes containing ESS, at different hours. ESS seeks to purchase electricity at low LMP and sell it at high LMP.

$$\text{Maximize} \quad \sum_{t=1}^{T}\sum_{b=1}^{B} \alpha_n(t) \cdot (p_b^{\mathrm{dis}}(t) - p_b^{\mathrm{ch}}(t)) \tag{19}$$

subject to:

$$(11), \quad (12) \tag{20}$$

$$\text{Maximize} \sum_{t=1}^{T} \Big(\sum_{n=1}^{N} \lambda_n^D \cdot d_n(t) + \sum_{b=1}^{B} \lambda_b^{\mathrm{ch}} \cdot p_b^{\mathrm{ch}}(t) - \sum_{i=1}^{I}\sum_{c=1}^{C} \lambda_{i,c}^G \cdot g_{i,c}(t) - \sum_{b=1}^{B} \lambda_b^{\mathrm{dis}} \cdot p_b^{\mathrm{dis}}(t) \Big) \tag{21}$$

subject to:

$$(5), \quad (13), \quad (14), \quad (16)-(18) \tag{22}$$

$$\begin{aligned} \sum_{w=1}^{W} k_w(t) + \sum_{b=1}^{B} p_b^{\mathrm{dis}}(t) + \sum_{i=1}^{I}\sum_{c=1}^{C} g_{i,c}(t) - \sum_{l=1|\{n,m\}\in l}^{L} pf_{n,m}^{-}(t) + \sum_{l=1|\{n,m\}\in l}^{L} pf_{n,m}^{+}(t) \\ = d_n(t) + \sum_{b=1}^{B} p_b^{\mathrm{ch}}(t) \quad : \alpha_n(t) \quad \forall n \in N, t \in T \end{aligned} \tag{23}$$

$$d_n(t) \leq d_n^{\max}(t) \quad : \chi_n(t) \quad \forall n \in N, t \in T \tag{24}$$

$$k_w(t) \leq K_w^{\max}(t) \quad : \vartheta_w(t) \quad \forall w \in W, t \in T \tag{25}$$

$$\theta_n(t) \leq \pi \quad : \mu_n^{\max}(t) \quad \forall n \in N \setminus n : \text{ref. bus}, t \in T \tag{26}$$

$$\theta_n(t) \geq -\pi \quad : \mu_n^{\min}(t) \quad \forall n \in N \setminus n : \text{ref. bus}, t \in T \tag{27}$$

$$\theta_n(t) = 0 \quad : v(t) \quad n : \text{ref. bus}, \forall t \in T \tag{28}$$

$$g_{i,c}(t) \geq 0 \quad \forall c \in C, i \in I, t \in T \tag{29}$$

$$k_w(t) \geq 0 \quad \forall w \in W, t \in T \tag{30}$$

$$d_n(t) \geq 0 \quad \forall n \in N, t \in T \tag{31}$$

Objective Function (19) is subject to the storage state of charge Constraints (11) and (12) and the market clearing model (21)–(31). The objective function of the market clearing model is to maximize social welfare, where ESS behaves as demand when charging and as generator when discharging.

The lower-level problem is subject to the generator block output limit (5), ESS charging and discharging Constraints (13) and (14), as well as power flow Constraints (16)–(18). Constraint (23) is the power balance constraint that includes renewable generation, ESS discharge, conventional generation, outbound flows, inbound flows, demand and ESS charging at each node, respectively. Constraint (24) limits demand per bus, while Constraint (25) limits renewable output per bus. Constraints (26)–(28) limit voltage angles and set the voltage angle of the reference bus to zero. Finally, Constraints (29)–(31) enforce non-negativity to generation, wind utilization and demand variables.

The bilevel problem (19)–(31) cannot be solved directly and needs to be reformulated as a mathematical problem with equilibrium constraints (MPEC). For this reason, we create the dual of the lower-level problem (32)–(43) and the strong duality equality (44).

$$\begin{aligned}\text{Minimize} \sum_{l=1}^{L}(\kappa_l^{\max}(t)-\kappa_l^{\min}(t))\cdot pf_l^{\max}+\sum_{i=1}^{I}\sum_{c=1}^{C}\gamma_{i,c}(t)\cdot g_{i,c}^{\max}+\sum_{n=1}^{N}\chi_n(t)\cdot d_n^{\max}(t)\\ +\sum_{b=1}^{B}\phi_b^{\text{dis}}(t)\cdot dis_b^{\max}\cdot x_b^{\text{dis}}(t)+\sum_{b=1}^{B}\phi_b^{\text{ch}}(t)\cdot ch_b^{\max}\cdot x_b^{\text{ch}}(t)\\ +\sum_{w=1}^{W}\vartheta_w(t)\cdot K_w^{\max}(t)+\sum_{n=1}^{N}(\mu_n^{\max}(t)-\mu_n^{\min}(t))\cdot\pi\end{aligned} \tag{32}$$

$$\alpha_{n(i)}(t)+\gamma_{i,c}(t)\geq-\lambda_{i,c}^{G}\quad\forall c\in C,i\in I,t\in T \tag{33}$$

$$-\alpha_n(t)+\chi_n(t)\geq\lambda_n^{D}\quad\forall n\in N,t\in T \tag{34}$$

$$\alpha_{n(b)}(t)+\phi_b^{\text{dis}}(t)\geq-\lambda_b^{\text{dis}}\quad\forall b\in B,t\in T \tag{35}$$

$$-\alpha_{n(b)}(t)+\phi_b^{\text{ch}}(t)\geq\lambda_b^{\text{ch}}\quad\forall b\in B,t\in T \tag{36}$$

$$\alpha_{n(w)}(t)+\vartheta_w(t)\geq 0\quad\forall w\in W,t\in T \tag{37}$$

$$-\alpha_{n(n(l))}(t)+\alpha_{n(m(l))}(t)+\beta_l(t)+\kappa_l^{\max}(t)-\kappa_l^{\min}(t)=0\quad\forall l\in L,t\in T \tag{38}$$

$$-\sum_{l=1|n(l)}^{L}sus_l\cdot\beta_l(t)+\sum_{l=1|m(l)}^{L}sus_l\cdot\beta_l(t)+\mu_n^{\max}(t)+\mu_n^{\min}(t)=0\quad\forall n\in N\setminus\text{ref. bus},t\in T \tag{39}$$

$$-\sum_{l=1|n(l)}sus_l\cdot\beta_l(t)+\sum_{l=1|m(l)}sus_l\cdot\beta_l(t)+v(t)=0\quad n=\text{ref. bus},t\in T \tag{40}$$

$$\alpha_n(t),\beta_l(t),v(t)\quad:\text{free variable}\quad\forall t\in T \tag{41}$$

$$\kappa_l^{\max}(t),\gamma_{i,c}(t),\chi_n(t),\mu_n^{\max}(t)\geq 0\quad\forall t\in T \tag{42}$$

$$\kappa_l^{\min}(t),\mu_n^{\min}(t)\leq 0\quad\forall t\in T \tag{43}$$

$$\begin{aligned}\sum_{n=1}^{N}\lambda_n^{D}\cdot d_n(t)+\sum_{b=1}^{B}\lambda_b^{\text{ch}}\cdot p_b^{\text{ch}}(t)-\sum_{i=1}^{I}\sum_{c=1}^{C}\lambda_{i,c}^{G}\cdot g_{i,c}(t)-\sum_{b=1}^{B}\lambda_b^{\text{dis}}\cdot p_b^{\text{dis}}(t)=\sum_{l=1}^{L}(\kappa_l^{\max}(t)-\kappa_l^{\min}(t))\cdot pf_l^{\max}\\ +\sum_{i=1}^{I}\sum_{c=1}^{C}\gamma_{i,c}(t)\cdot g_{i,c}^{\max}+\sum_{n=1}^{N}\chi_n(t)\cdot d_n^{\max}(t)+\sum_{b=1}^{B}\phi_b^{\text{dis}}(t)\cdot dis_b^{\max}\cdot x_b^{\text{dis}}(t)+\sum_{b=1}^{B}\phi_b^{\text{ch}}(t)\cdot ch_b^{\max}\cdot x_b^{\text{ch}}(t)\\ +\sum_{w=1}^{W}\vartheta_w(t)\cdot K_w^{\max}(t)+\sum_{n=1}^{N}(\mu_n^{\max}(t)-\mu_n^{\min}(t))\cdot\pi\quad\forall t\in T\end{aligned} \tag{44}$$

The final MPEC is:

$$\begin{gathered}(19)\\ \text{subject to}\quad(20),\quad(21)-(31),\quad(33)-(44).\end{gathered} \tag{45}$$

Linearization Using KKT Conditions

Objective Function (19) contains a non-linear product of the LMP variable $\alpha_n\ (t)$ and charging and discharging variables. We use some of the lower-level problem Karush–Kuhn–Tucker (KKT) conditions to rewrite the objective function in an equivalent linear way, similarly as in [23]. Since this linearization requires additional constraints, auxiliary variables $\phi_b^{\text{ch-}}(t)$ and $\phi_b^{\text{dis-}}(t)$ are used to implement the big M linearization method. Finally, non-linear objective Function (19) is replaced by its linear equivalent (46) and additional Constraints (47)–(50):

$$\begin{gathered}\text{Maximize} \sum_{t=1}^{T}\sum_{b=1}^{B}(\lambda_b^{\text{dis}} \cdot p_b^{\text{dis}}(t) - \lambda_b^{\text{ch}} \cdot p_b^{\text{ch}}(t) \\ +(\phi_b^{\text{dis}}(t) - \phi_b^{\text{dis}-}(t)) \cdot dis_b^{\max} + (\phi_b^{\text{ch}}(t) - \phi_b^{\text{ch}-}(t)) \cdot ch_b^{\max})\end{gathered} \tag{46}$$

$$-x_b^{\text{dis}}(t) \cdot M \le \phi_b^{\text{dis}}(t) - \phi_b^{\text{dis}-}(t) \le x_b^{\text{dis}}(t) \cdot M \quad \forall b \in B \tag{47}$$

$$-(1 - x_b^{\text{dis}}(t)) \cdot M \le \phi_b^{\text{dis}-}(t) \le (1 - x_b^{\text{dis}}(t)) \cdot M \quad \forall b \in B \tag{48}$$

$$-x_b^{\text{ch}}(t) \cdot M \le \phi_b^{\text{ch}}(t) - \phi_b^{\text{ch}-}(t) \le x_b^{\text{ch}}(t) \cdot M \quad \forall b \in B \tag{49}$$

$$-(1 - x_b^{\text{ch}}(t)) \cdot M \le \phi_b^{\text{ch}-}(t) \le (1 - x_b^{\text{ch}}(t)) \cdot M \quad \forall b \in B \tag{50}$$

Strong duality Constraint (44) also contains non-linear terms, i.e., multiplication of binary and continuous variables. Its linear equivalent is written below and requires the same linear constraints as (46).

$$\begin{gathered}\sum_{n=1}^{N}\lambda_n^D \cdot d_n(t) + \sum_{b=1}^{B}\lambda_b^{\text{ch}} \cdot p_b^{\text{ch}}(t) - \sum_{i=1}^{I}\sum_{c=1}^{C}\lambda_{i,c}^G \cdot g_{i,c}(t) - \sum_{b=1}^{B}\lambda_b^{\text{dis}} \cdot p_b^{\text{dis}}(t) = \sum_{l=1}^{L}(\kappa_l^{\max}(t) - \kappa_l^{\min}(t)) \cdot pf_l^{\max} \\ + \sum_{i=1}^{I}\sum_{c=1}^{C}\gamma_{i,c}(t) \cdot g_{i,c}^{\max} + \sum_{n=1}^{N}\chi_n(t) \cdot d_n^{\max}(t) + \sum_{b=1}^{B} dis_b^{\max} \cdot (\phi_b^{\text{dis}}(t) - \phi_b^{\text{dis}-}(t)) + \sum_{b=1}^{B} ch_b^{\max} \cdot (\phi_b^{\text{ch}}(t) - \phi_b^{\text{ch}-}(t)) \\ + \sum_{w=1}^{W}\vartheta_w(t) \cdot K_w^{\max}(t) + \sum_{n=1}^{N}(\mu_n^{\max}(t) - \mu_n^{\min}(t)) \cdot \pi \quad \forall t \in T\end{gathered} \tag{51}$$

3. Case Study and Results

Both of the proposed models are tested on a modernized IEEE RTS-96 system, as shown in Figure 1 [19], with wind power plants and ESS devices [23,25]. The case study network consists of three areas, where the first area contains nine wind farms (w1–w9) with overall capacity of 3900 MW; the second area contains six wind farms (w10–w16) with overall capacity of 2400 MW; and the third area contains three wind farms (w17–w19) with overall capacity of 300 MW. Although the test system is a generic IEEE network, the wind topography replicates the Electric Reliability Council Of Texas (ERCOT) system, where the power flows are directed from the west zone, with abundant wind generation, to the east zone, with large loads [26]. ESS units are connected to buses where the significant wind power is injected into the grid.

The test system contains 96 conventional generators (overall capacity 10,215 MW), 19 wind farms (overall capacity 6900 MW), two ESS units of 100 MW and 600 MWh each connected to Buses 120 and 202. Both charging and discharging efficiencies of ESS are 0.90. The initial and final ESS state of charge is 50%.

The generated wind output data are based on 10-min wind speed data applied to aggregated Vestas V90-3 MW wind turbines to obtain power outputs at locations in the western USA in the period of 2004–2006. These data are a part of the NREL's Western Wind dataset [27]. The dataset contains 32,043 sites, which are combined in order to signify the locations of large capacity wind farms connected at buses into the transmission network. The wind speed data from the database were first converted into the wind power data using the wind turbine power curve. The data from 2004–2005 were selected as input in the model, while the data from 2006 were used in the process of calibration. Similarly to [28], the first step is to normalize the wind speed data in a way that each point is subtracted by the average of the corresponding month, and the second step is to divide it by the standard deviation of the corresponding hour of the month. The following step is to obtain stationary Gaussian distributed series by the undesirable data with the empirical distribution function. These time series are fitted to normalized data, as elaborated in [19]. Every model is updated with a step of six hours in which data are used by the 120 most recent hours of wind data in 2006, and followed by each update, each model provides a new six-hour prediction. Following a scenario reduction technique from [29], we used four representative days from this dataset.

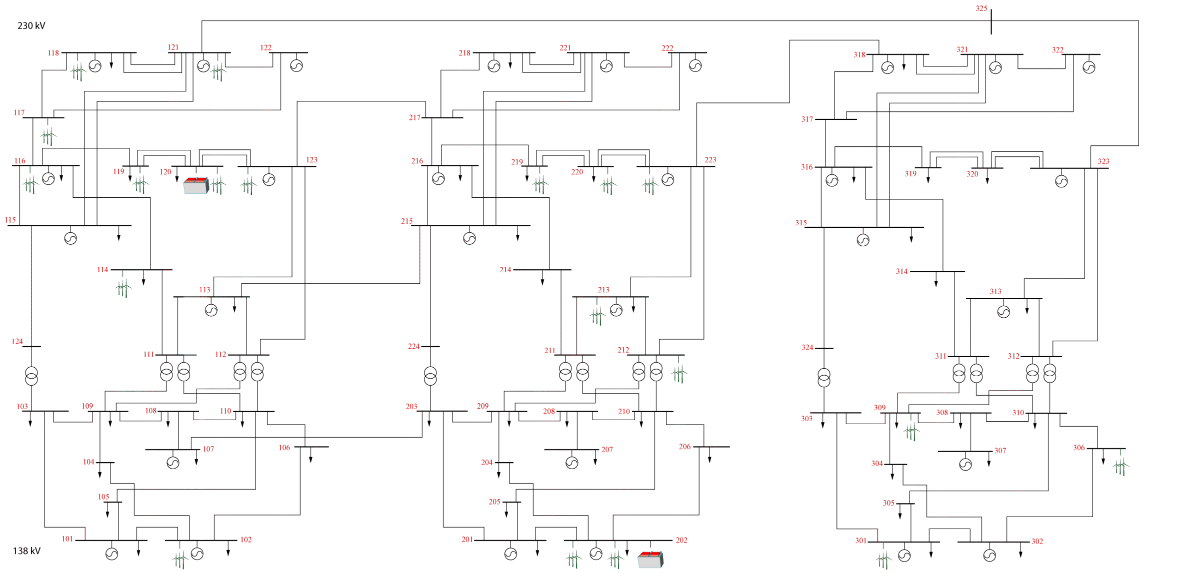

Figure 1. IEEE RTS network.

The production of wind farms is shown in Figure 2. We compare ESS performance for the following four cases: (1) high wind generation throughout the day; (2) low wind generation; (3) high wind generation in the second half of the day and (4) high wind generation in the first half of the day. Both models are tested on these four representative days.

3.1. Vertically-Integrated Power System

First, the model is tested without any ESS in order to determine the baseline result, which is compared to the results obtained with ESS in the system. The overall system cost with and without ESS is shown in Table 1 (last three rows). The presence of ESS brings savings in the range of 0.2–1.3%. The lowest savings are achieved on Day 2, which has the lowest wind output, while the highest savings are achieved on Day 1, which has the most wind. This indicates that ESS results in the highest operating cost savings on days with the most wind energy. ESS acts in a way to reduce wind curtailment. On Day 1, ESS operation reduces wind curtailment by 8.4% (last two rows in Table 2). On Day 2, due to low wind, there is no curtailment, even without ESS. Day 3 has very similar curtailment values of wind curtailment as Day 1, although the hourly distribution is different. Day 4 has lower wind curtailment than Day 1 and Day 3, and ESS operation reduces it by 9.3%.

Overall generation throughout the day changes in the presence of ESS. On the one hand, ESS reduces wind curtailment, which decreases the amount of electricity generators need to produce. On the other hand, ESS have round trip efficiencies that are lower than 100%. On Days 1, 2 and 4, the wind curtailment is greater than the electricity lost due to ESS inefficiency, resulting in decreased overall electricity produced by conventional generators (first two rows in Table 2). On Day 2, there is no wind curtailment, which means than any ESS activity increases the overall conventional electricity generation. ESS also affects the peak production of conventional generators. In all four cases, peak generation is reduced by 200 MW, which is the output capacity of ESS in the system (first two rows in Table 1). These results show the role ESS can have in the reduction of cycling of peaking units, but also in deferring generation capacity system-wide.

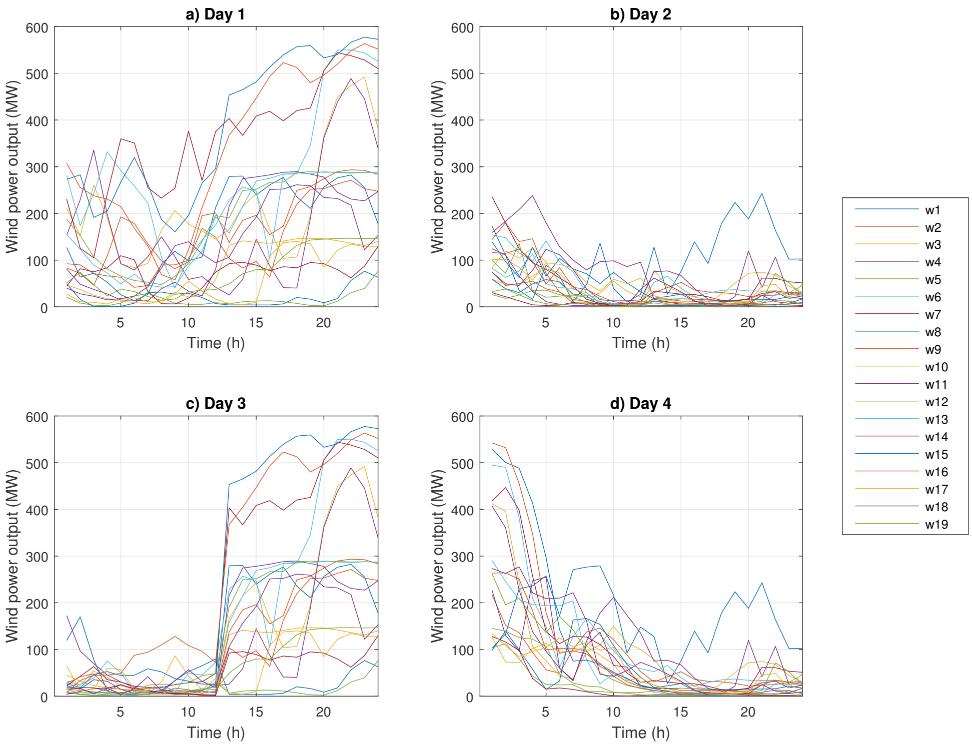

Figure 2. Wind production by 19 wind farms.

Table 1. Peak production and overall generation cost.

	Day 1	Day 2	Day 3	Day 4
Peak production of conventional generators with ESS (MW)	5436	6972	6598	6972
Peak production of conventional generators without ESS (MW)	5636	7172	6798	7172
Overall generation cost with ESS (€)	1,203,739	2,345,928	1,582,782	2,095,339
Overall generation cost without ESS (€)	1,219,185	2,351,232	1,599,738	2,111,110
Overall generation cost savings	1.3%	0.2%	1.1%	0.8%

Table 2. Overall daily production and wind curtailment with and without ESS in the vertically-integrated power system.

	Day 1	Day 2	Day 3	Day 4
Daily production of conventional generators with ESS (MWh)	79,436	132,381	97,189	119,067
Daily production of conventional generators without ESS (MWh)	79,861	132,229	97,561	119,515
Wind curtailment with ESS (MWh)	6568	0	6568	5828
Wind curtailment without ESS (MWh)	7168	0	7168	6428

Daily charging and discharging cycles of both ESS units during four representative days are presented in Figure 3. In all of the cases, both ESS are finished charging by Hour 7. On Day 1, ESS are fully discharged by Hour 11, when abundant wind output starts. High wind output supplies most of the load during the afternoon. Evening reduced load hours are used to charge the ESS to the requested 50% state of charge. Low wind output is used to fully charge ESS in the early hours of Day 2 (the maximum state of charge of ESS is 540 MWh, due to charging efficiency). Approximately 300 MWh is discharged from each ESS in 17–19 to reduce the running of peaking units for supplying the high evening load. The last hour is used for recharging ESS to the required 50% of state of charge. On Day 3, ESS are fully charged by the morning, and they discharge during the morning peak hours due to scarce wind production. Abundant wind power in the later hours is used to supply the evening peak consumption and to charge ESS. Day 4 operation of ESS is very similar to Day 2. Part of the copious wind generation in the early hours is used to charge ESS, but most of it is curtailed due to low consumption. ESS are discharge in the late afternoon and evening to reduce the impact of high-cost peaking units.

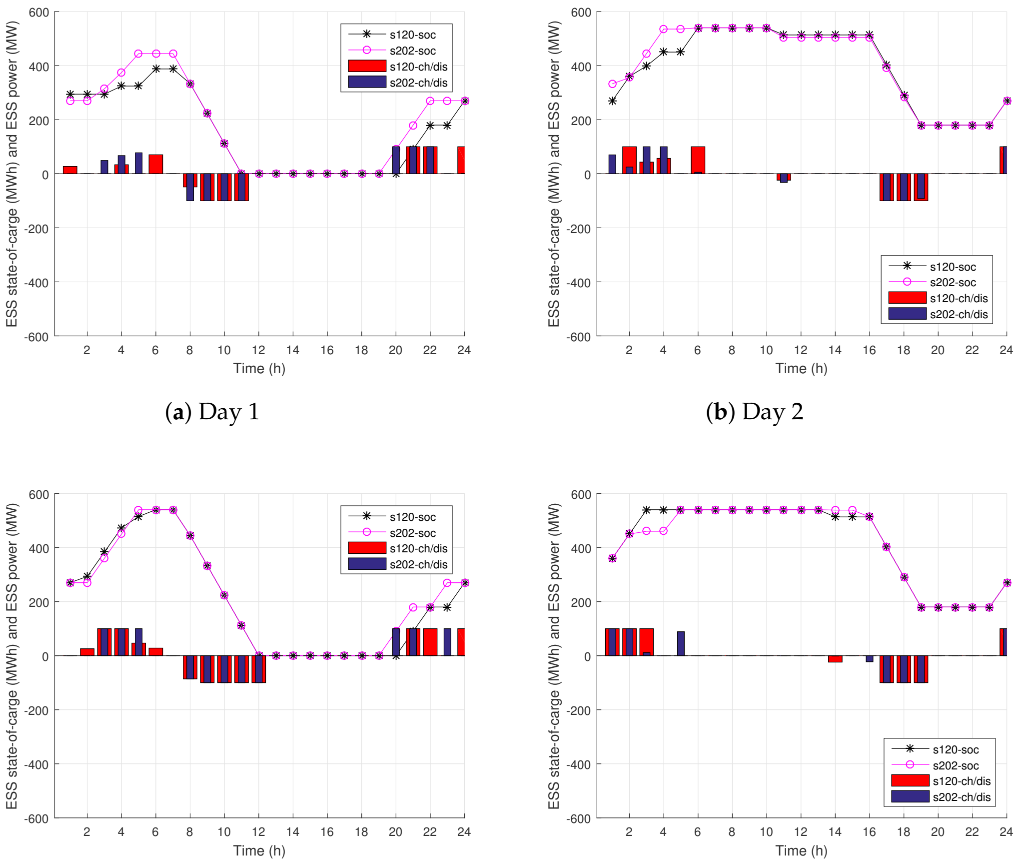

(**a**) Day 1 (**b**) Day 2

(**c**) Day 3 (**d**) Day 4

Figure 3. ESS operation in the vertically-integrated power system.

3.2. Market-Based Power System

The goal of the market-based model is to maximize the overall ESS profit. The overall ESS profit for each of the four days is shown in Table 3. ESS profit highly depends on the wind profile. Day 2, where wind generation is low throughout the day, provides very limited profit opportunities for ESS, resulting in only a 2272 € profit. Figure 4b shows a rather flat LMP profile at Buses 120 and 202. Day 1, on the other hand, has high wind generation throughout the day and results in much higher ESS profit. Figure 4a shows much higher variability of LMPs at both ESS buses. Days 3 and 4 have uneven wind generation throughout the day, which results in high differences in LMPs. Volatile LMPs enable ESS to attain a high difference in purchasing and selling prices, which results in over a 12,000 € profit on Day 3 and Day 4.

Table 3. ESS profit in the market-based power system.

Day 1 (€)	Day 2 (€)	Day 3 (€)	Day 4 (€)
9376	2272	12,377	12,018

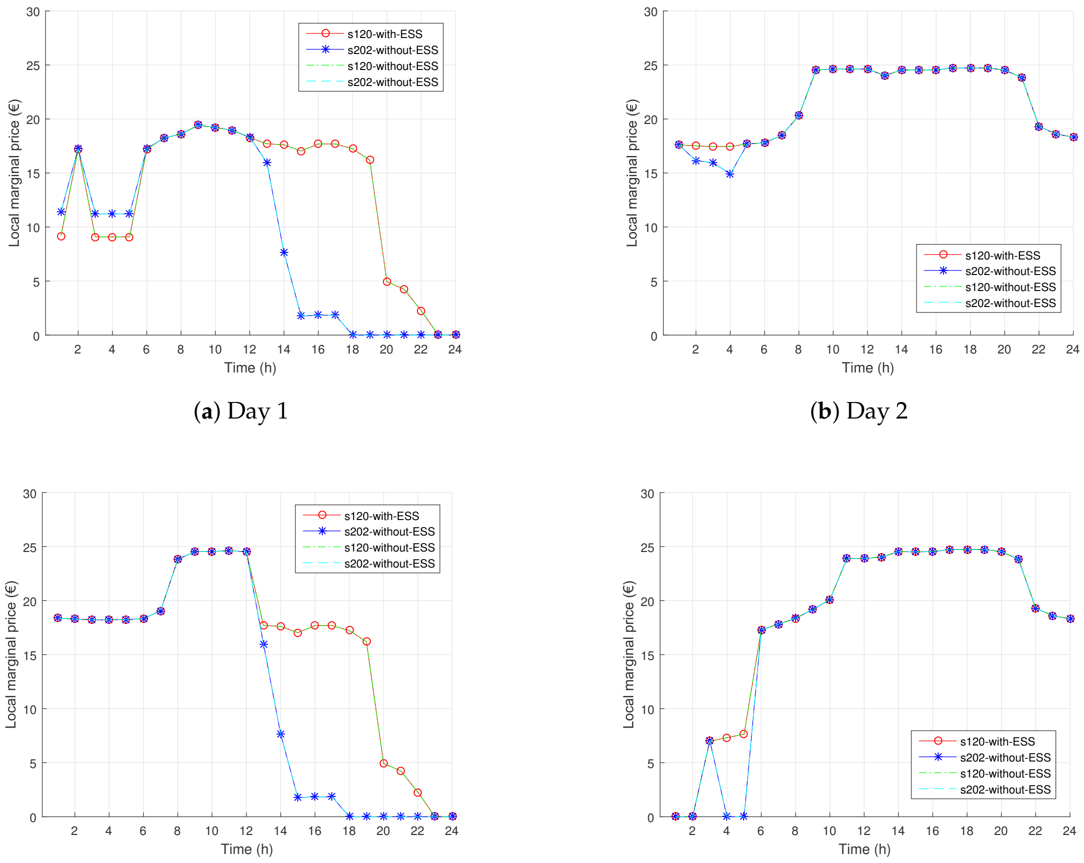

(**a**) Day 1 (**b**) Day 2 (**c**) Day 3 (**d**) Day 4

Figure 4. Local marginal prices at Buses 120 and 202.

ESS operation in market-based environment is shown in Figure 5. On representative Day 1, ESS at Bus 202 is not charged in the morning due to relatively high LMPs (compare with Figure 4a). Instead, only ESS at Bus 120 is charged, due to lower LMPs. Since the LMPs are highest in Time Periods 8–11, both ESS are discharged in the late morning. LMPs at Bus 202 fall to zero at Hour 18 and stay zero until the end of the day, which is why ESS at Bus 202 is charged to the required capacity in the late evening. LMPs at Bus 120 are lowest towards the end of the day, as well, making this time of the day favorable for charging. On Day 2, both ESS fully charge in the morning. Although the morning prices are higher than on Day 1, both ESS fully charge because the afternoon LMPs are much higher, making it profitable for ESS to perform arbitrage. Days 3 and 4 are similar in the way that ESS charge in the morning and discharge during peak price hours. For Day 3, these peak price hours are 8–12, while for Day 4, they occur in the late afternoon. Note that ESS at Bus 202 performs arbitrage between Hours 2 and 3 of Day 4 due to the local price spike.

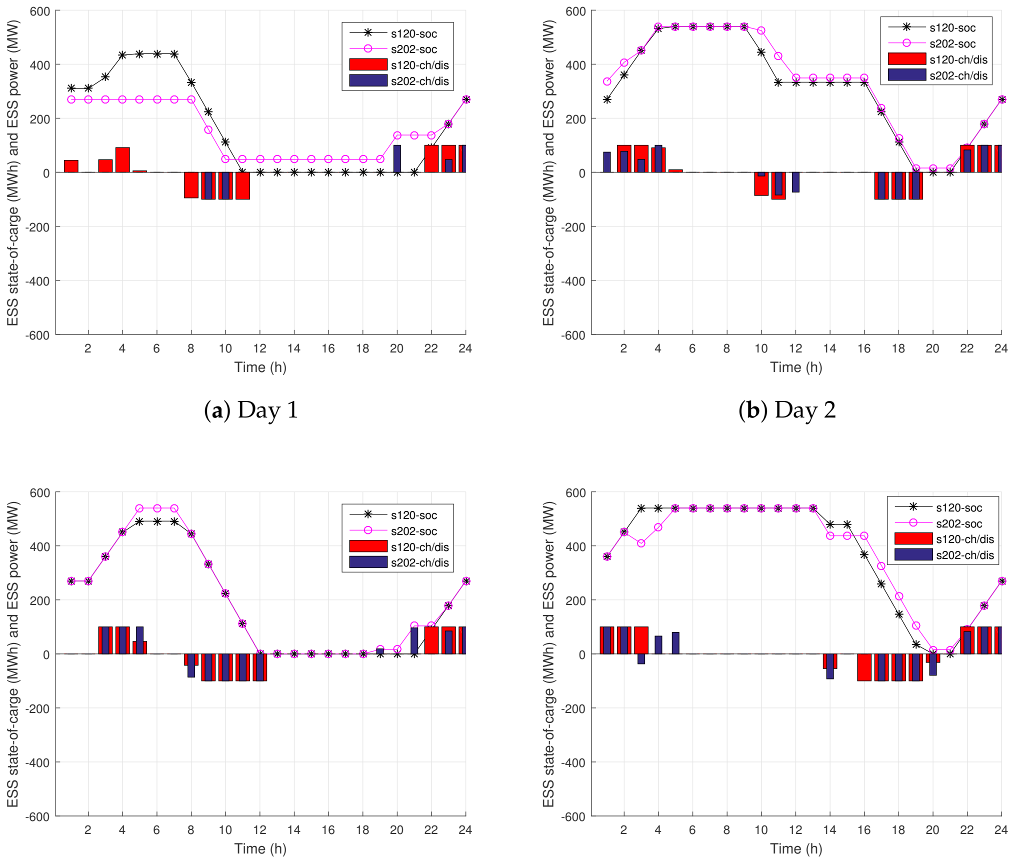

(**a**) Day 1 (**b**) Day 2

(**c**) Day 3 (**d**) Day 4

Figure 5. ESS operation in the market-based power system.

Social welfare for all four representative days in cases with and without ESS is presented in Table 4. The presence of ESS increases social welfare by up to 1%. It is interesting to compare ESS profit from Table 3 with the increase of social welfare in Table 4. The conclusion is that relatively small ESS profit results in much higher improvement of social welfare. For instance, a 9376 € ESS profit on Day 1 causes an 82,830 € increase in social welfare. This is because the social welfare is not only increased by storage offers and bids, but also because of higher utilization of wind energy.

Table 4. Social welfare in the market-based power system.

	Day 1	Day 2	Day 3	Day 4
Without ESS (€)	14,211,540	13,176,030	13,871,820	13,439,810
With ESS (€)	14,294,370	13,296,560	13,998,800	13,574,660
Improvement	0.6%	0.9%	0.9%	1.0%

Table 5 shows peak production, overall daily production and wind curtailment with and without ESS in the market-based power system. Like in the vertically-integrated model, peak production of conventional generating units is reduced by 200 MW, i.e., the ESS capacity. Overall generation is reduced on Days 1, 3 and 4, while on Day 2, it is increased due to low wind output (no wind curtailment even in the no ESS case). Wind curtailment is reduced on all representative days. Generally, wind curtailment is much lower in the market-based system as compared to the vertically-integrated system. This is the result of more stringent constraints in the vertically-integrated system, e.g., generator minimum generation, minimum up and down times, start-up costs. These constraints are not part of the market-based model. They are subject to self-scheduling and out-of-market corrections.

Table 5. Peak production, overall daily production and wind curtailment with and without ESS in the market-based power system.

	Day 1	Day 2	Day 3	Day 4
Peak production of conventional generators with ESS (MW)	5436	6972	6598	6972
Peak production of conventional generators without ESS (MW)	5636	7172	6798	7172
Production of conventional generators with ESS (MWh)	74,367	132,454	92,093	113,745
Production of conventional generators without ESS (MWh)	74,757	132,229	92,457	114,033
Wind curtailment with ESS (MWh)	1534	0	1483	425
Wind curtailment without ESS (MWh)	2064	0	2064	946

Figure 6 shows cumulative ESS profit throughout the day for each representative day. In almost all cases, ESS first purchases energy, resulting in negative profit, then sells energy, reaching its positive peak profit. The profit is then decreased in most of the cases because of the constraint imposing 50% state of charge at the end of the time horizon. During Day 1, ESS at Bus 202 does not start with negative profit (Figure 6a) because this ESS is not charged during the night (Figure 5a). During Day 4, ESS at Bus 202 is charged at zero LMP and performs arbitrage between Hours 2 and 3, which brings it to a positive profit in the early hours (Figure 6a).

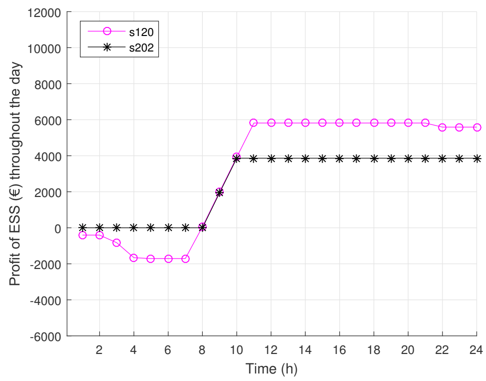

(**a**) Day 1

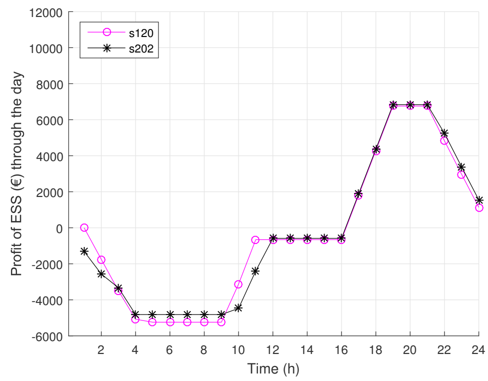

(**b**) Day 2

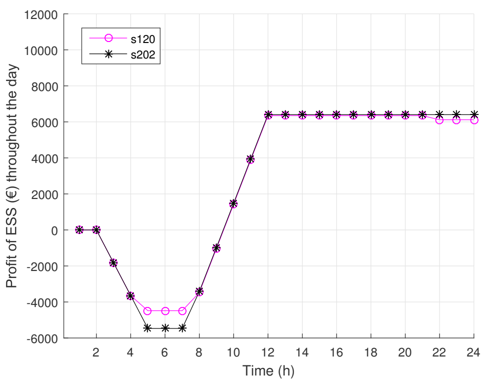

(**c**) Day 3

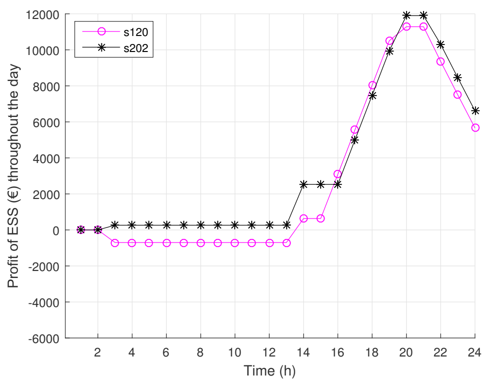

(**d**) Day 4

Figure 6. ESS profit throughout the day.

4. Conclusions

The presented simulation results indicate that ESS benefits in both vertically-integrated and market-based power systems. In the vertically-integrated system, the savings achieved by two distributed ESS result in saving up to 1.3%. The savings are greater for days with high wind outputs. This result indicates that power systems with high penetration of renewable generators benefit from ESS the most. Furthermore, ESS reduces wind curtailment, which reduces the generation of conventional generators. Peak production of conventional generators is reduced, as well.

In the market-based power system, ESS collects profit based on the difference in LMPs throughout the day. Even relatively low ESS profit results in a much higher (up to 10-times) increase in social welfare. One reason for this is the ESS market offers and bids, while the other reason, much more significant, is the reduction of wind curtailment. An additional finding is that ESS offers and bids for electricity in a way that is as neutral as possible for LMPs. ESS market actions that affect LMPs disrupt its profit opportunities. Therefore, one cannot expect significant price deviations as a result of ESS operation.

Although ESS can make a profit in the energy market, these profits are insufficient to justify such investment. Therefore, multiple streams of revenue need to be stacked together to justify investment in ESS. Our future work will be focused on ESS as a reserve provider and a temporary means for the deferral of investment in transmission and generation.

Acknowledgments: This work has been supported in part by Croatian Science Foundation and Croatian Transmission Operator System (TSO) under the project Smart Integration of RENewables (I-2583-2015).

Author Contributions: Hrvoje Pandžić conceived and designed the experiments; Zora Luburić performed the experiments and performed literature review; Tomislav Plavšić analyzed the data and designed the experiments.

Conflicts of Interest: The authors declare no conflict of interest.

Abbreviations

The following abbreviations are used in this manuscript:

ERCOT	Electric Reliability Council Of Texas
ESS	Energy storage system
GAMS	General algebraic modeling system
KKT	Karush–Kuhn–Tucker
LMP	Local marginal price
LOLP	Loss of load probability
MILP	Mixed integer programming problem
RES	Renewable energy sources
TSO	Transmission system operator

Nomenclature

Sets

B	energy system units, indexed by b
C	segments of generators cost curves, indexed by c
I	thermal generator units, indexed by i
L	lines, indexed by l
N	buses, indexed by n
T	time periods, indexed by t
W	wind farms, indexed by w

Parameters

$ch_b^{\max}$	maximum charging capacity of ESS b (MWh)
$d_n^{\max}(t)$	maximum demand at bus n during time period t (MW)
$dis_b^{\max}$	maximum discharging capacity of ESS b (MWh)
f_i	fixed production cost of generator i (€)

$g_{i,c}^{\max}$	maximum capacity of segment c of generator i cost curve (MW)
$g_i^{\min}$	minimum capacity of generator i cost curve (MW)
$g_i^{\text{on-off}}$	ON-OFF status of generator i at time t (1/0)
g_i^{down}	minimum down time of generator i (h)
g_i^{up}	minimum up time of generator i (h)
$K_w^{\max}(t)$	maximum power production of wind farm w during time period t (MW)
$o_{i,c}$	slope of the segment c of the cost curve of generator i (€/MW)
$pf_l^{\max}$	maximum power flow through line l (MW)
r_i^{down}	ramp-down limit of generator i (MW/h)
r_i^{up}	ramp-up limit of generator i (MW/h)
$soc_b^{\max}$	maximum capacity of ESS b (MWh)
$soc_b^{\min}$	minimum capacity of ESS b (MWh)
$sus_{n,m}$	susceptance of line connecting buses n-m (S)
η_b^{ch}	charging efficiency of ESS b (-)
η_b^{dis}	discharging efficiency of ESS b (-)
$V_i^{\text{down,min}}$	length of time that generator i must be OFF at the start of the planning horizon (h)
$V_i^{\text{up,min}}$	length of time that generator i must be ON at the start of the planning horizon (h)

Variables

$d_n(t)$	demand at bus n (MW) in dispatch hour t
$g_{i,c}(t)$	generator production i by block c (MW) in dispatch hour t
$k_w(t)$	power production of wind farm w (MW) in dispatch hour t
$pf_l(t)$	power flow through line l (MW) in dispatch hour t
$soc_b(t)$	state of charge of ESS b (MWh) in dispatch hour t
$start_i(t)$	start-up cost of generator i at time t (€)
$a_n(t)$	voltage angle at bus n (rad) in dispatch hour t
$p_b^{\text{ch}}(t)$	charging power purchased by ESS b (MW) in dispatch hour t
$p_b^{\text{dis}}(t)$	discharging power sold by ESS b (MW) in dispatch hour t

Binary Variables

$x_b^{\text{ch}}(t)$	enforces ESS b to bid; 1 when charging in dispatch hour t
$x_b^{\text{dis}}(t)$	enforces ESS b to offer; 1 when discharging in dispatch hour t
$x_i(t)$	1 if generator i is producing at time t, 0 otherwise
$y_i(t)$	1 if generator i is started at time t, 0 otherwise
$z_i(t)$	1 if generator i is shutdown at time t, 0 otherwise

References

1. US DOE Energy Information Administration/Electric Power Monthly. Available online: http://www.eia.gov/electricity/monthly/ (accessed on 25 April 2017).
2. EWEA (The European Wind Energy Association). *Wind in Power 2015 European Statistics*; EWEA: Leuven, Belgium, 2016.
3. Fabbri, A.; San Roman, T.G.; Abbad, J.R.; Quezada, V.H.M. Assessment of the Cost Associated with Wind Generation Prediction Errors in a Liberalized Electricity Market. *IEEE Trans. Power Syst.* **2005**, *20*, 1440–1446.
4. Ortega-Vazquez, M.; Kirschen, D.S. Assessing the Impact of Wind Power Generation on Operating Costs. *IEEE Trans. Smart Grid* **2010**, *1*, 295–301.
5. Baringo, L.; Conejo, A.J. Strategic Offering for a Wind Power Producer. *IEEE Trans. Power Syst.* **2013**, *28*, 4645–4654.
6. Zugno, M.; Morales, J.M.; Pinson, P.; Madsen, H. Pool Strategy of a Price-Maker Wind Power Producer. *IEEE Trans. Power Syst.* **2013**, *28*, 3440–3450.
7. Delikaraoglou, S.; Papakonstantinou, A.; Ordoudis, C.; Pinson, P. Price-Maker Wind Power Producer Participating in a Joint Day-Ahead and Real-Time Market. In Proceedings of the 12th International Conference on the European Energy Market (EEM), Lisbon, Portugal, 19–22 May 2015; pp. 1–5.
8. Aigner, T.; Jaehnert, S.; Doorman, G.L.; Gjengedal, T. The Effect of Large-Scale Wind Power on System Balancing in Northern Europe. *IEEE Trans. Sustain. Energy* **2012**, *3*, 751–759.

9. Taczi, I.; Szorenyi, G. *Pumped Storage Hydroelectric Power Plants: Issues and Applications*; Energy Regulators Regional Association (ERRA): Budapest, Hungary, 2016.
10. Office of Electricity Delivery and Energy Reliability. Available online: http://energy.gov/ (accessed on 8 May 2012).
11. Pozo, D.; Contreras, J.; Sauma, E.E. Unit Commitment With Ideal and Generic Energy Storage Units. *IEEE Trans. Power Syst.* **2014**, *29*, 2974–2984.
12. Yan, N.; Xing, Z.X.; Li, W.; Zhang, B. Economic Dispatch Application of Power System with Energy Storage Systems. *IEEE Trans. Appl. Superconduct.* **2016**, *26*, 0610205.
13. Li, N.; Uçkun, C.; Constantinescu, E.M.; Birge, J.R.; Hedman, K.W.; Botterud, A. Flexible Operation of Batteries in Power System Sceduling with Renewable Energy. *IEEE Trans. Power Sustain. Energy* **2016**, *7*, 685–696.
14. Kyriakopoulos, G.L.; Arabatzis, G. Electrical energy storage systems in electricity generation: Energy policies, innovative technologies, and regulatory regimes. *Renew. Sustain. Energy Rev.* **2016**, *56*, 1044–1067.
15. Kyriakopoulos, G.L.; Arabatzis, G.; Chalikias, M. Renewables exploitation for energy production and biomass use for electricity generation. A multi-parametric literature-based review. *AIMS Energy* **2016**, *4*, 762–803.
16. Sioshansi, R.; Madaeni, S.H.; Denholm, P. A Dynamic Programming Approach to Estimate the Capacity Value of Energy Storage. *IEEE Trans. Power Syst.* **2014**, *29*, 395–403.
17. Wogrin, S.; Gayme, D.F. Optimizing Storage Siting, Sizing, and Technology Portofolios in Transmission-Constrained Networks. *IEEE Trans. Power Syst.* **2015**, *30*, 3304–3313.
18. Meneses de Quevedo, P.; Contreras, J. Optimal Placement of Energy Storage and Wind Power under Uncertainty. *Energies* **2016**, *9*, 528.
19. Pandžić, H.; Wang, Y.; Qiu, T.; Dvorkin, Y.; Kirschen, D.S. Near-Optimal Method for Siting and Sizing of Distributed Storage in a Transmission Network. *IEEE Trans. Power Syst.* **2015**, *30*, 2288–2300.
20. Dvorkin, Y.; Fernandez-Blanco, R.; Kirschen, D.S.; Pandžić, H.; Watson, J.-P.; Silva-Monroy, C.A. Ensuring Profitability of Energy Storage. *IEEE Trans. Power Syst.* **2016**, *32*, 611–623.
21. Hu, Z.; Zhang, S.; Zhang, F.; Lu, H. SCUC with Battery Energy Storage System for Peak-Load Shaving and Reserve Support. In Proceedings of the 2013 IEEE Power and Energy Society General Meeting (PES), Vancouver, BC, Canada, 21–25 July 2013; pp. 1–5.
22. Sioshansi, R.; Denholm, P.; Jenkin, T. *Market and Policy Barriers to Deployment of Energy Storage*; Economics of Energy and Environmental Policy: Cleveland, OH, USA, 2012; p. 1.
23. Pandžić, H.; Kuzle, I. Energy Storage Operation in the Day-Ahead Electricity Market. In Proceedings of the IEEE Conference on the European Energy Market, Lisbon, Portugal, 19–22 May 2015; pp. 1–6.
24. Miranda, I.; Silva, N.; Bernardo, A.M. Assessment of the potential of Battery Energy Storage Systems in current European markets designs. In Proceedings of the 12th International Conference on the European Energy Market (EEM), Lisbon, Portugal, 19–22 May 2015; pp. 1–5.
25. The IEEE Reliability Test System. A report prepared by the Reliability Task Force of the Application of Probability Method Subcommittee. *IEEE Trans. Power Syst.* **1999**, *14*, 1010–1020.
26. Baldick, R. Wind and Energy Markets: A Case Study of Texas. *IEEE Syst. J.* **2012**, *6*, 27–34.
27. Potter, C.W.; Lew, D.; McCaa, J.; Cheng, S.; Eichelberger, S.; Grimit, E. Creating the Dataset For the Western Wind and Solar Integration Study (USA). *Wind Eng.* **2008**, *32*, 325–338.
28. Papavasiliou, A.; Oren, S.S. Multiarea Stochastic Unit Commitment For High Wind Penetration in a Transmission Constrained Network. *Oper. Res.* **2013**, *61*, 78–592.
29. Growe-Kuska, N.; Heitsch, H.; Romisc, W. Scenario Reduction and Scenario Tree Construction for Power Management Problems. In Proceedings of the IEEE Bologna Power Technology Conference, Bologna, Italy, 23–26 June 2003.

© 2017 by the authors. Licensee MDPI, Basel, Switzerland. This article is an open access article distributed under the terms and conditions of the Creative Commons Attribution (CC BY) license (http://creativecommons.org/licenses/by/4.0/).

Article 2 - FACTS Devices and Energy Storage in Unit Commitment

Luburić, Zora; Pandžić, Hrvoje, "FACTS devices and energy storage in unit commitment" International Journal of Electrical Power Energy Systems 104 (2019): 311-325.
DOI: https://doi.org/10.1016/j.ijepes.2018.07.013

– 15 pages

Electrical Power and Energy Systems 104 (2019) 311–325

Contents lists available at ScienceDirect

Electrical Power and Energy Systems

journal homepage: www.elsevier.com/locate/ijepes

FACTS devices and energy storage in unit commitment

Zora Luburić*, Hrvoje Pandžić

Faculty of Electrical Engineering and Computing, University of Zagreb, Croatia

ARTICLE INFO

Keywords:
FACTS devices
Energy storage
Unit commitment
Transmission power system

ABSTRACT

Both Flexible AC Transmission System (FACTS) devices and energy storage may provide benefits to the power system, e.g. reduced transmission losses, improved system stability, voltage regulation and reduced congestion. As a result, FACTS devices can diminish the value of the installed energy storage and vice versa. In order to assess their impact on each other, this paper formulates a unit commitment model that includes generic energy storage and FACTS devices in order to investigate characteristics of their joint operation assess how they cancel out each other's benefits. The results of four unit commitment models are presented: (i) with no storage or FACTS devices (base case); (ii) with FACTS devices only; (iii) with energy storage only; (iv) with both FACTS devices and energy storage. An analysis of the benefits of both technologies is performed and economic assessment is presented. The simulations are performed on IEEE RTS96 system using CPLEX 12 under GAMS.

1. Introduction

Intermittent power produced by renewable energy sources, especially wind, has introduced many challenges to Transmission System Operators, whose mission is to ensure reliability and stability of the transmission power system. This is a consequence of the reduced controllability, only partial generation predictability and locational dependence of the connected renewable sources [1]. Many countries have introduced measures to improve integration of renewable sources, e.g. feed-in-tariff incentives [2]. However, possible wind curtailment can drastically reduce savings in power system operating costs and reducing greenhouse gas emissions. Therefore, power network needs to be upgraded and new control methods should be included in operating procedures in order to maximize the utilization of renewable power. These include utilization of energy storage units and Flexible AC Transmission System (FACTS) devices, upgrading transmission lines, load management, sufficient provision of ancillary services and others. Power transmission lines are usually congested in areas with high capacity of installed renewable sources, which causes congestion and decreases transmission system adequacy [3]. Besides upgrading the existing or building new transmission lines, this problem can be tackled by using FACTS devices and energy storage. Both FACTS and energy storage can control power system flows in order to optimize the system operating costs. There are three categories of FACTS devices distinguishable by their connection to the grid: (i) series controllers, (ii) shunt controllers and (iii) combined series-shunt controllers. Each category contains several specific technical solutions. This paper is based on series controllers, i.e. Thyristor-Controlled Series Capacitor (TCSC), whose purpose is to modify the reactance of a power line to which it is connected [4]. TCSC consists of controlled reactors in parallel with sections of a capacitor bank, which enables a smooth control of the capacitive reactance. As a result, TCSCs contribute to a better utilization of the existing lines, resulting in increased transmission power capacity due to redistributed power flows from congested lines to non-congested parallel lines in the same direction. Energy storage affects power flows by consuming power at certain time periods and injecting it back into the grid later on. This reduces congestion, and consequently the curtailed wind generation.

1.1. Literature review

1.1.1. Unit commitment

Unit commitment is a well-researched problem in the research community. This is a short-term problem, usually consisted of 24 consecutive hours, comprising one day, whose goal is to determine optimal on/off status and dispatch of thermal generating units in order to minimize operating costs. Unit commitment formulations are constantly being improved. For instance, in [5] the authors propose more accurate thermal units start up and shut down trajectories. Another unit commitment model, which captures variability of wind generation at the sub-hourly level and considers uncertainty of renewable generation via stochastic scenarios, is proposed in [6]. Study on the feasibility of energy delivery in case of a large-scale wind integration is examined in [7]. The numerical results indicate that including a continuous piece-

* Corresponding author.
E-mail addresses: zora.luburic@fer.hr (Z. Luburić), hrvoje.pandzic@fer.hr (H. Pandžić).

https://doi.org/10.1016/j.ijepes.2018.07.013
Received 5 January 2018; Received in revised form 17 May 2018; Accepted 5 July 2018
0142-0615/ © 2018 Elsevier Ltd. All rights reserved.

wise sub-hourly linear formulation of power generation would enable effectively meeting the energy delivery requirement. Impact of wind power forecasting uncertainty on unit commitment problem is examined in [8]. This uncertainty is represented by wind scenarios that include cross-temporal dependency. The authors conclude that this type of representation of uncertainty has advantages over traditional deterministic unit commitment approach. Value of forecasting is also investigated in [9], where the authors present an adaptive unit commitment formulation based on rolling horizon approach. A unit commitment model that considers different sources of grid uncertainty, i.e. uncertainty related to the output of renewable generation, load uncertainty, generator contingencies and line outages, is formulated in [10]. This security constrained unit commitment model uses a heuristic genetic algorithm to obtain the optimal commitment schedule. The results indicate that power systems are more prone to contingencies at peak load hours and that the stochastic scheduling model is more robust than deterministic ones.

1.1.2. Energy storage

Energy storage can be operated by a regulated entity, i.e. System Operator, or by an independent owner. As shown in [11], energy storage is operated differently in case of a vertically integrated utility as opposed to an investor-owned energy storage. This is because the investor operates its storage to maximize its profit, while in vertically integrated utility the main goal is to minimize overall operating costs. In [12], a novel model of storage capacity auction is proposed which presents an efficient utilization of priced storage capacity rights, such as power capacity and energy capacity rights, for both competitively priced and unpriced services. In fact, it is shown that a storage owner receives the same revenue through the auction as it could collect through market bids. Operation of energy storage can be divided into few categories, e.g. energy arbitrage, reserve provision, and cooptimization with renewable plants, such as wind farms and photovoltaics, to ensure better position of renewables in the market. The authors in [13] analyse how the operation of strategic energy storage affects conventional generators in the day-ahead electricity market. They show that the energy storage profits are directly related to the electricity price volatility and that they are very low in case of relatively constant market prices throughout the day. A model that includes stochasticity of market prices is shown in [14]. Stochastic model, where an investor-owned independently-operated energy storage offers energy and reserves in the day-ahead market, is proposed in [15]. The authors use many wind generation scenarios to obtain profitability of energy storage. Similarly, the authors in [16] model energy storage in a single-stage transmission expansion planning model in which the line losses are linearized by segments. Their results show that investment in energy storage contributes to a decrease in power system operating costs and improves flexibility of the power system operation. Many papers propose a coordinated operation of renewable plants and energy storage, since energy storage can reduce the negative effects of poor predictability and intermittency of renewable plants. In [17], an energy storage unit is modelled to compensate for forecast errors in wind farm production as determined by the market transactions. The authors showed that large energy storage units contribute in complying delivery requirements in production of wind farms, and from economical point of view, ensure that their operation is more profitable. The authors in [18] formulate a problem for optimal production strategy for joint wind farm and pumped storage hydro unit. The approach is based on energy arbitrage and maximum utilization of wind energy. A thorough review of energy storage technologies for alleviating variability of renewable energy sources is available at [19]. A study on grid-scale energy storage is as an option to reduce wind curtailment in transmission network is presented in [20]. The results indicate that wind spillage can be reduced with energy storage costs as high as $780/kW and ten hours of storage capacity. Generally, batteries with higher power ratings result in less overall wind curtailment in the system. The sensitivity analysis showed the most sensitive parameters are wind subsidies, cost of transmission expansion, battery degradation and battery life cycle. A heuristic algorithm that solves a unit commitment problem that includes renewable generation and pumped-hydro energy storage is presented in [21]. The results of this paper indicate that higher forecast error of renewable generation increases operating cost of thermal units, which can be effectively counterbalanced with pumped-hydro storage plants. Interval unit commitment formulation that includes pumped-hydro storage units and their hydraulic constraints is proposed in [22]. The authors demonstrate that cost-effective regulating capabilities of the pumped-hydro storage units result in large savings in overall system operating costs. Mathematical formulations of energy storage investment models are much more complex than those of operating models. Minimization of investment costs for new technologies of generators, transmission lines and energy storages is proposed in [23]. This model is tested on the power system of Great Britain and the authors report that energy storage can contribute to the island power system by providing ancillary services, enabling balancing energy in real time, as well as reducing transmission investment in new lines. Modelling of siting and sizing of energy storage is provided in [24,25]. The former is focused on technical and economic aspects of the energy storage investment problem. The objective function of the proposed model minimizes the sum of the generation costs and the investment costs in energy storage reduced on a daily scale. The outcome of the model are optimal locations and capacities of distributed energy storage. Paper [25] formulates a linear programming model, which the authors use to show how the proper sizing of energy storage units can have an important role in providing flexibility in transmission grids. However, they also point out that siting has a minor role in the optimal operation of the power system.

1.1.3. FACTS devices

FACTS devices are commonly used in operations that require both rapid dynamic response and frequent variations in output. The most important role of FACTS devices is to increase utilization of transmission lines. In other words, they are used in areas where bottlenecks and less utilized power lines appear simultaneously. In this paper, the modelling of line's reactance is similar to the model proposed in [26], where the transmission grid is modelled with variable line impedance determined by the operation of FACTS devices. A characteristic of the model presented in [26] is that the same sign of the voltage angle difference in lines equipped with FACTS devices is imposed. The model finds the optimal number of FACTS devices in a power system, which results in maximum cost savings. The authors in [27] contribute with reformulating a non-linear problem into a MILP and optimize the operation of FACTS devices to improve the deliverability of reserves to ensure the day-ahead corrective operation. This approach minimizes the out-of-market corrections, such as re-dispatching units different from deliverable market plan and committing more costly power plants. Another method for converting a non-linear problem into a MILP is proposed in [28]. This method is based on Big M reformulation and applied to the economic dispatch problem. The results of the case study indicate that utilization of FACTS devices improves economics of power system operation. Moreover, in case of low power line capacities, altered line admittances, provided by FACTS devices, can find feasible solution when no such solution exists for fixed line admittances. Operations of both FACTS devices and wind farms are investigated in [29] to minimize wind curtailment. Model has two stages: market stage, which consists of the day-ahead and balancing market, and operational stage, which considers wind scenarios. The authors highlight the possibility of changing the TCSC reactance for each wind scenario to find the optimal solution. In [30], a split TSCS is used to fine tune power flows in order to increase the transmission line capacity. The fine tuning of the lice reactance is performed using the Newton Raphson power flow analysis method in order to compensate for small changes in power demand. Analysis of the impact of TCSC on the available transfer capacity in transmission system with wind and hydro generation is performed in [31]. The authors conclude that wind generation brings more variability to the available transfer capacity and that installation of TCSC generally improves available transfer capacity, especially since it removes the downward peaks upon sudden lack of wind generation. A model for optimal allocation of TCSC and unified power flow controllers is proposed in [32]. The optimization model is based on step-by-step variation of control parameters of these devices. The impact of these devices on LMPs and system voltage is investigated. The case study demonstrates the effectiveness of the proposed TCSC and unified power flow controller placement strategy. Few types of FACTS devices are modelled in the redispatching problem to enhance system security in [33], which uses AC power flow representation. The authors indicate a reduction in redispatching procedures in presence of an appropriate FACTS device. In addition, they show an increase in system stability and security if FACTS devices are installed. Using FACTS devices to improve available transfer capability of interconnecting lines in [34] results in up to 18% improvement in total transfer capability. The optimal multiplier Newton–Raphson method is used to maximize the power flows in the IEEE 118-bus system in [35]. Available Transfer Capacity enhancement of interconnectors was achieved, as well as improved transmission services in market-based power systems by modelling several FACTS devices, such as series, shunt and unified controllers. An investment model of FACTS devices is proposed in [36] by a generic algorithm. It consists of three investment parameters: location, type and value of the FACTS device. The authors model four types of FACTS devices for steady-state analysis of the IEEE 118-bus system and show increase in loadability of the power system. The most efficient solution is achieved by simultaneous use of several kinds of FACTS devices. Furthermore, results show that after a certain number of FACTS devices, the loadability of the system cannot be improved.

1.2. Contributions

With respect to the literature review above, the contributions of the paper are:

- Formulation of a unit commitment problem with energy storage and continuous variable admittance of power lines to which the FACTS devices are connected.
- A detailed analysis of effects of both the energy storage and the FACTS technologies (individually and combined) on power system economics and utilization of renewable power.
- A sensitivity analysis of the wind power penetration level and level of congestion, i.e. capacity of transmission lines.

2. Model

2.1. Nomenclature

Sets and Indices	
$a \in A$	Index and set of generator cost curve segments
$b \in B$	Index and set of nodes
$i \in I$	Index and set of all transmission lines
$l^{\mathrm{FACTS}} \in L^{\mathrm{FACTS}}$	Index and set of transmission lines l^{FACTS} with FACTS devices
$\bar{l} \in L$	Index and set of transmission lines $\bar{l}$ without FACTS devices
$s \in S$	Index and set of energy storage units
$t \in \mathrm{T}$	Index and set of time periods
$w \in W$	Index and set of wind farms
Parameters	
C_i^{fx}	Fixed production cost of generating unit i (\$)
C_i^{start}	Start-up cost of generating unit i (\$)
$ch_s^{\max}$	Maximum charging power of energy storage s (MW)
$D_{t,b}$	Demand at node b (MW) during period t
$dis_s^{\max}$	Maximum discharging power of energy storage s (MW)
g_i^{down}	Minimum down time of generator unit i (h)
$g_i^{\mathrm{down,init}}$	Time that generating unit i has been down at t = 0 (h)
g_i^{up}	Minimum up time of generator unit i (h)
$g_i^{\mathrm{up,init}}$	Time that generating unit i has been up at t = 0 (h)
$G_{i,a}^{\max}$	Capacity of segment a of the cost curve of generating unit i (MW)
$G_i^{\min}$	Minimum power output of generating unit i (MW)
$G_i^{\max}$	Maximum power output of generating unit i (MW)
M	Large number
$mc_{i,a}$	Generation cost on segment a of generating unit i's cost curve (\$/MW)
p_i^0	Initial power of generating unit i at t = 0(MW)
R_i^{down}	Ramp-down limit of generating unit i (MW/h)
R_i^{down}	Ramp-down limit of generating unit i (MW/h)
R_i^{up}	Ramp up limit of generating unit i (MW/h)
$RS_t^{\mathrm{up/down}}$	Minimum required up/down reserve during period t (MW)
$sus_{l^{\mathrm{FACTS}}}^{\max}$	Maximum susceptance of line $l^{\mathrm{FACTS}}$with FACTS devices (S)
$sus_{l^{\mathrm{FACTS}}}^{\min}$	Minimum susceptance of line l^{FACTS} with FACTS devices (S)
$sus_{\bar{l}}$	Susceptance of line l without FACTS devices (S)
$soc_s^{\max}$	Maximum state of charge of energy storage s (MWh)
$soc_s^{\min}$	Minimum state of charge of energy storage s (MWh)
$V_i^{\mathrm{up,min}}$	Time that generating unit i must stay on at the beginning of the operating horizon (h)
$V_i^{\mathrm{down,min}}$	Time that generating unit i must stay off at the beginning of the operating horizon (h)
$Z_{t,w}^{\max}$	Available output of wind farm w (MW)
$\eta_s^{\mathrm{ch/dis}}$	Charging/Discharging efficiency of energy storage s
η_s^{dis}	Discharging efficiency of energy storage s
Variables	
$flow_{t,l}$	Power flow through line $l \in L$ during period t (MW)
$flow_{t,\bar{l}}$	Power flow through line $\bar{l} \in \bar{L}$ during period t (MW)
$flow_{t,l^{\mathrm{FACTS}}}$	Power flow through line $l^{\mathrm{FACTS}} \in L^{\mathrm{FACTS}}$ during period t (MW)
$p_{t,s}^{\mathrm{ch}}$	Charging power of energy storage s during period t (MW)
$p_{t,s}^{\mathrm{dis}}$	Discharging power of energy storage s during period t (MW)
$p_{t,i}$	Output of generating unit i during period t (MW)
$p_{t,i,a}$	Output of generating unit i on cost curve segment a during period t (MW)
$p_{t,w}$	Output of wind farm w during period t (MW)
$r_{t,i}^{\mathrm{up/down}}$	Up/Down reserve provided by generating unit i during period t (MW)
$soc_{t,s}$	State of charge of energy storage s during period t (MWh)
$sus_{t,l^{\mathrm{FACTS}}}$	Susceptance of line l^{FACTS} with FACTS devices during period t (S)

$\vartheta_{t,b}$	Voltage angle at node b during period t (rad)
$u_{t,i}$	On/off (1/0) status of generating unit i during period t
$v_{t,i}$	Start up (1/0) of generating unit i during period t
$z_{t,i}$	Shut down (1/0) of generation unit i during period t
$x_{t,s}^{\mathrm{ch}}$	Charging (1/0) of energy storage s during period t
$x_{t,s}^{\mathrm{dis}}$	Discharging (1/0) of energy storage s during period t
x_l^{FACTS}	Voltage angle difference; 1 if positive, 0 if negative

2.2. Description

This section formulates a unit commitment model that incorporates both energy storage and FACTS devices. The objective function (1) aims to minimize overall generation cost of all generators. It comprises three terms: fixed operating cost, start up cost and variable cost of each generator. Wind farms are assumed to produce at zero cost.

$$\text{Minimize} \sum_{t=1}^{T}\sum_{i=1}^{I}\left(C_i^{\mathrm{fx}}\cdot u_{t,i} + C_i^{\mathrm{start}}\cdot v_{t,i} + \sum_{a=1}^{A} mc_{i,a}\cdot p_{t,i,a}\right) \tag{1}$$

This objective function is subject to a number of constraints.

Conventional generating unit constraints (2)–(21):

Eq. (2) represents logic constraints in operation of generating units. If generator i is started at time period t, then both $u_{t,i}$ and $v_{t,i}$ are equal to 1. Else, if generator i is shut down at period t, then $z_{t,i}$ is equal to 1, and $u_{t,i}$ is zero. Moreover, (3) imposes that generator i can only start up or shut down at any period of time t.

$$v_{t,i} - z_{t,i} = u_{t,i} - u_{t-1,i} \quad \forall\, i \in I,\, t \in T \tag{2}$$

$$v_{t,i} + z_{t,i} \leqslant 1 \quad \forall\, i \in I,\, t \in T \tag{3}$$

Constraints (4)–(7) ensure that generators operate between their minimum and maximum allowed outputs, while the overall output is comprised of multiple piecewise generation cost curves a.

$$p_{t,i} = \sum_{a=1}^{A} p_{t,i,a} \quad \forall\, a \in A,\, i \in I,\, t \in T \tag{4}$$

$$p_{t,i} - r_{t,i}^{\mathrm{down}} \geqslant G_i^{\min}\cdot u_{t,i} \quad \forall\, i \in I,\, t \in T \tag{5}$$

$$p_{t,i,a} \leqslant G_{i,a}^{\max} \quad \forall\, a \in A,\, i \in I,\, t \in T \tag{6}$$

$$p_{t,i} + r_{t,i}^{\mathrm{up}} \leqslant G_i^{\max}\cdot u_{t,i} \quad \forall\, i \in I,\, t \in T \tag{7}$$

The next block of generator constraints are minimum up and down time constraints (8)–(13), which use different start up states, depending on the time a generator had been on or off before being started. A detailed explanation of these constraints is available in [37].

Minimum up time constraints:

$$\sum_{t=1}^{V_i^{\mathrm{up,min}}} (1-u_{t,i}) = 0 \quad \forall\, i \in I \tag{8}$$

$$\sum_{tt=t}^{t+g_i^{\mathrm{up}}} u_{tt,i} \geqslant g_i^{\mathrm{up}}\cdot v_{t,i} \quad \forall\, i \in I,\, t \in [V_i^{\mathrm{up,min}}+1,\, T-g_i^{\mathrm{up}}+1] \tag{9}$$

$$\sum_{tt=t}^{T} (u_{tt,i} - v_{t,i}) \geqslant 0 \;\forall\, i \in I,\, t \in [T-g_i^{\mathrm{up}}+2,\, T] \tag{10}$$

where

$$V_i^{\mathrm{up,min}} = \max\{0,\, \min\{T,\, (g_i^{\mathrm{up}} - g_i^{\mathrm{up,init}})\cdot g_i^{\mathrm{on-off}}\}\}$$

Minimum down time constraints:

$$\sum_{t=1}^{V_i^{\mathrm{down,min}}} u_{t,i} = 0 \quad \forall\, i \in I \tag{11}$$

$$\sum_{tt=t}^{t+g_i^{\mathrm{down}}-1} (1-u_{tt,i}) \geqslant g_i^{\mathrm{down}}\cdot z_{t,i} \;\forall\, i \in I,\, t \in [V_i^{\mathrm{down,min}}+1,\, T-g_i^{\mathrm{down}}+1] \tag{12}$$

$$\sum_{tt=t}^{T} (1-u_{tt,i} - z_{t,i}) \geqslant 0 \quad \forall\, i \in I,\, t \in [T-g_i^{\mathrm{down}}+2,\, T] \tag{13}$$

where

$$V_i^{\mathrm{down,min}} = \max\{0,\, \min\{T,\, (g_i^{\mathrm{down}} - g_i^{\mathrm{down,init}})\cdot(1-g_i^{\mathrm{on-off}})\}\}$$

Constraints (14)–(17) are up and down ramp constraints, which consider both the expected output and the up and down reserve provision of each generating unit. Eqs. 18,19 impose up and down reserve requirements, which need to be fulfilled by all the generating units combined. When defining the minimum level of reserve in the system, we use the well-known 3 + 5% rule proposed by the National Renewable Energy Laboratory [38], which sets the required reserves to 3% of the load and 5% of the available wind power at each time period. This is imposed in (20) and (21).

Ramp constraints:

$$-p_{t,i} + r_{t,i}^{\mathrm{down}} + p_{t-1,i} + r_{t-1,i}^{\mathrm{up}} \leqslant R_i^{\mathrm{down}}\cdot u_{t,i} + G_i^{\min}\cdot z_{t,i} \quad \forall\, i \in I,\, t \in [2,\, T] \tag{14}$$

$$p_{t,i} + r_{t,i}^{\mathrm{up}} - p_{t-1,i} + r_{t-1,i}^{\mathrm{down}} \leqslant R_i^{\mathrm{up}}\cdot u_{t-1,i} + G_i^{\min}\cdot v_{t,i} \quad \forall\, i \in I,\, t \in [2,\, T] \tag{15}$$

$$-p_{t_1,i} + r_{t_1,i}^{\mathrm{down}} + p_i^0 \leqslant R_i^{\mathrm{down}}\cdot u_{t,i} \quad \forall\, i \in I,\, t \in [1] \tag{16}$$

$$p_{t_1,i} + r_{t_1,i}^{\mathrm{up}} - p_i^0 \leqslant R_i^{\mathrm{up}}\cdot u_{t,i} \quad \forall\, i \in I,\, t \in [1] \tag{17}$$

Ramp requirements:

$$\sum^{I} r_{t,i}^{\mathrm{up}} = RS_t^{\mathrm{up}} \quad \forall\, t \in T \tag{18}$$

$$\sum^{I} r_{t,i}^{\mathrm{down}} = RS_t^{\mathrm{down}} \quad \forall\, t \in T \tag{19}$$

$$RS_t^{\mathrm{up}} = 0.03\cdot \sum_{b}^{B} d_{t,b} + 0.05\cdot \sum_{w}^{W} Z_{t,w} \quad \forall\, t \in T \tag{20}$$

$$RS_t^{\mathrm{down}} = 0.03\cdot \sum_{b}^{B} d_{t,b} + 0.05\cdot \sum_{w}^{W} Z_{t,w} \quad \forall\, t \in T \tag{21}$$

Renewable generation constraints:

Renewable generation output is constrained by its available output at each time period in (22).

$$p_{t,w} \leqslant Z_w^{\max} \quad \forall\, w \in W,\, t \in T \tag{22}$$

Transmission constraints:

Constraints (23)–(35) are transmission constraints. Eq. (23) is the power balance at each bus b and at each time period t. It balances the power generated by generators and wind farms, power discharged by energy storage and power inflows with the demand, power charged by energy storage and power outflows. Eq. (24) computes power flows through lines, while (25) and (26) limit these power flows. Constraints (27) and (28) determine power flows through lines equipped with FACTS devices. However, Eq. (27) is non-linear because the susceptance of FACTS equipped lines is a variable, instead of parameter. As explained in [26], this model assumes that FACTS devices do not change direction of flows through the

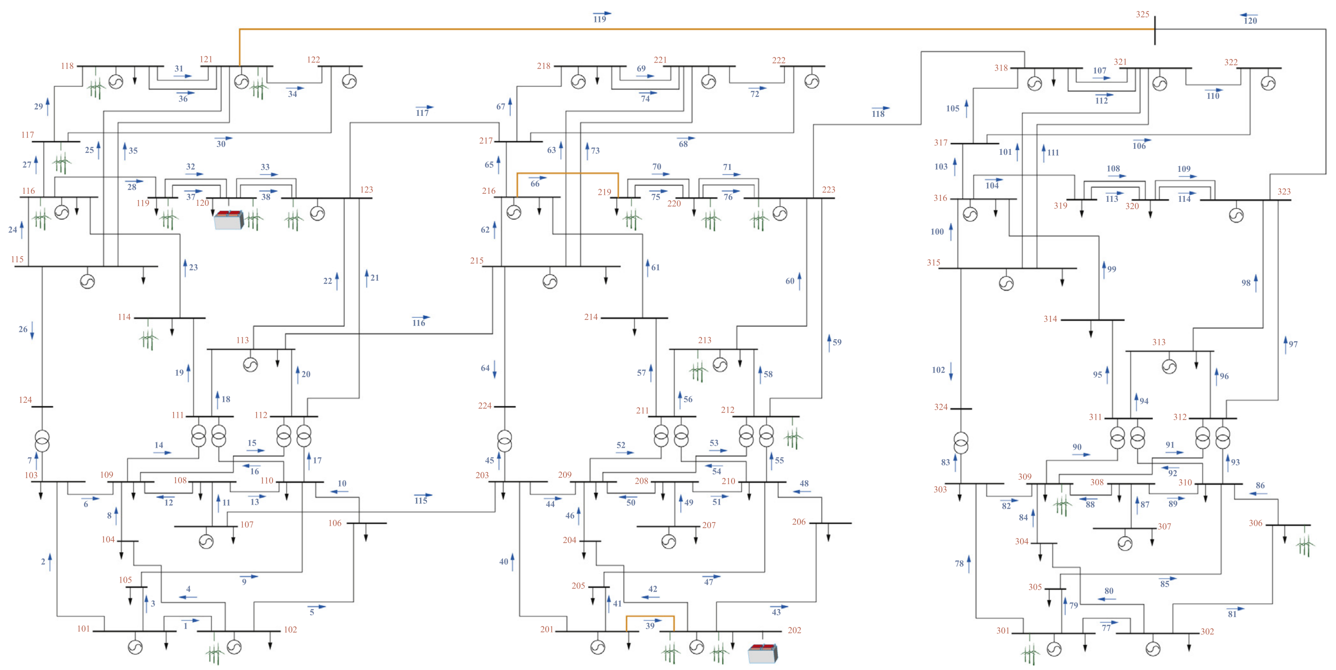

Fig. 1. IEEE RTS96 with 19 wind farms (green symbols), two energy storage units (battery symbols), and three lines with installed FACTS devices (orange color). Blue numbers represent lines, while red numbers represent bus numbers. (For interpretation of the references to colour in this figure legend, the reader is referred to the web version of this article.)

lines. Constraints (29)–(33) use binary variable $x_{t,l^{\mathrm{FACTS}}}$ to determine when there is a positive angle difference ($x_{t,l^{\mathrm{FACTS}}}$ is 1) and negative angle difference ($x_{t,l^{\mathrm{FACTS}}}$ is zero). Because of this, it is necessary to run the unit commitment without FACTS devices first to determine if there is a positive or a negative angle difference between the buses connected by the lines equipped with FACTS devices. Big M reformulation used to linearize the product of the binary and continuous variables is listed in Appendix A. Finally, constraints (34) and (35) limit voltage angles at each bus and set voltage angle at the reference bus to zero.

$$\sum_{i=1}^{I^b} p_{t,i} + \sum_{w=1}^{W^b} p_{t,w} + \sum_{s=1}^{S^b} p_{t,s}^{\mathrm{dis}} - \sum_{l=1,b(l)}^{L^b} flow_{t,l} + \sum_{l=1,n(l)}^{L^b} flow_{t,l} = D_{t,b} + \sum_{s=1}^{S^b} p_{t,s}^{\mathrm{ch}} \quad \forall\, b\in B,\, t\in T \tag{23}$$

$$flow_{t,\bar{l}} = sus_{\bar{l}}\cdot(\vartheta_{t,b}-\vartheta_{t,n}) \quad \forall\,\{b,n\}\in \bar{L},\, t\in T \tag{24}$$

$$flow_{t,\bar{l}} \leqslant flow_{\bar{l}}^{\max} \quad \forall\, \bar{l}\in \bar{L},\, t\in T \tag{25}$$

$$flow_{t,\bar{l}} \geqslant -flow_{\bar{l}}^{\max} \quad \forall\, \bar{l}\in \bar{L},\, t\in T \tag{26}$$

$$flow_{t,l^{\mathrm{FACTS}}} = sus_{t,l^{\mathrm{FACTS}}}\cdot(\vartheta_{t,b}-\vartheta_{t,n}) \quad \forall\, l^{\mathrm{FACTS}}\in L^{\mathrm{FACTS}},\, t\in T \tag{27}$$

$$sus_{l^{\mathrm{FACTS}}}^{\min} \leqslant sus_{t,l^{\mathrm{FACTS}}} \leqslant sus_{l^{\mathrm{FACTS}}}^{\max} \quad \forall\, l^{\mathrm{FACTS}}\in L^{\mathrm{FACTS}},\, t\in T \tag{28}$$

If $(\vartheta_{t,b}-\vartheta_{t,n}) \geqslant 0$:

$$sus_{l^{\mathrm{FACTS}}}^{\min}\cdot(\vartheta_{t,b}-\vartheta_{t,n}) \leqslant flow_{t,l^{\mathrm{FACTS}}} \leqslant sus_{l^{\mathrm{FACTS}}}^{\max}\cdot(\vartheta_{t,b}-\vartheta_{t,n}) \quad \forall\, l^{\mathrm{FACTS}}\in L^{\mathrm{FACTS}},\, t\in T \tag{29}$$

If $(\vartheta_b(t)-\vartheta_n(t)) \leqslant 0$

$$sus_{l^{\mathrm{FACTS}}}^{\max}\cdot(\vartheta_{t,b}-\vartheta_{t,n}) \leqslant flow_{t,l^{\mathrm{FACTS}}} \leqslant sus_{l^{\mathrm{FACTS}}}^{\min}\cdot(\vartheta_{t,b}-\vartheta_{t,n}) \quad \forall\, l^{\mathrm{FACTS}}\in L^{\mathrm{FACTS}},\, t\in T \tag{30}$$

$$(1-x_{t,l^{\mathrm{FACTS}}})\cdot sus_{l^{\mathrm{FACTS}}}^{\min} + x_{t,l^{\mathrm{FACTS}}}\cdot sus_{l^{\mathrm{FACTS}}}^{\max}\cdot(\vartheta_{t,b}-\vartheta_{t,n}) \geqslant flow_{t,l^{\mathrm{FACTS}}} \quad \forall\, l^{\mathrm{FACTS}}\in L^{\mathrm{FACTS}},\, t\in T \tag{31}$$

Table 1
Modified IEEE-RTS 96 power system.

Type	Capacity (MW)	# devices	Buses/lines
Wind farms	150	4	buses: 202,219,301,309
	300	9	buses: 102,114,118,121,123,202,212,213
	600	6	buses: 116,117,119,120,220,223
Energy Storage	150	2	buses: 120,202
FACTS	50 % X_l	3	lines: 39, 66, 119

$$(1-x_{t,l^{\mathrm{FACTS}}})\cdot sus_{l^{\mathrm{FACTS}}}^{\max} + x_{t,l^{\mathrm{FACTS}}}\cdot sus_{l^{\mathrm{FACTS}}}^{\min}\cdot(\vartheta_{t,b}-\vartheta_{t,n}) \leqslant flow_{t,l^{\mathrm{FACTS}}} \quad \forall\, l^{\mathrm{FACTS}}\in L^{\mathrm{FACTS}} \tag{32}$$

$$(1-x_{t,l^{\mathrm{FACTS}}})\cdot\vartheta_{t,n} + x_{t,l^{\mathrm{FACTS}}}\cdot\vartheta_{t,b} \geqslant (1-x_{t,l^{\mathrm{FACTS}}})\cdot\vartheta_{t,b} + x_{t,l^{\mathrm{FACTS}}}\cdot\vartheta_{t,n} \quad \forall\, l^{\mathrm{FACTS}}\in L^{\mathrm{FACTS}},\, t\in T \tag{33}$$

$$-\pi \leqslant \vartheta_{t,b} \leqslant \pi \quad \forall\, b\in B \setminus b\text{: ref. bus},\, t\in T \tag{34}$$

$$\vartheta_{t,s} = 0 \quad s\text{: ref. bus},\ \forall\, t\in T \tag{35}$$

Energy storage constraints:

The last block of constraints are energy storage constraints. Eq. (36) calculates the state of charge of each energy storage unit s at time period t, which consists of state of charge from the previous time period and charging and discharging powers at the current time period. Storage state of charge is constrained from the lower and upper side in (37). Maximum charging and discharging powers are imposed by (38) and (39), while constraint (40) disables simultaneous charging and

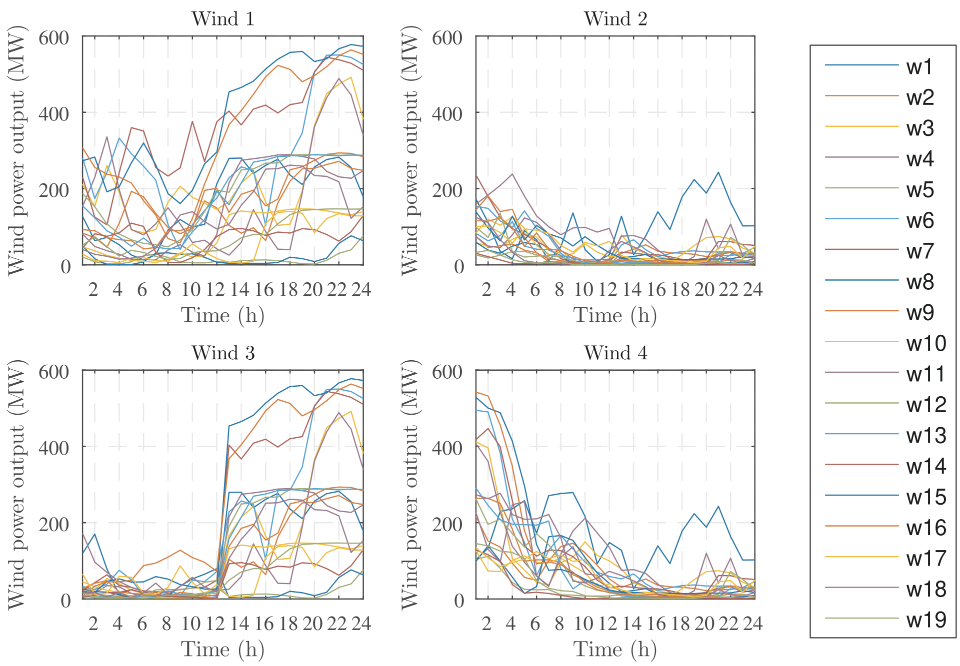

Fig. 2. Generation of 19 wind farms for all four wind scenarios.

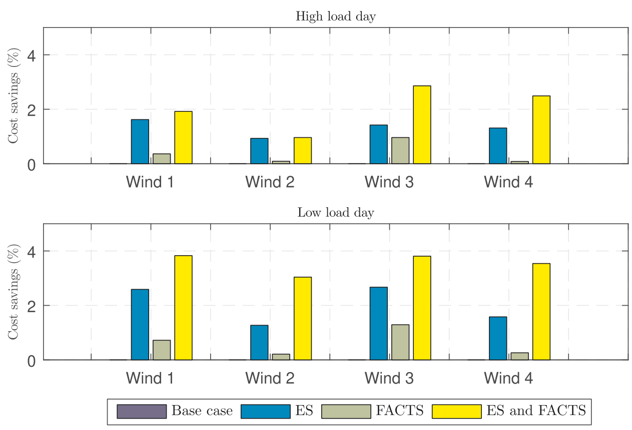

Fig. 3. Operating cost savings in all four cases for all four wind scenarios.

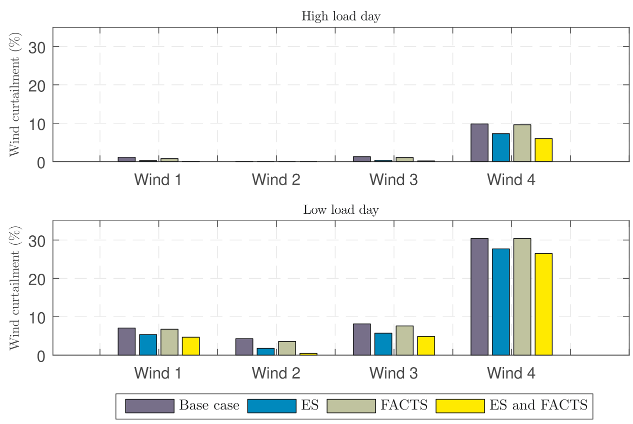

Fig. 4. Wind curtailment as a percentage of the available wind in all four cases for all four wind scenarios.

Table 2
System operating costs and wind curtailment for the high-load day.

		Wind 1	Wind 2	Wind 3	Wind 4
Case 1	Costs ($)	2,048,149	3,436,256	2,493,440	3,154,300
	Wind curtailment (MWh)	888	5	754	3,637
Case 2	Costs ($)	2,015,035	3,404,278	2,457,942	3,113,146
	Wind curtailment (MWh)	183	0	210	2,698
Case 3	Costs ($)	2,040,872	3,433,198	2,469,432	3,151,808
	Wind curtailment (MWh)	598	0	632	3,559
Case 4	Costs ($)	2,008,959	3,403,268	2,422,005	3,075,550
	Wind curtailment (MWh)	70	0	106	2,229

discharging.

$$soc_{t,s} = soc_{t-1,s} + p_{t,s}^{\mathrm{ch}} \cdot \eta_s^{\mathrm{ch}} - \frac{p_{t,s}^{\mathrm{dis}}}{\eta_s^{\mathrm{dis}}} \quad \forall\, s \in S,\, t \in T \tag{36}$$

$$soc_s^{\min} \leqslant soc_{t,s} \leqslant soc_s^{\max} \quad \forall\, s \in S,\, t \in T \tag{37}$$

$$p_{t,s}^{\mathrm{ch}} \leqslant ch_s^{\max} \cdot x_{t,s}^{\mathrm{ch}} \quad \forall\, s \in S,\, t \in T \tag{38}$$

$$p_{t,s}^{\mathrm{dis}} \leqslant dis_s^{\max} \cdot x_{t,s}^{\mathrm{dis}} \quad \forall\, s \in S,\, t \in T \tag{39}$$

$$x_{t,s}^{\mathrm{ch}} + x_{t,s}^{\mathrm{dis}} \leqslant 1 \quad \forall\, s \in S,\, t \in T \tag{40}$$

It is worth noting that, in most cases, constraint (40), as well as binary variables $x_{t,s}^{\mathrm{ch}}$ and $x_{t,s}^{\mathrm{dis}}$ in (38) and (39), can be omitted because it is not beneficial for the model to charge and discharge energy storage simultaneously. However, this can happen if the charging/discharging cycle efficiency is close to 100% and if the set optimality gap is not small enough.

Some of the energy storage devices, such as batteries, may have variable charging power limit instead of the constant one imposed by constraint (38). Also charging/discharging cycle efficiency might depend on the charging and discharging currents. However, this paper considers general energy storage constraints, which is common in power system economics studies, see [20–25].

Variable definition:

Continuous variables are defined in (41) and (42), and binary variables in (43):

$$p_{t,s}^{\mathrm{ch}},\, p_{t,s}^{\mathrm{dis}},\, p_{t,i,a},\, p_{t,i},\, p_{t,w},\, r_{t,i}^{\mathrm{down}},\, r_{t,i}^{\mathrm{up}},\, soc_{t,s} \geqslant 0 \tag{41}$$

Table 3
Number of committed generating units for all cases under the Wind 1 scenario and high-load day.

Hour	1	2	3	4	5	6	7	8	9	10	11	12	13	14	15	16	17	18	19	20	21	22	23	24
Case 1	60	45	30	21	22	36	47	48	48	48	47	44	39	37	33	33	33	33	33	32	26	26	25	22
Case 2	60	45	31	21	23	33	45	46	46	46	45	42	39	36	32	31	31	31	31	30	25	25	25	23
Case 3	60	45	29	21	23	34	48	48	48	48	48	43	40	37	33	33	33	33	32	31	27	25	23	21
Case 4	60	45	31	21	21	33	45	46	46	46	45	42	38	37	33	32	32	32	32	29	25	25	25	23

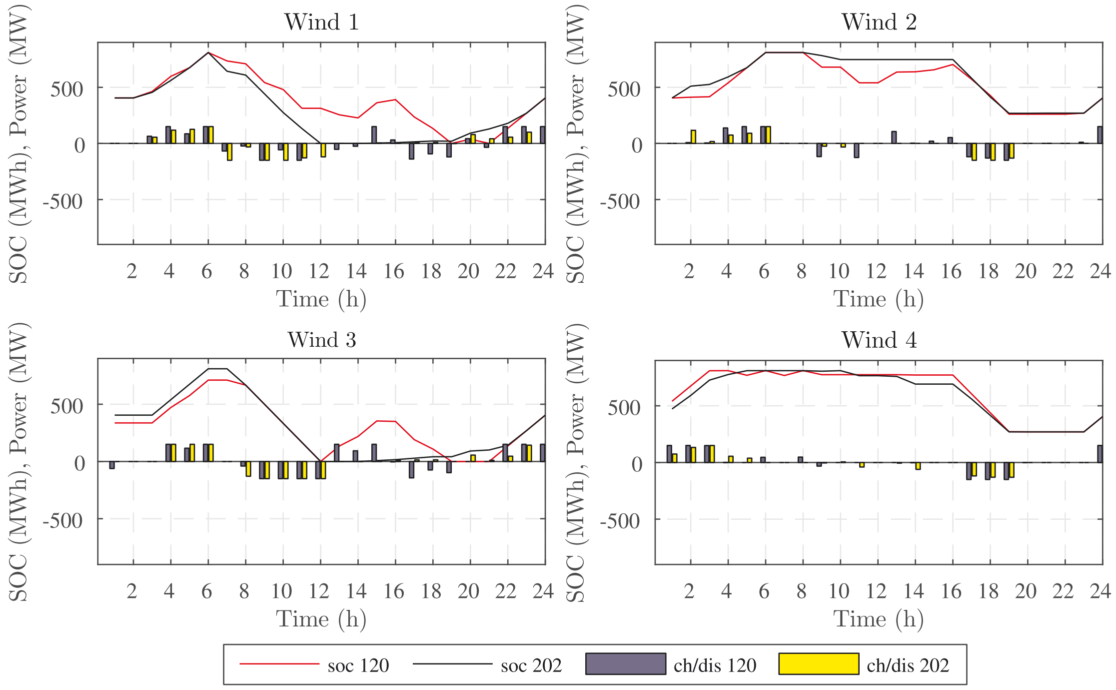

Fig. 5. Energy storage charging and discharging schedules for the high-load day – Case 2.

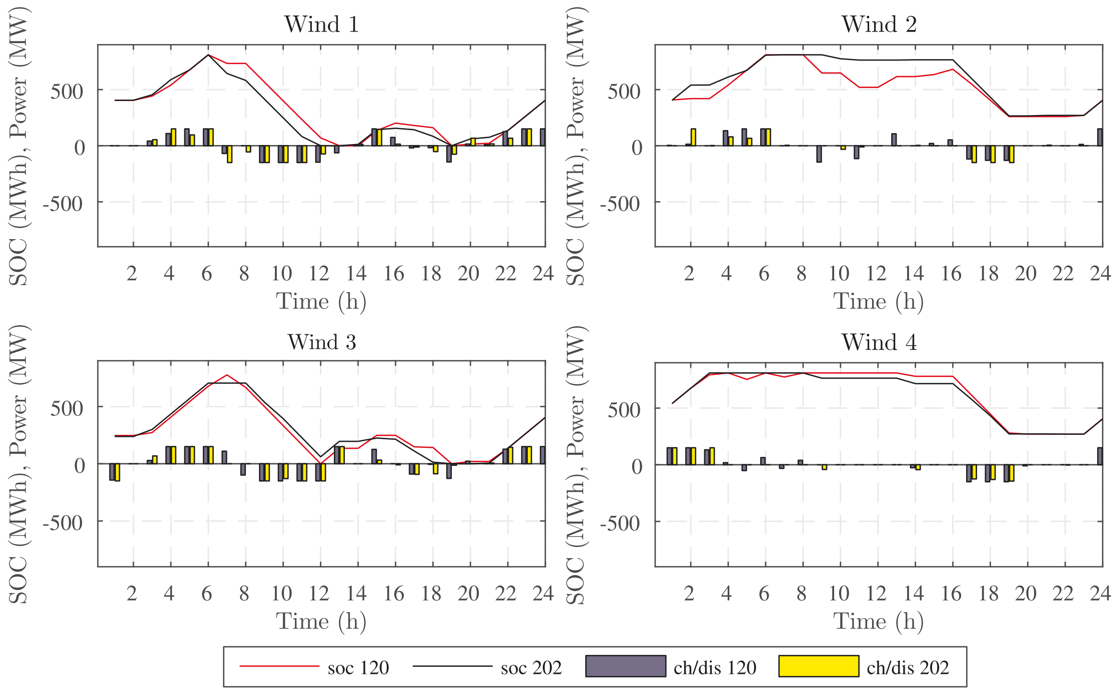

Fig. 6. Energy storage charging and discharging schedules for the high-load day – Case 4.

Table 4
System operating costs and wind curtailment for the low-load day.

		Wind 1	Wind 2	Wind 3	Wind 4
Case 1	Costs ($)	1,150,114	2,015,189	1,444,068	1,864,291
	Wind curtailment (MWh)	5,478	769	4,872	11,275
Case 2	Costs ($)	1,120,327	1,989,688	1,405,556	1,834,817
	Wind curtailment (MWh)	4,144	315	3,420	10,272
Case 3	Costs ($)	1,141,785	2,010,896	1,425,393	1,859,505
	Wind curtailment (MWh)	5,234	637	4,555	11,275
Case 4	Costs ($)	1,106,108	1,953,844	1,388,999	1,798,342
	Wind curtailment (MWh)	3,623	80	2,900	9,819

$$flow_{t,l},\ \vartheta_{t,b} \quad \text{free variable} \tag{42}$$

$$x_{t,s}^{\mathrm{ch}},\ x_{t,s}^{\mathrm{dis}},\ x_{t,l^{\mathrm{FACTS}}},\ u_{t,i},\ v_{t,i},\ z_{t,i} \in \{0,\ 1\} \tag{43}$$

3. Case study

3.1. Input data

The model presented in the previous section is tested on the three-area IEEE-RTS 96 system shown in Fig. 1. Wind farm and energy storage locations and capacity, as well as FACTS data are shown in Table 1. The detailed data on lines, load and generating units are available in [37]. All the simulations are performed at 80% of the original line capacity in order to incur congestion. The test system contains 19 wind farms with capacities 150 MW, 300 MW or 600 MW, resulting in 6,900 MW of overall capacity [24]. Both energy storage capacities are 150 MW and they are located at buses 120 and 202, as per findings of [24]. They are assumed to be of NaS type [39] with charging duration of 8 h and discharging duration of 6 h. Both the charging and the discharging efficiencies are 0.9.

Capacity of the FACTS devices is assumed to be 50% of the line reactance, which means that the reactance of these lines can be changed up to 50% in both directions. This percentage is considered to best balance between the investment cost and the achieved operating cost savings (see Fig. 3 in [26]). FACTS devices, namely the series controllers, such as TCSC, are particularly appropriate for very long power lines which are frequently congested. Therefore, it is reasonable to locate these FACTS devices at congested power lines, which are either the interconnecting lines or heavily loaded lines within one of the areas. Having this in mind, FACTS devices are assigned to lines 39, 66 and 119. Line 119 is an interconnection line between the first and the third area. First area has much more wind power than the third area, so this line is heavily loaded. The other two lines equipped with FACTS devices are within the second area, connecting buses 201 and 202 (exports abundant wind power available at bus 202) and buses 2016 and 219 (bus 219 contains a wind farm and is further connected to buses 220 and 223, both containing wind generation).

All simulations include four wind scenarios, as shown in Fig. 2. Overall available wind generation per wind scenario is as follows: 77,496 MWh in wind scenario 1, 17,960 MWh in wind scenario 2, 59,796 MWh in wind scenario 3, and 37,102 MWh in wind scenario 4. These are applied to two specific days: high load (the day with the highest daily consumption throughout the year) and low load (the day with the lowest daily consumption). The high-load day is a winter day with 187,347 MWh overall consumption, while the low-load day is an autumn day with 130,207 MWh overall consumption.

The results of four unit commitment models are represented as follows: Case (1) without energy storage or FACTS devices (base case); Case (2) with energy storage only; Case (3) with FACTS devices only; Case (4) with both FACTS devices and energy storage.

In the entire case study, it is assumed that all generators except the nuclear ones can provide reserve.

3.2. Simulation results

3.2.1. High-load day

This section analyses simulation results of the unit commitment models for the high-load day (overall consumption 187,347 MWh). Table 2 shows operating costs and wind curtailment for all four wind scenarios. Wind 1 scenario has the lowest operating costs in each case due to high available wind production, overall 77,496 MWh. On the other hand, Wind 2 scenario incurs the highest operating costs due to the low available wind generation, overall only 17,959 MWh. Operating cost savings are visualized in Fig. 3(top) with respect to the base case without energy storage and FACTS devices (Case 1). The highest savings (up to 2.86%) are achieved in Case 4 with both energy storage and FACTS devices in operation. Energy storage contributes more to these savings in all the cases. It is interesting to note that operation of only FACTS devices does not reduce operating costs significantly (only 0.08%) in Wind 2 scenario. This is the result of high production of thermal generators and low production of wind farms, which diminishes the impact of FACTS devices located in vicinity of the wind power plants.

Fig. 4(top) shows overall system wind curtailment for all four cases as a percentage of the available wind. The highest wind curtailment occurs for Wind 4 scenario due to high wind output during the first six hours, i.e. the low load time periods. The installed storage capacity is insufficient to store all the excess wind generation for later use. However, energy storage is more successful at reducing wind curtailment than the FACTS devices. Wind 1 and Wind 3 scenarios have similar wind curtailment levels because Wind 3 scenario coincides with the evening peak load, although the overall available wind generation is lower than in the Wind 1 scenario. In all four cases, the lowest levels of wind curtailment are achieved in Case 4 (combination of energy storage and FACTS devices).

Table 3 shows the number of committed thermal generating units under the Wind 1 scenario in all four Cases. Green numbers indicate less and red numbers more online generating units as compared to the base case (Case 1). In most hours, Cases 1, 2 and 3 result in the same number or fewer online generating units. Case 3 has one committed generating unit more than Case 1 in hours 5, 7, 11, 13, and 21, but in hours 3, 6, 12, 19–20, and 22–24 it commits one or two generating units less. This is because FACTS devices relieve congestion, resulting in a more efficient commitment schedule. Case 2 also commits less generating units in most time periods, but in hours 3, 5 and 24 this number is increased. To better understand this phenomenon, results from Table 3 should be compared with energy storage charging/discharging schedules in Fig. 5 (top left graph). The increase in the number of committed generator at hours 3 and 5 is the result of storage charging process at these hours.

Table 5
Number of committed generating units for all cases under the Wind 1 scenario and low-load day

Time (h)	1	2	3	4	5	6	7	8	9	10	11	12	13	14	15	16	17	18	19	20	21	22	23	24
Case 1	59	37	23	25	25	18	29	31	31	31	28	28	24	20	21	23	23	23	24	22	22	21	20	19
Case 2	59	39	23	23	24	17	25	27	27	27	25	25	20	20	22	23	22	22	24	23	23	22	20	20
Case 3	59	37	23	25	25	17	28	32	32	31	29	27	24	21	21	23	22	23	24	23	23	21	20	19
Case 4	59	39	23	23	25	17	25	27	27	26	26	25	20	20	21	22	21	22	23	22	22	21	20	19

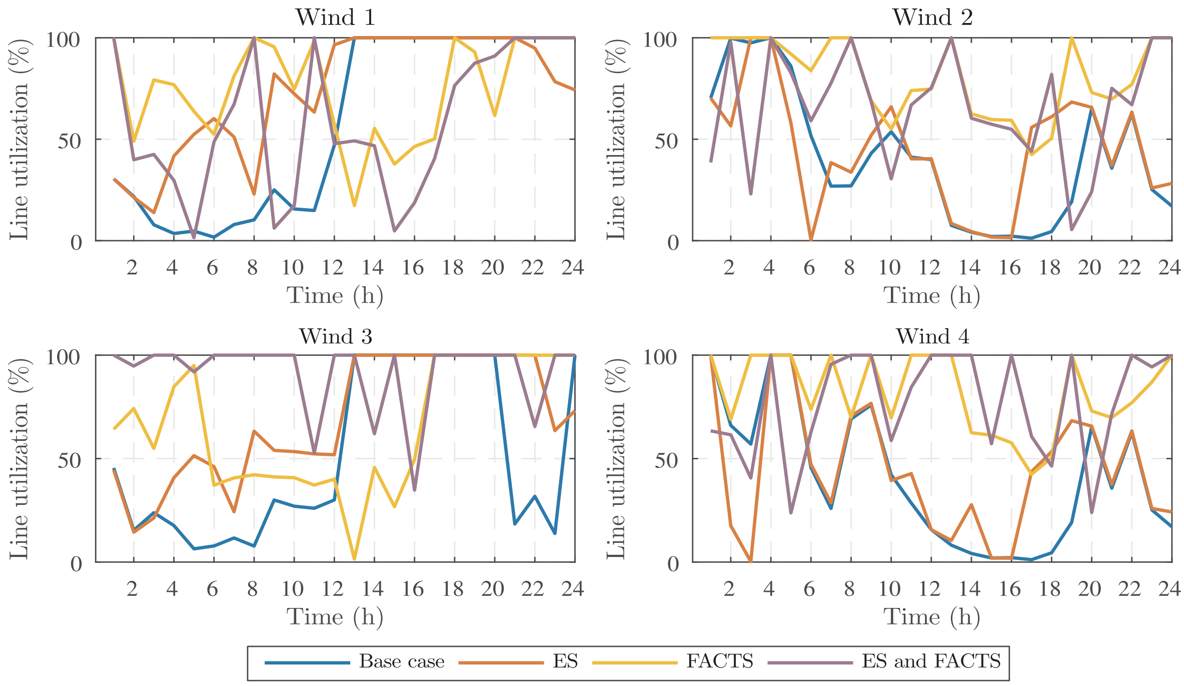

Fig. 7. Utilization of line 39 during the high-load day.

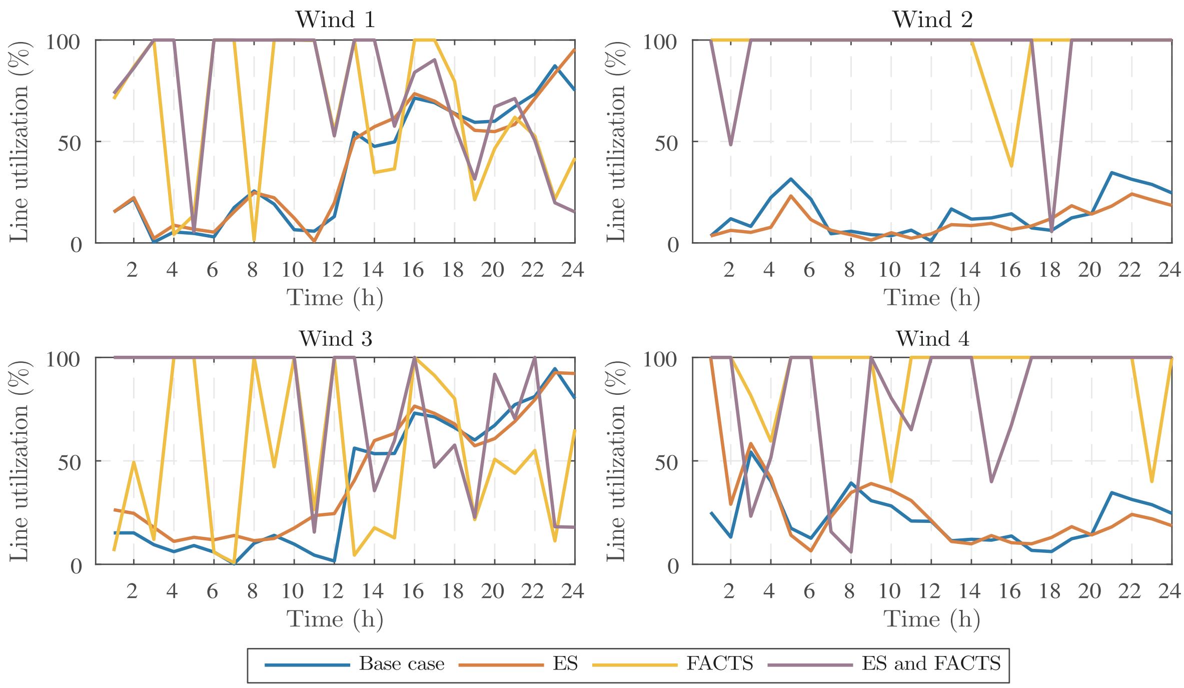

Fig. 8. Utilization of line 66 during the high-load day.

Storage unit at bus 202 completely discharges by hour 12, while the storage at bus 120 discharges at slower pace until hour 14, after which it slightly charges and then fully discharges at hour 19. These discharging actions result in a reduced number of committed generating units in the afternoon and evening hours. The increased number of committed generating units in hour 24 is because energy storage units are charging in order to meet their initial state of charge. It is important to notice that the number of committed units is not strictly proportional to storage actions, e.g. in hour 6 the storage units are being charged, but the number of committed generating units is lower than in the base case. This is due to inter-temporal constraints on generators, i.e. minimum up and down times, ramp up and down constraints, and start-up costs. Case 4, i.e. coordination of FACTS devices and energy storage, results in the least committed generating units throughout the day. The only two hours with more committed units are 3, when storage units are being charged to meet the morning peak load, and 24, when they are charged to meet the initial state of charge level.

Fig. 5 also shows energy storage scheduling for all four wind scenarios. Storage operation schedules are very similar for Wind 1 and Wind 3 (both with abundant wind levels later in the day, providing the opportunity to charge to the initial state of charge level), as well as for Wind 2 and Wind 4 (both with low wind at the end of the day, resulting in fewer charging/discharging actions). As a result, energy storage is more utilized in Wind 1 and Wind 3 scenarios. Energy storage is never

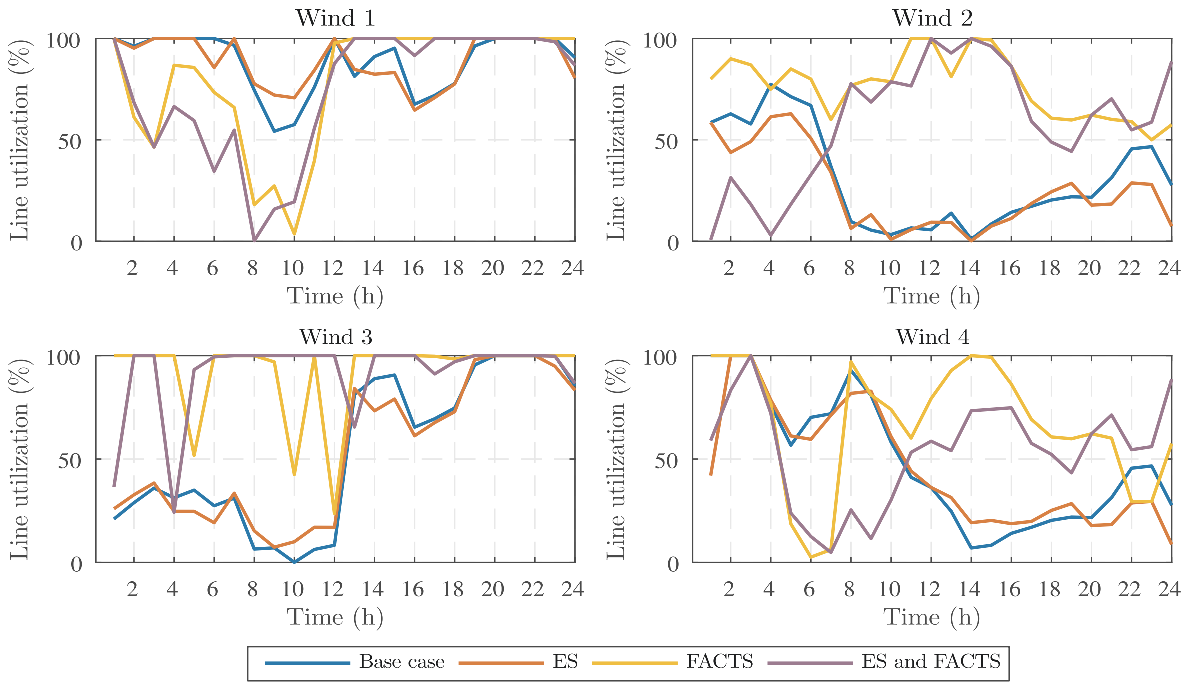

Fig. 9. Utilization of line 119 during the high-load day.

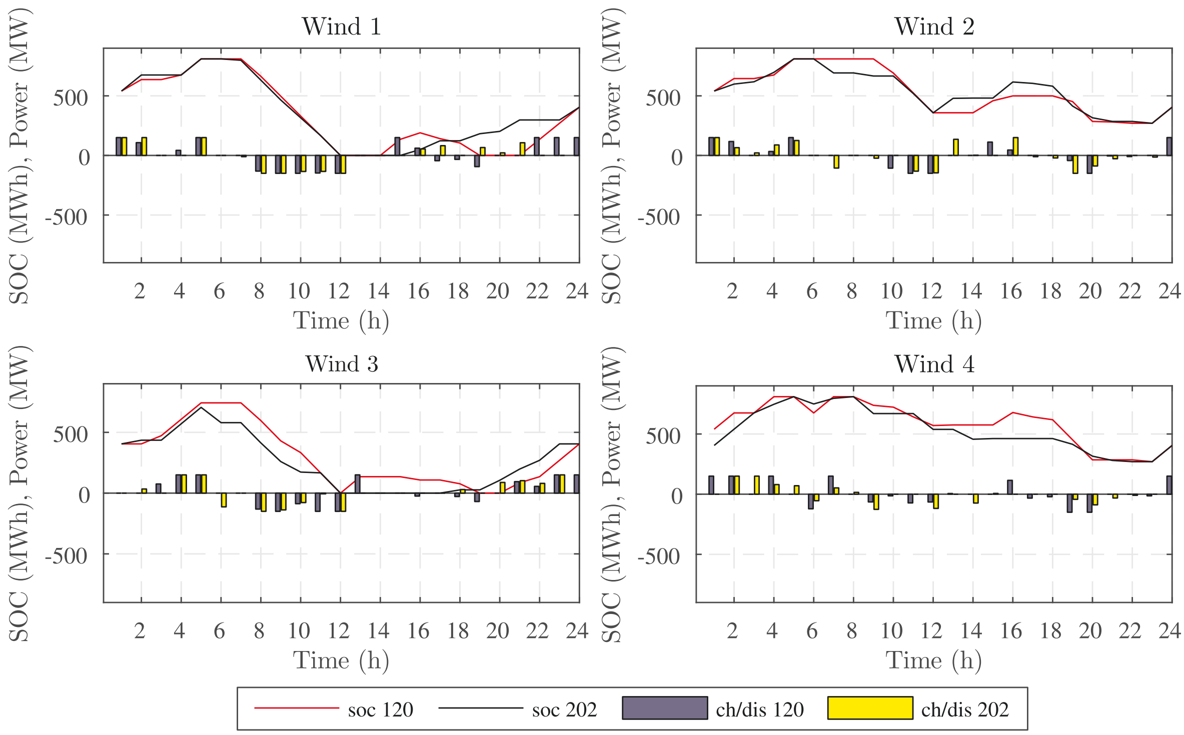

Fig. 10. Energy storage charging and discharging schedules for the low-load day – Case 2.

fully discharged in Wind 2 and Wind 4 scenarios. This is because of low wind power in the other half o the day in those two scenarios. Therefore, the stored energy is discharged during the peak-load hours 17–19.

Fig. 6 shows energy storage operation for Case 4. The charging/discharging schedules are only slightly altered by the presence of FACTS devices. The biggest difference if observed for Wind 1 scenario, where energy storage at bus 120 is fully discharged at hour 13 (there is no full discharge at hour 13 in Case 2). Also, there is a difference in Wind 3 scenario, where energy storage at bus 202 is more active in the afternoon hours instead of energy storage at bus 120, which is the opposite as in Case 2 (compare lower left graphs in Fig. 5 and 6).

To analyze power flows through lines equipped with FACTS devices, Fig. 7–9 show utilization of lines 39, 66 and 119 in all four cases and for all four wind scenarios. Line 39 for Wind 1 scenario, is more utilized in the first half of the day, as compared to the base case, and is relieved in the second half of the day. This relief is mostly caused by FACTS devices, as Case 2 keeps this line congested in hours 13–21. In Wind 2 and Wind 4 scenarios, line 39 is more utilized throughout the day, also

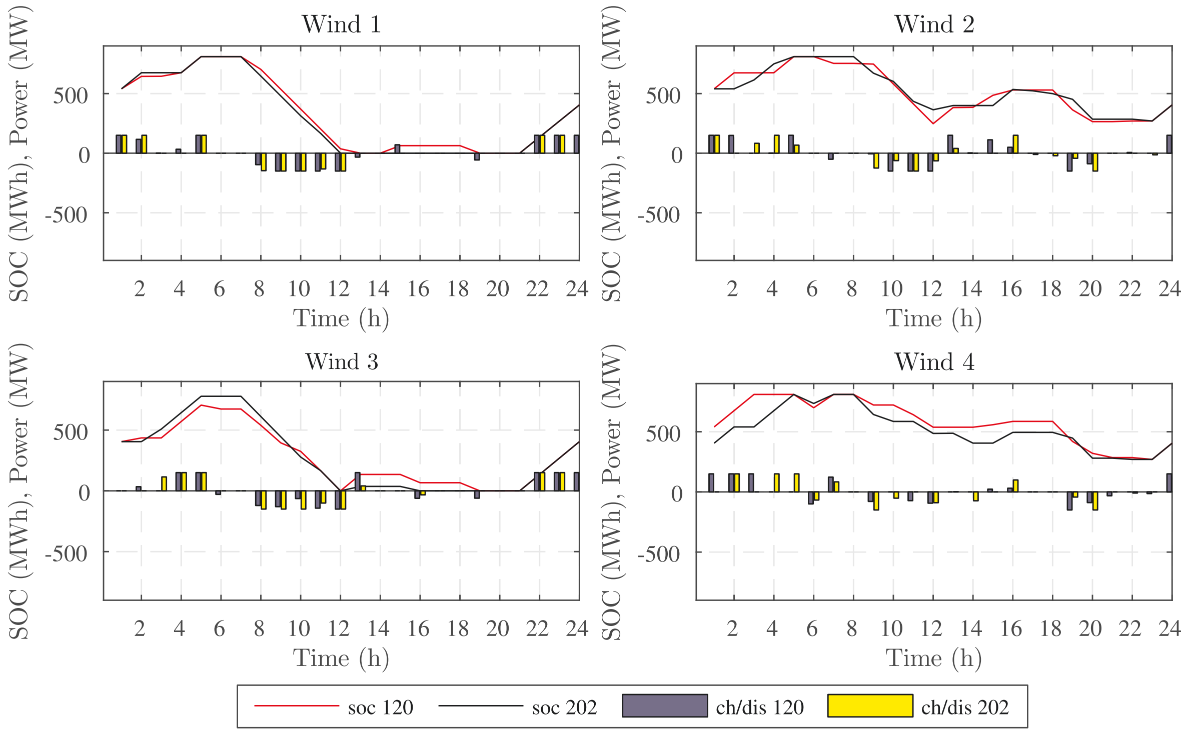

Fig. 11. Energy storage charging and discharging schedules for the low-load day – Case 4.

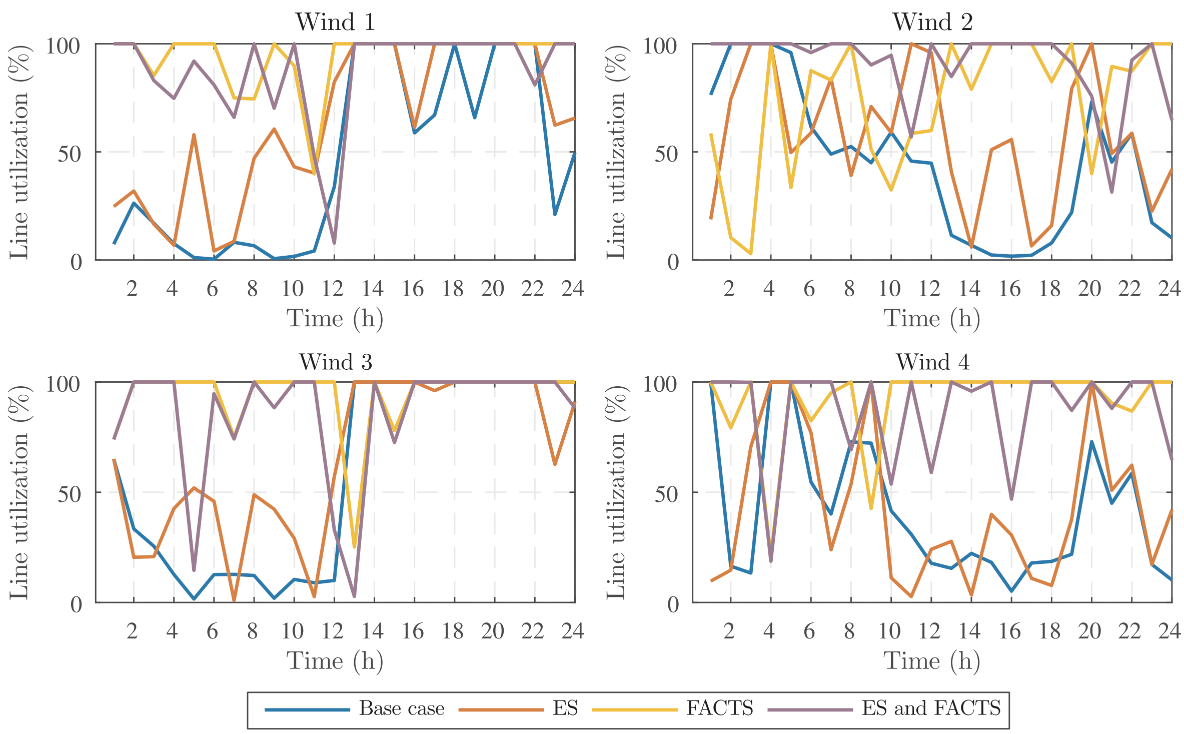

Fig. 12. Utilization of line 39 on the low-load day.

mostly as a result of optimal operation of FACTS devices. Optimal operation of FACTS device at line 66 significantly increases its loading as compared to the Cases 1 and 2, allowing higher power flows and evacuation of cheap wind power from buses 219, 220, and 223. In Fig. 9, Case 2 improves the utilization of line 119 by charging and discharging energy storage units, but this utilization is even more increased in Cases 3 and 4, where FACTS devices rearrange power flows in a more cost effective way.

3.2.2. *The low-load day*

Table 4 shows operating costs and wind curtailment for all cases and wind scenarios of the low-load day, whose daily consumption is 130,206 MWh. Generally, operating costs are lower and wind curtailment higher than on the high-load day (compare to Table 2). Again, Wind 2 scenario incurs the highest, while Wind 1 scenario incurs the lowest operating costs. Introduction of FACTS devices and energy storage reduces operating costs and wind curtailment. Cost savings

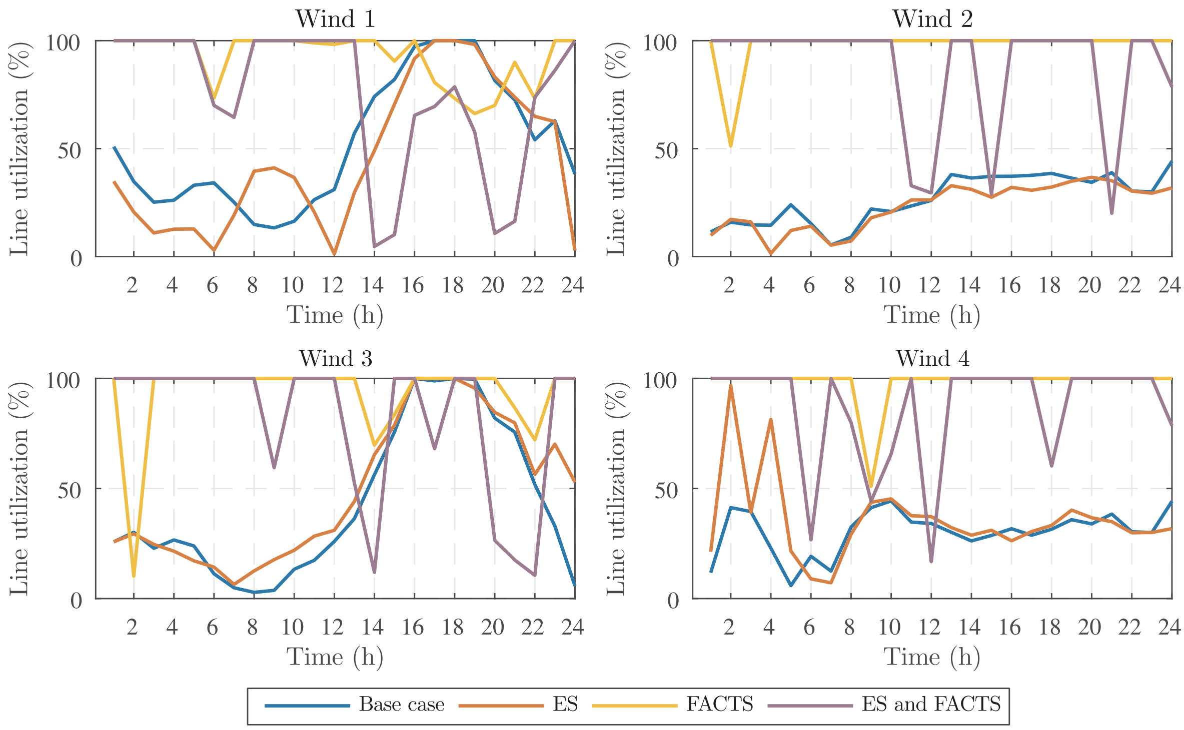

Fig. 13. Utilization of line 66 on the low-load day.

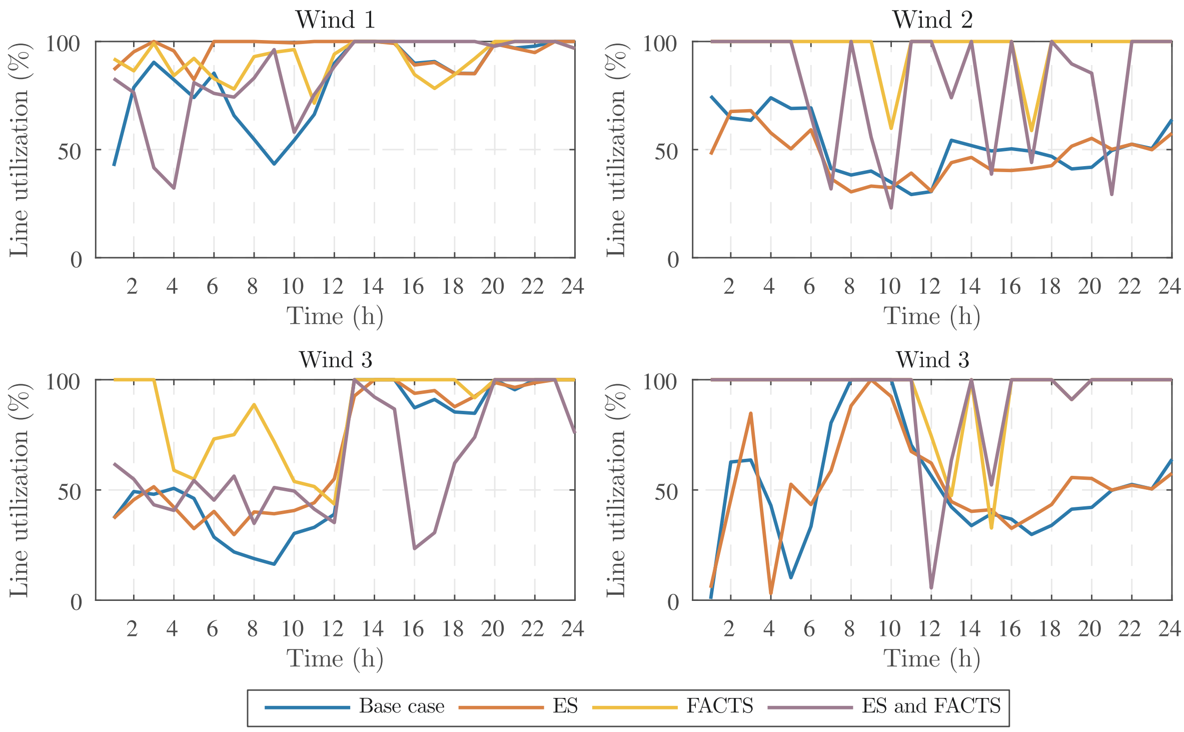

Fig. 14. Utilization of line 119 on the low-load day.

compared to Case 1 are visualized in the lower graph of Fig. 3. Maximum cost savings are 3.83% in Case 4 for the Wind 1 scenario. Similarly as in the high-load day, energy storage contributes more to cost savings, which are percentually higher than for the high-load day.

Impact of energy storage and FACTS devices on wind curtailment for the low-load day is shown in the lower graph of Fig. 4. Energy storage reduces wind curtailment much more than FACTS devices in all the cases. They are very similar to the high-load day, but with higher amounts due to a lower demand. Wind 1 and Wind 3 scenarios have similar wind curtailment level because of the similar wind production in the second part of the day (after hour 12). In Wind 4 scenario, energy storage is better at reducing wind curtailment as it takes advantage of the early morning high wind production that can be stored for later use.

Table 5 shows the number of committed generating units at each hour, where red colour presents higher and green colour lower number of committed generating units as compared to Case 1. Case 2 generally results in a lower number of committed generating units, except in hours 2, 15, 20, 22, and 24. At hours 2 and 15, energy storage units are

Table 6
System operating costs for different line rating on the high-load day

Line rating		60%	80%	100%
Wind 1	Case 1	2,078,324 (+1.47%)	2,048,149	2,042,726 (-0.26%)
	Case 2	2,045,735 (+1.52%)	2,015,035	2,040,343 (-0.23%)
	Case 3	2,058,779 (+0.87%)	2,040,872	2,038,821 (-0.10%)
	Case 4	2,027,135 (+0.91%)	2,008,959	2,007,479 (-0.07%)
Wind 2	Case 1	3,442,651 (+0.19%)	3,436,256	3,435,591 (-0.02%)
	Case 2	3,407,346 (+0.09%)	3,404,278	3,404,270 (-0.00%)
	Case 3	3,435,349 (+0.06%)	3,433,198	3,433,182 (-0.00%)
	Case 4	3,405,693 (+0.07%)	3,403,268	3,403,213 (-0.00%)
Wind 3	Case 1	2,527,094 (+1.35%)	2,493,440	2,487,574 (-0.24%)
	Case 2	2,486,793 (+1.17%)	2,457,942	2,454,094 (-0.16%)
	Case 3	2,484,838 (+0.63%)	2,469,432	2,467,586 (-0.07%)
	Case 4	2,438,175 (+0.67%)	2,422,005	2,420,738 (-0.05%)
Wind 4	Case 1	3,161,123 (+0.22%)	3,154,300	3,153,659 (-0.02%)
	Case 2	3,117,410 (+0.14%)	3,113,146	3,112,580 (-0.01%)
	Case 3	3,155,585 (+0.12%)	3,151,808	3,151,577 (-0.00%)
	Case 4	3,079,955 (+0.14%)	3,075,550	3,075,510 (-0.00%)

being charged (upper left graph in Fig. 10), resulting in a higher net load. The charging of energy storage to meet the initial state of charge level results in a higher number of committed generating units at hours 20, 22 and 24. Operation of FACTS devices (Case 3) results with one committed generating unit more than in Case 1 in hours 8, 9 and 11. Combination of FACTS devices and energy storage in Case 4 results in the lowest number of committed generating units throughout the day except in hour 2 due to charging of generating units (upper left graph in Fig. 11).

Figs. 10 and 11 indicate more active storage operation for Wind 1 and Wind 3 scenarios as compared to Wind 2 and Wind 4 scenarios. However, in comparison to the high-load day (Fig. 7 and 8), Wind 2 and Wind 4 scenarios result in more storage charging/discharging actions. Again, because of the significantly lower wind production, energy storage is never fully discharged in these scenarios.

Utilization of lines 39, 66 and 119 are presented in Figs. 12–14. Similarly to the high-load day, energy storage and FACTS devices increase utilization of these lines, thus transferring more electricity from wind farms to load centres and reducing wind curtailment. Lines 39 and 66 are less utilized in the first half of the day in scenarios Wind 1 and Wind 3. Introduction of energy storage (Case 2) slightly increases the loading of these lines in the first half of the day. However, FACTS devices change power flows in a way to significantly increase the loading of these lines (Case 3 and Case 4). Another example how FACTS devices increase loading of transmission lines is the loading of line 66 (Fig. 13) under Wind 2 and Wind 4 scenarios.

3.3. Sensitivity analysis

Sensitivity analysis is performed by three different line capacity cases: 100%, 80% (the one used in the previous subsection) and 60% of original line capacity of IEEE RTS96. Comparison of operating costs is shown in Table 6. The results indicate that line ratings have highest impact on the system operating cost for Wind 1 and Wind 3 scenarios. Reducing line ratings in Wind 1 scenario from 80% to 60% results in 1.47% higher operating costs for the base case (Case 1), while in Case 4 the operating costs are 0.9% higher. On the other hand, increased line rating (80% - > 100%) result in lower savings in operating costs (up to 0.26%). The differences in operating costs for different line ratings in Wind 2 scenario are much more modest (up to 0.19%). Again, they are the highest for Case 1. Results for Wind 3 scenario are very similar to the ones for Wind 1 scenario due to high wind output that cannot reach the load centers due to congestion. Under Wind 4 scenario, the objective function changes only slightly with the change of the line ratings, similarly as under the Wind 2 scenario.

Wind curtailment for different line ratings is shown in Fig. 15. For Wind 1 scenario,and line ratings 60%, combination of FACTS devices and energy storage can reduce wind curtailment from 3.9% to 2.8%. Wind curtailment is much lower for 80% line ratings, while for 100% line ratings energy storage can almost completely eliminate wind curtailment. In Wind 2 scenario, only the base case has a small amount of wind curtailment for line ratings 60% and 80%. Wind curtailment levels in Wind 3 scenario are very similar to the ones in Wind 1 scenario,

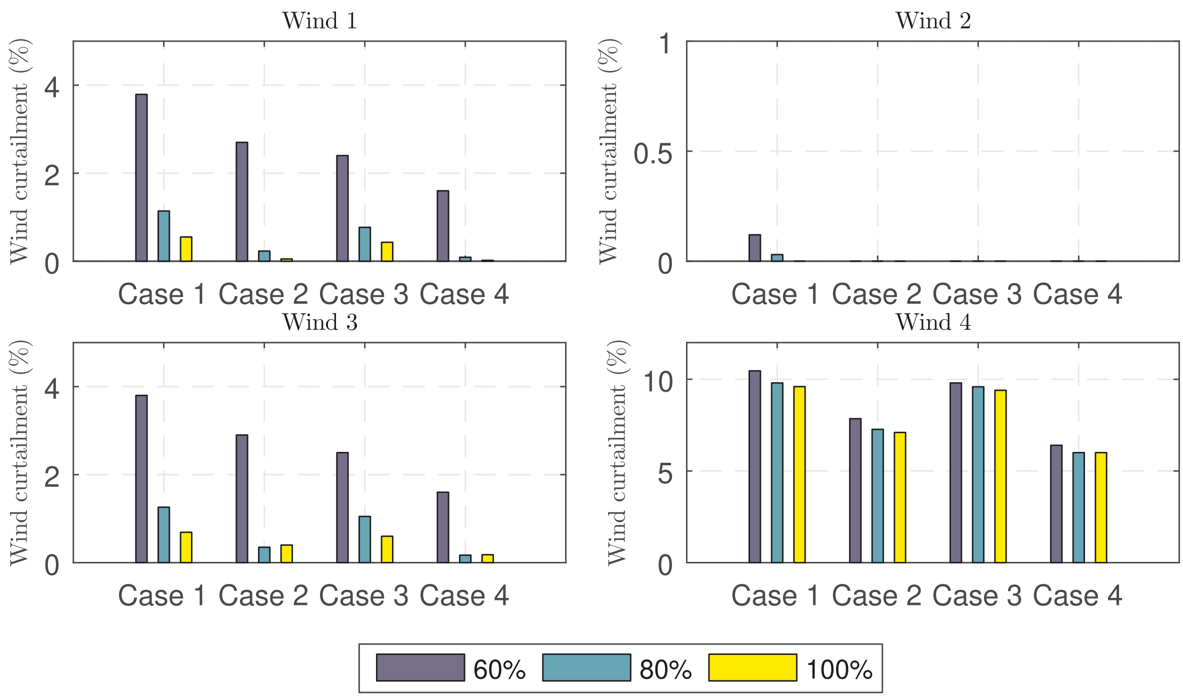

Fig. 15. Sensitivity analysis of wind curtailment in percentage of the available wind for three line ratings on the high-load day.

with the difference that even storage cannot completely eliminate wind curtailment. Wind 4 scenario results in the highest wind curtailment levels, but increased line ratings do not severely reduce them.

4. Conclusions

This paper presented four different unit commitment models considering energy storage and FACTS devices. The following conclusions are derived:

- Energy storage is more efficient at reducing system operating costs than FACTS devices, while the wind curtailment is effectively reduced by both technologies. However, the effectiveness of energy storage at reducing system operating costs and wind curtailment significantly depends on the wind profile.
- FACTS devices can significantly increase line loadings, though a large number of these devices is needed in order to effectively control power flows in the entire system.
- Both energy storage and FACTS devices are efficient at reducing the number of committed generating units. The highest reduction in the number of committed generating units is achieved in the case of their coordinated operation. However, energy storage can increase the number of committed generating units at certain time periods due to charging requirements.
- Although energy storage outperformed FACTS devices in the presented case study, energy storage is a more expensive technology than FACTS. Considering the FACTS prices from [40] and assuming NaS battery cost to be $450/kWh, the overall installation cost of the FACTS devices in the case study is M$17.7, while the installation costs of energy storage is over M$405. This indicates that, at least for the case study at hand, FACTS devices are economically more viable option.

Future work will be focused on implementation of AC power flow model, which will enable to assess the impact of energy storage and FACTS devices on voltage levels and reactive power flows. Also, an important line of research is implementation of a security constrained unit commitment model. Energy storage and FACTS devices could act quickly after a contingency in a corrective manner in order to provide enough time to the system operator to perform re-dispatch of the generators. Another line of research worth pursuing is finding an optimal investment in FACTS devices and energy storage in terms of the locations and capacities.

Acknowledgement

This work has been supported in part by Croatian Science Foundation and Croatian Transmission Operator System (HOPS) under the project Smart Integration of RENewables – SIREN (I-2583-2015) and through European Union's Horizon 2020 research and innovation program under project CROSSBOW – CROSS BOrder management of variable renewable energies and storage units enabling a transnational Wholesale market (Grant No. 773430).

Appendix A. Big M formulation

In order to linearize the product of binary variable $x_{t,l^{\mathrm{FACTS}}}$ and continuous variable $\vartheta_{t,b}$, the following big M reformulation is used:

$$x_{t,l^{\mathrm{FACTS}}}\cdot sus_{l^{\mathrm{FACTS}}}^{\min}\cdot(\vartheta_{t,b}-\vartheta_{t,n})-(1-x_{t,l^{\mathrm{FACTS}}})\cdot M \leqslant flow_{t,l^{\mathrm{FACTS}}} \quad \forall\, l^{\mathrm{FACTS}} \in L^{\mathrm{FACTS}},\, t \in T \tag{A.1}$$

$$(1-x_{t,l^{\mathrm{FACTS}}})\cdot sus_{l^{\mathrm{FACTS}}}^{\max}\cdot(\vartheta_{t,b}-\vartheta_{t,n})-x_{t,l^{\mathrm{FACTS}}}\cdot M \leqslant flow_{t,l^{\mathrm{FACTS}}} \quad \forall\, l^{\mathrm{FACTS}} \in L^{\mathrm{FACTS}},\, t \in T \tag{A.2}$$

$$x_{t,l^{\mathrm{FACTS}}}\cdot sus_{l^{\mathrm{FACTS}}}^{\max}\cdot(\vartheta_{t,b}-\vartheta_{t,n}) + (1-x_{t,l^{\mathrm{FACTS}}})\cdot M \geqslant flow_{t,l^{\mathrm{FACTS}}} \quad \forall\, l^{\mathrm{FACTS}} \in L^{\mathrm{FACTS}},\, t \in T \tag{A.3}$$

$$(1-x_{t,l^{\mathrm{FACTS}}})\cdot sus_{l^{\mathrm{FACTS}}}^{\min}\cdot(\vartheta_{t,b}-\vartheta_{t,n}) + x_{t,l^{\mathrm{FACTS}}}\cdot M \geqslant flow_{t,l^{\mathrm{FACTS}}} \quad \forall\, l^{\mathrm{FACTS}} \in L^{\mathrm{FACTS}},\, t \in T \tag{A.4}$$

$$\vartheta_{t,b} + (1-x_{t,l^{\mathrm{FACTS}}})\cdot M \geqslant \vartheta_{t,n} \;\forall\, l^{\mathrm{FACTS}} \in L^{\mathrm{FACTS}},\, t \in T \tag{A.5}$$

$$\vartheta_{t,n} + x_{t,l^{\mathrm{FACTS}}}\cdot M \geqslant \vartheta_{t,b} \quad \forall\, l^{\mathrm{FACTS}} \in L^{\mathrm{FACTS}},\, t \in T \tag{A.6}$$

$$M > \max\{flow_{t,l} + sus_l\cdot(\vartheta_{t,n}-\vartheta_{t,b})\} \tag{A.7}$$

References

[1] Commission IE, et al., Grid integration of large capacity renewable energy sources and use of large-capacity electrical energy storage, IEC White Paper, Geneva: International Electrotechnical Commission,www.iec.ch/whitepaper/pdf/iecWP-gridintegrationlargecapacity-LR-en.pdf (last accessed March 2015).
[2] Punda L, Capuder T, Pandžić H, Delimar M. Integration of renewable energy sources in southeast Europe: a review of incentive mechanisms and feasibility of investments. Renew Sustainable Energy Rev 2017;71:77–88. https://doi.org/10.1016/j.rser.2017.01.008.
[3] Zbunjak Z, Bašić H, Pandžić H, Kuzle I, autotransformer Phase shifting. transmission switching and battery energy storage systems to ensure n-1 criterion of stability. Energija: časopis Hrvatske elektroprivrede 2015;64:285. doi:http://journalofenergy.com/specIss/JournalofEnergy2015VOL64.pdf.
[4] Mathur RM, Varma RK. Thyristor-based FACTS controllers for electrical transmission systems. John Wiley & Sons; 2002. URLhttp://research.iaun.ac.ir/pd/bahador.fani/pdfs/UploadFile8100.pdf.
[5] Morales-España G, Raírez-Elizondo L, Hobbs BF. Hidden power system inflexibilities imposed by traditional unit commitment formulations. Appl Energy 2017;191:223–38. https://doi.org/10.1016/j.apenergy.2017.01.089.
[6] Wang J, Wang J, Liu C, Ruiz JP. Stochastic unit commitment with sub-hourly dispatch constraints. Appl Energy 2013;105:418–22. https://doi.org/10.1016/j.apenergy.2013.01.008.
[7] Yang Y, Wang J, Guan X, Zhai Q. Subhourly unit commitment with feasible energy delivery constraints. Appl Energy 2012;96:245–52. https://doi.org/10.1016/j.apenergy.2011.11.008.
[8] Wang J, Botterud A, Bessa R, Keko H, Carvalho L, Issicaba D, Sumaili J, Miranda V. Wind power forecasting uncertainty and unit commitment. Appl Energy 2011;88(11):4014–23. https://doi.org/10.1016/j.apenergy.2011.04.011.
[9] Delarue E, D'haeseleer W. Adaptive mixed-integer programming unit commitment strategy for determining the value of forecasting. Appl Energy 2008;85(4):171–81. https://doi.org/10.1016/j.apenergy.2007.07.007.
[10] Quan H, Srinivasan D, Khambadkone AM, Khosravi A. A computational framework for uncertainty integration in stochastic unit commitment with intermittent renewable energy sources. Appl Energy 2015;152:71–82. https://doi.org/10.1016/j.apenergy.2015.04.103.
[11] Luburić Z, Pandžić H, Plavšić T. Comparison of energy storage operation in vertically integrated and market-based power system. 2016 IEEE 16th International Conference on Environment and Electrical Engineering (EEEIC) IEEE; 2016. p. 1–6. https://doi.org/10.1109/EEEIC.2016.7555524.
[12] Sioshansi R. Using storage-capacity rights to overcome the cost-recovery hurdle for energy storage. IEEE Trans Power Syst 2017;32(3):2028–40. https://doi.org/10.1109/TPWRS.2016.2607153.
[13] Pandžić H, Kuzle I. Energy storage operation in the day-ahead electricity market. 2015 12th International Conference on the European Energy Market (EEM) IEEE; 2015. p. 1–6. https://doi.org/10.1109/EEM.2015.7216754.
[14] Kefayati M, Baldick R. On optimal operation of storage devices under stochastic market prices. 2013 IEEE 52nd Annual Conference on Decision and Control (CDC) IEEE; 2013. p. 7576–81. https://doi.org/10.1109/CDC.2013.6761092.

[15] Akhavan-Hejazi H, Mohsenian-Rad H. Optimal operation of independent storage systems in energy and reserve markets with high wind penetration. IEEE Trans Smart Grid 2014;5(2):1088–97. https://doi.org/10.1109/TSG.2013.2273800.
[16] Zhang F, Hu Z, Song Y. Mixed-integer linear model for transmission expansion planning with line losses and energy storage systems. IET Gener, Trans Distrib 2013;7(8):919–28. https://doi.org/10.1049/iet-gtd.2012.0666.
[17] Dicorato M, Forte G, Pisani M, Trovato M. Planning and operating combined wind-storage system in electricity market. IEEE Trans Sustainable Energy 2012;3(2):209–17. https://doi.org/10.1109/TSTE.2011.2179953.
[18] Khatod DK, Pant V, Sharma J. Optimized daily scheduling of wind-pumped hydro plants for a day-ahead electricity market system. 2009. ICPS'09. International Conference on Power Systems IEEE; 2009. p. 1–6. https://doi.org/10.1109/ICPWS.2009.5442767.
[19] Beaudin M, Zareipour H, Schellenberglabe A, Rosehart W. Energy storage for mitigating the variability of renewable electricity sources: an updated review. Energy Sustainable Devel 2010;14(4):302–14. https://doi.org/10.1016/j.esd.2010.09.007.
[20] JohnsonRobertDe JX, Keoleian KA. Assessment of energy storage for transmission-constrained wind. Appl Energy 2014;124:377–88. https://doi.org/10.1016/j.apenergy.2014.03.006.
[21] Wang W, Li C, Liao X, Qin H. Study on unit commitment problem considering pumped storage and renewable energy via a novel binary artificial sheep algorithm. Appl Energy 2017;187:612–26. https://doi.org/10.1016/j.apenergy.2016.11.085.
[22] Bruninx K, Dvorkin Y, Delarue E, Pandžić H, D'haeseleer W, Kirschen DS. Coupling pumped hydro energy storage with unit commitment. IEEE Trans Sustainable Energy 2016;7(2):786–96. https://doi.org/10.1109/TSTE.2015.2498555.
[23] Pudjianto D, Aunedi M, Djapic P, Strbac G. Whole-systems assessment of the value of energy storage in low-carbon electricity systems. IEEE Trans Smart Grid 2014;5(2):1098–109. https://doi.org/10.1109/TSG.2013.2282039.
[24] Pandžić H, Wang Y, Qiu T, Dvorkin Y, Kirschen DS. Near-optimal method for siting and sizing of distributed storage in a transmission network. IEEE Trans Power Syst 2015;30(5):2288–300. https://doi.org/10.1109/TPWRS.2014.2364257.
[25] Fiorini L, Pagani GA, Pelacchi P, Poli D, Aiello M. Sizing and siting of large-scale batteries in transmission grids to optimize the use of renewables. IEEE J Emerging Selected Topics Circuits Syst 2017;7(2):285–94. https://doi.org/10.1109/JETCAS.2017.2657795.
[26] Sahraei-Ardakani M, Hedman KW. A fast lp approach for enhanced utilization of variable impedance based facts devices. IEEE Trans Power Syst 2016;31(3):2204–13. https://doi.org/10.1109/PESGM.2016.7741200.
[27] Sahraei-Ardakani M, Hedman KW. Day-ahead corrective adjustment of facts reactance: a linear programming approach. IEEE Trans Power Syst 2016;31(4):2867–75. https://doi.org/10.1109/TPWRS.2015.2475700.
[28] Ding T, Bo R, Li F, Sun H. Optimal power flow with the consideration of flexible transmission line impedance. IEEE Trans Power Syst 2016;31(2):1655–6. https://doi.org/10.1109/TPWRS.2015.2412682.
[29] Nasri A, Conejo AJ, Kazempour SJ, Ghandhari M. Minimizing wind power spillage using an opf with facts devices. IEEE Trans Power Syst 2014;29(5):2150–9. https://doi.org/10.1109/TPWRS.2014.2299533.
[30] Meikandasivam S, Nema RK, Jain SK. Fine power flow control by split tcsc. Int J Electr Power Energy Syst 2013;45(1):519–29. https://doi.org/10.1016/j.ijepes.2012.09.012.
[31] Gupta A, Kumar A. Impact of tcsc installation on atc in a system incorporating wind and hydro generations. Procedia Technol 2016;25:743–50. https://doi.org/10.1016/j.protcy.2016.08.168.
[32] Dawn S, Tiwari PK. Improvement of economic profit by optimal allocation of tcsc & upfc with wind power generators in double auction competitive power market. Int J Electr Power Energy Syst 2016;80:190–201. https://doi.org/10.1016/j.ijepes.2016.01.041.
[33] Zarate-Minano R, Conejo A, Milano F. Opf-based security redispatching including facts devices. IET Gener, Transm, Distrib 2008;2(6):821–33. https://doi.org/10.1049/iet-gtd:20080064.
[34] Choudhury NBD, Jena R. Available transfer capability enhancement in constrained network conditions using tcsc. 2014 International Conference on Advances in Engineering and Technology Research (ICAETR) IEEE; 2014. p. 1–7. https://doi.org/10.1109/ICAETR.2014.7012804.
[35] Xiao Y, Song Y, Liu C-C, Sun Y. Available transfer capability enhancement using facts devices. IEEE Trans Power Syst 2003;18(1):305–12. https://doi.org/10.1109/TPWRS.2002.807073.
[36] Gerbex S, Cherkaoui R, Germond AJ. Optimal location of multi-type facts devices in a power system by means of genetic algorithms. IEEE Trans Power Syst 2001;16(3):537–44. https://doi.org/10.1109/PICA.2001.932321.
[37] Pandzic H, Qiu T, Kirschen DS. Comparison of state-of-the-art transmission constrained unit commitment formulations. Power and Energy Society General Meeting (PES), 2013 IEEE IEEE; 2013. p. 1–5. https://doi.org/10.1109/PESMG.2013.6672719.
[38] Western wind and solar integration study, Tech. rep., National Renewable Energy Lab. (NREL), Golden, CO (United States), 2010.
[39] Zarate-Minano R, Conejo A, Milano F. Opf-based security redispatching including facts devices. IET Gener, Trans, Distrib 2008;2(6):821–33. https://doi.org/10.1049/iet-gtd:20080064.
[40] Cai LJ, Erlich I, Stamtsis G. Optimal choice and allocation of facts devices in deregulated electricity market using genetic algorithms. IEEE PES Power Systems Conference and Exposition, 2004, vol. 1. 2004. p. 201–7. https://doi.org/10.1109/PSCE.2004.1397562.

Article 3 - Transmission Expansion Planning Model Considering Battery Energy Storage, TCSC and Lines Using AC OPF

Luburić, Zora; Pandžić, Hrvoje; Carrión, Miguel, "Transmission Expansion Planning Model Considering Battery Energy Storage, TCSC and Lines Using AC OPF," IEEE Access, vol. 8, pp. 203429-203439, 2020
DOI: 10.1109/ACCESS.2020.3036381.

– 10 pages

IEEE Access
Multidisciplinary | Rapid Review | Open Access Journal

Received October 16, 2020, accepted November 2, 2020, date of publication November 6, 2020, date of current version November 19, 2020.

Digital Object Identifier 10.1109/ACCESS.2020.3036381

Transmission Expansion Planning Model Considering Battery Energy Storage, TCSC and Lines Using AC OPF

ZORA LUBURIĆ[1], (Member, IEEE), HRVOJE PANDŽIĆ[2,3], (Senior Member, IEEE), AND MIGUEL CARRIÓN[4], (Member, IEEE)

[1]Croatian Transmission System Operator-HOPS, 10000 Zagreb, Croatia
[2]Innovation Centre Nikola Tesla, 10000 Zagreb, Croatia
[3]Faculty of Electrical Engineering and Computing, University of Zagreb, 10000 Zagreb, Croatia
[4]School of Industrial and Aerospace Engineering, University of Castilla-La Mancha, 13001 Toledo, Spain

Corresponding author: Zora Luburić (zora.luburic@hops.hr)

The research leading to these results has received funding from the European Union's Horizon 2020 research and innovation programme under grant agreement No 864298 (project ATTEST). The sole responsibility for the content of this document lies with the authors. It does not necessarily reflect the opinion of the Innovation and Networks Executive Agency (INEA) or the European Commission (EC). INEA or the EC are not responsible for any use that may be made of the information contained therein.

ABSTRACT Flexibility has become a requirement for modern power systems dominated by renewable generation sources. It can be extracted from different assets, ranging from demand response to fast generating units. This paper proposes an investment model that finds an optimal mix of transmission-level non-generation flexible assets: battery energy storage (BES), thyristor-controlled series compensators (TCSC), and transmission lines. The role of BES is to offset renewable generation in time, but its power converter is additionally utilized to provide voltage regulation by injecting/withdrawing reactive power. TCSC is used to alter power flows and increase existing lines' capacity, while new power lines are used to increase bulk power transfer. The proposed planning model uses a linearized AC OPF and employs Benders' decomposition to develop an iterative procedure for obtaining the optimal solution. The presented case study illustrates usefulness of the model for different BES costs and investment policies.

INDEX TERMS Battery energy storage, Benders' decomposition, FACTS devices, TCSC, transmission planning.

NOMENCLATURE

A. SETS

Ω^D	Set of representative days indexed with d
Ω^G	Set of piecewise blocks indexed with g
Ω^I	Set of thermal generators indexed with i
Ω^L	Set of lines consisting of existing lines, existing lines with TCSC and new lines $\Omega^L = \Omega^{L^{\text{EX}}} \cup \Omega^{L^{\text{TCSC}}} \cup \Omega^{L^{\text{NEW}}}$ and indexed with l
Ω^N	Set of network buses indexed with n
Ω^R	Set of R-sided convex polygon slices indexed with r
Ω^S	Set of BES units indexed with s
Ω^T	Set of time periods indexed with t
Ω^W	Set of wind farms indexed with w
Ω^Z	Set of TCSC compensation blocks indexed with z

The associate editor coordinating the review of this manuscript and approving it for publication was S. Ali Arefifar.

B. VARIABLES

$ch_s^{\max}$	Rated power of converter of BES unit s (MVA)
$p_{d,t,s}^{\text{ch/dis}}$	Active (dis)charging power of BES s in period t on day d (MW)
$p_{d,t,l}^{\text{nm/mn}}$	Active power flow through line l from bus $n(m)$ to bus $m(n)$ in period t on day d (MW)
$\Delta p_{d,t,l}^{\text{TCSC, max}}$	Active power flow through line l with TCSC in period t on day d (MW)
$pg_{d,t,i}$	Active power output of thermal generator i in period t on day d (MW)
$pls_{d,t,l}$	Active power losses on line l in period t on day d (MW)
$pw_{d,t,w}$	Active power output of wind farm w in period t on day d (MW)
$q_{d,t,s}^{\text{ch/dis}}$	Reactive (dis)charging power of BES s in period t on day d (Mvar)

This work is licensed under a Creative Commons Attribution 4.0 License. For more information, see https://creativecommons.org/licenses/by/4.0/

$q_{d,t,l}^{\mathrm{nm/mn}}$	Reactive power flow through line l from bus $n(m)$ to bus $m(n)$ in period t in day d (Mvar)
$\Delta q_{d,t,l}^{\mathrm{TCSC,\,max}}$	Reactive power flow through line l with TCSC in period t on day d (Mvar)
$qg_{d,t,i}$	Reactive power output of thermal generator i in period t on day d (Mvar)
$qls_{d,t,l}$	Reactive power losses on line l in period t on day d (Mvar)
$soc_{d,t,s}$	State of charge of BES s in period t on day d (MWh)
$soc_{s}^{\max}$	Installed capacity of BES s (MWh)
$v_{d,t,n}$	Voltage magnitude at bus n in period t on day d (kV)
$ws_{t,w}$	Wind spillage at farm w in period t on day d (MW)
$\theta_{d,t,n}$	Voltage angle at bus n in period t on day d (rad)
$\theta_{d,t,l}^{+}, \theta_{d,t,l}^{-}$	Slack variables on + and – voltage angle difference across line l in period t on day d (rad)
$\Delta v_{d,t,n}$	Voltage deviation at bus n in period t on day d
$\Delta\theta_{d,t,l,g}$	Size of gth linear block of angle difference across line l in period t on day d
$\xi_{d,s}^{\mathrm{BESpow}(\upsilon)}$	Dual variable of constraint on variable $ch_{s}^{\max}$
$\xi_{d,s}^{\mathrm{BESsoc}}$	Dual variable of constraint on variable $soc_{s}^{\max}$
$\xi_{d,l}^{\mathrm{TCSC}}$	Dual variable of constraint on variable $\kappa_{l,z}^{\mathrm{TCSC}}$
$\xi_{d,l}^{\mathrm{LINES}}$	Dual variable of the constraint on variable ν_l
ν_l	Binary variable equal to 1 if line l is built
$\kappa_{l,z}^{\mathrm{TCSC}}$	Binary variable equal to 1 if TCSC capacity block z is selected
$p_{d,t,l}$	Variable equal to $\max\left\{p_{d,t,l}^{\mathrm{nm}}, p_{d,t,l}^{\mathrm{mn}}\right\}$
$q_{d,t,l}$	Variable equal to $\max\left\{q_{d,t,l}^{\mathrm{nm}}, q_{d,t,l}^{\mathrm{mn}}\right\}$

PARAMETERS

B_l	Series susceptance of line l (S)
B_{l}^{sh}	Shunt susceptance of line l (S)
$B_{l,z}^{\mathrm{TCSC}}$	Series susceptance of line l with TCSC (S)
C_{s}^{BESen}	Battery investment cost of BES unit s (\$/MWh)
C_{s}^{BESpow}	Converter investment cost of BES unit s (\$/MVA)
$C_{l,z}^{\mathrm{TCSC}}$	Investment cost of TCSC block z on line l (\$)
C_{l}^{line}	Investment cost of new lines l (\$)
G_l	Series conductance of transmission line l (S)
$G_{l,z}^{\mathrm{TCSC}}$	Series conductance of line l with TCSC (S)
K_g	Slope of the gth piecewise linear block
$\ell_{d,t,l}$	Takes value 1 if $\theta_{d,t,l}^{(\upsilon)} \geq 0$ on line l in period t on day d, and 0 otherwise
M	Big enough constant
O_{i}^{gen}	Production cost of thermal generator i (\$/MW)
O_{w}^{wind}	Production cost of wind farm w (\$/MW)
$PD_{d,t,n}$	Active power demand at bus n in period t on day d (MW)
$Pg_{i}^{\max}$	Maximum active power output of generator i (MW)
$Pw_{d,t,w}^{\det}$	Available power at wind farm w in period t on day d (MW)
$QD_{d,t,n}$	Reactive power demand at bus n in period t on day d (Mvar)
$Qg_{t,i}^{\max}, Qg_{t,i}^{\min}$	Maximum and minimum reactive power output of thermal generator i (Mvar)
RD_i	Maximum ramp-down of thermal generator i (MW/h)
RU_i	Maximum ramp-up of thermal generator i (MW/h)
$S_{l}^{\max}$	Power rating of line l (MVA)
$Sg_{i}^{\max}$	Maximum apparent power output of generator i (MVA)
X_l	Reactance of line l (Ω)
$\theta^{\max}$	Maximum allowed voltage angle (rad)
χ_d	Number of days in a year represented by day d
$\sigma_{l,z}^{\mathrm{TCSC}}$	Compensation level z of TCSC on line l
$\Delta V_{n}^{\max}$	Maximum voltage magnitude deviation at bus n

I. INTRODUCTION

A. BACKGROUND AND MOTIVATION

One of major system-wide challenges in integrating renewable energy sources (RES) is their intermittent nature. This is a major change as compared to traditional, robust power systems characterized by steady, foreseeable and controllable generation [1]. Therefore, there is no doubt that new flexible assets need to be introduced and take a role in preserving the balance of generation and consumption [2]. Assuming that future generation will be based (almost) exclusively on RES, the system operator needs to ensure flexible assets at the transmission level as well to maximize utilization of non-controllable RES generation assets. Traditionally, the system operator may invest in new transmission lines to reduce congestion and improve utilization of RES generation, i.e. minimize its curtailment. However, line construction is very time-consuming and the investments are bulky making them economically inefficient. This inefficiency is especially apparent when utilization of the existing generation resources would be much more effective if parameters of specific lines are only slightly changed, which can be accomplished using specific devices based on power electronics. Thyristor-controlled series capacitors (TCSC) comprise controlled reactors in parallel with sections of a capacitor bank. They change overall reactance of the line, thus affecting the power flows in the surrounding network. Installation of such devices can thus affect power flows and increase the utilization of RES generation in congested parts of the grid [3]. The third tool at the disposal to the system operator is battery energy storage (BES), which enables shifting energy in time, from periods of RES overproduction to periods of insufficient RES output. Although there are various applications of BES [4], and most of them are merchant oriented, in this paper we focus on the applications that improve social welfare and grid variables. Bidirectional AC/DC converters used to connect batteries to the AC grid inherently contain inductors and capacitors that can be utilized to inject/withdraw reactive power to/from the grid and control local voltage levels. This reactive power manipulation does not affect the battery state of charge, but reduces the available battery charging and discharging power.

To realistically model the power system operation and incorporate the effects of TCSC and BES on reactive power flows and voltage levels, this paper uses a linearized AC OPF (optimal power flow) model in which network losses and voltage magnitudes are variables. Since AC OPF is a nonlinear and nonconvex problem, linearization techniques are used to obtain the proposed network planning model looking at a target year. It simulates operation over a number of representative days that meticulously portray the entire year. Due to complexity of the proposed transmission expansion planning (TEP) problem, the iterative Benders' decomposition [5] is used to decompose it into a mixed-integer linear program (MILP) that serves as the investment master problem, and to several linear problems (LP), one for each representative day, that represent the operational sub-problems.

B. LITERATURE REVIEW

TEP models have had an important position in scientific literature for a long time. Since they consider the future power system topology and operating conditions, they often include uncertainty. For instance, in [6] the authors present a transmission network expansion planning problem considering uncertainty in demand. Due to a high complexity of such models, TEP problems either rely on heuristic methods, e.g. [7], or decomposition techniques, e.g. [8]. Furthermore, in order to preserve computational tractability of the model, power flows in these paper are represented by the DC model, which ignores voltage levels, losses and reactive power flows.

TEP problems have recently started considering BES assets, on top of transmission lines. This introduced a new dimension to TEP because BES move electricity in time, which complements transmission lines that move electricity in space. Therefore, BES does not entirely substitute transmission lines, but complements them depending on the power system characteristics, as shown in [9]. A mixed-integer model that considers only BES expansion in transmission systems is proposed in [10]. The model is solved in three stages, where the first stage determines optimal location of the BES, the second stage sets optimal BES size at each location, and the final stage determines actual operating costs used to calculate the economic viability of the installation. A stochastic multistage TEP model that considers both BES and transmission lines is presented in [11]. It utilizes BES both as a long-term solution and to defer investments in transmission lines under different renewable generation and load increase scenarios. A trilevel model where the upper-level problem optimizes the system operator's transmission line and BES investments, the middle-level determines the merchant energy storage investment decisions, and the lower-level simulates the market clearing process for representative days is formulated in [12]. The paper concludes that, even at low cost of BES, the system operator will give advantage to transmission lines since they are more lasting than BES. Also, increase in social welfare is mainly driven by the system operator's investments in transmission lines.

Another option to reduce bulky investments in new transmission lines, but still somewhat affect power flows and increase bandwidth of the transmission network, is to equip some of the existing lines with series compensation, as demonstrated in [13]. Fixed series compensation is especially suitable for networks with only slight congestion, often a result of the RES integration. To reduce RES curtailment, the model proposed in [14] minimizes investment costs in new lines, TCSC and reactive power sources. The model uses the linearized AC OPF formulation to assess reactive power flows, network losses, and voltage magnitudes. TCSC devices are modeled using binary variables. Each binary variable defines the level of installed compensation capacity at a specific line. In [15], optimal allocation of TCSC devices in an AC OPF model is proposed using a generalized Benders' decomposition approach. The proposed model is a two-stage stochastic program, where the first stage determines optimal locations and upper limits on TCSC devices. The second stage checks the AC feasibility of the obtained solution based on nonlinear programming (NLP). The results show that the number of allowed TCSC devices and computation time are not in direct correlation. Also, changing the maximum compensation level and the operating voltage range significantly affects the transmission lines selected for compensation. The authors in [16] find optimal location and size of TCSC devices to minimize the generation costs. An adaptive parallel seeker optimization algorithm is employed to solve a multi-objective OPF problem while a linear recursive sequence tool is utilized to reduce the search space.

C. CONTRIBUTION

With respect to the literature review above, this paper proposes an optimisation methodology for incorporating BES, series compensation (TCSC) and traditional reinforcement into transmission planning practice. Besides the model itself, we introduce two novelties to the literature. First, we model dynamic operation of TCSC in a mixed-integer linear fashion

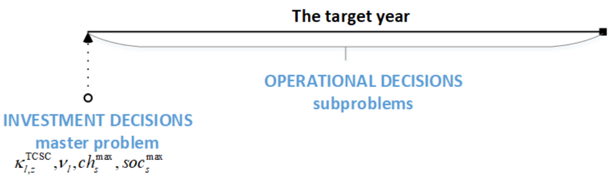

FIGURE 1. The relationship between the investment and the operation stages.

(the one in [15] is nonlinear). Dynamic TCSC operation means that compensation value of TCSC is actively adjusted at each operating time period between zero and the installed compensation capacity. Second, we use BES not only to inject or withdraw active power by discharging or charging the battery, which is customarily in the literature, but its AC/DC converter is also used to inject or withdraw reactive power, thus affecting network voltages. This adds another stream of value to the BES installation that has so far been ignored in the literature.

II. METHODOLOGY

Since computational tractability of a TEP problem using the linearized AC OPF is inadequate, we employ Benders' decomposition to dissolve the problem into two parts: i) Master problem – determines optimal investments in BES, TCSC and lines, and ii) Subproblem – solves the operational problem. The investment decisions from the master problem are then fixed in the subproblems to calculate the operating costs on representative days, as shown in Fig 1. In case the optimal solution is not achieved, the subproblems' sensitivities are used to construct the Benders' cut and the updated master problem is solved. Since the considered battery storage is a short-term storage (matter of hours), there is no need for coupling between the days, as in the case of long-term storage [17].

A. MASTER PROBLEM

Master problem is formulated as follows:

$$
\begin{aligned}
\underset{\aleph^{MP}}{\text{Minimize}}\ E^{\text{down}(\upsilon)} &= \sum_{l\in\Omega^{L^{\text{NEW}}}} C_l^{\text{line}} \cdot \nu_l^{(\upsilon)} \\
&+ \sum_{s\in\Omega^S} \left(C_s^{\text{BESpow}} \cdot ch_s^{\max(\upsilon)} + C_s^{\text{BESen}} \cdot soc_s^{\max(\upsilon)} \right) \\
&+ \sum_{l\in\Omega^{L^{\text{TCSC}}}} \sum_{z\in\Omega^Z} C^{\text{TCSC}} \cdot \kappa_{l,z}^{\text{TCSC}(\upsilon)} \cdot \sigma_{l,z}^{\text{TCSC}}(\upsilon) \cdot X_l \\
&+ \alpha^{(\upsilon)} \qquad (1)
\end{aligned}
$$

$$
\begin{aligned}
\text{subject to: } \alpha^{(\upsilon)} &\geq \sum_{d\in\Omega^D} E_d^{\text{SP}(k)} + \sum_{d\in\Omega^D} \sum_{l\in\Omega^{L^{\text{NEW}}}} \xi_{d,l}^{\text{LINE}(k)} \\
&\cdot \left(\nu_l^{(\upsilon)} - \nu_l^{(k)} \right) \\
&+ \sum_{d\in\Omega^D} \sum_{l\in\Omega^{L^{\text{TCSC}}}} \sum_{z\in\Omega^Z} \xi_{d,l}^{\text{TCSC}(k)} \\
&\cdot \left(\kappa_{l,z}^{\text{TCSC}(\upsilon)} - \kappa_{l,z}^{\text{TCSC}(k)} \right) \\
&+ \sum_{d\in\Omega^D} \sum_{s\in\Omega^S} \xi_{d,s}^{\text{BESpow}(k)} \cdot \left(ch_s^{\max(\upsilon)} - ch_s^{\max(k)} \right) \\
&+ \xi_{d,s}^{\text{BESsoc}(k)} \cdot \left(soc_s^{\max(\upsilon)} - soc_s^{\max(k)} \right) \\
&\forall k = 1, \ldots, \upsilon - 1 \qquad (2)
\end{aligned}
$$

$$
\sum_{z\in\Omega^Z} \kappa_{l,z}^{\text{TCSC}(\upsilon)} \leq 1 \quad \forall l \in \Omega^{L^{\text{TCSC}}} \qquad (3)
$$

$$
\begin{aligned}
&\alpha^{(\upsilon)} \geq \alpha^{\text{down}} \\
&\aleph^{\text{MP}} = \left\{ \kappa_{l,z}^{\text{TCSC}(\upsilon)}, \alpha^{(\upsilon)}, \nu_l^{(\upsilon)}, E^{\text{down}(\upsilon)}, \right. \\
&\left. ch_s^{\max(\upsilon)}, soc_s^{\max(\upsilon)} \right\}. \qquad (4)
\end{aligned}
$$

Master problem objective function (1) minimizes total investment cost in new lines (first row), BES (second row) and TCSC (third row). All the investment costs are levelized to annual values in order to make them comparable to overall annual operating costs obtained from the subproblems. In other words, investment in a new transmission asset will be chosen if and only if the levelized daily cost of this investment in the master problem is lower than the sum of the weighed savings it achieves in the subproblems. Line investments are decided based on binary variable $\nu_l^{(\upsilon)}$ (1 – built; 0 – not built in iteration υ). On the other hand, BES investment is decided by two variables, $ch_s^{\max(\upsilon)}$, which sets the power capacity of the AC/DC converter for both (dis)charging the battery and reactive power compensation, and $soc_s^{\max(\upsilon)}$, which defines energy capacity of the battery. TCSC investment is based on binary variable $\kappa_{l,z}^{\text{TCSC}(\upsilon)}$, which decides the reactance block z within parameter $\sigma_{l,z}^{\text{TCSC}(\upsilon)}$ to be installed. This sets the maximum reactance compensation level of the existing line l in the subproblems. Investment in multiple TCSC blocks for each line is prohibited in constraint (3). The final item $\alpha^{(\upsilon)}$ in the objective function, defined in constraint (2), presents the Benders' cuts that include the subproblems' constraint sensitivities. Their function is to approximate the levelized operational costs formulated in the subproblems. Constraint (4) imposes the lower bound on Benders' cuts generated in (2) for each iteration. Master problem is represented by a set of variables in $\aleph^{\text{MP}}$ referring to Benders' iteration υ.

B. SUBPROBLEMS

The subproblems formulated in (5)–(57) represent the operational problems where the investment variables obtained in the master problem are fixed. Variables from the subproblem set $\aleph^{\text{SP}}$ are determined for each Benders' iteration υ.

$$
\begin{aligned}
\underset{\aleph^{\text{SP}}}{\text{Minimize}}\ & E_d^{\text{SP}(\upsilon)} \\
&= \chi_d \cdot \sum_{t\in\Omega^T} \left(\sum_{i\in\Omega^I} pg_{d,t,i}^{(\upsilon)} \cdot O_i^{\text{gen}} \right. \\
&\left. + \sum_{w\in\Omega^W} pw_{d,t,w}^{(\upsilon)} \cdot O_w^{wind} \right) \qquad (5)
\end{aligned}
$$

subject to:

1) POWER BALANCE CONSTRAINTS

$$\sum_{w\in M^n} pw_{d,t,w}^{(\upsilon)} + \sum_{i\in M^n} pg_{d,t,i}^{(\upsilon)} + \sum_{o(l)\in M^n} p_{d,t,l}^{\mathrm{nm}(\upsilon)} + \sum_{d(l)\in M^n} p_{d,t,l}^{\mathrm{mn}(\upsilon)} - 0.5\sum_{l\in M^n} pls_{d,t,l}^{(\upsilon)} + \sum_{s\in M^n} p_{d,t,s}^{\mathrm{dis}(\upsilon)} = PD_{d,t,n} + \sum_{s\in M^n} p_{d,t,s}^{\mathrm{ch}(\upsilon)} \quad \forall n\in\Omega^N, t\in\Omega^T, d\in\Omega^D \tag{6}$$

$$\sum_{i\in M^n} qg_{d,t,i}^{(\upsilon)} + \sum_{o(l)\in M^n} q_{d,t,l}^{\mathrm{nm}(\upsilon)} + \sum_{d(l)\in M^n} q_{d,t,l}^{\mathrm{mn}(\upsilon)} - 0.5\sum_{l\in M^n} qls_{d,t,l}^{(\upsilon)} + \sum_{s\in M^n} q_{d,t,s}^{\mathrm{dis}(\upsilon)} = QD_{d,t,n} + \sum_{s\in M^n} q_{d,t,s}^{\mathrm{ch}(\upsilon)} \quad \forall n\in\Omega^N,\ t\in\Omega^T,\ d\in\Omega^D \tag{7}$$

Objective function (5) of subproblem d minimizes operating costs of conventional generators and wind power plants. Active power balance at each bus n is assured by constraint (6), which includes production of wind and thermal power plants, outgoing (from bus n to bus m) and incoming (from bus m to bus n) power flows, half of the active power line losses, power (dis)charging from BES and active power load. Reactive power balance in (7) includes reactive power injection/absorption of conventional generators, outgoing and incoming reactive power flows and losses, reactive power (dis)charging from BES, and reactive power load. Reactive power from BES units is based on the converter topology capable of producing capacitive and inductive power.

2) POWER FLOW CONSTRAINTS

$$p_{d,t,l}^{\mathrm{nm}(\upsilon)} = G_l\cdot\left(\Delta v_{d,t,n}^{(\upsilon)} - \Delta v_{d,t,m}^{(\upsilon)}\right) + B_l\cdot\theta_{d,t,l}^{(\upsilon)} \quad \times\forall\{n,m\}\in l\in\Omega^{L^{\mathrm{EX,\,NEW}}},\quad t\in\Omega^T,\ d\in\Omega^D \tag{8}$$

$$p_{d,t,l}^{\mathrm{mn}(\upsilon)} = -G_l\cdot\left(\Delta v_{d,t,n}^{(\upsilon)} - \Delta v_{d,t,m}^{(\upsilon)}\right) - B_l\cdot\theta_{d,t,l}^{(\upsilon)} \quad \times\forall\{m,n\}\in l\in\Omega^{L^{\mathrm{EX,\,NEW}}},\quad t\in\Omega^T,\ d\in\Omega^D \tag{9}$$

$$q_{d,t,l}^{\mathrm{nm}(\upsilon)} = -B_l^{\mathrm{sh}}\cdot\left(1+2\Delta v_{d,t,n}^{(\upsilon)}\right) - G_l\cdot\theta_{d,t,l}^{(\upsilon)} + B_l\cdot\left(\Delta v_{d,t,n}^{(\upsilon)} - \Delta v_{d,t,m}^{(\upsilon)}\right) \quad \times\forall\{n,m\}\in l\in\Omega^{L^{\mathrm{EX,\,NEW}}},\quad t\in\Omega^T,\ d\in\Omega^D \tag{10}$$

$$q_{d,t,l}^{\mathrm{mn}(\upsilon)} = -B_l^{\mathrm{sh}}\cdot\left(1+2\Delta v_{d,t,m}^{(\upsilon)}\right) + G_l\cdot\theta_{d,t,l}^{(\upsilon)} - B_l\cdot\left(\Delta v_{d,t,n}^{(\upsilon)} - \Delta v_{d,t,m}^{(\upsilon)}\right) \quad \times\forall\{m,n\}\in l\in\Omega^{L^{\mathrm{EX,\,NEW}}},\quad t\in\Omega^T,\ d\in\Omega^D \tag{11}$$

$$\left(\nu_l^{(\upsilon)}-1\right)\cdot M \le p_{d,t,l}^{\mathrm{nm}(\upsilon)} - \Delta p_{d,t,l}^{(\upsilon)} \le \left(1-\nu_l^{(\upsilon)}\right)\cdot M \quad \times\forall\{n,m\}\in l\in\Omega^{L^{\mathrm{NEW}}},\quad t\in\Omega^T,\ d\in\Omega^D \tag{12}$$

$$\left(\nu_l^{(\upsilon)}-1\right)\cdot M \le p_{d,t,l}^{\mathrm{mn}(\upsilon)} - \Delta p_{d,t,l}^{(\upsilon)} \le \left(1-\nu_l^{(\upsilon)}\right)\cdot M \quad \times\forall\{m,n\}\in l\in\Omega^{L^{\mathrm{NEW}}},\quad t\in\Omega^T,\ d\in\Omega^D \tag{13}$$

$$\left(\nu_l^{(\upsilon)}-1\right)\cdot M \le q_{d,t,l}^{\mathrm{nm}(\upsilon)} - \Delta q_{d,t,l}^{(\upsilon)} \le \left(1-\nu_l^{(\upsilon)}\right)\cdot M \quad \times\forall\{n,m\}\in l\in\Omega^{L^{\mathrm{NEW}}},\quad t\in\Omega^T,\ d\in\Omega^D \tag{14}$$

$$\left(\nu_l^{(\upsilon)}-1\right)\cdot M \le q_{d,t,l}^{\mathrm{mn}(\upsilon)} - \Delta q_{d,t,l}^{(\upsilon)} \le \left(1-\nu_l^{(\upsilon)}\right)\cdot M \quad \times\forall\{m,n\}\in l\in\Omega^{L^{\mathrm{NEW}}},\quad t\in\Omega^T,\ d\in\Omega^D \tag{15}$$

Active and reactive power flow constraints for both the existing and new lines are imposed through eqs. (8)–(11). The formulation calculates their values for each direction as explained in [18]. Constraints (12)–(15) are used to force active and reactive power flows through newly constructed lines (these are candidate lines whose binary variable ν_l is equal to 1) to $\Delta p_{d,t,l}^{(\upsilon)}$ and $\Delta q_{d,t,l}^{(\upsilon)}$, which are defined as the right-hand sides of (8) and (10). The *big M* method is used to avoid nonlinearity due to binary variable determining if a line is built or not.

Maximum and minimum bounds on power flows on lines equipped with TCSC are set as follows:

$$\Delta p_{d,t,l,z}^{\mathrm{TCSC,max}(\upsilon)} = G_{l,z}^{\mathrm{TCSC}}\cdot\left(\Delta v_{d,t,n}^{(\upsilon)} - \Delta v_{d,t,m}^{(\upsilon)}\right) + B_{l,z}^{\mathrm{TCSC}}\cdot\theta_{d,t,l}^{(\upsilon)} \quad \times\forall z\in\Omega^Z,\quad \{n,m\}\in l\in\Omega^{L^{\mathrm{TCSC}}},\quad t\in\Omega^T,\quad d\in\Omega^D \tag{16}$$

$$\Delta q_{d,t,l,z}^{\mathrm{TCSC,max}(\upsilon)} = -B_l^{\mathrm{sh}}\cdot\left(1+2\Delta v_{d,t,n}^{(\upsilon)}\right) + B_{l,z}^{\mathrm{TCSC}}\cdot\left(\Delta v_{d,t,n}^{(\upsilon)} - \Delta v_{d,t,m}^{(\upsilon)}\right) - G_{l,z}^{\mathrm{TCSC}((\upsilon)\cdot\theta_{d,t,l}^{(\upsilon)}} \quad \times\forall z\in\Omega^Z,\quad \{n,m\}\in l\in\Omega^{L^{\mathrm{TCSC}}},\quad t\in\Omega^T,\quad d\in\Omega^D \tag{17}$$

$$\Delta p_{d,t,l,z}^{\mathrm{TCSC,min}(\upsilon)} := \Delta p_{d,t,l}^{(\upsilon)} \tag{18}$$

$$\Delta q_{d,t,l,z}^{\mathrm{TCSC,min}(\upsilon)} := \Delta q_{d,t,l}^{(\upsilon)} \tag{19}$$

$$G_{l,z}^{\mathrm{TCSC}} = \frac{R_l}{(R_l)^2 + \left(X_l\cdot\left(1-\sigma_{l,z}^{\mathrm{TCSC}}\right)\right)^2} \quad \times\forall z\in\Omega^Z,\quad \{n,m\}\in l\in\Omega^{L^{\mathrm{TCSC}}} \tag{20}$$

$$B_{l,z}^{\mathrm{TCSC}} = \frac{X_l \cdot \left(1-\sigma_{l,z}^{\mathrm{TCSC}}\right)}{(R_l)^2 + \left(X_l \cdot \left(1-\sigma_{l,z}^{\mathrm{TCSC}}\right)\right)^2} \times \forall z \in \Omega^Z, \quad \{n,m\} \in l \in \Omega^{L^{\mathrm{TCSC}}} \tag{21}$$

Eqs. (16) and (17) calculate maximum active and reactive power flows using susceptance and conductance values of the installed TCSC capacity block determined in (20)–(21), as further explained in [14]. Eqs. (18)–(19) set the minimum power flows to the values without TCSC. Thus, power flows through a line with TCSC can be increased up to the level determined by the installed TCSC capacity.

Active power flows through lines equipped with TCSC are calculated as follows:

$$\kappa_{l,f}^{\mathrm{TCSC}(\upsilon)} \cdot M - \sum_{z\in\Omega^Z|z\neq f} \kappa_{l,z}^{\mathrm{TCSC}(\upsilon)} \cdot M + \ell_{d,t,l} \cdot \Delta p_{d,t,l,f}^{\mathrm{TCSC,min}(\upsilon)} - (1-\ell_{d,t,l}) \cdot M - M \leq p_{d,t,l,f}^{(\upsilon)} \times \forall f \in \{1,\ldots,Z\}, l \in \Omega^{L^{\mathrm{TCSC}}}, \quad t \in \Omega^T, \ d \in \Omega^D \tag{22}$$

$$-\kappa_{l,f}^{\mathrm{TCSC}(\upsilon)} \cdot M + \sum_{z\in\Omega^Z|z\neq f} \kappa_{l,z}^{\mathrm{TCSC}(\upsilon)} \cdot M + \ell_{d,t,l} \cdot \Delta p_{d,t,l,f}^{\mathrm{TCSC,max}(\upsilon)} + (1-\ell_{d,t,l}) \cdot M + M \geq p_{d,t,l,f}^{(\upsilon)} \times \forall f \in \{1,\ldots,Z\}, \quad l \in \Omega^{L^{\mathrm{TCSC}}}, \ t \in \Omega^T, \ d \in \Omega^D \tag{23}$$

$$\kappa_{l,f}^{\mathrm{TCSC}(\upsilon)} \cdot M - \sum_{z\in\Omega^Z|z\neq f} \kappa_{l,z}^{\mathrm{TCSC}(\upsilon)} \cdot M - (1-\ell_{d,t,l}) \cdot \Delta p_{d,t,l,f}^{\mathrm{TCSC,max}(\upsilon)} - \ell_{d,t,l} \cdot M - M \leq p_{d,t,l,f}^{(\upsilon)} \times \forall f \in \{1,\ldots,Z\}, \quad l \in \Omega^{L^{\mathrm{TCSC}}}, \ t \in \Omega^T, \ d \in \Omega^D \tag{24}$$

$$-\kappa_{l,f}^{\mathrm{TCSC}(\upsilon)} \cdot M + \sum_{z\in\Omega^Z|z\neq f} \kappa_{l,z}^{\mathrm{TCSC}(\upsilon)} \cdot M - (1-\ell_{d,t,l}) \cdot \Delta p_{d,t,l,f}^{\mathrm{TCSC,min}(\upsilon)} + \ell_{d,t,l} \cdot M + M \geq p_{d,t,l}^{(\upsilon)} \times \forall f \in \{1,\ldots,Z\}, \quad l \in \Omega^{L^{\mathrm{TCSC}}}, \ t \in \Omega^T, \ d \in \Omega^D \tag{25}$$

Set of constraints (22)–(25) determines power flows on lines with installed TCSC based on decision variable $\kappa_{l,f}^{\mathrm{TCSC}}$ from the master problem. Parameter $\ell_{d,t,l}$ takes value 1 if $\theta_{d,t,l}^{(\upsilon)} \geq 0$ and 0 otherwise. It is used to define the actual direction of the line flow and is determined before solving the TEP problem. Further information on the role of this parameter is available in [19]. Dynamic change of TCSC reactance adjusts line flow to optimal value within the given range of the installed compensation level at each time period. Fig. 2 visualizes how (22)–(25) work. Eq. (22) sets the lower bound to the power flow without TCSC, while (23) sets the power flow upper bound, i.e. the maximum possible power flow with TCSC installed. Negative power flow direction is bounded by (24) and (25). Eqs. (22)–(25) have their corresponding counterparts for reactive power where letter p is replaced by letter q.

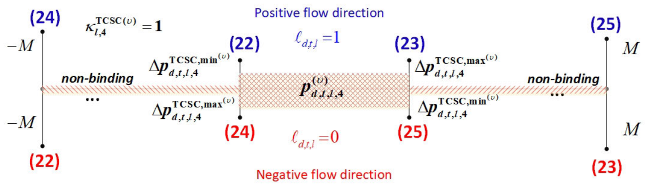

FIGURE 2. The explanations of TCSC constraints (22)–(25) on active power flow (e.g. if the compensation level 4 is installed).

Power flow limits on newly installed power lines are imposed using binary variable ν_l:

$$-\nu_l^{(\upsilon)} \cdot S_l^{\max} \leq p_{d,t,l}^{(\upsilon)} \leq \nu_l^{(\upsilon)} \cdot S_l^{\max} \times \forall l \in \Omega^{L^{\mathrm{NEW}}}, \quad t \in \Omega^T, \ d \in \Omega^D \tag{26}$$

$$-\nu_l^{(\upsilon)} \cdot S_l^{\max} \leq q_{d,t,l}^{(\upsilon)} \leq \nu_l^{(\upsilon)} \cdot S_l^{\max} \times \forall l \in \Omega^{L^{\mathrm{NEW}}}, \quad t \in \Omega^T, \ d \in \Omega^D \tag{27}$$

The second-order cone constraint on maximum active and reactive power flows are limited by constraint (28). To avoid nonlinearity, the feasible region is described as an R-sided convex regular polygon [20].

$$\left(p_{d,t,l}^{(\upsilon)}\right)^2 + \left(q_{d,t,l}^{(\upsilon)}\right)^2 \leq \left(S_l^{\max}\right)^2 \quad \forall l \in \Omega^L, \ t \in \Omega^T, \ d \in \Omega^D \tag{28}$$

Constraint on voltage magnitude is defined as:

$$0 \leq \Delta v_{d,t,n}^{(\upsilon)} \leq \Delta V_n^{\max} \quad \forall n \in \Omega^N, \ t \in \Omega^T, \ d \in \Omega^D \tag{29}$$

Constraints representing piecewise-linearized losses are:

$$\theta_{d,t,l}^{(\upsilon)} = \theta_{d,t,l}^{+(\upsilon)} - \theta_{d,t,l}^{-(\upsilon)} \quad \forall l \in \Omega^L, \ t \in \Omega^T, \ d \in \Omega^D \tag{30}$$

$$\sum_{g\in\Omega^G} \Delta\theta_{d,t,l,g}^{(\upsilon)} = \theta_{d,t,l}^{+(\upsilon)} + \theta_{d,t,l}^{-(\upsilon)} \quad \forall g \in \Omega^G, \ l \in \Omega^L, \ t \in \Omega^T, \quad d \in \Omega^D \tag{31}$$

$$0 \leq \Delta\theta_{d,t,l,g}^{(\upsilon)} \leq \frac{\theta^{\max}}{G} \quad \forall g \in \Omega^G, \ l \in \Omega^L, \ t \in \Omega^T, \ d \in \Omega^D \tag{32}$$

$$\Delta\theta_{d,t,l,g}^{(\upsilon)} \leq \Delta\theta_{d,t,l,g-1}^{(\upsilon)} \quad \forall g \in \Omega^G, \ l \in \Omega^L, \ t \in \Omega^T, \quad d \in \Omega^D \tag{33}$$

$$0 \leq \Delta\theta_{d,t,l,g}^{(\upsilon)} \leq \frac{\theta^{\max}}{G} + \frac{\left[\left(1-\nu_l^{(\upsilon)}\right)\cdot\pi\right]}{G} \times \forall g \in \Omega^G, \quad l \in \Omega^{L^{\mathrm{NEW}}}, \ t \in \Omega^T, \ d \in \Omega^D \tag{34}$$

$$pls_{d,t,l}^{(\upsilon)} = G_l \cdot \sum_{g\in\Omega^G} K_g \cdot \Delta\theta_{d,t,l,g}^{(\upsilon)} \times \forall g \in \Omega^G, \quad l \in \Omega^L, \ t \in \Omega^T, d \in \Omega^D \tag{35}$$

$$0 \leq pls_{d,t,l}^{(\upsilon)} \leq \nu_l^{(\upsilon)} \cdot G_l \cdot \left(\theta^{\max}\right)^2 \quad \forall l \in \Omega^{L^{\text{NEW}}}, \quad t \in \Omega^T, \quad d \in \Omega^D \tag{36}$$

$$0 \leq -pls_{d,t,l}^{(\upsilon)} + G_l \cdot \sum_{g \in \Omega^G} K_g \cdot \Delta\theta_{d,t,l,g}^{(\upsilon)} \leq \left(1 - \nu_l^{(\upsilon)}\right) \cdot M \quad \forall l \in \Omega^{L^{\text{NEW}}}, \ t \in \Omega^T, \ d \in \Omega^D \tag{37}$$

$$qls_{d,t,l}^{(\upsilon)} = -B_l \cdot \sum_{g \in \Omega^G} K_g \cdot \Delta\theta_{d,t,l,g}^{(\upsilon)} \times \forall g \in \Omega^G, \quad l \in \Omega^L, \ t \in \Omega^T, \ d \in \Omega^D \tag{38}$$

$$0 \leq qls_{d,t,l}^{(\upsilon)} \leq \nu_l^{(\upsilon)} \cdot B_l \cdot \left(\theta^{\max}\right)^2 \quad \forall l \in \Omega^{L^{\text{NEW}}}, \ t \in \Omega^T, d \in \Omega^D \tag{39}$$

$$0 \leq -qls_{d,t,l}^{(\upsilon)} - B_l \cdot \sum_{g \in \Omega^G} K_g \cdot \Delta\theta_{d,t,l,g}^{(\upsilon)} \leq \left(1 - \nu_l^{(\upsilon)}\right) \cdot M \quad \forall g \in \Omega^G, \ l \in \Omega^{L^{\text{NEW}}}, \ t \in \Omega^T, \quad d \in \Omega^D \tag{40}$$

$$K_g = (2g - 1) \cdot \frac{\theta^{\max}}{G} \quad \forall g \in \Omega^G \tag{41}$$

Active and reactive power losses in (30)–(41) are denoted with $pls_{d,t,l} \approx G_l \cdot \theta_{d,t,l}^2$ and $qls_{d,t,l} \approx -B_l \cdot \theta_{d,t,l}^2$ and modeled using piecewise linearization of the square of voltage angles [18]. Two slack variables in (30) are used to replace the absolute value of voltage angle $\theta_{d,t,l}^{(\upsilon)}$. Constraint (31) forces both positive and negative values to be calculated in the first quadrant. Constraint (32) limits variable $\Delta\theta_{d,t,l,g}$. Constraint (33) is used to avoid fictitious network losses, while (34) stands only for new lines. Active power losses are then calculated in (35), while (36)–(37) are binding only if new lines are built. Constraints (38)–(40) are reactive counterparts of constraints (35)–(37). Eq. (41) calculates slope K_g at each linearized block of the quadratic voltage magnitude.

3) GENERATION CONSTRAINTS

Constraints on the operation of conventional generation units:

$$0 \leq pg_{d,t,i}^{(\upsilon)} \leq Pg_i^{\max} \quad \forall i \in \Omega^I, \ t \in \Omega^T, \ d \in \Omega^D \tag{42}$$

$$pg_{d,t,i}^{(\upsilon)} - pg_{d,t-1,i}^{(\upsilon)} \leq RU_i \quad \forall i \in \Omega^I, \ t \in \Omega^T, \ \forall d \in \Omega^D \tag{43}$$

$$pg_{d,t,i}^{(\upsilon)} - pg_{d,t-1,i}^{(\upsilon)} \geq -RD_i \quad \forall i \in \Omega^I, \ t \in \Omega^T, \ d \in \Omega^D \tag{44}$$

$$Qg_{d,t,i}^{\min} \leq qg_{d,t,i}^{(\upsilon)} \leq Qg_{d,t,i}^{\max} \quad \forall i \in \Omega^I, \ t \in \Omega^T, \ d \in \Omega^D \tag{45}$$

$$\left(pg_{d,t,i}^{(\upsilon)}\right)^2 + \left(qg_{d,t,i}^{(\upsilon)}\right)^2 \leq \left(Sg_i^{\max}\right)^2 \quad \forall i \in \Omega^I, \ t \in \Omega^T, \ d \in \Omega^D \tag{46}$$

Maximum active power production limits of conventional generators are set in (42), while their up and down ramp limits are imposed in (43) and (44). Maximum and minimum reactive power output is limited in (45). Second-order cone constraint (46) represents the feasible operation area of generators, whose implementation is linearized as in [20].

Available wind power output is partitioned between utilized wind power and wind spillage:

$$pw_{d,t,w}^{(\upsilon)} + ws_{d,t,w}^{(\upsilon)} = Pw_{d,t,w}^{\text{det}} \quad \forall w \in \Omega^W, \ t \in \Omega^T, \ d \in \Omega^D \tag{47}$$

4) BATTERY ENERGY STORAGE CONSTRAINTS

$$0 \leq p_{d,t,s}^{\text{ch}(\upsilon)} \leq ch_s^{\max(\upsilon)} \quad \forall s \in \Omega^S, \ t \in \Omega^T, \ d \in \Omega^D \tag{48}$$

$$0 \leq p_{d,t,s}^{\text{dis}(\upsilon)} \leq ch_s^{\max(\upsilon)} \quad \forall s \in \Omega^S, \ t \in \Omega^T, \ d \in \Omega^D \tag{49}$$

$$0 \leq q_{d,t,s}^{\text{ch}(\upsilon)} \leq ch_s^{\max(\upsilon)} \quad \forall s \in \Omega^S, \ t \in \Omega^T, \ d \in \Omega^D \tag{50}$$

$$0 \leq q_{d,t,s}^{\text{dis}(\upsilon)} \leq ch_s^{\max(\upsilon)} \quad \forall s \in \Omega^S, \ t \in \Omega^T, \ `d \in \Omega^D \tag{51}$$

$$\left(p_{d,t,s}^{\text{ch}(\upsilon)}\right)^2 + \left(q_{d,t,s}^{\text{ch}(\upsilon)}\right)^2 \leq \left(ch_s^{\max(\upsilon)}\right)^2 \times \forall s \in \Omega^S, \quad t \in \Omega^T, \ d \in \Omega^D \tag{52}$$

$$\left(p_{d,t,s}^{\text{dis}(\upsilon)}\right)^2 + \left(q_{d,t,s}^{\text{dis}(\upsilon)}\right)^2 \leq \left(ch_s^{\max(\upsilon)}\right)^2 \times \forall s \in \Omega^S, \quad t \in \Omega^T, \ d \in \Omega^D \tag{53}$$

$$0 \leq soc_{d,t,s}^{(\upsilon)} \leq soc_s^{\max(\upsilon)} \quad \forall s \in \Omega^S, \ t \in \Omega^T, \ d \in \Omega^D \tag{54}$$

$$soc_{d,t,s}^{(\upsilon)} = soc_{d,t-1,s}^{(\upsilon)} + p_{d,t,s}^{\text{ch}(\upsilon)} \cdot \eta^{\text{ch}} - \frac{p_{d,t,s}^{\text{dis}(\upsilon)}}{\eta^{\text{dis}}} \quad \forall s \in \Omega^S, \ t \in \Omega^T, \quad d \in \Omega^D \tag{55}$$

Constraints on active and reactive (dis)charging power of BES, i.e. rated power of its AC/DC converter, are set by (48)-(51). Quadratic constraints (52)-(53) describing the operation area of the converter are linearized in the same way as (28). The inverter can use its entire rating to supply reactive power, however, in that case the battery cannot be charged nor discharged. Battery state of charge is in (54) limited by the maximum state of charge determined in the master problem. State of charge in (55) is determined based on the amount of injected/absorbed active power during the discharging/charging.

5) INTERACTION WITH THE MASTER PROBLEM

Constraints on the decision variables from the master problem:

$$\nu_l^{(\upsilon)} = \nu_l^{\text{fixed}(\upsilon)} : \xi_{d,l}^{\text{LINES}(\upsilon)} \quad \forall l \in \Omega^{L^{\text{NEW}}}, \ d \in \Omega^D \tag{56}$$

$$\kappa_{l,z}^{\mathrm{TCSC}(\upsilon)} = \kappa_{l,z}^{\mathrm{TCSC,fixed}(\upsilon)} : \xi_{d,l}^{\mathrm{TCSC}(\upsilon)} \quad \forall l \in \Omega^{L^{\mathrm{TCSC}}}, \; d \in \Omega^{D} \tag{57}$$

$$soc_s^{\max(\upsilon)} = soc_s^{\max,\mathrm{fixed}(\upsilon)} : \xi_{d,s}^{\mathrm{soc}(\upsilon)} \quad \forall s \in \Omega^S, \; d \in \Omega^D \tag{58}$$

$$ch_s^{\max(\upsilon)} = ch_s^{\max,\mathrm{fixed}(\upsilon)} : \xi_{d,s}^{\mathrm{BESpow}(\upsilon)} \quad \forall s \in \Omega^S, \; d \in \Omega^D \tag{59}$$

$$\begin{aligned} E^{\mathrm{up}(\upsilon)} = &\sum_{d\in\Omega^D} E_d^{\mathrm{SP}(\upsilon)} + \sum_{l\in\Omega^{L^{\mathrm{NEW}}}} \nu_l^{\mathrm{fixed}} \cdot C_l^{\mathrm{line}} \\ &+ \sum_{s\in\Omega^S} \Big(C^{\mathrm{BESpow}} \cdot ch_s^{\max,\mathrm{fixed}} + C^{\mathrm{BESen}} \\ &\cdot soc_s^{\max,\mathrm{fixed}} \Big) \\ &+ \sum_{l\in\Omega^{L^{\mathrm{TCSC}}}} C^{\mathrm{TCSC}} \cdot \kappa_{l,z}^{\mathrm{TCSC,fixed}(\upsilon)} \cdot \sigma_{l,z}^{\mathrm{TCSC}} \cdot X_l \end{aligned} \tag{60}$$

Investment variables in (56)–(59) are fixed to the decisions derived in the master problem. The upper bound of the original problem is obtained in (60). The variables in the subproblem are:

$$\begin{aligned} \aleph^{\mathrm{SP}} = \Big\{ &pg_{d,t,i}^{(\upsilon)}, p_{d,t,l}^{(\upsilon)}, p_{d,t,l}^{\mathrm{nm}(\upsilon)}, p_{d,t,l}^{\mathrm{mn}(\upsilon)}, qg_{d,t,i}^{(\upsilon)}, q_{d,t,l}^{(\upsilon)}, p_{d,t,l}^{(\upsilon)}, \\ &q_{d,t,l}^{\mathrm{nm}(\upsilon)}, q_{d,t,l}^{\mathrm{mn}(\upsilon)}, \Delta v_{d,t,n}^{(\upsilon)}, \theta_{d,t,n}^{(\upsilon)}, \theta_{d,t,l}^{+(\upsilon)}, \theta_{d,t,l}^{-(\upsilon)}, pls_{d,t,l}^{(\upsilon)}, \\ &qls_{d,t,l}^{(\upsilon)}, \Delta\theta_{d,t,l,g}^{(\upsilon)}, pw_{d,t,w}^{(\upsilon)}, ws_{d,t,w}^{(\upsilon)}, soc_{d,t,s}^{(\upsilon)}, p_{d,t,s,}^{\mathrm{ch}(\upsilon)}, \\ &p_{d,t,s,}^{\mathrm{dis}(\upsilon)}, \nu_l^{(\upsilon)}, \kappa_{l,z}^{\mathrm{TCSC}(\upsilon)}, ch_s^{\max(\upsilon)}, soc_s^{\max(\upsilon)} \Big\}. \end{aligned}$$

C. THE PROPOSED BENDERS' ALGORITHM

1) Initialization: Set $\upsilon = 1$, $E^{\mathrm{down}(\upsilon)} = -\infty$, and complicating decision variables: $\nu_l^{\mathrm{fixed}(\upsilon)} = 0$, $\kappa_{l,z}^{\mathrm{TCSC,fixed}(\upsilon)} = 0$, $soc_s^{\max,\mathrm{fixed}(\upsilon)} = 0$, $ch_s^{\max,\mathrm{fixed}(\upsilon)} = 0$.
2) Initial subproblem and time period: Consider day $d = 1$, time period $t = 1$.
3) Subproblems solution: Solve (5) – (59) for each day d and time period t and calculate $E^{\mathrm{up}(\upsilon)}$ as in (60).
4) Convergence check: If $\left|E^{\mathrm{up}(\upsilon)} - E^{\mathrm{down}(\upsilon)}\right| \leq \epsilon$, the optimal solution with level of accuracy ϵ has been obtained. Otherwise, calculate the sensitivities to build the Benders' cut. Then, set $\upsilon \leftarrow \upsilon + 1$.
5) Master problem solution: Solve (1) – (4), calculate $E^{\mathrm{down}(\upsilon)}$ and update the values of complicating decision variables. Then, continue to step 3.

III. CASE STUDY

A. INPUT DATA

The proposed model is applied to a modified IEEE 24-bus system with high installed wind power capacity. Detailed data on this power system can be found in [21]. The target year is modeled by a set of five representative days with hourly periods selected based on the scenario reduction algorithm described in [22]. It uses an iterative approach to select days that minimize the probability distance between the original set of 365 days and the reduced one. Each representative day has its assigned weight according to its occurrence frequency in the target year. Wind production and demand for five characteristic days are shown Fig. 3 and Fig. 4. As reported in [23] and confirmed in our own numerical experiments, five representative days are sufficient to ensure numerical stability of the solution.

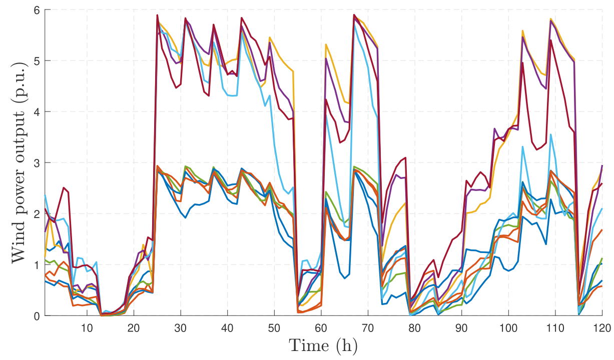

FIGURE 3. Wind production scenarios over five representative days.

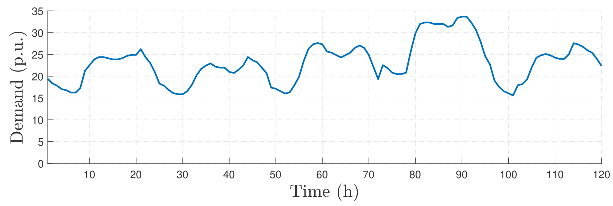

FIGURE 4. Demand profile over five representative days.

BES installation is allowed at three preselected buses: $s102$, $s114$, and $s120$. TCSC installation is enabled at lines connecting buses $s102$–$s104$ ($l4$) and $s115$–$s121$ ($l25$), both belonging to a group of long-distance lines. Maximum allowed TCSC compensation level is 0.6 [24]. Four discrete maximum compensation levels are allowed: 0.15, 0.3, 0.45, and 0.6. The third investment option are new power lines between buses $s101$–$s102$ ($l41$), $s116$–$s117$ ($l39$), $s116$–$s119$ ($l40$), and $s117$–$s118$ ($l42$). Preselection of the candidates for BES, TCSC and new lines highly reduces the feasible area and improves computational performance. In reality, such preselecation is based on operator's experience as well as geographical and legal constraints, especially when it comes to the construction of new lines.

Investment costs are calculated using capital recovery factor as in [12], with annual interest rate 5%, BES lifetime 15 years, TCSC lifetime 20 years, and lines lifetime 40 years. Since the investment is aimed for the target year, all investment costs are scaled to one year. We consider three distinct BES investment costs: \$17/kWh and \$425/kW (high), \$13/kWh and \$325/kW (medium), and \$10/kWh and \$250/kW (low). TCSC investment costs are based on the cost function from [25] and shown in Table 1. Line investments are based on data from [26], resulting in 153,120\$/year for $l39$, 138,040\$/year for $l40$, 32,712\$/year for $l41$, and 92,800\$/year for $l42$.

TABLE 1. Investment costs of TCSC devices ($/year).

TCSC lines	Compensation level (p.u.) 0.15	0.3	0.45	0.6
$l4$	64,569	129,139	193,709	258,278
$l25$	161,278	322,557	483,836	645,115

TABLE 2. Investment results.

Options	Line	BES (MWh/MVA)	TCSC	Costs (m$)	CPU (min)
high.all	$l41$	x	x	0.032	6.78
high.flex	-	x	$l4$(0.6)	0.258	8.95
medium.all	$l41$	$s120$(150;23.8)	x	0.811	14.59
medium.flex	-	$s120$(124;20.5)	$l4$(0.45)	0.864	27.36
low.all	$l41$	$s102$(150;27.7) $s114$(150;27.7) $s120$(150;27.7)	x	2.059	37.46
low.flex	-	$s114$(150;27.7) $s120$(150;27.7)	$l4$(0.6)	1.612	58.01

B. RESULTS

Optimal investments for three BES costs are shown in Table 2. Allowing investment in all three technologies (option *all*) results in investment in line $l41$ for all three BES costs. In case of the high BES cost, this is the only investment in the network. For medium cost of BES, the optimal investment plan also includes a 150 MWh/23.8 MW BES at bus $s120$. The low BES cost scenario results in even higher BES capacity divided across buses $s102$, $s114$ and $s120$. No investment in TCSC is observed in any of these cases. In order to further examine the behavior of the proposed model, we include *flex* option, which allows only installation of TCSC and BES. The high BES cost results in a TCSC installation on line $l4$. This investment, but with reduced capacity, exist for the medium BES cost as well, but is supplemented with BES investment at bus $s120$. The low BES cost scenario keeps the TCSC at bus $l4$ and installs 150 MWh/27.7 MW BES at buses $s114$ and $s120$.

The computation times reached by each option are provided in Table 2. The solution times range from 6.78 minutes for the *high.all* option to 58.01 minutes for *low.flex* option. The solution times increase as the prices of BES are lower due to multiple attractive options on siting and sizing of BES. Also, the optimizations with *all* options is in general completed quicker than for *flex* options as it considers more assets.

Fig. 5 shows the convergence rate of the Benders' algorithm for each option. The convergence is slower as BES starts to be more attractive option due to reduced price (low option). The spread on the number of iterations is quite wide, as option *high.all* requires only 17 iterations to reach the optimal solution, the option *low.flex* requires 119 iterations to reach the ϵ-criterion specified under subsection II-C.

Operation results are shown in Table 3. Generally, the savings are higher in *all* options cases (0.974% for the high BES cost) than for *flex* options cases (0.292% for the high BES cost). As the BES costs reduce, the increased investment in BES further reduce the system operating costs. Wind curtailment is also reduced with increased investments, reaching 6% for the *low.all* option. Reduction of losses is slightly higher when investment in new line is performed (option *high.all*) than for installation of TCSC (option *high.flex*). Network losses are generally reduced by 1-2% after the investments. The lowest reduction is achieved for option *low.all* (0.151%). This is caused by installation of BES at bus $s102$, which reduces wind curtailment at that bus, but increases losses on the surrounding lines. The increased losses are explained by increased flows in hours when the BES is discharged and this electricity, along with electricity produced by inexpensive generators at bus $s102$, is transferred to the northern part of the grid with high loads.

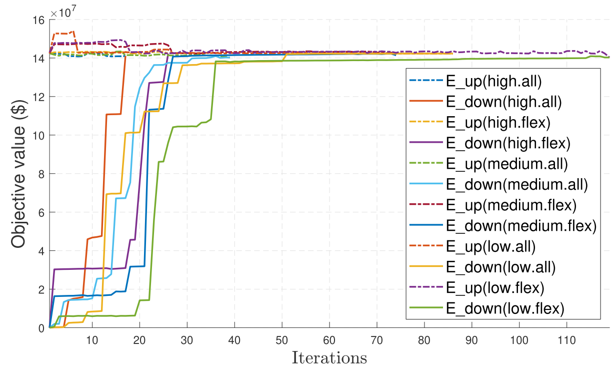

FIGURE 5. Number of iterations to obtain optimal solution.

TABLE 3. Operating costs, wind curtailment and energy losses.

Options	Total costs ($)	Wind curtailment (MWh)	Losses (MWh)
no investment	142,416,862	1,279,322	357,750
high.all	-0.974%	-0.189%	-1.692%
high.flex	-0.292%	-0.175%	-1.500%
medium.all	-1.528%	-2.062%	-1.891%
medium.flex	-0.685%	-1.963%	-0.811%
low.all	-2.664%	-5.976%	-0.151%
low.flex	-1.497%	-4.422%	-1.121%

Installation of TCSC helps power line loadability, as shown in Fig. 6. Higher TCSC compensation levels significantly increases utilization of line $l4$. The red line corresponds to line loading in *high.flex* option (compensation level 0.6), while the blue line shows load levels for *medium.flex* option (compensation level 0.45). Increased loadability helps both to increase the production of cheaper generators and decrease wind curtailment at bus $s102$. An additional benefit is a decreased reactive power flow through line $l4$.

Voltage deviations at buses $s102$ and $s104$ are shown in in Fig. 7. Voltage magnitudes at bus $s102$ are slightly decreased after TCSC installation, while the opposite effect is observed at bus $s104$. In periods of lower power flows, i.e. during the first 8 hours and during the night, voltage

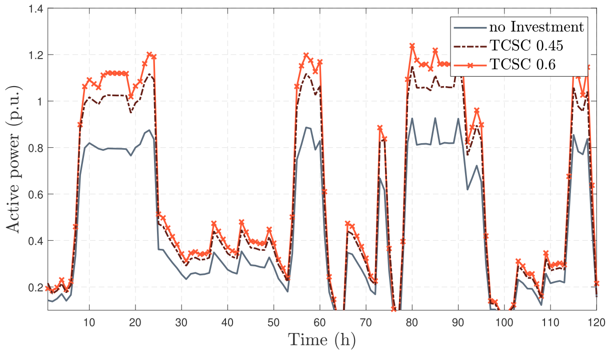

FIGURE 6. Compensation effects of TCSC on power transfer through line *l*4.

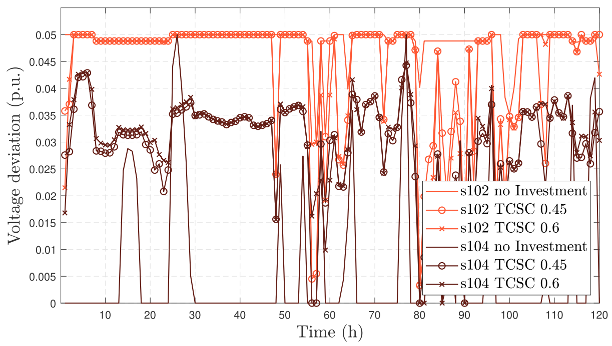

FIGURE 7. Voltage effects of TCSC installed at line *l*4 (buses *s*102–*s*104).

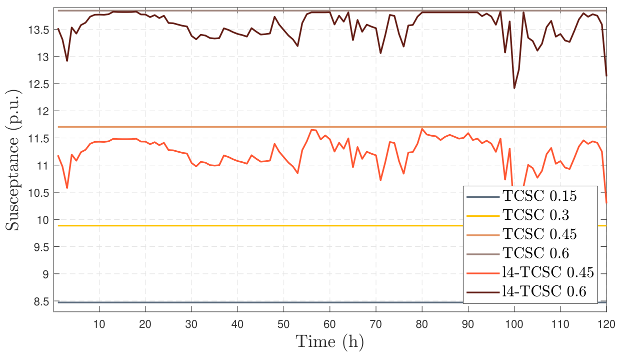

FIGURE 8. Change of susceptance of TCSC installed at line *l*4 considering compensation levels 0.45 and 0.6.

magnitudes are higher because of the low consumption and increased reactive power flows.

Dynamic change of susceptance of TCSC installed on line *l*4 is shown in Fig. 8. The TCSC susceptance changes over time in the subproblem within the range set in the master problem to optimally distribute power flows and affect voltage levels. Correlation between voltage magnitudes, BES operation at bus *s*102 in *low.all* option, and TCSC operation at line *l*4 in *low.flex* option is shown in Fig. 9. A representative day in which production of the local wind farm is high during the night is shown. This highly affects the charging schedule of BES, as it charges during the first six hours and discharges as necessary until hour 18. Reactive power is controlled by the BES's converter in order to reduce overall reactive power

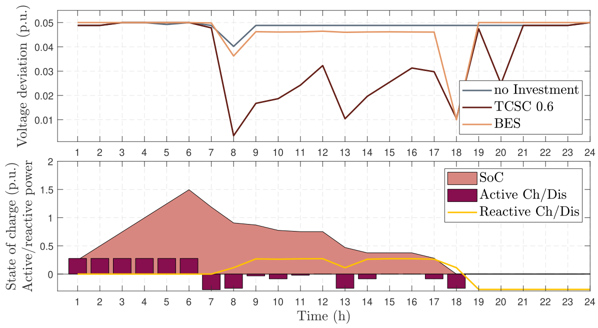

FIGURE 9. Voltage magnitude when BES is installed at bus *s*102 in *low.all*, and TCSC at line *l*4 in *low.flex* option.

flows and losses in the surrounding network while preserving voltage deviations within the given range.

IV. CONCLUSION

This paper proposes a mathematical formulation of the TEP problem considering investments in flexible devices (BES and TCSC) and power lines using a linearized form of AC OPF. The novelty of the paper is the possibility of continuous adjustment of power line reactance in the subproblems (operational problem) after the optimal size of TCSC is determined in the master problem while preserving linearity of the model. Additionally, the paper considers BES providing reactive power control instead of only active power arbitrage. The results of the case study indicate that for the current prices of BES and TCSC, investment in new line is still the most attractive option. However, for lower BES costs, the model results in BES installations at multiple buses, reducing the wind curtailment, but also taking part in voltage control. Investment in TCSC is less attractive and yields lower returns than the investment in new lines. However, it also complements the BES and can come handy at locations where installation of new lines is not possible.

ACKNOWLEDGMENT

The sole responsibility for the content of this document lies with the authors. It does not necessarily reflect the opinion of the Innovation and Networks Executive Agency (INEA) or the European Commission (EC). INEA or the EC are not responsible for any use that may be made of the information contained therein.

REFERENCES

[1] B. Dandrade, *The Power Grid: Smart, Secure, Green and Reliable*. New York, NY, USA: Academic, 2017.
[2] *Renewables 2018-Global Status Report*, REN21, Paris, France, 2018.
[3] R. M. Mathur and R. K. Varma, *Thyristor-Based FACTS Controllers for Electrical Transmission Systems*. Hoboken, NJ, USA: Wiley, 2002.
[4] M. Miletić, Z. Luburić, I. Pavić, and T. Capuder, "A review of energy storage systems applications," in *Proc. MEDPOWER*, Dubrovnik, Croatia, 2018, pp. 1–6.
[5] A. J. Conejo, E. Castillo, R. Minguez, and R. Garcia-Bertrand, *Decomposition Techniques in Mathematical Programming: Engineering and Science Applications*. Cham, Switzerland: Springer, 2006.
[6] I. De J. Silva, M. J. Rider, R. Romero, and C. A. F. Murari, "Transmission network expansion planning considering uncertainty in demand," *IEEE Trans. Power Syst.*, vol. 21, no. 4, pp. 1565–1573, Nov. 2006.

[7] M. Moeini-Aghtaie, A. Abbaspour, and M. Fotuhi-Firuzabad, ''Incorporating large-scale distant wind farms in probabilistic transmission expansion planning—Part I: Theory and algorithm,'' *IEEE Trans. Power Syst.*, vol. 27, no. 3, pp. 1585–1593, Aug. 2012.

[8] X. Zhang and A. J. Conejo, ''Robust transmission expansion planning representing Long- and short-term uncertainty,'' *IEEE Trans. Power Syst.*, vol. 33, no. 2, pp. 1329–1338, Mar. 2018.

[9] C. Bustos, E. Sauma, S. de la Torre, J. A. Aguado, J. Contreras, and D. Pozo, ''Energy storage and transmission expansion planning: Substitutes or complements?'' *IET Gener., Transmiss. Distrib.*, vol. 12, no. 8, pp. 1738–1746, 2018.

[10] H. Pandzic, Y. Wang, T. Qiu, Y. Dvorkin, and D. S. Kirschen, ''Near-optimal method for siting and sizing of distributed storage in a transmission network,'' *IEEE Trans. Power Syst.*, vol. 30, no. 5, pp. 2288–2300, Sep. 2015.

[11] T. Qiu, B. Xu, Y. Wang, Y. Dvorkin, and D. S. Kirschen, ''Stochastic multistage coplanning of transmission expansion and energy storage,'' *IEEE Trans. Power Syst.*, vol. 32, no. 1, pp. 643–651, Jan. 2017.

[12] K. Pandžić, H. Pandžić, and I. Kuzle, ''Coordination of Regulated and Merchant Energy Storage Investments,'' *IEEE Trans. Sustain. Energy*, vol. 9, no. 3, pp. 1244–1254, Jul. 2018.

[13] M. Rahmani, G. Vinasco, M. J. Rider, R. Romero, and P. M. Pardalos, ''Multistage transmission expansion planning considering fixed series compensation allocation,'' *IEEE Trans. Power Syst.*, vol. 28, no. 4, pp. 3795–3805, Nov. 2013.

[14] F. Ugranli and E. Karatepe, ''Coordinated TCSC allocation and network reinforcements planning with wind power,'' *IEEE Trans. Sustain. Energy*, vol. 8, no. 4, pp. 1694–1705, Oct. 2017.

[15] O. Ziaee and F. F. Choobineh, ''Optimal location-allocation of TCSC devices on a transmission network,'' *IEEE Trans. Power Syst.*, vol. 32, no. 1, pp. 94–102, Jan. 2017.

[16] M. B. Shafik, H. Chen, G. I. Rashed, and R. A. El-Sehiemy, ''Adaptive multi objective parallel seeker optimization algorithm for incorporating TCSC devices into optimal power flow framework,'' *IEEE Access*, vol. 7, pp. 36934–36947, 2019.

[17] D. A. Tejada-Arango, S. Wogrin, and E. Centeno, ''Representation of storage operations in network-constrained optimization models for Medium- and long-term operation,'' *IEEE Trans. Power Syst.*, vol. 33, no. 1, pp. 386–396, Jan. 2018.

[18] H. Zhang, G. T. Heydt, V. Vittal, and J. Quintero, ''An improved network model for transmission expansion planning considering reactive power and network losses,'' *IEEE Trans. Power Syst.*, vol. 28, no. 3, pp. 3471–3479, Aug. 2013.

[19] M. Sahraei-Ardakani and K. W. Hedman, ''A fast LP approach for enhanced utilization of variable impedance based FACTS devices,'' *IEEE Trans. Power Syst.*, vol. 31, no. 3, pp. 2204–2213, May 2016.

[20] T. Akbari and M. Tavakoli Bina, ''A linearized formulation of AC multi-year transmission expansion planning: A mixed-integer linear programming approach,'' *Electric Power Syst. Res.*, vol. 114, pp. 93–100, Sep. 2014.

[21] H. Pandžić, Y. Dvorkin, T. Qiu, Y. Wang, and D. S. Kirschen. Unit commitment under Uncertainty–GAMS Models. REAL Lab Library, University of Washington, Seattle, WA, USA. Accessed: Oct. 1, 2020. [Online]. Available: www.ee.washington.edu/research/real/gams_code.html

[22] N. Growe-Kuska, H. Heitsch, and W. Romisch, ''Scenario reduction and scenario tree construction for power management problems,'' in *Proc. IEEE Bologna Power Tech Conf.*, Bologna, Italy, 2003, pp. 1–7.

[23] M. Carrion, Y. Dvorkin, and H. Pandzic, ''Primary frequency response in capacity expansion with energy storage,'' *IEEE Trans. Power Syst.*, vol. 33, no. 2, pp. 1824–1835, Mar. 2018.

[24] N. Acharya and N. Mithulananthan, ''Locating series FACTS devices for congestion management in deregulated electricity markets,'' *Electr. Power Syst. Res.*, vol. 77, nos. 3–4, pp. 352–360, Mar. 2007.

[25] L. Cai, I. Erlich, and G. Stamtsis, ''Optimal choice and allocation of FACTS devices in deregulated electricity market using genetic algorithms,'' in *Proc. IEEE PES Conf. Expo*, New York, NY, USA, Oct. 2004, pp. 201–207.

[26] M. J. Rider, A. V. Garcia, and R. Romero, ''Power system transmission network expansion planning using AC model,'' *IET Gener., Transmiss. Distrib.*, vol. 1, no. 5, pp. 731–742, Sep. 2007.

ZORA LUBURIĆ (Member, IEEE) received the M.E.E. degree from the Faculty of Electrical Engineering and Computing, University of Zagreb, Croatia, in 2015, where she is currently pursuing the Ph.D. degree. She was a Research Assistant with the Department of Energy and Power Systems, University of Zagreb, for a period of three years. She is also with the Market Department, Balancing Services, Croatian Transmission System Operator. Her research interests include planning, operation, and economics of power and energy systems.

HRVOJE PANDŽIĆ (Senior Member, IEEE) received the M.E.E. and Ph.D. degrees from the Faculty of Electrical Engineering and Computing, University of Zagreb, Zagreb, Croatia, in 2007 and 2011, respectively. From 2012 to 2014, he was a Postdoctoral Researcher with the University of Washington, Seattle, WA, USA. He is currently an Associate Professor and the Head of the Department of Energy and Power Systems with the Faculty of Electrical Engineering and Computing, University of Zagreb. His research interests include planning, operation, control, and economics of power and energy systems.

MIGUEL CARRIÓN (Member, IEEE) received the degree and the Ph.D. degree in industrial engineering from the University of Castilla–La Mancha, Ciudad Real, Spain, in 2003 and 2008, respectively. He is currently an Associate Professor with the University of Castilla–La Mancha, Toledo. His research interests include planning, operation, and economics of power and energy systems.

Conference 1 - Valuation of Energy Storage Operation in an AC Power Flow Model

Luburić, Zora; Pandžić, Hrvoje; Carrión, Miguel; Plavšić Tomislav, "Valuation of Energy Storage Operation in an AC Power Flow Model" // In 2018 IEEE International Conference on Environment and Electrical Engineering and 2018 IEEE Industrial and Commercial Power Systems Europe (EEEIC/ICPS Europe), pp. 1-6. IEEE, 2018.
DOI: 10.1109/EEEIC.2018.8493859

– 6 pages

Valuation of Energy Storage Operation in an AC Power Flow Model

Zora Luburić and Hrvoje Pandžić
Faculty of Electrical Engineering and Computing, University of Zagreb
Zagreb, Croatia
zora.luburic@fer.hr;
hrvoje.pandzic@fer.hr

Miguel Carrión
School of Industrial Engineering of Toledo, University of Castilla-La Mancha, Toledo, Spain
miguel.carrion@uclm.es

Tomislav Plavšić
Croatian TSO
HOPS
Zagreb, Croatia
tomislav.plavsic@hops.hr

***Abstract*—High integration of renewable sources in power systems requires additional assets that can sustain reduced controllability and increased variability of these sources. Energy storage has emerged as a flexible asset that increases flexibility and ensures a more economic and secure power system operation. This paper integrates large-scale battery energy storage in power system under different levels of wind power penetration. As opposed to many models already available, we use the full AC model approach that accurately represents power system operation, but at a cost of high computational burden. The proposed model is applied to the IEEE 24-bus test case modeled in GAMS environment and solved with. The power system operation is simulated with and without battery energy storage to show its contribution to the reduction of power system operating costs.**

Keywords: unit commitment, active and reactive optimal power flow, energy storage

I. Introduction

Unit commitment is a short-term decision-making problem, usually solved for the 24-hour time horizon [1]. It determines the generator commitment decisions and estimates their production levels at each hour while meeting the generator, system, network, and environmental constraints [2]. With the integration of renewable power sources into power systems, the operation of battery energy storage (BES) units is becoming more and more common [3]. Although there are different BES ownership models (see [4]), effects of BES on power system operation is best understood in typical unit commitment models, e.g. [5] and [6].

In this paper, we also assume a typical unit commitment problem, where the system operator is in charge of delivering electricity to its customers, as well as setting the operating points of generators and BES in the most cost-effective way. The objective function is the minimization of total system operating costs. Power system operation is represented using a rectangular representation of optimal power flow constraints, which is related to the full AC model [7].

Most research papers accommodate models that use the DC representation of power flows, which considers only active power flows and disregard network losses, to obtain convex solutions and shorter computation times. For instance, the authors in [5] propose a method for siting and sizing of energy storage in the highly renewable power system. The proposed approach consists of a three-stage planning procedure, where the optimal operation of new storage units is determined to alleviate congestion in the network and, consequently, reduce power system operating costs. It is concluded that the location and capacity of storage units is dependent on the distribution of wind resources and their level of penetration. Another use of DC power flow is demonstrated in [9], where a significant reduction of wind curtailment is obtained by introducing energy storage system in both the unit commitment and market clearing environment. Deterministic unit commitment model proposed in [10], also uses the DC representation of power flows and co-optimizes controllable conventional generators and energy storage units. The decrease in operating costs is obtained without distortion of the system reliability.

In general, if a renewable-dominant environment is considered, many models use a stochastic unit commitment model. The impact of significant uncertainties in both wind production and load are researched in [11]. Authors show that, by comparing the operating costs with the planned operation and the performance of the provided schedules, the stochastic optimization results in lower system operating costs. Also, they conclude that with a high value of wind production, the need for reserve is decreased. An important conclusion is that the peaking units' operation and power flows on interconnections are significantly modified. A parallel implementation of the Lagrangian relaxation is presented in [12] to solve the stochastic unit commitment under a set of scenarios using two different approaches: i) narrowing the duality gap of the Lagrangian, and ii) increasing the number of scenarios in order to obtain a more efficient power system operation schedule. It is shown that the first tested approach yields comparable benefits to the one with an increased scenario set, in the case of a reliable scenario selection algorithm.

As opposed to [4]-[12], which use DC power flow representation, AC network models that consider both the active and reactive power flows are used in [13]-[18]. Full AC models cannot be easily applied to large networks. The

This work has been supported in part by Croatian Science Foundation and Croatian Transmission System Operator (HOPS) under the project Smart Integration of RENewables (I-2583-2015) and with the project DPI2015-71280-R MINECO/FEDER, UE.

978-1-5386-5186-5/18/$31.00 © 2018 IEEE

authors in [15] examine the DC and the AC model with Benders decomposition. They conclude that switching from the DC representation to the AC should be accompanied with additional auxiliary constraints. The importance of balancing economic and security issues in restructured markets is discussed in [16]. The proposed model is a security-constrained unit commitment model with additional system constraints: time-limited emergency controls for a given contingency and fuel and emission limits. Moreover, to solve a non-convex mixed-integer nonlinear program, authors in [17] propose a solution technique that co-optimizes both active and reactive power scheduling and dispatch under the AC optimal power flow and unit commitment constraints. The proposed model can be extended to use security constraints.

II. Methodology

The following assumptions are considered: i) we assume an economic dispatch problem, where binary variables modeling the generator commitments are neglected; ii) as common in the literature, energy scheduling of energy storage and wind power units is made considering that they only provide active power. The proposed model is tested with and without energy storage units and its formulation includes active and reactive power flow constraints using real complex equations.

Unlike the DC formulation, the full AC formulation includes the voltage magnitudes, reactive power flows, and network losses. The proposed model uses a rectangular representation of the optimal power flow constraints and is based on model from [14]. For convenience, the notation used in this formulation is listed in appendix at the end of the paper.

$$\underset{\aleph_t}{\text{Minimize}} \sum_t \sum_i Pg_{t,i} \cdot o_i \cdot \mathrm{Z} \tag{1}$$

subject to:

$$\sum_{w \in M^n} Pw_{t,w} + \sum_{i \in M^n} Pg_{t,i} - \sum_{o(l) \in M^n} P_{t,l} + \sum_{d(l) \in M^n} P_{t,l} = PD_{t,n} \forall n \in \Omega^N,\ \forall t \in \Omega^T \tag{2}$$

$$\sum_{i \in M^n} Qg_{t,i} - \sum_{o(l) \in M^n} Q_{t,l} + \sum_{d(l) \in M^n} Q_{t,l} = QD_{t,n} \quad \forall n \in \Omega^N,\ \forall t \in \Omega^T \tag{3}$$

$$0 \leq Pg_{t,i} \leq Pg_i^{\max} \quad \forall i \in \Omega^I,\ \forall t \in \Omega^T \tag{4}$$

$$Qg_{t,i}^{\min} - \kappa_{t,i}^{Q\min} \leq Qg_{t,i} \leq Qg_{t,i}^{\max} + \kappa_{t,i}^{Q\max} \quad \forall i \in \Omega^I,\ \forall t \in \Omega^T \tag{5}$$

$$P_{t,l} = Y_l \left[V_{t,n}^2 \cdot \cos(\vartheta_l) - V_{t,n} \cdot V_{t,m} \cdot \cos(\theta_{t,n} - \theta_{t,m} - \vartheta_l)\right] \quad \forall \{n,m\} \in l \in \Omega^L,\ \forall t \in \Omega^T \tag{6}$$

$$Q_{t,l} = -Y_l \left[V_{t,n}^2 \cdot \sin(\vartheta_l) + V_{t,n} \cdot V_{t,m} \cdot \sin(\theta_{t,n} - \theta_{t,m} - \vartheta_l)\right] \quad \forall \{n,m\} \in l \in \Omega^L,\ \forall t \in \Omega^T \tag{7}$$

$$P_{t,l}^2 + Q_{t,l}^2 \leq (S_l^{\max})^2 \quad l \in \Omega^L,\ \forall t \in \Omega^T \tag{8}$$

$$V_n^{\min} - \kappa_{t,n}^{V\min} \leq V_{t,n} \leq V_n^{\max} + \kappa_{t,n}^{V\max} \quad \forall n \in \Omega^N,\ \forall t \in \Omega^T \tag{9}$$

$$Pg_{t,i} - Pg_{t-1,i} \leq RU_i \quad \forall i \in \Omega^I,\ \forall t \in \Omega^T \tag{10}$$

$$Pg_{t,i} - Pg_{t-1} \geq -RD_i \ \forall i \in \Omega^I,\ \forall t \in \Omega^T \tag{11}$$

$$soc_{t,s} = soc_{t,s}^{\text{in}} + p_{t,s}^{\text{ch}} \cdot \eta_s^{\text{ch}} - \frac{p_{t,s}^{\text{dis}}}{\eta_s^{\text{dis}}} \quad \forall s \in \Omega^S, t \in 1 \tag{12}$$

$$soc_{t,s} = soc_{t-1,s} + p_{t,s}^{\text{ch}} \cdot \eta_s^{\text{ch}} - \frac{p_{t,s}^{\text{dis}}}{\eta_s^{\text{dis}}} \quad \forall s \in \Omega^S, t \in \Omega^T \setminus \{1, T\} \tag{13}$$

$$soc_{t,s} \geq soc_{t,s}^{\text{in}} \quad \forall s \in \Omega^S, t \in T \tag{14}$$

$$soc_s^{\min} \leq soc_{t,s} \leq soc_s^{\max} \quad \forall s \in \Omega^S, t \in \Omega^T \tag{15}$$

$$p_{t,s}^{\text{ch}} \leq ch_s^{\max} \cdot x_{t,s}^{\text{ch}} \quad \forall s \in \Omega^S, t \in \Omega^T \tag{16}$$

$$p_{t,s}^{\text{dis}} \leq dis_s^{\max} \cdot (1 - x_{t,s}^{\text{ch}}) \quad \forall s \in \Omega^S, t \in \Omega^T \tag{17}$$

$$-\theta^{\max} \leq \theta_{t,n} \leq \theta^{\max} \quad \forall n \in \Omega^N,\ \forall t \in \Omega^T \tag{18}$$

$$Pw_{t,w} + ws_{t,w} = Pw_{t,w}^{\text{det}} \quad \forall w \in \Omega^W,\ \forall t \in \Omega^T \tag{19}$$

Optimization variables of full AC model are the elements of set:

$$\aleph_t = \left\{g_{t,i},\ P_{t,l},\ Qg_{t,i},\ Q_{t,l},\ \kappa_{t,i}^{Q\min},\ \kappa_{t,i}^{Q\max},\ V_{t,n},\ \theta_{t,n},\ Pw_{t,w},\ ws_{t,w},\ soc_{t,s}, p_{t,s}^{\text{ch}},\ p_{t,s}^{\text{dis}},\ x_{t,s}^{\text{ch}}\right\}.$$

Objective function (1) minimizes total generation costs. Equations (2)-(3) present active and reactive power balance at each bus n. Inequality (4) limits the generators' production between their maximum and minimum power outputs (assumed to be zero), while inequality (5) imposes minimum and maximum limits of their reactive power outputs. Active power flows are determined by equation (6), and reactive power flows by (7). Their relationship is established by inequality (8), which defines a circular P-Q plane of the possible solutions. Voltage magnitudes are limited by their lower and upper bounds in (9). Ramp up and down limits are imposed by (10)-(11). Battery energy storage constraints are (12)-(17).

Battery state of charge depends on the initial battery state of charge, as formulated in (12). The first item considers the initial state of charge, and depending on the charging or discharging period, the battery is charged by the second item, or discharged by the third item. Equation (13) calculates the state of charge for the remaining time periods. The state of charge in the last hour should not be lower than the initial one, which is set by (14). Minimum and maximum limits on storage state of charge are imposed by constraint (15). Power charging and discharging limits are enforced by (16) and (17). Upper and lower limits on voltage angles are imposed by (18). Used wind power and wind power spillage are equal to the available wind power production in (19).

III. Case Study

The proposed models are tested on a case study based on the IEEE 24-bus system test case [18]. The original system has been modified including 7 wind farms in the upper part of the power system, and two battery energy storage units at buses 15 and 19, as shown in Figure 1. Data for this case study are taken from [19]. All simulations are performed under GAMS 24.9.1 on a Linux-based server with 11 2.9-GHz processors and 250 GB of RAM. CONOPT solver is used for solving the full AC formulation without BES units and DICOPT for solving the full AC formulation with BES units. Load data (active and reactive power) used in this model are represented in the upper graph in Figure 2. Peak active load is 2,513 MW and it appears during the late afternoon in hours 18-19. Overall daily active energy consumption is 50 GWh, and reactive is 5 GVArh.

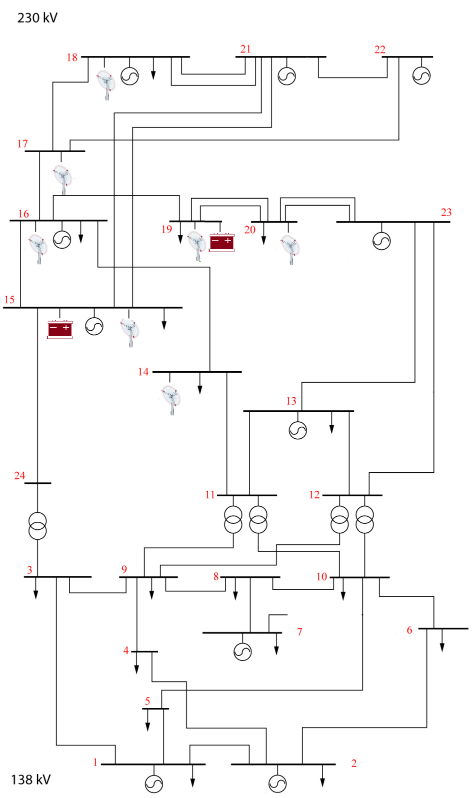

Fig. 1. IEEE 24-bus system test case

The lower graph in Figure 2 shows the wind production available in the considered day by each wind farm. This case is considered as wind factor $f = 1.0$. Total wind production is 49 GWh and is denoted as $Pw_{t,w}^{\text{det,ini}}$. Wind speed data are available in [19]. Wind production is very high throughout the day, but varies across location. For example, wind farm w4 produces at its maximum until hour 14, and then in the second part of day its production drops almost to 30% of its installed capacity. Wind farm w6 produces almost 100% the first two hours and during hours 4-10 does not produce at all. After hour 10, the available wind output is around 50% of the installed capacity and at hours 23-24 it reaches the maximum production level. These two wind farm output examples show how much variability wind power can introduce in a power system.

In case when there is more available wind power than

TABLE I
TOTAL OPERATING COSTS (TOC) IN THE FULL AC MODEL WITH/WITHOUT BES UNDER DIFFERENT LEVELS OF WIND PENETRATION

Model	Wind factor f	TOC without BES (€)	TOC with BES (€)	TOC savings with BES (%)
Full AC	0	713,741	713,294	0.06
	0.5	275,003	273,230	0.65
	1	48,135	46,049	4.33
	1.5	13,869	11,218	19.11

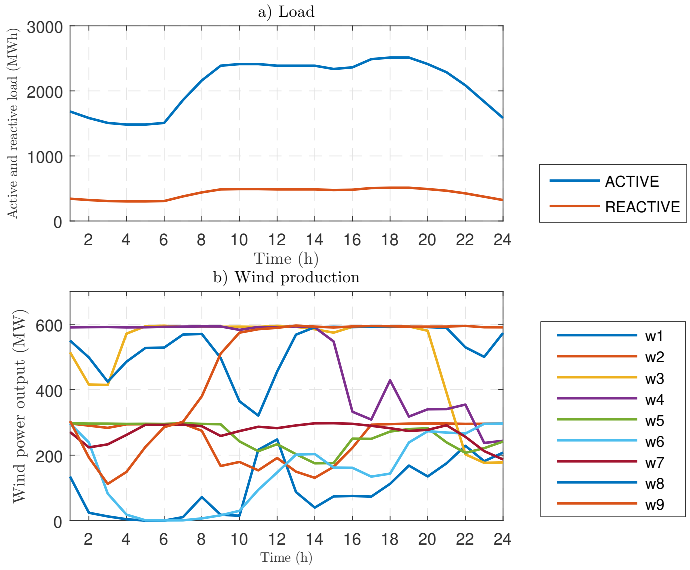

Fig. 2. Active and reactive load (upper graph), and wind production of 7 wind farms under the initial wind factor (lower graph).

needed in the power system, a part of the wind power production is curtailed. In these cases the battery storage systems take their major role, as they store excess electricity and inject it back into the network when needed. This article analyzes how different wind factor levels (lower and higher than the power outputs in the lower graph of Figure 2) affect the total generation costs. Each BES unit has maximum state of charge 120 MWh and maximum charging/discharging power 40 MW. It is assumed that the energy efficiencies of both charging and discharging processes are 0.9.

IV. RESULTS

Table I shows the total operating costs (TOC) under different wind penetration levels pertaining to factor f. In this manner, the available wind power production is computed as $Pw_{t,w}^{\text{det}} = f \cdot Pw_{t,w}^{\text{det,ini}}$. With no wind in the system, TOC obtained using the full AC power flow formulation are the highest and amount to €713,741. Observe that the differences between TOC obtained in proposed model decreases as the wind power penetration increases. It should be noted that introducing BES decreases TOC in all cases. In case when there is no wind in the system, TOC are only slightly decreased, by 0.06%. For wind penetration factor f of 0.5, TOC are reduced by 0.65%. TOC savings for wind penetration factor 1 are significantly higher, 4.33%. When increasing wind factor to 1.5, the proposed model has very low TOC, only €13,869 without BES with additional 19.11% savings with BES operation.

Figure 3 shows the overall wind curtailment for different wind power penetration factors. For factor 0.5, there is no wind spillage. However, for wind energy penetration factor 1.0 wind curtailment increases raises to 3,375 MWh without the BES devices and 3,155 MWh with BES in operation. The highest wind curtailment (23,221 MWh) is achieved for 1.5

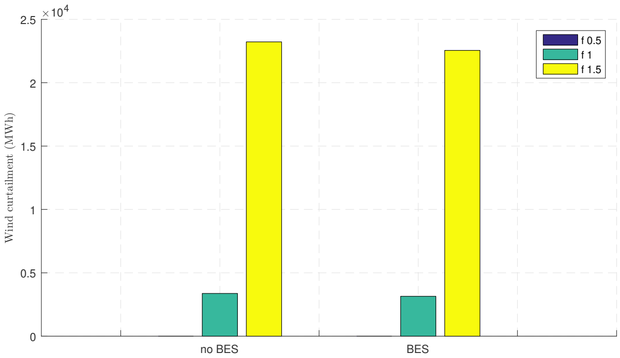

Fig. 3. Wind curtailment for different wind penetration factors

wind penetration factor when there is no BES. Introduction of BES devices reduces slightly wind spillage by 2.89%.

Active power losses are shown in Table II. With increased wind generation, active power losses in the full AC model increase as well. The most noticeable difference in active power losses under different factor is the one between the state where there is no wind and under wind power factor of 0.5, where the active power losses are increased by 692 MWh. Introducing BES in the power system with no wind power results in 2 MWh reduced active power losses. For all the other wind factors, the active power losses are slightly increased after the introduction of BES.

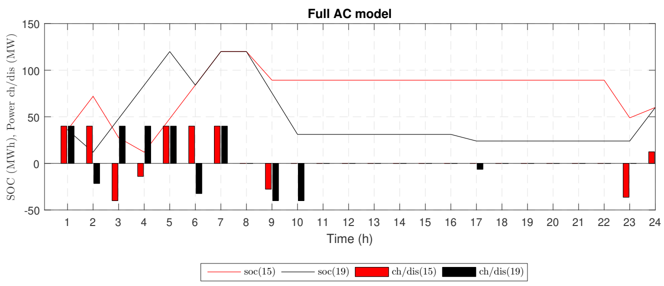

Fig. 4. BES state of charge and charging and discharging quantities at buses 15 and 19 in the full AC model for wind penetration level equal to 1

Figure 4 represents the BES operation for wind penetration level equal to 1. BES units are more active in the first part of the day. The main reason is high level of wind power and low demand during the night and, consequently, absence of thermal generation until hour 8, as can be seen in Figure 5. Low BES activity in the second part of the day is closely related to the available wind generation shown in the lower graph in Figure 2. Both BES units are charged in hour 1 and then discharged in hour 2. BES at bus 15 is charged in hours 3-4 and then discharged in hour 5 due to low wind production of wind farm w2 at the same bus. However, it is charged up to its capacity in hour 7. The other BES unit (bus 19) is charged in hour 3, discharged in hour 4, and then charged up to its capacity in hour 7 as well. Both BES units discharge during the morning peak hours 9-10, and the BES at bus 19 performs a small discharge in the afternoon, while the BES unit at bus 15 discharges in hour 23. Finally, this BES charges in the last hour to reach the required 50% state of charge at the end of the day.

To better understand the resulting total operation costs of the proposed model with BES operation and for wind penetration level equal to 1, generator committed statuses are shown in Figure 5. The most used generators are 22 and 23 at buses 18 and 21, respectively. These generators are nuclear and operate at the lowest cost. All generating units are started at hour 8. Referring to these results, it can be seen that high level of renewable power in the system results in few generating units in operation. The full AC model without BES has higher generation cost due to committed unit 12 in hours 9-10 with cost of 17.19 €/MWh, and unit 9 in hour 23 with cost of 17.59 €/MWh. BES unit replaces these generators units and decreases overall system operating costs.

Figure 6 shows voltage magnitudes at buses 15 and 19 and the differences in voltage levels with and without the BES in operation. The different voltage levels appear only during BES operation - compare to Figure 4. During the charging process of the BES unit in hours 1 and 2, voltage magnitude at bus 15 is slightly decreased, and while the BES is discharged in hours 3-4, voltage magnitude is higher. Again, the voltage is decreased due to charging of the BES in hours 5-7. In hours 9-10, the voltage magnitudes are closer to their nominal value (1 p.u.). There are no voltage magnitude differences in the second part of the day due to the BES inactivity in this period. Similar results are obtained for bus 19, where the other BES is installed. In general, voltage magnitudes at buses 15 and 19 are very close to their nominal value (1 p.u.).

Execution times of the proposed model are listed in Table III. Generally, the formulation that includes BES operation

TABLE II
TOTAL ACTIVE POWER LOSSES IN THE FULL AC MODEL WITH AND WITHOUT BES FOR DIFFERENT LEVELS OF WIND PENETRATION

Model	Wind factor f	Active power losses without BES (MWh)	Active power losses with BES (MWh)
Full AC	0	338	336
	0.5	1,030	1,041
	1	1,766	1,774
	1.5	1,804	1,809

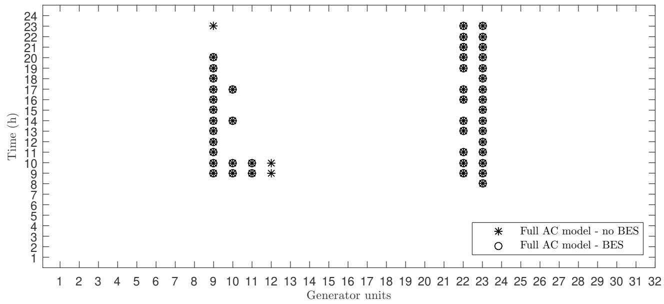

Fig. 5. Generator on/off statuses for the full AC model with and without BES in operation for wind penetration level equal to 1

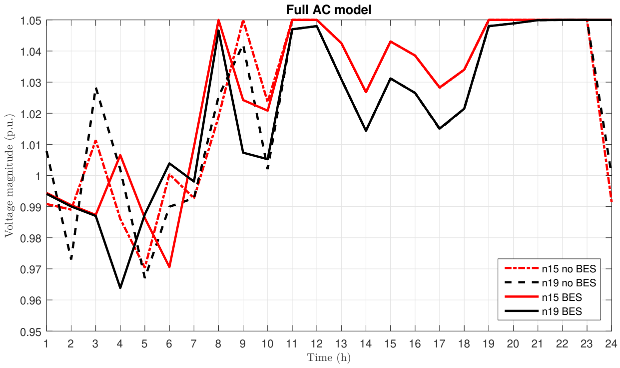

Fig. 6. Voltage magnitudes at buses 15 and 19 with and without the BES for wind penetration level equal to 1

requires more time due to additional binary variables that impose simultaneous charging and discharging. Execution time of the full AC model without the BES is 57.8 s and the number of variables is 8,789. This high number of variables is a result of additional constraints that calculate network losses across transmission lines and voltage levels. Introducing the BES units in the full AC model yields a mixed-integer nonlinear problem (MINLP) and execution time for DICOPT solver is much higher (252 s), while the number of variables is increased to 9,555.

V. Conclusion

This paper proposes and analyzes a formulation for the unit commitment problem considering battery energy storage under the full AC model. We compare its performance with and without the BES and for different factors of wind power penetration levels: 0, 0.5, 1, 1.5. The results show the following main conclusions:

1) By increasing the wind penetration level, TOC of the full AC model is decreased in comparison when there is no wind in the power system: from 61.47% under wind penetration factor 0.5, 93.25% under initial wind penetration factor, and 98.06% under wind penetration factor 1.5.
2) By introducing BES units into the power system, total wind curtailment is generally decreased. The voltage magnitudes are less variable and less dependent on the wind generation since energy storage evens out the copious and scarce wind generation. Also, the number of committed generators is decreased.
3) The full AC formulation requires lower execution time without BES units than the full AC formulation with BES units due to addition of binary variables in the model.

Finally, the formulated AC models contribute with more realistic solutions and provide better insight in the operation of a power system since they capture losses, voltage magnitudes and reactive power flows.

TABLE III
Execution times and number of variables in the models

Model	Without BES		With BES	
	Time (s)	Number of continuous and binary variables	Time (s)	Number of continuous and binary variables
Full AC	57.80	8,789	252.00	9,555

Appendix(Nomenclature)

Sets and Indices

$i \in \Omega^I$ Index of thermal generator i, belonging to set of thermal generators Ω^I.

$l \in \Omega^L$ Index of transmission line l, belonging to set of transmission linesΩ^L.

$n \in \Omega^N$ Index of bus n, belonging to set of network busesΩ^N.

$s \in \Omega^S$ Index of BES unit s, belonging to set of BES units Ω^S.

$t \in \Omega^T$ Index of time period t, belonging to set of periods Ω^T.

$w \in \Omega^W$ Index of wind farm w, belonging to set of wind farms Ω^W.

Parameters:

b_l Series susceptance of transmission line l (S).
$ch_s^{\max}$ Maximum charging power of BES unit s (MW).
$dis_s^{\max}$ Maximum discharging power of BES unit s (MW).
o_i Generating cost of thermal generator i (€/MWh).
$PD_{t,n}$ Active power demand at bus n in period t (MW).
$Pg_i^{\max}$ Maximum active power output of thermal generator i (MW).
$Pw_{t,w}^{\text{det}}$ Maximum power output of wind farm w under wind factor f (MW).
$Pw_{t,w}^{\text{det,ini}}$ Maximum power output of wind farm w under the initial factor 1 (MW).
$QD_{t,n}$ Reactive power demand at bus n in period t (MVAr).
$Qg_{t,i}^{\max}$ Maximum reactive power output of thermal generator i (MVAr).
$Qg_{t,i}^{\min}$ Minimum reactive power output of thermal generator i (MVAr).
RD_i Maximum ramp down of thermal generator i (MW/h).
RU_i Maximum ramp up of thermal generator i (MW/h).
$S_l^{\max}$ Maximum power rating of transmission line l (MVA).
$soc_{t,s}^{\text{in}}$ Initial value of state of charge of BES unit s (MWh).
$soc_s^{\max}$ Maximum state of charge of BES unit s (MWh).
$V_n^{\max}$ Maximum voltage magnitude at bus n (p.u.).
$V_n^{\min}$ Minimum voltage magnitude at bus n (p.u.).
Y_l Admittance of transmission line l (S).
Z Nominal value that converts from p.u.
ϑ_l Admittance angle of transmission line l (rad).
θ^{max} Maximum allowed voltage angle (rad).
η_s^{ch} Efficiency of charging BES unit s (-).
η_s^{dis} Efficiency of discharging BES unit s (-).

Variables:

$P_{t,l}$ Active power through transmission line l in period t (MW).

$p^{\text{ch}}_{t,s}$ Charging power of BES unit s in period t (MW).

$p^{\text{dis}}_{t,s}$ Discharging power of BES unit s in period t (MW).

$Pg_{t,i}$ Active power output of thermal generator i in period t (MW).

$Pw_{t,w}$ Power output of wind farm w in period t (MW).

$Q_{t,l}$ Reactive power through transmission line l in period t (MVAr).

$Qg_{t,i}$ Reactive power output of thermal generator i in period t (MVAr).

$soc_{t,s}$ State of charge of BES unit s in period t (MWh).

$V_{t,n}$ Voltage magnitude at bus n in period t (rad).

$ws_{t,w}$ Wind spillage of wind farm w in period t (MWh).

$\kappa^{Q\max}_{t,i}$ Slack variable ensuring feasibility of constraint on maximum reactive power output of thermal generator i in period t (MVAr).

$\kappa^{Q\min}_{t,i}$ Slack variable ensuring feasibility of constraint on minimum reactive power output of thermal generator i in period t (MVAr).

$\kappa^{V\max}_{t,n}$ Slack variable helping in ensuring feasibility of constraint on maximum voltage magnitude at bus n in period t (rad).

$\kappa^{V\min}_{t,n}$ Slack variable ensuring feasibility of constraint on minimum voltage magnitude at bus n in period t (rad).

$\theta_{t,n}$ Voltage angle at bus n in period t (rad).

Binary variable:

$x^{\text{ch}}_{t,s}$ Binary variable equal to 1 when BES unit s is being charged during time period t, and 0 otherwise.

REFERENCES

[1] R. Baldick, "The generalized unit commitment problem," *IEEE Transactions on Power Systems*, vol. 10, no. 1, pp. 465-475, 1995.

[2] E. Denny, and M. O'Malley, " Wind generation, power system operation, and emissions reduction," *IEEE Transactions on power systems*, vol. 21, no. 1, pp. 341-347, 2006.

[3] Y. Zhang, V. Gevorgian, C. Wang, X. Lei, E. Chou, R. Yang and L. Jiang, "Grid-Level Application of Electrical Energy Storage: Example Use Cases in the United States and China," *IEEE Power and Energy Magazine*, vol. 15, no. 5, pp. 51-58, 2017.

[4] K. Pandžić, H. Pandžić, I. Kuzle, "Coordination of Regulated and Merchant Energy Storage Investments," *IEEE Transactions on Sustainable Energy*, early access.

[5] H. Pandžić, Y. Wang, T. Qiu, Y. Dvorkin D. S. and Kirschen, "Near-optimal method for siting and sizing of distributed storage in a transmission network," *IEEE Transactions on Power Systems*, vol. 30, no. 5, 2288-2300, 2015.

[6] M. Carrión, Y. Dvorkin and H. Pandžić, "Primary Frequency Response in Capacity Expansion," *IEEE Transactions on Power Systems*, vol. 33, no. 2, pp 1824-1835, 2018.

[7] A. G. Expósito, A. Gomez-Exposito, A. J. Conejo and C. Canizares, "Electric energy systems: analysis and operation," *CRC Press*, 2016.

[8] H. Pandžić, Y. Dvorkin, T. Qiu, Y. Wang and D. S. Kirschen, "Toward cost-efficient and reliable unit commitment under uncertainty," *IEEE Transactions on Power Systems*, vol. 31, no. 2, pp. 970-982, 2016.

[9] Z. Luburić, H. Pandžić and T. Plavšić, "Assessment of Energy Storage Operation in Vertically Integrated Utility and Electricity Market," *Energies*, vol. 10, no. 5, pp. 683, 2017.

[10] K. Bruninx and E. Delarue, "Improved energy storage system and unit commitment scheduling," *in Proceedings of IEEE PowerTech 2017 Manchester*, pp. 1-6, June 2017.

[11] A. Tuohy, P. Meibom, E. Denny and M. O'Malley, "Unit commitment for systems with significant wind penetration," *IEEE Transactions on Power Systems*, vol. 24, no. 2, pp. 592-601, 2009.

[12] A. Papavasiliou, S. S. Oren and B. Rountree, "Applying high performance computing to transmission-constrained stochastic unit commitment for renewable energy integration," *IEEE Transactions on Power Systems*, vol. 30, no. 3, pp. 1109-1120, 2015.

[13] A. Nikoobakht, M. Mardaneh, J. Aghaei, V. Guerrero-Mestre and J. Contreras, "Flexible power system operation accommodating uncertain wind power generation using transmission topology control: an improved linearised AC SCUC model," *IET Generation, Transmission and Distribution*, vol. 11, no. 1, pp. 142-153, 2017.

[14] A. Nasri, S. J. Kazempour, A. J. Conejo and M. Ghandhari, "Network-constrained AC unit commitment under uncertainty: A benders' decomposition approach," *IEEE Transactions on Power Systems*, vol. 31, no. 1, pp. 412-422, 2016.

[15] A. Lotfjou, M. Shahidehpour, Y. Fu and Z. Li, "Security-constrained unit commitment with AC/DC transmission systems," *IEEE Transactions on Power Systems*, vol. 25, no.1, pp. 531-542, 2010.

[16] Y. Fu, M. Shahidehpour and Z. Li, "AC contingency dispatch based on security-constrained unit commitment," *IEEE Transactions on Power Systems*, vol. 21, no. 2, pp. 897-908, 2006.

[17] A. Castillo, C. Laird, C. A. Silva-Monroy, J. P. Watson and R. P. O'Neill, "The unit commitment problem with AC optimal power flow constraints," *IEEE Transactions on Power Systems*, vol. 31, no. 6, pp. 4853-4866, 2016.

[18] C. Grigg, P. Wong, P. Albrecht, R. Allan, M. Bhavaraju, R. Billinton and W. Li, "The IEEE reliability test system-1996. A report prepared by the reliability test system task force of the application of probability methods subcommittee," *IEEE Transactions on Power Systems*, vol. 14, no. 3, pp. 1010-1020, 1996.

[19] H. Pandžić, Y. Dvorkin, T. Qiu, Y. Wang, and D. Kirschen, "Unit Commitment under Uncertainty - GAMS Models," Library of the Renewable Energy Analysis Lab (REAL), University of Washington, Seattle, USA. [Online]. Available at: www.ee.washington.edu/research/real/gams_code.html.

Conference 2 - A Review of Energy Storage Systems Applications

Miletić, Marija; Luburić, Zora; Pavić, Ivan; Capuder, Tomislav; Pandžić, Hrvoje; Andročec, Ivan; Marušić, Anton, "A Review of Energy Storage Systems Applications" // 11th Mediterranean Conference on Power Generation, Transmission, Distribution and Energy Conversion (MEDPOWER 2018), Dubrovnik, Croatia, 2018. 94-6.
DOI: 10.1049/cp.2018.1926

– 7 pages

A Review of Energy Storage Systems Applications

Marija Miletić, Zora Luburić, Ivan Pavić, Tomislav Capuder, and Hrvoje Pandžić
Faculty of Electrical Engineering and Computing
University of Zagreb
Zagreb, Croatia

Ivan Andročec
Croatian Power Utility - HEP d.d.
Zagreb, Croatia

Anton Marušić
Croatian DSO - HEP ODS
Zagreb, Croatia

***Abstract*—Energy storage systems can be used in a wide range of applications in power system. Some of these applications can be procured as services through market mechanisms, while others can be a part of grid infrastructure or merchant installations. This paper reviews all these applications categorized in three main groups: system-level applications, transmission and distribution grid applications and end-user applications. Energy storage systems could be tailored for a specific usage, but they are usually profitable only when multiple applications are stacked. Applications stacking cannot be achieved for all combinations, especially when these applications are not market services or when storage ownership prevents it, e.g. system operator owned storage. The importance of service stacking and issues of storage ownership are recognized and addressed.**

***Index Terms*—energy storage systems, ancillary services, service stacking, energy market, reserve market**

I. Introduction

Energy storage systems (ESS) convert electrical energy into a storable form to be saved for later use. This stored energy is converted back to electricity when required. Various storage technologies can be managed independently or combined with other technologies for different applications in the power system.

The best known type of ESS are pumped hydro-power plants, which have been a mature technology for over a century. Pumped hydro-power plants are traditionally used for energy arbitrage and securing system stability and they were one of the first technologies considered for wind power generation balancing. According to Department of Energy's Global Energy Storage Database [1], pumped hydro storage constitutes 94.3% of the world's storage systems in terms of power, but the largest number of projects are based on electrochemical technologies. For comparison, there are 352 pumped hydro storage projects in the world, as compared to 1076 electrochemical storage projects. This indicates that pumped storage projects generally have much higher installed capacity than electrochemical storage projects. According to the same source, the most common ESS applications are energy arbitrage, electric bill management and renewable generation balancing (Figure 1). More detailed description of energy storage technologies and potential use cases can be found in [2], [3].

As many of the energy storage technologies slowly reach market maturity, it is useful to consider possible benefits they can bring to the power system and its users. For instance, a possibility of using an ESS to ensure N-1 criterion of power system stability is analysed in [4]. Model of an ESS providing contingency reserve is proposed in [5]. ESS behaviour in case of contingency, aiming to ensure system adequacy and security, is modelled in [6]. Authors in [7] propose a strategy for ESS acting as a virtual synchronous machine to provide virtual inertia and damping. Energy arbitrage is commonly used storage application and it could be cost-effective when large price variations occur, especially when bidding in short term markets, such as balancing and reserve markets. The day-ahead energy market is observed in majority case studies found in literature concerning ESS. ESS is in [8] used to postpone investments in distribution network, while offering services of energy arbitrage and frequency control as well. This combined use of an ESS for different services is known as stacking and is also considered in [9] for reserve and balancing markets. Similarly, in [10], [11] and [12], [13] arbitrage stacked with reserve and balancing markets can be found, respectively. The authors in [12] showed, by using historical data from Finland, that pumped-hydro storage as a price-taker makes at most 25% of its profit in energy market when combining arbitrage and

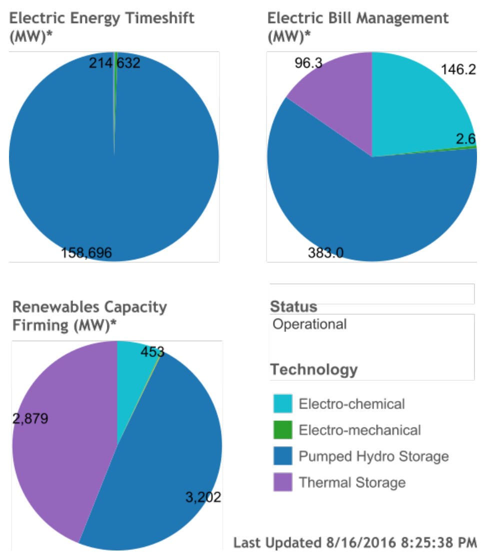

Fig. 1. Three most common applications of ESS: energy arbitrage (timeshift), renewables capacity firming and electric bill management with corresponding technologies [1]

balancing services. In [13] similar results are presented for Germany. The common conclusion is that without stacking, the commercial energy storage cannot be profitable. An idea of future market scheme proposed in [14] is called local balancing market, which is operated by a distribution market operator where storage is combined with wind power plant.

Considering behaviour of an ESS in the market, it can be modelled either as a price-taker or a price-maker. Price-maker is a strategic market participant that has influence the price-setting mechanism as in [9], [10]. On the other hand, a price-taker model takes market prices as given and cannot influence their values. It is usually the first choice for modelling ESS participating in large-scale power markets because ESS usually does not have the capacity to make a significant change to the market prices. Examples of these markets can be found in [11], [12], [13].

Purpose of this paper is to provide a thorough analysis of possible applications of the ESS. The possible applications of an ESS are presented in three separate groups. The first group contains services that an ESS can provide to the power system regardless of its location, the second contains services that are grid-location specific and the third group are potential benefits for the end-users with integrated ESS.

The organisation of the paper is as follows: Section II examines locationally independent, mostly market applications of ESS, Section III investigates locationally dependent ancillary services and Section IV describes end-user level applications. Requirements for ESS used for multiple applications are given in V, while the question of ESS ownership is discussed in VI.

II. System-Level Applications

System-level applications are services that an ESS can provide to the electrical power system regardless of its location. They are mostly connected to electricity and ancillary services market participation or power balancing issues. The possible use cases is provided below.

1) Energy Arbitrage: Energy arbitrage means buying electricity when the market prices are low and selling when they are high. It is the most common usage of ESS (Figure 1). Profitability of an ESS performing arbitrage depends on the difference between the buying and the selling price, cost of storing energy and charging and discharging efficiencies. As it requires many charge-discharge cycles to be profitable, cycle life and degradation rate are the most important properties of an ESS performing arbitrage. Different storage technologies use different time frames for the arbitrage, therefore pumped-hydro power plants often shift energy between seasons, while battery storage is more useful for intra-day load shifting.

2) Power System Adequacy: Adequacy is the ability of the power system to supply its peak load through electricity generation or imports, under normal operating conditions. Consumption of electricity is always growing so the peak load is the main strategic parameter for the system adequacy planning. ESS can help secure system adequacy by discharging at time periods of high electricity consumption. Renewable energy sources are lowering the market prices and therefore pushing the conventional power plants out of the electricity markets. Production of renewable energy sources is uncertain, so they cannot be used to increase system adequacy.

To ensure adequacy of a future power system, capacity remuneration mechanisms are created. There are several types of these mechanisms, e.g. capacity markets, strategic reserve, and some countries have allowed storage to participate in them. Rules for ESS participating in these mechanisms are stricter than those for generators, which limits the income of the ESS owners. In the UK capacity market, de-rating factors have been introduced for duration-limited storage systems. For example, an ESS with discharge time of 1 hour can offer up to 40.41% of their available capacity in the primary (T-1), and 36.44% in the secondary (T-4) capacity market, while the ones with discharge time over than 4 hours can bid up to 96.11% in both markets [15].

3) Power Grid Balancing: Matching supply and demand of active power is one of the main tasks of system operators. Ancillary services related to grid balancing are primary, secondary and tertiary frequency control. Primary control is automatic and can be mandatory or market procured, while secondary and tertiary control reserves are usually market procured. Because of their fast response times, battery storage systems are a suitable choice for providing primary control.

From 2015, storage systems in Germany are allowed to offer control reserve through the German control reserve market, where German, Belgian, Dutch, Austrian, Swiss and French transmission system operators procure control reserve. To participate in the market, a battery system should be able to supply primary reserve for at least 30 minutes while keeping its state of energy within a prescribed range [16]. ESS mostly offer primary reserve in this market, but secondary reserve market is being reorganising to allow the ESS to provide secondary control reserve as well. The following changes are the most beneficial for the ESS: 1) auction will be conducted daily, 2) two types of the product, positive and negative secondary control reserve will be traded, each in three 4-hour time intervals and 3) bid quantities lower than 5 MW will be accepted [17].

New technologies, such as hybrid energy storage-gas turbine systems in Edison's Center Peaker and Grapeland Peaker plants in Southern California, use battery storage combined with gas turbine to offer spinning reserve (secondary frequency control) during the low electricity consumption periods, avoiding high fuel costs [18].

4) Balancing Responsibility: According to the European Commission regulations on electricity market, all market participants are responsible for the imbalances they cause in the system. Balancing can be done individually or through a representative that aggregates imbalances caused by multiple participants. Market participants who take responsibility for imbalances on behalf of themselves or larger groups are Balance Responsible Parties (BRP). BRPs can use an ESS to correct deviations from the planned schedule within their group and thus avoid paying for the balancing energy.

5) Demand Turn Up - Footroom: A service that encourages large energy users and generators to either increase demand or reduce generation at times of high renewable output and low energy demand. This typically occurs during the night and weekend afternoons in the summer. This service can be provided by an ESS charging overnight and discharging during the day, similar to energy arbitrage. Entities offering Footroom cannot offer any other balancing service [19].

6) Flexiramp: A novel type of ramping ancillary service in the US real-time markets, where market participants are payed to be able to change their generated power in order to mitigate short-term imbalances due to variability and uncertainties. Such imbalances become relevant in electricity markets with high penetration of renewables. Flexiramp has been in use in several US electricity markets (CAISO, MISO, SPP).

7) Providing Virtual Inertia: Inertia is a parameter of the power system important for frequency control. ESS is connected to the network by power electronics, which can be transformed into virtual synchronous machine by programming the inverters to mimic synchronous generators. This is useful in systems with high penetration of solar and wind resources. This application is still in the development phase.

III. Network-Level Applications

Network-level applications are services specific to the location of the ESS grid connection. ESS can be connected to the transmission or distribution network, depending on its size, function and local regulations. For example, California ISO (CAISO) in its initiative *Storage as a transmission asset* proposed to enable ESS connected to the transmission network to offer transmission services under a cost-of-service framework [20]. A list of possible network-level applications of ESS that acts as a part of network infrastructure, similar to a line or a transformer, is given below.

1) Congestion Management in Transmission Systems: Congestion happens when there is not enough transmission capacity to support least cost power flow between generators and consumers. ESS can be installed in areas with congestion issues to avoid high energy costs, market decoupling and units redispatching. ESS used for congestion management charges when there is no congestion and discharges during the congestion, effectively increasing generation capability in areas otherwise affected with congestion. Required discharging capacity of the ESS performing congestion management depends on the transmission system topology and ratings. Congestion usually happens few times a year and lasts for several consecutive hours.

2) Deferral of Investments in Network Infrastructure: ESS can be used to postpone investments in two ways. The first way is to postpone investments in new elements or upgrades of parts of the infrastructure (transformers, lines, cables, etc.). This is achieved through reduction of power flows during peak loads. The requirements for ESS used to defer upgrades or replacements are similar as for ESS performing congestion management. The main difference, however, is that if a ESS does not perform as planned in the congestion management scheme, the prices will go up because the power flows will be diverge from the optimal one but all consumers will be supplied. On the other hand, if the ESS does not operate in investment deferral scheme, some of the consumers will be not be supplied since grid infrastructure would be overloaded.

The second category of investment deferral is prolonging the lifetime of network equipment by decreasing the power flows through old and time-worn parts of the equipment. This slows down the further wear and tear of the equipment. Investing in ESS for this reason causes better utilisation of the existing resources and can help avoid risk of uncertain load growth in some parts of the grid.

3) Supporting the (N-1) Criterion for System Stability: ESS can be used to secure the (N-1) criterion in areas where it is too expensive or unpractical to do it by laying down a parallel line or a line to a connect to another transformer station. This is common on islands and in the areas with low consumption. One of the examples of an ESS used to maintain system security is a 1 MW / 3 MWh lithium-ion battery system in Canary Islands. It is a part of the Spanish transmission system operator's project Almacena and was installed in 2013 [21].

4) Voltage and Reactive Power Compensation: Similar to the application of an ESS as a virtual synchronous generator for active power and frequency control, coupling the energy storage with a static synchronous compensator (STATCOM) results in a device that can be used for reactive power compensation. This device based on power electronics is called STATCOM with energy storage (STATCOM-ES). The reactive power generation/consumption is not connected to energy storage but to its voltage-sourced inverter with a possibility to work in all four quadrants. As in synchronous generator, if STATCOM-ES generates/consumes reactive power, the capability to generate/consume active power is decreased. This possible application of ESS is still being researched.

5) Black Start: Black start is a process of restoring part of an electric grid to operation without help from the external transmission network. First step in the black start process is usually done by diesel generators but it has been successfully proven that battery storage can perform this service too. For example, Alaska Energy Authority uses 27 MW NiCd battery to energise the Anchorage-Fairbanks transmission line [22].

6) Minimising Network Losses: Network losses from system operator's standpoint are caused by inadequate network infrastructure configuration, old equipment, big differences in the load profile through the year and metering errors. Electrical losses in the power system are proportional to the square of the current and are therefore very high during peak hours. By using storage for load shifting, these losses can be reduced significantly, which has been shown in [23] and [24].

IV. End-user Applications

End-users in power system include: households (both as passive consumers and prosumers), industry, electric vehicle charging stations or battery-swapping stations, conventional power plants and renewable energy sources. All of them can benefit from installation of an ESS in terms of cost reduction or increase of the quality and reliability of power supply. Possible useful applications for ESS at end-user level are examined below.

1) Peak Shaving and Load Shifting: Industrial consumers are, besides for energy, charged for peak power as well [25]. Peak power remuneration could be seen as penalisation of peak power, especially if it deviates from the contracted value. These costs can be avoided using an ESS for load shifting. Peak load can occur daily, when the ESS is charged during the base-load hours and discharged during the peak hours to avoid high power costs, or can occur more rarely, enabling the ESS can also be used to offer other services to the system. New consumers can use an ESS for load flattening to cut the required capacity while negotiating the grid connection fee. Thermal and battery storage systems are mostly installed at the end-user level to manage electricity bills, as shown in Figure 1.

2) Retail Arbitrage: Consumers can use an ESS for retail arbitrage, if the time-of-use rates or other flexible pricing schemes are available for them, to shift their load from the high-price to the low-price hours during the day. Retail arbitrage could be observed as load shifting due to the grid tariff rates or due to the supplier's dynamic rates. The former could be done in most countries through the existing two-tariff schemes (day/night), but it generally does not yield enough monetary incentives to invest in ESS. The latter is currently unavailable for 62% of the EU households [26, p. 209]. The option of using an ESS for load shifting might gain popularity in Europe in the light of the latest EU plans for changing Electricity market design [27].

3) Voltage Quality: Industrial consumers pay for excessive use of reactive power. These users might install STATCOM-ES devices (see Section III-4) for reactive power compensation and power factor correction.

4) Backup Power: End-users need to secure electricity supply for their businesses if the main grid suffers from a failure. ESS can be combined with Diesel generators or used independently to supply power and maintain frequency within the required range during the island operation. The inverter of an ESS used independently for this purpose must be able to synchronise with the grid after the normal operation has been established, as well as to maintain the frequency when in island operation. The ESS is usually used to start-up Diesel generators or as a short-term supply before the Diesel generators take over.

5) Hybrid Systems: None of the energy storage technologies, except open-loop pumped hydro power plants, have access to unlimited source of energy. To be able to offer any services, they need to procure energy in the market. If an ESS is installed within a conventional or non-conventional power plant, it can obtain energy as part of the plant's auxiliary power consumption. This way the operation of the ESS becomes more profitable when bidding in capacity or reserve Markets. These systems are known as hybrid or combined systems.

Energy storage has been successfully coupled with renewable energy sources to be used for both on-grid and off-grid applications. Many remote settlements in Tanzania have combination of photovoltaics and lead-acid storage as the main electricity supply [28]. A lot of different hybrid solar-ESS systems exist in the market. The prices of the whole system range between \$0.30 and \$0.89 per kWh if it is used for one cycle a day [29].

6) Monitoring Energy Consumption/Production: Hybrid systems, as described in the previous subsection, can be used by consumers, both industrial and households, to monitor their power consumption and balance their power intake. ESS can also be used by wind or solar farms to balance their power output. A number of experimental hybrid projects are under construction, such as Bulgana wind farm in Australia [30], or already in operating, such as Babcock Ranch Solar Energy Center [31].

7) Relaxing the Constraints of Conventional Power Plants: Many traditional generating units do not have sufficient flexibility to participate in capacity or reserve markets. ESS installation improves flexibility of these resources, enabling their participation in these markets. One of the first projects is a 4 MW / 4 MWh battery storage system installed at Buck and Byllesby hydro-power plant to provide additional flexibility. It is currently waiting for the system operator's approval to participate in frequency regulation [32]. Another example is Heilbronn coal-fired power plant in Heilbronn, Germany, which has a 5 MW / 5 MWh lithium-ion battery added to participate in the German control reserve market [33].

V. SERVICE STACKING

As the installation costs of battery energy storage are still high, single applications of the ESS that can ensure an attractive return of investment are rare. Therefore, it is required to stack different ESS services to increase revenue streams.

Authors in [3] provide guidelines for planning investments in ESS. After choosing the primary role, location and technology, the investor should consider secondary services the its ESS can provide. Secondary services should be compatible with its primary services in multiple ways. First, technical parameters of the ESS should meet the minimum requirements to perform both services. Next, the offered services might coincide, partially overlap or not overlap at all, changing the requirements on storage duration. This is why the timing of the services is an important deciding factor. The last one is flexibility of the services, which depends on the scheduling time and duration of the service contracts. It is recommended to consider less flexible services first and then use the remaining capacity for the more flexible ones.

To illustrate this, Figures 2 and 3 show the ESS day-ahead plans and real-time operation, respectively, of an ESS participating in five markets: black start, day-ahead energy, secondary reserve day-ahead, real-time balancing and intraday market. First, the ESS procures a contract on the black-start market where auctions take place on monthly basis. This means its State-Of-Energy (SOE) must remain above a certain limit, which is actually beneficial for battery storage, as it degrades faster at lower SOE. Energy reserved for black start

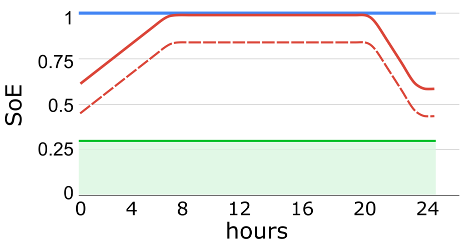

Fig. 2. Day-ahead plan of an ESS (p.u.): SoE - red solid line; green shaded area - energy reserved for black-start contract; red dashed line - minimum expected SoE, secondary reserve; blue solid line - maximum SoE

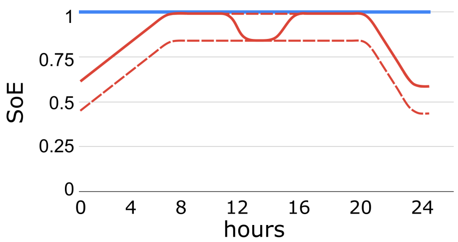

Fig. 3. Real-time operation of an ESS (p.u.): SoE - red solid line, intraday market; red dashed line - minimum and maximum expected SoE, from DAM; blue solid line - maximum SoE

is represented as the shaded area in Figure 2. Using ESS in other markets should never result in SOE within this shaded area. The second market where the ESS participates is a energy day-ahead market (DAM). To participate in energy DAM, the ESS must send its bids for charging/discharging to the electricity exchange operator. After the bids are accepted, its plans for charging/discharging are sent to the system operator. In our example, energy storage plans (all bids in he DAM are accepted) to charge during night hours (SOE increases in hours 0-7) and to discharge during the evening peak hours (SOE decreases in hours 20-23). The planned DAM SOE trajectory is denoted with solid line in Figure 2. The third market are secondary up reserve auctions taking place on the daily basis organised by the system operator. For the ESS, secondary up reserve means discharging a part of its SOE when the system operator calls for this service. ESS in our example bids the same amount of secondary up reserve throughout the day. ESS now has the obligation to discharge whenever called to activate up reserve. Therefore, the SOE constraint for secondary reserve must always be lower then the day-ahead SOE trajectory for the amount of the contracted discharging power and at the same time higher then other constraints, such as black start constraint (shaded area). The minimum SOE constraint (in respect to the DAM trajectory) due to secondary reserve obligation is represented as dashed line. In case that in the real-time balancing market (the fourth market) at time 11-12 the system operator calls for secondary up reserve, the ESS discharges and its SOE decreases (3). The operating point (the SOE) of the ESS is now below its planned SOE and it could cause problems when the ESS starts the planned discharge at evening or if the system operator calls for the service again. The stored energy would be lower than the required to follow the ESS's day-ahead plans. To resolve this issue, the ESS uses intraday market to recharge before the DAM planned evening discharging or before another up secondary reserve call is made. In hours 14-15 ESS recharge using intraday market (fifth market) and its SOE is back at the day-ahead trajectory. Solid red line in Figure 3 represents the actual SOE. If there is the need to provide black start, the system is in emergency mode and other market plans could be ignored.

VI. The Question of Ownership

There are three possible ownership structures for an ESS:

- ESS as a property of a private investor,
- ESS owned by a regulated natural monopoly, i.e. system operator,
- Separated ownership of the ESS physical assets and the energy stored within.

Private investors can use their ESS to participate in different markets, providing energy or ancillary services. This possibility of service stacking increases profitability of an ESS. The objective of the private investor is profit maximisation, and this profit is highest when the difference between buying and selling price is also highest. For this reason, the ESS owner performing arbitrage avoids bids that could affect market prices, even if it means not using the ESS's full capacity.

Natural monopolies, i.e. distribution and transmission system operators, might be able to own ESS the same way they own distribution or transmission lines. This involves little or no risk for the companies because the risk is usually transferred to the end-users by means of network fees and taxes. System operators' objective is overall system cost minimization, which means that the ESS is used to reduce congestion and, consequently, market prices whenever possible. This model of ownership indicates that the ESS is built for s specific application, e.g. congestion management, and since the regulated natural monopolies are not allowed to take part in energy markets (except to cover their energy losses, provide balancing energy or compensate losses for the cross-border exchanges), this model of ownership does not include service stacking.

If the ownership of physical assets is separated from the ownership of the energy stored within, the ESS could be used by different system users at different times. Physical assets in this model are owned by either regulated subjects or market participants. A decision to build this type of ESS can be made by the system operator to meet the need for a service, e.g. congestion management, and the investor is then chosen through an auction. When the ESS is operational, traders or system operators rent storage capacity by either auctioning or continuous bidding.

Necessary conditions for the ESS to offer ancillary services to the power system are organised wholesale market and compatible legal framework. European regulations on the ESS are confusing and differ between countries. This is why ENTSO-E recommends making separate regulation on storage and differentiate it from generation and consumption [34].

One of the main questions in the dialog about the ESS in Europe is whether it should be owned by regulated entities. General conclusion is that system operators are best suited to assess value of an ESS in the network as they operate it, but the first attempt on installation of the ESS should be done through a transparent market mechanism. If this process happens to be unsuccessful, the network operators can invest in the ESS themselves. This position is held by majority of the interested parties: Eurelectric, ENTSO-E, and Association of European DSOs (EDSO). EDSO recommends that the costs of building and operating the ESS to procure system stability should be recovered through network tariffs if the owner is a regulated entity. European Association for Storage of Energy (EASE) holds the position that *it is crucial to give the largest possible freedom to storage owners/operators as well as to offtakers of storage services (including regulated entities) in order to experiment innovative operation and remuneration schemes* [35]. European Agency for the cooperation of Energy Regulators (ACER) recommends DSOs should be prohibited from owning ESS to ensure their neutrality [36].

VII. Conclusion

This paper analyzes the benefits an ESS can bring to the system if the regulations are favourable. Various countries have different regulations regarding ESS and not all services are available for the ESS.

It is important to consider, while planning investments, many different ways the system can benefit from the installation of an ESS. Consideration of service stacking for the ESS is necessary to ensure its profitability. Service stacking should be planned with regard to technical parameters of the ESS, as well as time of scheduling and timing of the considered services.

Another way of ensuring return of ESS investments is combination of an ESS with other technologies, from conventional generators to consumers. This opens the way for the ESS to participate in even more markets it would otherwise not have access to.

Acknowledgment

This work has been supported by the Croatian Science Foundation and the Croatian Transmission System Operator (HOPS) under project *Smart Integration of RENewables - SIREN* (grant no. I-2583-2015) and the Croatian Environmental Protection and Energy Efficiency Fund under H2020 ERA-Net Smart Grids+ project *microGRId Positioning - uGRIP*.

References

[1] Sandia National Laboratories. (2018) DOE Global Energy Database. [Online]. Available: www.energystorageexchange.org/projects/data_visualization

[2] X. Luo, J. Wang, M. Dooner, and J. Clarke, "Overview of current development in electrical energy storage technologies and the application potential in power system operation," *Applied Energy*, vol. 137, pp. 511 – 536, 2015.

[3] A. A. Akhil, G. Huff, A. B. Currier, B. C. Kaun, D. M. Rastler, S. B. Chen, A. L. Cotter, D. T. Bradshaw, and W. D. Gauntlett, "DOE/EPRI Electricity Storage Handbook in Collaboration with NRECA," Sandia National Laboratories, Tech. Rep., January 2015.

[4] Z. Zbunjak, H. Bašić, H. Pandžić, and I. Kuzle, "Phase shifting autotransformer, transmission switching and battery energy storage systems to ensure n-1 criterion of stability," *Energija*, vol. 64, pp. 285–298, Oct. 2015.

[5] V. Guerrero-Mestre, Y. Dvorkin, R. Fernández-Blanco, M. A. Ortega-Vazquez, and J. Contreras, "Incorporating energy storage into probabilistic security-constrained unit commitment," *IET Generation, Transmission Distribution*, vol. 12, no. 18, pp. 4206–4215, 2018.

[6] Z. Luburić, H. Pandžić, T. Plavšić, L. Teklić, and V. Valentić, "Role of energy storage in ensuring transmission system adequacy and security," *Energy*, vol. 156, pp. 229 – 239, 2018.

[7] C. Yuan, C. Liu, T. Zhao, X. Xiao, and N. Tang, "Energy storage configuration strategy for virtual synchronous machine," in *2016 IEEE Energy Conversion Congress and Exposition (ECCE)*, Sept 2016, pp. 1–6.

[8] A. S. Tsagkou, E. D. K. D. I. Doukas, D. P. Labridis, A. G. Marinopoulos, and T. Tengnér, "Stacking grid services with energy storage techno-economic analysis," in *2017 IEEE Manchester PowerTech*, June 2017, pp. 1–6.

[9] H. Pandžić and I. Kuzle, "Energy storage operation in the day-ahead electricity market," in *2015 12th International Conference on the European Energy Market (EEM)*, May 2015, pp. 1–6.

[10] J. Lagarto, F. Fernandes, J. A. M. Sousa, and J. Santana, "Multi-market optimal scheduling of a power generation portfolio with a price-maker pumped-storage hydro unit," in *2016 13th International Conference on the European Energy Market (EEM)*, June 2016, pp. 1–5.

[11] E. Drury, P. Denholm, and R. Sioshansi, "The value of compressed air energy storage in energy and reserve markets," *Energy*, vol. 36, no. 8, pp. 4959 – 4973, 2011.

[12] B. Zakeri and S. Syri, "Economy of electricity storage in the nordic electricity market: The case for finland," in *11th International Conference on the European Energy Market (EEM14)*, May 2014, pp. 1–6.

[13] B. Zakeri, S. Syri, and F. Wagner, "Economics of energy storage in the German electricity and reserve markets," in *2017 14th International Conference on the European Energy Market (EEM)*, June 2017, pp. 1–6.

[14] M. Farrokhseresht, N. G. Paterakis, M. Gibescu, and J. G. Slootweg, "Participation of a combined wind and storage unit in the day-ahead and local balancing markets," in *2018 15th International Conference on the European Energy Market (EEM)*, June 2018, pp. 1–5.

[15] Government Department for Business, Energy and Industrial Strategy, *Capacity Market Consultation – Improving the Framework*. UK, 2017.

[16] A. Zeh, M. Müller, M. Naumann, H. Hesse, A. Jossen, and R. Witzmann, "Fundamentals of using battery energy storage systems to provide primary control reserves in germany," *Batteries*, vol. 2, pp. 1–21, Sept. 2016.

[17] F. Mayr and S. Adam. (2017) The German Secondary Control Reserve market: Will recent regulatory updates finally pave the way for energy storage? [Online]. Available: www.apricum-group.com/german-secondary-control-reserve-market-will-recent-regulatory-updates-finally-pave-way-energy-storage/

[18] S. Patel. (2017) Two sce gas-battery hybrid projects revolutionize peaker performance. [Online]. Available: https://www.powermag.com/two-sce-gas-battery-hybrid-projects-revolutionize-peaker-performance/

[19] N. Grid. (2018) Demand turn up. [Online]. Available: https://www.nationalgrideso.com/balancing-services/reserve-services/demand-turn?overview

[20] California ISO, *Storage as a Transmission Asset: Issue paper*, March 2018.

[21] R. E. de España. (2016) Almacena project. [Online]. Available: www.ree.es/en/sustainability/noteworthy-projects/rdi-projects-that-contribute-to-the-business/almacena-project

[22] D. A. Meyer, J. W. Cote, and D. W. Burlingame, "Pre/Post - Watana Transmission Study; Draft report," Alaska Energy Authority, Tech. Rep., 2014.

[23] A. Nourai, V. I. Kogan, and C. M. Schafer, "Load Leveling Reduces Line Losses," *IEEE Transactions on Power Delivery*, vol. 23, no. 4, pp. 2168–2173, Oct. 2008.

[24] H. Saboori and H. Abdi, "Application of a grid scale energy storage system to reduce distribution network losses," in *18th Electric Power Distribution Conference*, April 2013, pp. 1–5.

[25] H. Pandžić, "Optimal battery energy storage investment in buildings," *Energy and Buildings*, vol. 175, pp. 189 – 198, 2018.

[26] Ipsos-London Economics-Deloitte consortium, "Second consumer market study on the functioning of the retail electricity markets for con-

sumers in the eu," Consumers, Health, Agriculture and Food Executive Agency, Tech. Rep., Sept. 2016.
[27] European Comission, "New electricity market design: a fair deal for consumers," Tech. Rep., 2016.
[28] S. P. Ayeng'o, T. Schirmer, K.-P. Kairies, H. Axelsen, and D. U. Sauer, "Comparison of off-grid power supply systems using lead-acid and lithium-ion batteries," *Solar Energy*, vol. 162, pp. 140 – 152, 2018.
[29] Solarquotes. (2018) Solar Battery Storage Comparison Table. [Online]. Available: www.solarquotes.com.au/battery-storage/comparison-table/
[30] Bulgana Green Power Hub Overview. (2018). [Online]. Available: bulganawindfarm.com.au
[31] FPL Babcock Ranch Solar Energy Center, "Babcock Ranch Solar Factsheet," 2018.
[32] D. Waitkus. (2018) Appalachian Power's Byllesby Plant Inducted Into Hydro Hall of Fame. [Online]. Available: aepretirees.com/2018/08/22/appalachian-powers-byllesby-plant-inducted-into-hydro-hall-of-fame/
[33] B. Rusch. (2018) The large Heilbronn power plant gets pow. [Online]. Available: www.hannovermesse.de/en/news/the-large-heilbronn-power-plant-gets-pow-84480.xhtml
[34] European Network of Transmission System Operators for Electricity, *Energy storage and storage services*, October 2016.
[35] EASE - European Association for Storage of Energy, *EASE Reply to European Commission's Questions on "The Future of Energy Storage in the EU"*, Sept. 2018.
[36] Agency for the Cooperation of Energy Regulators (ACER), *European Energy Regulators' White Paper #2 - The Role of the DSO - Relevant to European Commission's Clean Energy Proposals*, May 2017.

Bibliography

[1] IRENA. Renewable energy statistics 2020, 2020. URL https://www.irena.org/publications/2020/Jul/Renewable-energy-statistics-2020.

[2] European Commission. Stepping up europe's 2030 climate ambition - investing in a climate-neutral future for the benefit of our people. September 2020.

[3] EU European Commission. Clean energy for all europeans package, May 2019. URL https://ec.europa.eu/energy/topics/energy-strategy/clean-energy-all-europeans_en.

[4] IRENA. Renewable power generation costs in 2018. May 2019.

[5] IRENA. *Power System Flexibility For the Energy Transition, Part 1: Overview for policy makers*. International Renewable Energy Agency, Abu Dhabi, 2018.

[6] ETIP SNET. Digitalisation of the energy system and customer participation: Description and recommendations of technologies, use cases and cybersecurity. November 20.

[7] Prabha Kundur, Neal J Balu, and Mark G Lauby. *Power system stability and control*, volume 7. McGraw-hill New York, 1994.

[8] Kennedy Mwanza and You Shi. Congestion management: re-dispatch and application of facts. Master's thesis, 2006.

[9] Xiaohe Yan, Chenghong Gu, Xin Zhang, and Furong Li. Robust optimization-based energy storage operation for system congestion management. *IEEE Systems Journal*, 2019.

[10] C Opathella, Ayman Elkasrawy, Amr A Mohamed, and B Venkatesh. Optimal scheduling of merchant-owned energy storage systems with multiple ancillary services. *IEEE Open Access Journal of Power and Energy*, 7:31–40, 2019.

[11] Raymond H Byrne, Tu A Nguyen, David A Copp, Babu R Chalamala, and Imre Gyuk. Energy management and optimization methods for grid energy storage systems. *IEEE Access*, 6:13231–13260, 2017.

[12] Robert A Huggins and Robert A Huggins. *Energy storage: fundamentals, materials and applications*. Springer, 2016.

[13] U.S. Department of Energy. Doe global energy storage database, 2020. URL `https://www.sandia.gov/ess-ssl/global-energy-storage-database-home/`.

[14] S Jalal Kazempour, M Parsa Moghaddam, MR Haghifam, and GR Yousefi. Electric energy storage systems in a market-based economy: Comparison of emerging and traditional technologies. *Renewable energy*, 34(12):2630–2639, 2009.

[15] Hossam A Gabbar. *Energy Conservation in Residential, Commercial, and Industrial Facilities*. John Wiley & Sons, 2018.

[16] Seamus D Garvey and Andrew Pimm. Compressed air energy storage. In *Storing energy*, pages 87–111. Elsevier, 2016.

[17] Canan Acar. A comprehensive evaluation of energy storage options for better sustainability. *International Journal of Energy Research*, 42(12):3732–3746, 2018.

[18] Christopher K Dyer. Fuel cells for portable applications. *Journal of Power Sources*, 106 (1-2):31–34, 2002.

[19] JM Zhao and ZM Zhang. Electromagnetic energy storage and power dissipation in nanostructures. *Journal of Quantitative Spectroscopy and Radiative Transfer*, 151:49–57, 2015.

[20] Adrian Schneuwly. High reliability power backup with advanced energy storage. *Maxwell Technologies White Paper*, 2006.

[21] Feng Ju, Qiao Zhang, Weiwen Deng, and Jingshan Li. Review of structures and control of battery-supercapacitor hybrid energy storage system for electric vehicles. In *2014 IEEE International Conference on Automation Science and Engineering (CASE)*, pages 143–148. IEEE, 2014.

[22] Venkata Suresh Vulusala G and Sreedhar Madichetty. Application of superconducting magnetic energy storage in electrical power and energy systems: a review. *International Journal of Energy Research*, 42(2):358–368, 2018.

[23] Diana Enescu, Gianfranco Chicco, Radu Porumb, and George Seritan. Thermal energy storage for grid applications: Current status and emerging trends. *Energies*, 13(2):340, 2020.

[24] Huili Zhang, Jan Baeyens, Gustavo Caceres, Jan Degreve, and Yongqin Lv. Thermal energy storage: Recent developments and practical aspects. *Progress in Energy and Combustion Science*, 53:1–40, 2016.

[25] C Castellón, M Medrano, J Roca, M Nogués, A Castell, and LF Cabeza. Use of microencapsulated phase change materials in building applications. *ASHRAE. project ENE2005-08256-C02-01/ALT*, 2007.

[26] Gilles Flamant, Daniel Gauthier, Hadrien Benoit, J-L Sans, Benjamin Boissière, Renaud Ansart, and Mehrdji Hemati. A new heat transfer fluid for concentrating solar systems: Particle flow in tubes. *Energy Procedia*, 49:617–626, 2014.

[27] Gilles Flamant, Daniel Gauthier, Hadrien Benoit, Jean-Louis Sans, Roger Garcia, Benjamin Boissière, Renaud Ansart, and Mehrdji Hemati. Dense suspension of solid particles as a new heat transfer fluid for concentrated solar thermal plants: On-sun proof of concept. *Chemical Engineering Science*, 102:567–576, 2013.

[28] HL Zhang, Jan Baeyens, J Degrève, and G Cacères. Concentrated solar power plants: Review and design methodology. *Renewable and sustainable energy reviews*, 22:466–481, 2013.

[29] Sylvie Genies Christian Glaize. *Lithium Batteries and Other Electrochemical Storage Systems*. Electrical Engineering Series. Wiley-ISTE, 2013. ISBN 978-1-84821-496-5.

[30] Yushu Sun, Zhenxing Zhao, Min Yang, Dongqiang Jia, Wei Pei, and Bin Xu. Overview of energy storage in renewable energy power fluctuation mitigation. *CSEE Journal of Power and Energy Systems*, 6(1):160–173, 2019.

[31] Xing Luo, Jihong Wang, Mark Dooner, and Jonathan Clarke. Overview of current development in electrical energy storage technologies and the application potential in power system operation. *Applied energy*, 137:511–536, 2015.

[32] Haisheng Chen, Thang Ngoc Cong, Wei Yang, Chunqing Tan, Yongliang Li, and Yulong Ding. Progress in electrical energy storage system: A critical review. *Progress in natural science*, 19(3):291–312, 2009.

[33] Fritz Beck and Paul Rüetschi. Rechargeable batteries with aqueous electrolytes. *Electrochimica Acta*, 45(15-16):2467–2482, 2000.

[34] Wenhua H Zhu, Ying Zhu, Zenda Davis, and Bruce J Tatarchuk. Energy efficiency and capacity retention of ni–mh batteries for storage applications. *Applied Energy*, 106:307–313, 2013.

[35] MA Fetcenko, SR Ovshinsky, B Reichman, K Young, C Fierro, J Koch, A Zallen, W Mays, and T Ouchi. Recent advances in nimh battery technology. *Journal of Power Sources*, 165(2):544–551, 2007.

[36] Battery University. Learn about batteries, 2020. URL `https://batteryuniversity.com/learn/article/bu_210a_why_does_sodium_sulfur_need_to_be_heated`.

[37] White Paper International Electrotechnical Commission (IEC). Electrical energy storage, 2019. URL `https://www.iec.ch/whitepaper/pdf/iecWP-energystorage-LR-en.pdf`.

[38] Joan Rocabert, Ruben Capó-Misut, Raúl Santiago Muñoz-Aguilar, José Ignacio Candela, and Pedro Rodriguez. Control of energy storage system integrating electrochemical batteries and supercapacitors for grid-connected applications. *IEEE Transactions on Industry Applications*, 55(2):1853–1862, 2018.

[39] Wesley Cole and Allister Frazier. Cost projections for utility-scale battery storage: 2020 update. doi: 10.2172/1665769. URL `https://www.osti.gov/biblio/1665769`.

[40] Ran Fu Ashwin Ramdas Jal Desai Feldman, David and Robert Margolis. U.s.solar photovoltaic system and energy storage cost benchmark: Q1 2019. *NREL/TP6A20-75161. Golden, CO: National Renewable Energy Laboratory*, 2019.

[41] Energy Storage World Forum. Energy storage standardization and specifications: What steps are being taken and where can they go further? 2020.

[42] Lexuan Meng, Jawwad Zafar, Shafiuzzaman K Khadem, Alan Collinson, Kyle C Murchie, Federico Coffele, and Graeme M Burt. Fast frequency response from energy storage systems—a review of grid standards, projects and technical issues. *IEEE Transactions on Smart Grid*, 11(2):1566–1581, 2019.

[43] Enerdata Trinomics Artelys, Directorate-General for Energy (European Commission). Study on energy storage contribution to the security of the electricity supply in europe.

[44] N. Hajia and B. Venkatesh. Soc model of high power lithium-ion battery. In *IEEE Electrical Power and Energy Conference (EPEC)*, page 6, 2015.

[45] David M Rosewater, David A Copp, Tu A Nguyen, Raymond H Byrne, and Surya Santoso. Battery energy storage models for optimal control. *IEEE Access*, 7:178357–178391, 2019.

[46] Patrick T Moseley and Jurgen Garche. *Electrochemical energy storage for renewable sources and grid balancing*. Newnes, 2014.

[47] Mark E Fuller. A battery model for constant-power discharge including rate effects. *Energy conversion and management*, 88:199–205, 2014.

[48] WM Saslow. How batteries discharge: A simple model. *American Journal of Physics*, 76(3):218–223, 2008.

[49] Marijn R Jongerden and Boudewijn R Haverkort. Which battery model to use? *IET software*, 3(6):445–457, 2009.

[50] Anna Tomaszewska, Zhengyu Chu, Xuning Feng, Simon O'Kane, Xinhua Liu, Jingyi Chen, Chenzhen Ji, Elizabeth Endler, Ruihe Li, Lishuo Liu, et al. Lithium-ion battery fast charging: a review. *ETransportation*, 1:100011, 2019.

[51] Richtek. Understanding the characteristics of li-ion batteries and richtek power management solutions. *Richtek Technology Corporation*, pages 1–22, 2014.

[52] Xiao-Guang Yang and Chao-Yang Wang. Understanding the trilemma of fast charging, energy density and cycle life of lithium-ion batteries. *Journal of Power Sources*, 402: 489–498, 2018.

[53] Marc Doyle, Thomas F Fuller, and John Newman. Modeling of galvanostatic charge and discharge of the lithium/polymer/insertion cell. *Journal of the Electrochemical society*, 140(6):1526, 1993.

[54] David Rosewater, Summer Ferreira, David Schoenwald, Jonathan Hawkins, and Surya Santoso. Battery energy storage state-of-charge forecasting: Models, optimization, and accuracy. *IEEE Transactions on Smart Grid*, 10(3):2453–2462, 2018.

[55] Hrvoje Pandžić and Vedran Bobanac. An accurate charging model of battery energy storage. *IEEE Transactions on Power Systems*, 34(2):1416–1426, 2018.

[56] Hrvoje Pandžić and Igor Kuzle. Energy storage operation in the day-ahead electricity market. In *2015 12th International Conference on the European Energy Market (EEM)*, pages 1–6. IEEE, 2015.

[57] Stylianos I Vagropoulos and Anastasios G Bakirtzis. Optimal bidding strategy for electric vehicle aggregators in electricity markets. *IEEE Transactions on power systems*, 28(4): 4031–4041, 2013.

[58] R Mohan Mathur and Rajiv K Varma. *Thyristor-based FACTS controllers for electrical transmission systems*. John Wiley & Sons, 2002.

[59] Narain G Hingorani and Laszlo Gyugyi. Facts concept and general system considerations. 2000.

[60] Joe H Chow and Juan J Sanchez-Gasca. *Power System Modeling, Computation, and Control*. John Wiley & Sons, 2020.

[61] Narain G.. Hingorani and Laszlo Gyugyi. *Understanding FACTS: concepts and technology of flexible AC transmission systems*. IEEE press, 2000.

[62] Huilian Liao and Jovica V Milanović. On capability of different facts devices to mitigate a range of power quality phenomena. *IET Generation, Transmission & Distribution*, 11 (5):1202–1211, 2016.

[63] Sauvik Biswas and Paresh Kumar Nayak. State-of-the-art on the protection of facts compensated high-voltage transmission lines: a review. *High voltage*, 3(1):21–30, 2018.

[64] Zhengyu Huang, Yinxin Ni, CM Shen, Felix F Wu, Shousun Chen, and Baolin Zhang. Application of unified power flow controller in interconnected power systems-modeling, interface, control strategy, and case study. *IEEE Transactions on Power Systems*, 15(2): 817–824, 2000.

[65] Sangeeta Jamhoria and Laxmi Srivastava. Applications of thyristor controlled series compensator in power system: an overview. In *2014 International Conference on Power Signals Control and Computations (EPSCICON)*, pages 1–6. IEEE, 2014.

[66] Xiaohu Zhang, Di Shi, Zhiwei Wang, Bo Zeng, Xinan Wang, Kevin Tomsovic, and Yanming Jin. Optimal allocation of series facts devices under high penetration of wind power within a market environment. *IEEE Transactions on Power Systems*, 33(6):6206–6217, 2018.

[67] Zahra Moravej, Mohammad Pazoki, and Mojtaba Khederzadeh. New pattern-recognition method for fault analysis in transmission line with upfc. *IEEE Transactions on Power Delivery*, 30(3):1231–1242, 2014.

[68] Yuanrui Sang and Mostafa Sahraei-Ardakani. The interdependence between transmission switching and variable-impedance series facts devices. *IEEE Transactions on Power Systems*, 33(3):2792–2803, 2017.

[69] Ebrahim Vaahedi. Power system operation optimization. 2014.

[70] Marija Miletić, Hrvoje Pandžić, and Dechang Yang. Operating and investment models for energy storage systems. *Energies*, 13(18):4600, 2020.

[71] Yuping Huang, Panos M Pardalos, and Qipeng P Zheng. Deterministic unit commitment models and algorithms. In *Electrical Power Unit Commitment*, pages 11–47. Springer, 2017.

[72] Samer Takriti, John R Birge, and Erik Long. A stochastic model for the unit commitment problem. *IEEE Transactions on Power Systems*, 11(3):1497–1508, 1996.

[73] Aharon Ben-Tal and Arkadi Nemirovski. Robust convex optimization. *Mathematics of operations research*, 23(4):769–805, 1998.

[74] Yang Wang, Qing Xia, and Chongqing Kang. Unit commitment with volatile node injections by using interval optimization. *IEEE Transactions on Power Systems*, 26(3): 1705–1713, 2011.

[75] Pu Li, Harvey Arellano-Garcia, and Günter Wozny. Chance constrained programming approach to process optimization under uncertainty. *Computers & chemical engineering*, 32(1-2):25–45, 2008.

[76] David J Rader. *Deterministic operations research: models and methods in linear optimization*. John Wiley & Sons, 2010.

[77] E Ela, M Milligan, and B Kirby. Operating reserves and variable generation. doi: 10.2172/1023095. URL `https://www.osti.gov/biblio/1023095`.

[78] Tao Hong, Pierre Pinson, Yi Wang, Rafał Weron, Dazhi Yang, Hamidreza Zareipour, et al. Energy forecasting: A review and outlook. *WORking papers in Management Science (WORMS)*, (WORMS/20/08), 2020.

[79] L Suganthi and Anand A Samuel. Energy models for demand forecasting—a review. *Renewable and sustainable energy reviews*, 16(2):1223–1240, 2012.

[80] Martin T Hagan and Suzanne M Behr. The time series approach to short term load forecasting. *IEEE transactions on power systems*, 2(3):785–791, 1987.

[81] Ibrahim Moghram and Saifur Rahman. Analysis and evaluation of five short-term load forecasting techniques. *IEEE Transactions on power systems*, 4(4):1484–1491, 1989.

[82] XQ Liu, BW Ang, and TN Goh. Forecasting of electricity consumption: a comparison between an econometric model and a neural network model. In *[Proceedings] 1991 IEEE International Joint Conference on Neural Networks*, pages 1254–1259. IEEE, 1991.

[83] S Sp Pappas, L Ekonomou, D Ch Karamousantas, GE Chatzarakis, SK Katsikas, and P Liatsis. Electricity demand loads modeling using autoregressive moving average (arma) models. *Energy*, 33(9):1353–1360, 2008.

[84] Kyung-Bin Song, Young-Sik Baek, Dug Hun Hong, and Gilsoo Jang. Short-term load forecasting for the holidays using fuzzy linear regression method. *IEEE transactions on power systems*, 20(1):96–101, 2005.

[85] Halim Ceylan and Harun Kemal Ozturk. Estimating energy demand of turkey based on economic indicators using genetic algorithm approach. *Energy Conversion and Management*, 45(15-16):2525–2537, 2004.

[86] Jatin Bedi and Durga Toshniwal. Empirical mode decomposition based deep learning for electricity demand forecasting. *Ieee Access*, 6:49144–49156, 2018.

[87] GWEC Market Intelligence. Global wind report 2019, 2020. URL `https://gwec.net/global-wind-report-2019/`.

[88] Jakob W Messner, Pierre Pinson, Jethro Browell, Mathias B Bjerregård, and Irene Schicker. Evaluation of wind power forecasts—an up-to-date view. *Wind Energy*, 23 (6):1461–1481, 2020.

[89] Dennis W Van der Meer, Joakim Widén, and Joakim Munkhammar. Review on probabilistic forecasting of photovoltaic power production and electricity consumption. *Renewable and Sustainable Energy Reviews*, 81:1484–1512, 2018.

[90] Germán Morales-España, Álvaro Lorca, and Mathijs M de Weerdt. Robust unit commitment with dispatchable wind power. *Electric Power Systems Research*, 155:58–66, 2018.

[91] Dimitris Bertsimas and Melvyn Sim. The price of robustness. *Operations research*, 52 (1):35–53, 2004.

[92] Hrvoje Pandžić, Yury Dvorkin, Ting Qiu, Yishen Wang, and Daniel S Kirschen. Toward cost-efficient and reliable unit commitment under uncertainty. *IEEE Transactions on Power Systems*, 31(2):970–982, 2015.

[93] Yury Dvorkin, Hrvoje Pandžić, Miguel A Ortega-Vazquez, and Daniel S Kirschen. A hybrid stochastic/interval approach to transmission-constrained unit commitment. *IEEE Transactions on Power Systems*, 30(2):621–631, 2014.

[94] David Pozo and Javier Contreras. A chance-constrained unit commitment with an *nk* security criterion and significant wind generation. *IEEE Transactions on Power systems*, 28(3):2842–2851, 2012.

[95] Qianfan Wang, Yongpei Guan, and Jianhui Wang. A chance-constrained two-stage stochastic program for unit commitment with uncertain wind power output. *IEEE Transactions on Power Systems*, 27(1):206–215, 2011.

[96] U Aytun Ozturk, Mainak Mazumdar, and Bryan A Norman. A solution to the stochastic unit commitment problem using chance constrained programming. *IEEE Transactions on Power Systems*, 19(3):1589–1598, 2004.

[97] Hrvoje Pandžić, Ting Qiu, and Daniel S Kirschen. Comparison of state-of-the-art transmission constrained unit commitment formulations. In *2013 IEEE power & energy society general meeting*, pages 1–5. IEEE, 2013.

[98] Saleh Y Abujarad, MW Mustafa, and JJ Jamian. Recent approaches of unit commitment in the presence of intermittent renewable energy resources: A review. *Renewable and Sustainable Energy Reviews*, 70:215–223, 2017.

[99] Carlos Suazo-Martinez, Eduardo Pereira-Bonvallet, Rodrigo Palma-Behnke, and Xiao-Ping Zhang. Impacts of energy storage on short term operation planning under centralized spot markets. *IEEE Transactions on Smart Grid*, 5(2):1110–1118, 2013.

[100] Marija Miletic, Zora Luburic, Ivan Pavic, Tomislav Capuder, Hrvoje Pandžic, Ivan Androcec, and Anton Marušic. A review of energy storage systems applications. 2018.

[101] Yunfeng Wen, Chuangxin Guo, Hrvoje Pandžić, and Daniel S Kirschen. Enhanced security-constrained unit commitment with emerging utility-scale energy storage. *IEEE Transactions on power Systems*, 31(1):652–662, 2015.

[102] Yuzhou Zhou, Qiaozhu Zhai, and Lei Wu. Multistage transmission-constrained unit commitment with renewable energy and energy storage: Implicit and explicit decision methods. *IEEE Transactions on Sustainable Energy*, 2020.

[103] Mads Almassalkhi, Yury Dvorkin, Jennifer Marley, Ricardo Fernández-Blanco, Ian Hiskens, Daniel Kirschen, Jonathon Martin, Hrvoje Pandžič, Ting Qiu, Mushfiqur Sarker, et al. Incorporating storage as a flexible transmission asset in power system operation

procedure. In *2016 Power Systems Computation Conference (PSCC)*, pages 1–7. IEEE, 2016.

[104] Abdollah Ahmadi, Ali Esmaeel Nezhad, and Branislav Hredzak. Security-constrained unit commitment in presence of lithium-ion battery storage units using information-gap decision theory. *IEEE Transactions on Industrial Informatics*, 15(1):148–157, 2018.

[105] Nan Li and Kory W Hedman. Economic assessment of energy storage in systems with high levels of renewable resources. *IEEE Transactions on Sustainable Energy*, 6(3): 1103–1111, 2014.

[106] Kristina Jurković, Hrvoje Pandzić, and Igor Kuzle. Robust unit commitment with large-scale battery storage. In *2017 IEEE Power & Energy Society General Meeting*, pages 1–5. IEEE, 2017.

[107] Yongchao Wang, Kai Dong, Kaiwen Zeng, Xinbin Lan, Wei Zhou, Minjing Yang, and Wenhuan Hao. Robust unit commitment model based on optimal uncertainty set. *IEEE Access*, 2020.

[108] Zhe Chen, Zhengshuo Li, Chuangxin Guo, Yi Ding, and Yubin He. Two-stage chance-constrained unit commitment based on optimal wind power consumption point considering battery energy storage. *IET Generation, Transmission & Distribution*, 14(18):3738–3749, 2020.

[109] Yan Xu, Tianyang Zhao, Shuqian Zhao, Jianhua Zhang, and Yang Wang. Multi-objective chance-constrained optimal day-ahead scheduling considering bess degradation. *CSEE Journal of Power and Energy Systems*, 4(3):316–325, 2018.

[110] Kenneth Bruninx, Yury Dvorkin, Erik Delarue, Hrvoje Pandžić, William D'haeseleer, and Daniel S Kirschen. Coupling pumped hydro energy storage with unit commitment. *IEEE Transactions on Sustainable Energy*, 7(2):786–796, 2015.

[111] David Pozo, Javier Contreras, and Enzo E Sauma. Unit commitment with ideal and generic energy storage units. *IEEE Transactions on Power Systems*, 29(6):2974–2984, 2014.

[112] Raphael Saavedra, Alexandre Street, and Jose M Arroyo. Day-ahead contingency-constrained unit commitment with co-optimized post-contingency transmission switching. *IEEE Transactions on Power Systems*, 2020.

[113] Kári Hreinsson, Anna Scaglione, and Bita Analui. Continuous time multi-stage stochastic unit commitment with storage. *IEEE Transactions on Power Systems*, 34(6):4476–4489, 2019.

[114] Zao Tang, Yikui Liu, Lei Wu, Junyong Liu, and Hongjun Gao. Reserve model of energy storage in day-ahead joint energy and reserve markets: A stochastic uc solution. *IEEE Transactions on Smart Grid*, 2020.

[115] Hongyu Wu, Mohammad Shahidehpour, Zuyi Li, and Wei Tian. Chance-constrained day-ahead scheduling in stochastic power system operation. *IEEE Transactions on Power Systems*, 29(4):1583–1591, 2014.

[116] Dawei He, Zhenyu Tan, and Ronald G Harley. Chance constrained unit commitment with wind generation and superconducting magnetic energy storages. In *2012 IEEE Power and Energy Society General Meeting*, pages 1–6. IEEE, 2012.

[117] Nhung Nguyen-Hong and Yosuke NAKANISHI. Frequency-constrained unit commitment considering battery storage system and forecast error. In *2018 IEEE Innovative Smart Grid Technologies-Asia (ISGT Asia)*, pages 1171–1176. IEEE, 2018.

[118] Ryan T Elliott, Ricardo Fernandez-Blanco, Kelly Kozdras, Josh Kaplan, Brian Lockyear, Jason Zyskowski, and Daniel S Kirschen. Sharing energy storage between transmission and distribution. *IEEE Transactions on Power Systems*, 34(1):152–162, 2018.

[119] Yingyun Sun, Jianliang Zhong, Zuyi Li, Wei Tian, and Mohammad Shahidehpour. Stochastic scheduling of battery-based energy storage transportation system with the penetration of wind power. *IEEE Transactions on Sustainable Energy*, 8(1):135–144, 2016.

[120] Victoria Guerrero-Mestre, Yury Dvorkin, Ricardo Fernández-Blanco, Miguel A Ortega-Vazquez, and Javier Contreras. Incorporating energy storage into probabilistic security-constrained unit commitment. *IET Generation, Transmission & Distribution*, 12(18): 4206–4215, 2018.

[121] Yu Xia, Scott G Ghiocel, Daniel Dotta, Daniel Shawhan, Andrew Kindle, and Joe H Chow. A simultaneous perturbation approach for solving economic dispatch problems with emission, storage, and network constraints. *IEEE transactions on smart grid*, 4(4): 2356–2363, 2013.

[122] Ahmad Nikoobakht, Jamshid Aghaei, Masood Parvania, and Mostafa Sahraei-Ardakani. Contribution of facts devices in power systems security using milp-based opf. *IET Generation, Transmission & Distribution*, 12(15):3744–3755, 2018.

[123] Abraham Charnes and William W Cooper. Chance-constrained programming. *Management science*, 6(1):73–79, 1959.

[124] Zechun Hu. *Energy storage for power system planning and operation*. Wiley, 2020.

[125] PJM. Lmp supports competitive wholesale power markets. 2020.

[126] Europe Union. Directive (eu) 2019/944 of the european parliament and of the council of 5 june 2019 on common rules for the internal market for electricity and amending directive 2012/27/eu. 2019.

[127] Sirja-Leena Penttinen, Pami Aalto, and Teresa Haukkala. Eu electricity market reform and the adoption of the clean energy package addressing system flexibility. *Regulation (EU)*, 328:210–230, 2018.

[128] Europe Union. Commission regulation (eu) 2017/2195 of 23 november 2017 establishing a guideline on electricity balancing. 2017.

[129] Anthony Papavasiliou, Mette Bjørndal, Gerard Doorman, and Nicolas Stevens. Hierarchical balancing in zonal markets. In *2020 17th International Conference on the European Energy Market (EEM)*, pages 1–6. IEEE, 2020.

[130] Jeremiah Deboever and Santiago Grijalva. Optimal scheduling of large-scale price-maker energy storage. In *2016 IEEE Power and Energy Conference at Illinois (PECI)*, pages 1–6. IEEE, 2016.

[131] Nitin Padmanabhan, Mohamed Ahmed, and Kankar Bhattacharya. Battery energy storage systems in energy and reserve markets. *IEEE Transactions on Power Systems*, 35(1): 215–226, 2019.

[132] Hrvoje Pandžić, Juan M Morales, Antonio J Conejo, and Igor Kuzle. Offering model for a virtual power plant based on stochastic programming. *Applied Energy*, 105:282–292, 2013.

[133] Ehsan Nasrolahpour, Jalal Kazempour, Hamidreza Zareipour, and William D Rosehart. A bilevel model for participation of a storage system in energy and reserve markets. *IEEE Transactions on Sustainable Energy*, 9(2):582–598, 2017.

[134] Ehsan Nasrolahpour, Jalal Kazempour, Hamidreza Zareipour, and William D Rosehart. Impacts of ramping inflexibility of conventional generators on strategic operation of energy storage facilities. *IEEE Transactions on Smart Grid*, 9(2):1334–1344, 2016.

[135] Dheepak Krishnamurthy, Canan Uckun, Zhi Zhou, Prakash R Thimmapuram, and Audun Botterud. Energy storage arbitrage under day-ahead and real-time price uncertainty. *IEEE Transactions on Power Systems*, 33(1):84–93, 2017.

[136] Gilles Bertrand and Anthony Papavasiliou. Adaptive trading in continuous intraday electricity markets for a storage unit. *IEEE Transactions on Power Systems*, 35(3):2339–2350, 2019.

[137] Ioannis Boukas, Damien Ernst, Anthony Papavasiliou, and Bertrand Cornélusse. Intraday bidding strategies for storage devices using deep reinforcement learning. In *International Conference on the European Energy Market, Łódź 27-29 June 2018*, page 6, 2018.

[138] Mykel J Kochenderfer. *Decision making under uncertainty: theory and application*. MIT press, 2015.

[139] Antonio J Conejo, Luis Baringo, S Jalal Kazempour, and Afzal S Siddiqui. Investment in electricity generation and transmission. *Cham Zug, Switzerland: Springer International Publishing*, 119, 2016.

[140] Carlos Bustos, Enzo Sauma, Sebastian de la Torre, José A Aguado, Javier Contreras, and David Pozo. Energy storage and transmission expansion planning: substitutes or complements? *IET Generation, Transmission & Distribution*, 12(8):1738–1746, 2017.

[141] Bolun Xu, Yishen Wang, Yury Dvorkin, Ricardo Fernández-Blanco, Cesar A Silva-Monroy, Jean-Paul Watson, and Daniel S Kirschen. Scalable planning for energy storage in energy and reserve markets. *IEEE Transactions on Power systems*, 32(6):4515–4527, 2017.

[142] Daniel J Olsen and Daniel S Kirschen. Profitable emissions-reducing energy storage. *IEEE Transactions on Power Systems*, 35(2):1509–1519, 2019.

[143] Ahmad Nikoobakht, Jamshid Aghaei, Miadreza Shafie-khah, and João PS Catalão. Allocation of fast-acting energy storage systems in transmission grids with high renewable generation. *IEEE Transactions on Sustainable Energy*, 2019.

[144] Hrvoje Pandžić, Yishen Wang, Ting Qiu, Yury Dvorkin, and Daniel S Kirschen. Near-optimal method for siting and sizing of distributed storage in a transmission network. *IEEE Transactions on Power Systems*, 30(5):2288–2300, 2014.

[145] Ricardo Fernández-Blanco, Yury Dvorkin, Bolun Xu, Yishen Wang, and Daniel S Kirschen. Optimal energy storage siting and sizing: A wecc case study. *IEEE transactions on sustainable energy*, 8(2):733–743, 2016.

[146] Yongli Zhu, Chengxi Liu, Kai Sun, Di Shi, and Zhiwei Wang. Optimization of battery energy storage to improve power system oscillation damping. *IEEE Transactions on Sustainable Energy*, 10(3):1015–1024, 2018.

[147] Ehsan Nasrolahpour, S Jalal Kazempour, Hamidreza Zareipour, and William D Rosehart. Strategic sizing of energy storage facilities in electricity markets. *IEEE Transactions on Sustainable Energy*, 7(4):1462–1472, 2016.

[148] Luis N Vicente and Paul H Calamai. Bilevel and multilevel programming: A bibliography review. *Journal of Global optimization*, 5(3):291–306, 1994.

[149] Kristina Pandžić, Hrvoje Pandžić, and Igor Kuzle. Coordination of regulated and merchant energy storage investments. *IEEE Transactions on Sustainable Energy*, 9(3):1244–1254, 2017.

[150] Yury Dvorkin, Ricardo Fernandez-Blanco, Yishen Wang, Bolun Xu, Daniel S Kirschen, Hrvoje Pandžić, Jean-Paul Watson, and Cesar A Silva-Monroy. Co-planning of investments in transmission and merchant energy storage. *IEEE Transactions on Power Systems*, 33(1):245–256, 2017.

[151] Reza Hemmati, Miadreza Shafie-Khah, and João PS Catalão. Three-level hybrid energy storage planning under uncertainty. *IEEE Transactions on Industrial Electronics*, 66(3): 2174–2184, 2018.

[152] Faruk Ugranli and Engin Karatepe. Coordinated tcsc allocation and network reinforcements planning with wind power. *IEEE Transactions on Sustainable Energy*, 8(4):1694–1705, 2017.

[153] Mostafa Sahraei-Ardakani and Kory W Hedman. Computationally efficient adjustment of facts set points in dc optimal power flow with shift factor structure. *IEEE Transactions on Power Systems*, 32(3):1733–1740, 2016.

[154] Faisal B Alhasawi and Jovica V Milanovic. Techno-economic contribution of facts devices to the operation of power systems with high level of wind power integration. *IEEE Transactions on Power Systems*, 27(3):1414–1421, 2012.

[155] Omid Ziaee and F Fred Choobineh. Optimal location-allocation of tcsc devices on a transmission network. *IEEE Transactions on Power Systems*, 32(1):94–102, 2016.

[156] Antonio J Conejo, Enrique Castillo, Roberto Minguez, and Raquel Garcia-Bertrand. *Decomposition techniques in mathematical programming: engineering and science applications*. Springer Science & Business Media, 2006.

[157] Mahdi Habibi, Vahid Vahidinasab, Abolfazl Pirayesh, Miadreza Shafie-khah, and João PS Catalão. An enhanced contingency-based model for joint energy and reserve markets operation by considering wind and energy storage systems. *IEEE Transactions on Industrial Informatics*, 2020.

[158] Zora Luburić, Hrvoje Pandžić, and Tomislav Plavšić. Assessment of energy storage operation in vertically integrated utility and electricity market. *Energies*, 10(5):683, 2017.

[159] Zora Luburić and Hrvoje Pandžić. Facts devices and energy storage in unit commitment. *International Journal of Electrical Power & Energy Systems*, 104:311–325, 2019.

[160] Zora Luburić, Hrvoje Pandžić, and Miguel Carrión. Transmission expansion planning model considering battery energy storage, tcsc and lines using ac opf. *IEEE Access*, 8: 203429–203439, 2020.

Acronyms

AC	Alternating Current
ARIMA	An Autoregressive Integrated Moving Average
BES	Battery Energy Storage
CAES	Compressed Air Energy Storage
CC	Constant Current
CC-UC	Chance-constrained unit commitment
CEP	Clean Energy Package
CV	Constant Voltage
DC	Direct Current
DoD	Depth-of-Discharge
DSO	Distribution System Operator
DUC	Deterministic unit commitment
ES	Energy Storage
EU	Europe Union
EV	Electric Vehicle
FACTS	Flexible Alternating Current Transmission Systems
GAMS	The General Algebraic Modeling System
IUC	Interval unit commitment
LHS	Latent Heat Storage

Li-ion Lithium-ion

LMP Local Marginal Pricing

LP Linear Program

MC Market Coupling

MILP Mix Integer Linear Program

NaS Sodium Sulphur

NiCd Nickel Cadmium

NiMH Metal Hydride

OPF Optimal Power Flow

PHS Pumped Hydro Storage

PST Phase Shifting Transformer

RES Renewable Energy Sources

RUC Robust unit commitment

SHS Sensible Heat Storage

SoC State of Charge

SoH State of Health

SSSC Static Synchronous Series Compensator

SUC Stochastic unit commitment

SVC Static Var Compensator

STATCOM Static Synchronous Compensator

UC Unit Commitment

UPFC Unified Power Flow Controller

UPS Uninterruptible Power Supply

TCR Thyristor-Controlled Reactor

TCSC Thyristor-Controlled Series Capacitor

TEP Transmission Expansion Planning

TS Transmission Switching

TSO Transmission System Operator

VSR Variable Series Reactor

List of Figures

List of Tables

Biography

Zora Luburić was born on September 26, 1991 in Mostar, Bosnia and Herzegovina. After graduating from high school, in 2010 she started the undergraduate program Electrical Engineering and Information Technology at the University of Zagreb Faculty of Electrical Engineering and Computing, Croatia (UNIZG-FER), where she received her bachelor's degree in July 2013 and immediately continued her graduate study Electrical Power Engineering at the same institution. She received her master's degree (MSc) in July 2015. In December of the same year, she was employed as a research assistant at the Department of Energy and Power Systems at UNIZG-FER on project Smart Integration of Renewables (SIREN) under the leadership of Prof. Hrvoje Pandžić, PhD. She started the PhD program in February 2016 under the supervision of Prof. Hrvoje Pandžić, PhD. In the winter semester of academic year 2017/2018, she was on a research exchange at the University of Castilla-La Mancha, School of Industrial Technical Engineering in Toledo, Spain under the supervision of professor Miguel Carrión, PhD.

Since January 2019, she has been with the Croatian Transmission System Operator (HOPS). Her research interests include planning and operation of power systems. She is an author / coauthor of 5 journal papers and 5 conference papers with international review and 7 conference paper with national review. She speaks English and she is a member of IEEE.

Journal publications

1. Luburić, Zora; Pandžić, Hrvoje; Plavšić Tomislav, "Assessment of energy storage operation in vertically integrated utility and electricity market" Energies 10, no. 5 (2017): 683. DOI: https://doi.org/10.3390/en10050683
2. Luburić, Zora; Pandžić, Hrvoje, "FACTS devices and energy storage in unit commitment" International Journal of Electrical Power Energy Systems 104 (2019): 311-325. DOI: https://doi.org/10.1016/j.ijepes.2018.07.013
3. Luburić, Zora; Pandžić, Hrvoje; Carrión, Miguel, "Transmission Expansion Planning Model Considering Battery Energy Storage, TCSC and Lines Using AC OPF," IEEE

Access, vol. 8, pp. 203429-203439, 2020 DOI: 10.1109/ACCESS.2020.3036381.

4. Luburić, Zora; Pandžić, Hrvoje; Plavšić Tomislav; Teklić Ljupko; Valentić Vladimir, "Role of energy storage in ensuring transmission system adequacy and security" Energy 156 (2018): 229-239. DOI: 10.1016/j.energy.2018.05.098
5. Pavić, Ivan; Luburić, Zora; Pandžić, Hrvoje; Capuder, Tomislav; Andročec Ivan, "Defining and evaluating use cases for battery energy storage investments: case study in Croatia" Energies 12, no. 3 (2019): 376. DOI: https://doi.org/10.3390/en12030376

Conference publications with international revision

1. Luburić, Zora; Pandžić, Hrvoje; Plavšić, Tomislav, "Comparison of energy storage operation in vertically integrated and market-based power system" // In 2016 IEEE 16th International Conference on Environment and Electrical Engineering (EEEIC), pp. 1-6. IEEE, 2016.
2. Luburić, Zora; Pandžić, Hrvoje; Plavšić, Tomislav; Teklić, Ljupko; Valentić, Vladimir, "Role of Energy Storage in Ensuring Transmission System Adequacy and Stability" // 12th Conference on Sustainable Development of Energy, Water and Environment Systems - SDEWES 2017, Dubrovnik, Croatia (2017): 1.
3. Luburić, Zora; Pandžić, Hrvoje; Plavšić, Tomislav; Teklić, Ljupko; Valentić, Vladimir, "Assessment of N-1 criteria using energy storage" // In 2017 IEEE International Conference on Environment and Electrical Engineering and 2017 IEEE Industrial and Commercial Power Systems Europe (EEEIC/ICPS Europe), pp. 1-6. IEEE, 2017.
4. Luburić, Zora; Pandžić, Hrvoje; Carrión, Miguel; Plavšić Tomislav, "Valuation of Energy Storage Operation in an AC Power Flow Model" // In 2018 IEEE International Conference on Environment and Electrical Engineering and 2018 IEEE Industrial and Commercial Power Systems Europe (EEEIC/ICPS Europe), pp. 1-6. IEEE, 2018. DOI: 10.1109/EEEIC.2018.8493859
5. Miletić, Marija; Luburić, Zora; Pavić, Ivan; Capuder, Tomislav; Pandžić, Hrvoje; Andročec, Ivan; Marušić, Anton, "A Review of Energy Storage Systems Applications" // 11th Mediterranean Conference on Power Generation, Transmission, Distribution and Energy Conversion (MEDPOWER 2018), Dubrovnik, Croatia, 2018. 94-6.
DOI: 10.1049/cp.2018.1926

Conference publications with national revision

1. Luburić, Zora; Bašić, Hrvoje; Pandžić, Hrvoje; Plavšić, Tomislav, "Uloga spremnika energije u elektroenergetskom sustavu" // 12. simpozij o sustavu vođenja EES-a, HRO CIGRE 2016, Split, Croatia 2016. pp. 1-10
2. Luburić, Zora; Pandžić, Hrvoje, "Integracija obnovljivih izvora korištenjem spremnika energije i FACTS uređaja" // 13. savjetovanje HRO CIGRÉ, Šibenik, Croatia 2017. pp. 1-10
3. Luburić, Zora; Pandžić, Hrvoje; Plavšić, Tomislav, "Spremnici energije u modelu s izmjeničnim tokovima snaga" // 13. simpozij o sustavu vođenja EES-a, HRO CIGRE 2018, Rovinj, Croatia, 2018. pp. 1-10
4. Gržanić, Mirna; Luburić, Zora; Tomšić, Željko, "Pregled postojećih regulatornih okvira za integraciju spremnika energije u EES - prednosti i barijere" // 13. simpozij o sustavu vođenja EES-a, Rovinj, Croatia 2018. pp. 1-9
5. Luburić, Zora; Andrić, Antun; Tadin, Tonči, "Europska platforma za razmjenu sekundarne rezerve (PICASSO) – Analiza pristupanja operatora prijenosnog sustava"// 14. savjetovanje HRO CIGRÉ Šibenik, Croatia, 2019. pp. 1-9
6. Luburić, Zora; Andrić, Antun; Tadin, Tonči, "Mehanizmi za razvoj tržišta kapaciteta – osiguravanje dostatnosti sustava omogućavanjem prekograničnog sudjelovanja pružatelja usluge"// 14. simpozij o sustavu vođenja EES-a Opatija, Croatia, 2020. pp. 1-11
7. Luburić, Zora; Andrić, Antun; Tadin, Tonči; Ponoćko, Jelena; Wang, Mengxuan; Rebić, Bojan; Škrba, Obrad; Milanović, Jovica V., "Provision of the experiments by coordination of demand side response units in the region of southeast Europe within the CROSSBOW project - HOPS case"// 14. simpozij o sustavu vođenja EES-a Opatija, Croatia, 2020. pp. 1-10

Životopis

Zora Luburić rođena je 26. rujna 1991. godine u Mostaru. Po završetku srednjoškolskog obrazovanja, 2010. godine upisuje preddiplomski studij Elektrotehnike i informacijske tehnologije na Fakultetu elektrotehnike i računarstva, Sveučilište u Zagrebu, Hrvatska (UNIZG-FER) koji završava u srpnju 2013. te odmah na istom fakultetu nastavlja diplomski studij, smjer Elektroenergetika. Diplomirala je u srpnju 2015. godine. U prosincu iste godine zaposlena je na radnom mjestu asistenta na Zavodu za visoki napon i energetiku na FER-u na projektu Napredna integracija obnovljivih izvora (SIREN) pod vodstvom izv. prof. dr. sc. Hrvoja Pandžića. Poslijediplomski studij upisuje u veljači 2016. godine na istom fakultetu pod mentorstvom izv. prof. dr. sc. Hrvoja Pandžića. U zimskom semestru akademske godine 2017./2018. bila je na razmjeni u sklopu znanstvenog usavršavanja na Sveučilištu Castilla-La Mancha, Škola industrijskog tehničkog inženjerstva u Toledu, Španjolska pod mentorstvom izv. prof. dr. sc. Miguel Carrióna.
Od siječnja 2019. godine zaposlena je u Hrvatskom operatoru prijenosnog sustava. Profesionalni interesi uključuju planiranje i pogon elektroenergetskog sustava. Objavila je 5 znanstvenih radova u časopisima i 5 znanstvenih radova na međunarodnim konferencijama te 7 stručnih radova na domaćim konferencijama. Govori engleski i članica je IEEE-a.